3rd World Conference on Byproducts of Palms & their Applications (ByPalma)

Selected peer-reviewed extended articles based on abstracts presented at the 3rd World Conference on Byproducts of Palms & their Applications (ByPalma 2023)

Edited by:
Dr. Mohamad Midani
Prof. Othman Y. Alothman
Prof. Mohammad Jawaid

TRANS TECH PUBLICATIONS

3rd World Conference on Byproducts of Palms & their Applications (ByPalma)

Selected peer-reviewed extended articles based on abstracts presented at the 3rd World Conference on Byproducts of Palms & their Applications (ByPalma 2023)

Edited by
Dr. Mohamad Midani
Prof. Othman Y. Alothman
Prof. Mohammad Jawaid

3rd World Conference on Byproducts of Palms & their Applications (ByPalma)

Selected peer-reviewed extended articles based on abstracts presented at the 3rd World Conference on Byproducts of Palms & their Applications (ByPalma 2023)

Aggregated Book

Edited by

Dr. Mohamad Midani, Prof. Othman Y. Alothman and Prof. Mohammad Jawaid

Scientific.Net

Trans Tech Publications Ltd
Seestrasse 24c
CH-8806 Baech
Switzerland
https://www.scientific.net

Volume 159 of
Scientific Books Collection
ISBN 978-3-0364-0294-9

Full text available online at *https://www.scientific.net*

***Distributed** worldwide by*

Trans Tech Publications Ltd
Seestrasse 24c
CH-8806 Baech
Switzerland

Phone: +41 (44) 922 10 22
e-mail: sales@scientific.net

Foreword

The Palmae family includes a wide variety of species, and they are considered the main source of livelihood for a significant portion of the world population.

Unfortunately, their byproducts (secondary products) are often regarded as waste, despite that they represent a sustainable material base for a wide spectrum of industries ranging from compost, wood substitutes, and pulp to fiber reinforcements for advanced composites.

ByPalma is the only conference solely focusing on the byproducts of palm plantation around the globe and their current and potential applications. This includes all Palmae family, such as Date palms, Coconut palms, Oil palms, Doum palms, sugar palms,…etc.

This conference highlights the great potential of valorization of palm byproducts towards a sustainable bioeconomy!

The main aims of the ByPalma 2023 conference:

- Bringing together researchers and practitioners working in the area of industrial utilization of palm byproducts and providing a live dialogue and exchanging experiences between them.
- Rediscovering palm by-products and maximizing their added value via industrial technological advancement that can help in the environmental sustainability and circular bioeconomy.
- Establishing an international network of scientists, engineers, artisans, and industry professionals active in the area of palm byproducts R&D, manufacturing, and crafts.

ByPalma 2023 conference covered a wide range of trends in palm byproducts in wood substitutes, composite reinforcements, biotechnology, fertilizers, food, paper, textiles, and bioenergy.

ByPalma 2023 conference was held concurrently with the International Conference and Exhibition for Dates, organized by our strategic partner the National Center for Palms and Dates, bridging the gap in the palm economy by integrating the primary and secondary products of palms.

ByPalma 2023 was the main gathering for celebrating and rediscovering palm byproducts!

Majid L. Altamimi
Conference Chairman
Hamed El-Mously
Conference Co-Chair

Committees

Organizing Committee

Dr. Majid L. Altamimi (Conference Chair), King Saud University, Saudi Arabia
Prof. Hamed El-Mously (Conference Co-Chair), International Association for Palm Byproducts, Egypt
Prof. Othman Y. Alothman, King Saud University, Saudi Arabia
Dr. Mohamad Midani, German University in Cairo, Egypt
Dr. Abdulrahman Z. Bin-jumah, King Saud University, Saudi Arabia
Dr. Mohammed F. Alnuwairan, Saudi National Center for Palms and Dates, Saudi Arabia
Dr. Abdullah Y. AlFaify, King Saud University, Saudi Arabia
Prof. Mohammed F. AlAjmi, King Saud University, Saudi Arabia
Eng. Abd El-Aty Edrees (Committee Secretariat), King Saud University, Saudi Arabia

Scientific Committee

Prof. Othman Y. Alothman (Chair), King Saud University, Saudi Arabia
Dr. Mohamad Midani (Co-Chair), German University in Cairo, Egypt
Prof. Mohammad Jawaid, University Putra Malaysia, Malaysia
Prof. Arno Fruehwald, University of Hamburg, Germany
Prof. Hamed Elmously, Ain Shams University, Egypt
Prof. Mohammad I. Alwabel, King Saud University, Saudi Arabia
Dr. Navin K. Rastogi, Central Food Technological Research Institute, India
Dr. Ramzi Khiari, University of Grenoble Alpes, France
Dr. Mohanad El-Harbawi , King Saud University, Saudi Arabia
Prof. Abdelouahed Kriker, University of Ouargla, Algeria
Prof. Abou El-kacem Qaiss, Moroccan Foundation for Advanced Science Innovation and Research, Morocco
Prof. Abel Olorunnisola, University of Ibadan, Nigeria
Dr. Ahmed Hassanin, Alexandria University, Egypt
Dr. Tamer Hamouda, National Research Center, Egypt
Prof. Julia Ramos, University of Sao Paulo, Brazil
Prof. Carlo Santuli, Universita di Camerino, Italy
Prof. Rob Elias, Bangor University, UK
Prof. S.M. Sapuan, University Putra, Malaysia
Prof. Paridah Md Tahir, University Putra, Malaysia
Dr. Showkat Ahmad Bhawani, Universiti Malaysia Sarawak, Malaysia
Dr. Habil Suchart Siengchin King Mongkut's University of Technology North Bangkok, Thailand
Prof. Carlos A.Cardona, Universidad Nacional de Colombia Sede Manizales, Colombia
Prof. Luiz Augusto H Nogueira, Federal University of Itajuba, Colombia
Dr. Maiada Mohamed El-Dawayati, Agricultural Research Center, Egypt
Prof. Basim Abu-Jdayil, United Arab Emirates University, UAE
Dr. Mohamed Al-Farsi, Plant Research Centre, Oman
Dr. Chad A. Ulven, North Dakota State University, USA
Dr. Eman A. Darwish, Ain Shams University, Egypt
Prof. Saeed Al-Zahrani, King Saud University, Saudi Arabia
Prof. Ahussein Al-Awaadh, King Saud University, Saudi Arabia

Dr. Fahed Alrshoudi, King Saud University, Saudi Arabia
Dr. Maher Alrashid, King Saud University, Saudi Arabia
Prof. Mohammad Asif, King Saud University, Saudi Arabia
Prof. Bel Abbes Bachir Bouiadjra, University of Sidi Bel Abbes, Algeria
Prof. Mohamed Elsayed Ali, King Saud University, Saudi Arabia
Prof. Abdullah Al-Enizi, King Saud University, Saudi Arabia
Dr. Mansour Alhoshan, King Saud University, Saudi Arabia
Prof. Basheer Alshammari, KACST, Saudi Arabia
Dr. Sohail Khan, Florida International University, USA
Prof. Mohammad J. Al-Shannag, King Saud University, Saudi Arabia
Dr. REKBI Fares Mohammed Laid, Research Centre in Industrial Technologies (CRTI), Algeria

Executive Committee

Dr. Abdulrahman Z. Bin Jumah (Chair), King Saud University, Saudi Arabia
Dr. Abdulaziz S. Bentaleb, King Saud University, Saudi Arabia
Eng. Ateyah Z. Alzahrani, King Saud University, Saudi Arabia
Mr. Saud A. Alsaif, King Saud University, Saudi Arabia
Mr. Hassan M. Alamri, King Saud University, Saudi Arabia
Mr. Abdulaziz S. Alkhamis, King Saud University, Saudi Arabia
Eng. Ashraf K. Y. Sulieman, King Saud University, Saudi Arabia
Mr. Soubhi M. Alnamly, King Saud University, Saudi Arabia
Mr. Ali F. Almalki, King Saud University, Saudi Arabia
Mr. Faisal T. Alghamdi, King Saud University, Saudi Arabia

Organizers

ByPalma Association

جامعة الملك سعود
King Saud University
1957

Sponsors and Partners

المركز الوطني للنخيل و التمور
NATIONAL CENTRE FOR PALMS & DATES

Strategic Partner

سرك SIRC
الشركة السعودية الاستثمارية لإعادة التدوير
Saudi Investment Recycling Company

Bronze Sponsor

SPRINGER NATURE

Publishing Partner

Scientific.Net
Publisher in Materials Science & Engineering

Publishing Partner

KFU جامعة الملك فيصل
KING FAISAL UNIVERSITY
مركز التميز البحثي في النخيل والتمور
Date Palm Research Center of Excellence

Scientific Partner

المجلس الدولي للتمور
International Dates Council

Community Partner

بنك الجزيرة
BANK ALJAZIRA

Community Partner

AF.DATES
ARAB FEDERATION FOR DATES
الإتحاد العربي للتمور

Community Partner

جمعية هدية عالم
Scientist's Gift Organization

Cultural Partner

VALORIZEN
RESEARCH AND INNOVATION CENTER

Industry Partner

PalmwoodNet

Industry Partner

Table of Contents

CHAPTER 1:

Preparation Techniques and Properties of Biocomposites

Published in: Materials Science Forum
ISSN: 1662-9752, Vol. 1126, pp 61-75
doi:10.4028/p-7WGruG

Submitted: 2023-12-17
Revised: 2024-03-06
Accepted: 2024-03-26
Online: 2024-09-27

Mechanical Properties of Nano Date Palm versus Nano Titanium Dioxide Particles Reinforced Composites: Experimental Characterization

Mahmoud Alsafy[1,2,a], Nasr Al-Hinai[1,b] and Khalid Alzebdeh[1,c*]

[1]Department of Mechanical and Industrial Engineering, College of Engineering, Sultan Qaboos University, P.O. BOX 33, Al Khoud, PC 123, Sultanate of Oman

[2]Department of Mechanical Engineering, Higher Technological Institute Tenth of Ramadan City, Cairo, Egypt

[a]s128777@student.squ.edu.om, [b]nhinai@squ.edu.om, [c]alzebdeh@squ.edu.om

*alzebdeh@squ.edu.om

Keywords: Nanocomposites, Natural fiber, Mechanical properties, Nano date palm, Recycled Polypropylene, Bio-composites, Nano Titanium.

Abstract. This research work is about characterization of the mechanical properties of two newly developed nanocomposite materials. The produced nanocomposites are made by mixing either Nano date palm particles (NDPP) or Nano Titanium Dioxide particles ($NTiO_2P$), as a reinforcement filler, with recycled polypropylene (rPP). Particularly, downsizing the date palm microfibers generated from waste to Nano-sized lignocellulose fillers has been accomplished by using a ball milling machine. The powdering process is conducted at a high speed of 12 cycles (2 cycles per hour). The manufacturing process involves making composite sheets using a twin-screw extruder in a hot melt state followed by compression molding. After that, test specimens are prepared following ASTM standards and then tested in a Universal Testing Machine (UTM) setup. Results revealed that the highest tensile strength of the reinforced polymer can be accomplished at 3% wt. NDPP and 6% wt. $NTiO_2P$. These filler loadings increased the tensile strength by 48% and 63% over the neat rPP, respectively. Moreover, the flexural strength of NDPP-based nanocomposite increased by 30% at 3% wt. while the strength of $NTiO_2P$-based composite was improved by 33% at 6% wt. over the neat polymer. Due to the soft nanofillers, both nanoparticles exhibited a slight decrease in Young's modulus; 10.7% and 7.8% at 3% wt. NDPP and 6% wt. $NTiO_2P$, respectively. Similarly, the increase in elongation at break and flexural modulus for both nanocomposites contribute to improving the ductility of the neat polymer. The results from the morphological analysis using Field Emission Scanning Electron Microscope (FESEM) revealed that $NTiO_2P$ with 6% wt. has better interlocking with the polymeric matrix and better filler distribution over 3% wt. NDPP. Results showed that the viscosity of NDPP-based nanocomposites exceeded that of $NTiO_2P$-based nanocomposites while the density of NDPP was less. This study indicates that nanocomposites produced from NDPP are economically feasible as natural fiber and ecologically friendly materials with a great potential for use in a variety of industrial applications.

1. Introduction

In recent decades, an increasing interest has emerged to explore alternatives to synthetic fibers prepared from chemicals or petroleum resources due to environmental concerns. One of the challenges associated with synthetic fibers and composites is their impact on the environment, which includes increased carbon footprints, pollution, energy-intensive manufacturing processes, and waste management [1]. Thus, industrial applications often prioritize the use of natural materials. Many research efforts have been carried out to investigate natural fibers as potential fillers in polymers [2]. Specifically, their biodegradability, low cost, non-toxicity, and adequate mechanical capabilities, the ecological lignocellulosic fiber made them extensively researched to mitigate the undesired environmental impact [3]. In addition, the new environmental legislation emphasizes the use of sustainable alternative materials to reduce the greenhouse gas emissions caused by plastic materials.

These rules promote the use of bio-composites derived from a range of natural fibers in a number of applications.

Several studies were performed to investigate the mechanical, chemical, and thermal properties of extracted fibers from date palm trees, as well as their potential application to strengthen polymers [4]. To reinforce a polyester composite, date palm fiber (DPF) is recognized as a significant substitute for several traditional synthetic fibers [5]. In comparison with other natural fiber sources, DPF is one of the most easily obtainable as waste from a date palm tree is more economical due to its low processing cost [6], [7]. In a recent research work, it was found that micro DPFs provide extra strength and ductility to polymer composites [8] due to their inherited properties [9].

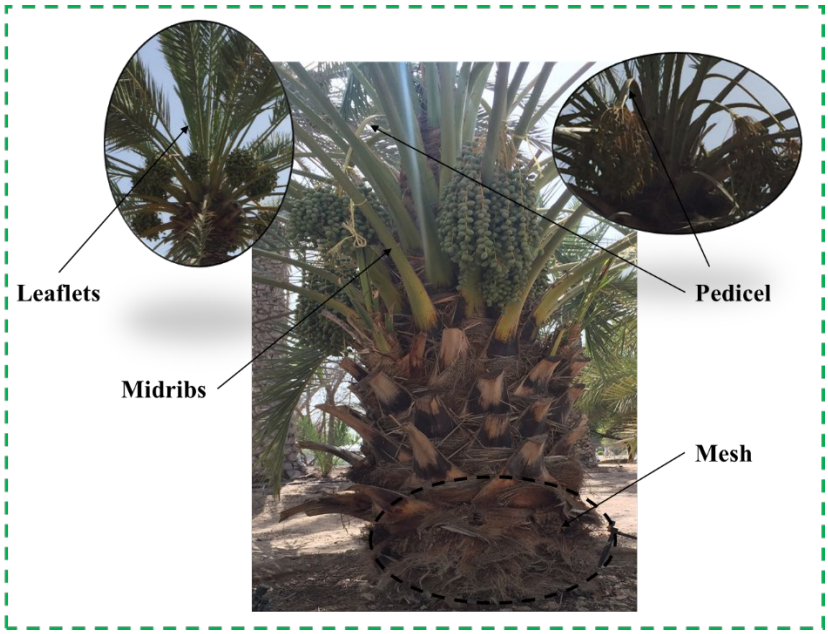

Fig. 1 Date palm tree parts.

Date palm fibers are extracted from different parts of the palm tree including stem, netting, leaflet, pedicel, and midrib as shown in Fig. 1. Filler materials extracted from date palm midribs and spadix can be used in thermoplastics, thermosets, and bio-composites [10], [11]. Furthermore, polypropylene (PP), a popular thermoplastic belonging to the polyolefin family [12], has a linear structure that enables it to be melted and remolded several times [13]. It is a versatile, hydrophobic polymer that can be used in a wide range of applications [14]. Due to its high softening point and maintains consistent mechanical properties at ambient temperature [15]. Other notable features of PP include dimensional consistency, impact resistance, and a high strength-to-weight ratio [16]. As a result, PP has been widely used in commercial applications while being reinforced with a variety of synthetic fibers and particles [17]. Despite some efforts to use post-consumer plastic polymers as matrices for fiber reinforced polymer applications [18], the feasibility of using natural fiber composites is limited due to several factors. The inhomogeneous distribution of particles and the misalignment of fibers in the surrounding polymer have a significant impact on the overall performance of bio-composites, which limits their applicability for load-bearing applications. As a result, they are not yet fully commercialized.

Research showed that powdering fibers into micro scale can enhance their homogeneity in the polymer matrix. Examples from literature include rice husk with a particle size of 500 µm [19], pine nutshell and corn straw micro fiber [20], DPF with 150 µm particles [21], and snail shell (53-63 µm) [22]. In general, incorporation of microfibers improved interlocking between fiber and matrix that resulted in improving the mechanical performance and thermal stability of the bio-composites. Although, the natural microfibers have showed prominent improvement in mechanical properties of

underlying bio-composites, the use of nanoparticle fillers can be further investigated to explore possible further developments [23]. If successful, several industries concerned with for example food packaging applications, aerospace, automotive, electronics, and biotechnology, may show interest in producing nanosized biomass fibers due to their higher surface area and aspect ratio, as well as its promising characteristics associated with possible cost reduction [24], [25]. Along this direction, [23], [26] highlighted the potential use of Nano date palm particles (NDPP) from mesh-part in the palm tree to reinforce polymer composites. The nanocomposite comprises oil palm bio-ash/phenol-formaldehyde (PF) with 1 % wt. filler content improved internal bonding strength, thermal stability, and crystal degree of these composite [27]. Moreover, the Nano eggshell/PP with 4% wt. enhanced physical, thermal, and mechanical characteristics [27] and Nano eggshell/rLDPE with 10 % wt. increased the tensile strength, flexural strength and hardness of the composite but impact energy decreased with 12 % wt. [28]. In addition, both Nano clay/rPP with 5 % wt. [29] and Nano clay/PP with 4 % wt. [30] used compatibilizers to improve the mechanical performance of the nanocomposites.

Recently, numerous nanoscale additives have been exploited in reinforcing virgin polymeric materials. For example, Nano Titanium Dioxide particles ($NTiO_2P$) is one of the potential inorganic Nano particles that are utilized to enhance mechanical properties in glass fiber reinforced polymers [31], [32]. Findings showed that the addition of 0.1 % wt. TiO_2 reduced the coefficient of water diffusion by 9% and improved the residual bending strength by 19%. It also increased the residual inter laminar shear strength by 18% among the nanocomposites [33]. Additionally, the incorporation of $NTiO_2P$ into Polyvinyl Alcohol (PVA)–chitosan (CHI) biodegradable PVA–CHI films resulted in better water vapor and gas barrier characteristics as well as improved mechanical and antibacterial properties.

The objective of this study is to create and analyze new nanocomposites made from $NTiO_2P$ and NDPP, which will enhance the strength of recycled polypropylene (rPP). NDPP, a reinforcing material, will be extracted from date palm agro-residue and processed using ball milling technique for 3 hours to create a mechanically powdered form. Afterwards, both nanoparticles will be mixed with the polymer matrix to produce various nanocomposite materials. Finally, the performance of the created nanocomposites will be characterized experimentally, as well as analyzing their microstructural morphology to validate the experimental findings.

2. Materials and Methods

The recycled post-consumer polypropylene (rPP) was generously provided by a local recycling facility in the form of powder. The date palm filler was extracted from the agro-residues of pedicel part of date palm tree. Firstly, the agro-residues were cleaned by tap water to remove impurities and dust particles, and then kept in fresh water for one day at room temperature. After that, it was dried at 105 °C for 15 minutes to ensure moisture release. As shown in Fig. 2, the branches were chopped into small pieces (8-10 cm) with an electrical sawing machine. It was then crushed using industrial herbs crush powdering machine (spice & Herb Grinder HR-50B) with 25,000 rpm, 4500 watts, and a capacity of 1 kg to obtain fine powder (micro-size). Then, microfibers were filtered into an Octagon 200 shaking machine for 1 hour using 75 μm with ASTM D5510 standard before being processed by ball milling machine powdered to nano-size. A planetary ball-milling machine linked to a liquid Nitrogen tank with a 50L capacity was used to further grind the microfibers to nano scale size particles (MITR Co. China). The milling procedure was carried out following the process reported in [34]. It is worthwhile to mention that no chemical treatment was used to produce NDPP. The material of the chamber and balls made of zirconium oxide materials, and the rotational speed was 400 rpm.

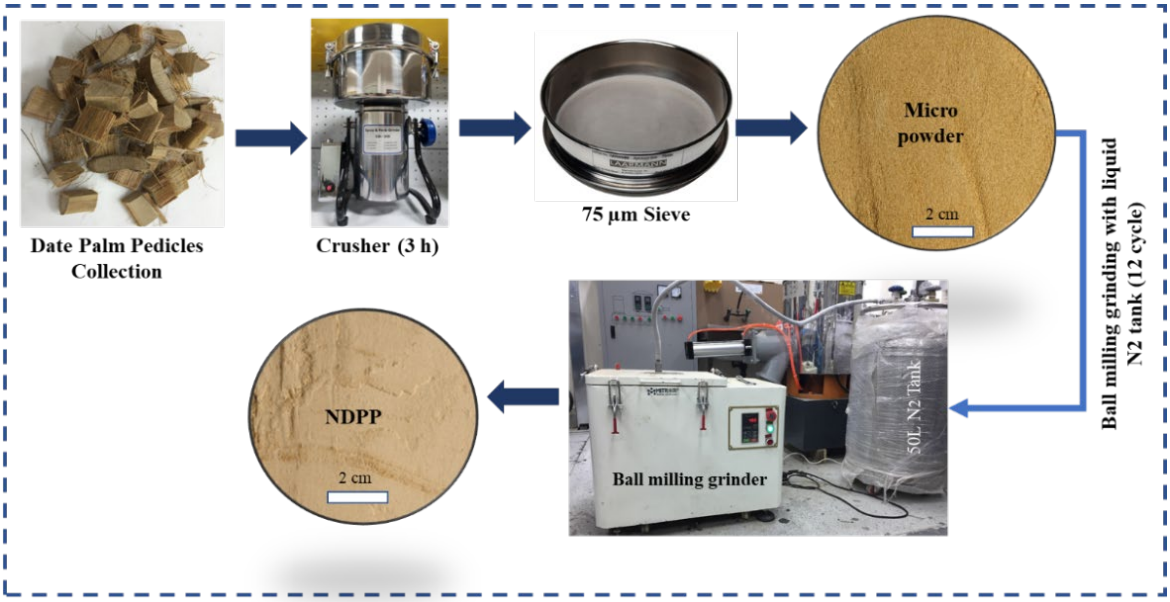

Fig. 2 Flow chart showing NDPP production.

Next, in a laboratory-sized double screw extruder (Nanjing TengDa Machinery Co., Ltd., China) with ten 180 °C heating zones, the extracted NDPP was blended with the rPP-powder as indicated in Fig. 3. The 160-rpm double screw spinning speed was maintained consistently. The extruded material was cooled down at room temperature and crushed into small pellets using crusher machine attached to double screw extruder prior to compression. The following step involved using a compression molding machine (Carver, USA) and a stainless-steel mold with dimensions of 230x230x3 mm to create sheets with (3, 5, and 10) % wt. for Nano Date Palm Composites (NDPC) at 260 °C with 40 MPa pressure under two heated plates. After maintaining the compression for 15 minutes, the heating elements were turned off to let the sheet cool down for an hour at room temperature. The next step was to remove the dried sheets from the mold and cut them using a CNC router to create test specimens. The same process was followed to produce Nano Titanium Composites (NTiC) sheets but with (5, 6, and 7) % wt., respectively.

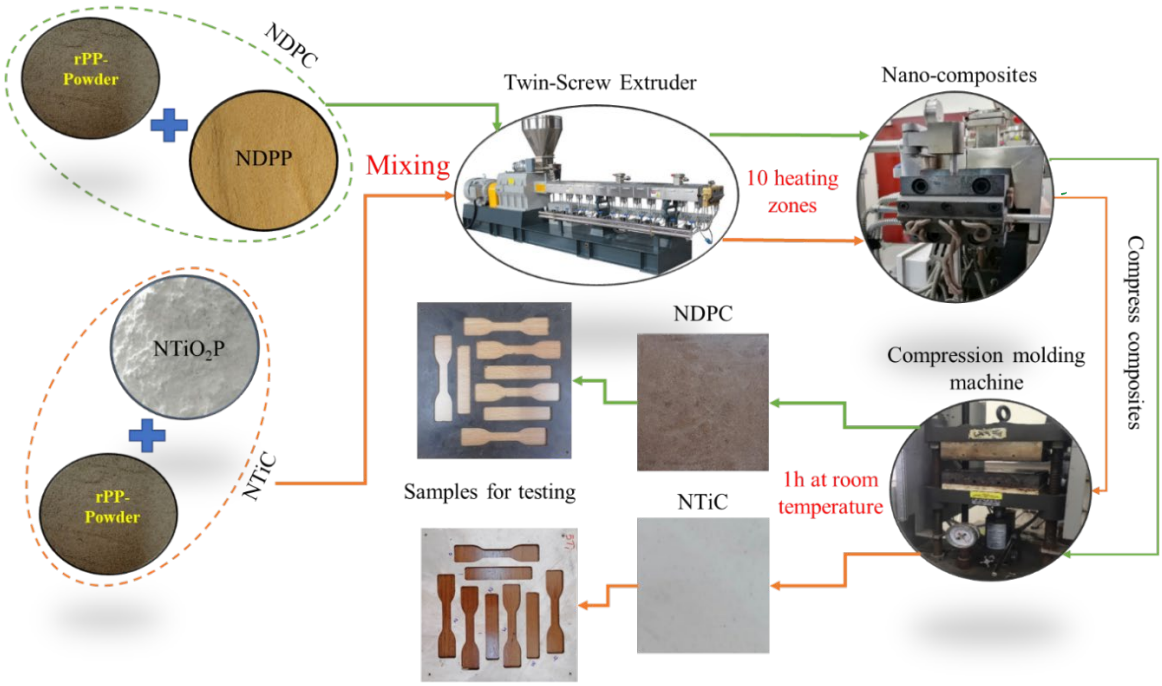

Fig. 3 Nanocomposite fabrication.

3. Testing and Characterization

The morphological, physical and mechanical properties of the manufactured nanocomposites specimens were characterized through experimental methods. Using a JEM-1400 field-emission electron microscope (JEOL, Japan) operated at an accelerating voltage of 120 kV, Transmission Electron Microscopy (TEM) imaging was performed to investigate the morphology of the Nano particles. The Nano particles were combined with ethanol during sample preparation and then applied on a copper grid substrate to dry before displaying.

Additional morphological characterization was carried out using a Scanning Electron Microscope (SEM), including elemental studies (JSM-7800F, Japan) to evaluate the filler geometry. A small amount of dry powder was sonicated in ethanol for 30 minutes before being placed on a conductive carbon tape of the sampling stub. All of the specimens were gold sputtered before being observed.

According to ASTM D638 and ASTM D790, the mechanical properties of test samples were measured using a UTM machine (tensile strength, Young's modulus, and elongation at break) and a three-point bending test (flexural strength) to measure the flexural modulus and flexural strength. Accordingly, the five samples' mechanical characteristics were assessed, and their average testing results are recorded as discussed in Section 4.

The Melt Flow Index (MFI) test was used to assess viscosity of the material in melt solid state following the standards ASTM D1238. Melt flow rate was used for NDPC and NTiC at 240°C, 2.16 kg. Furthermore, the samples' densities were measured using a densitometer (MZ-A300, Shenzhen Qun Long Instrument Equipment, China) according to ASTM D792-13 by using Archimedes' principle. About 50 g of each nanocomposite specimen were cut and submerged in distilled water at room temperature, and the volumetric change of the water was calculated. Consequently, the average of three samples is discussed in Section 4.

4. Results and Discussion

4.1 Morphological characteristics

4.1.1 TEM

TEM was used to investigate the morphology of both types of Nano particles and estimate the particle size. As shown in Fig.4 (a), the average particle size measurements of NDPP after 3h of powdering was found to be in the range of 80 to 122 nm, while the particle size of $NTiO_2P$ was found between 47nm to 66 nm, as illustrated in Fig.4 (b). TEM revealed an inhomogeneous distribution of circular and asymmetrical particle shapes [24]. This indicates that the ball milling process associated with liquid nitrogen tank had successfully broken down the micro natural fibers into several Nano-sized components [25]. It appears that the circular-shaped particle's pack-like structure could provide them with a highly preserved rigidity for useful application in reinforcing composite materials.

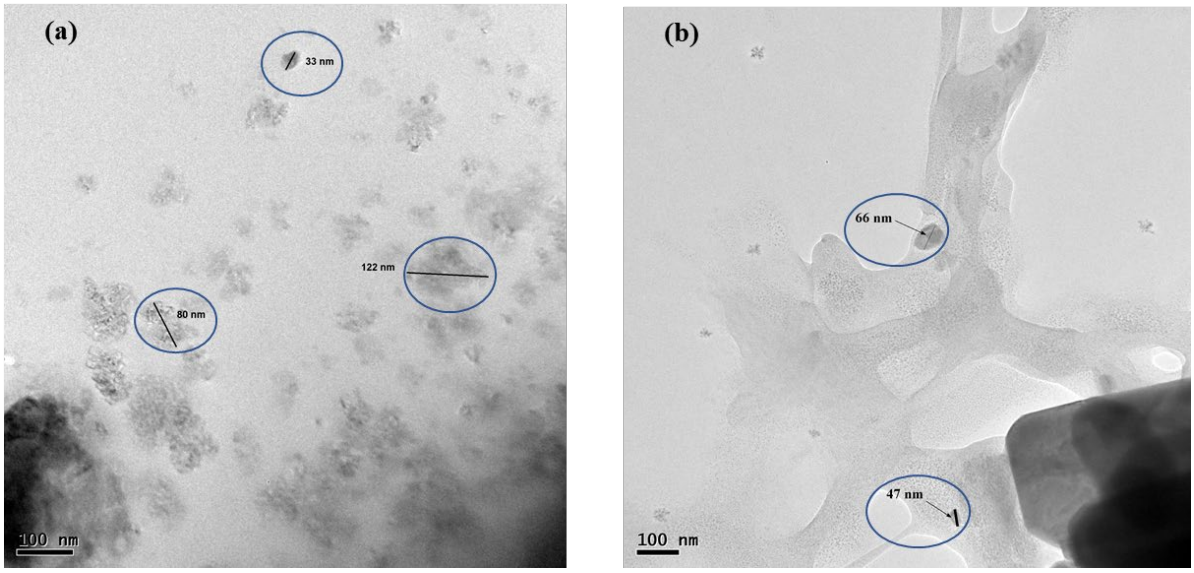

Fig. 4 TEM (a) NDPP and (b) $NTiO_2P$ particle size.

4.1.2 SEM

Fig. 5 (a) reveals that the surface of NDPP is rough and randomly shaped due to the excessive impact and shear forces generated by ball milling which assisted in disintegrating the lignin and hemicellulose components on outer surface of the particle [35], [36]. In addition, it shows that accumulation of particles becomes more apparent when particle size is further reduced. This poses a challenge to produce effective nanocomposite material. Fig. 5 (b) provides insight into the shape of $NTiO_2P$ that demonstrates smooth surface of the particles with less randomness compared to NDPP. It has been noted that $NTiO_2P$ frequently form spherical aggregates [37]. Several studies have stated that the development of spherical Nano particles was crucial for a variety of applications because it enhance their mechanical properties [38]. Consequently, there was an obvious agreement between grain size measurements revealed by SEM and TEM techniques for the structure and morphological characterization of both NDPP and $NTiO_2P$.

SEM at the fractured surfaces was performed to assess the interlocking between Nano particles and surrounding matrix after blending to make composite. The rough surface and low filler content of NDPP promotes good interlocking with the matrix and in turn improves mechanical properties of the nanocomposite, as supported by Fig 6(a). The Nano size (47-66 nm) and well dispersion of the $NTiO_2P$ in rPP are recognized to improve the matrix/fiber interfacial linkage, as shown in Fig. 6(b). However, Fig. 6(c) and (d), confirm the aggregation of the nanoparticles after increasing contents of NDPP and $NTiO_2P$ to 10% and 7%, respectively. At these conditions, achieving uniform dispersion of nanoparticles becomes difficult [39]. By acting as stress concentration regions and introducing defects, typically these agglomerates cause cracks and premature breakdowns in nanocomposites.

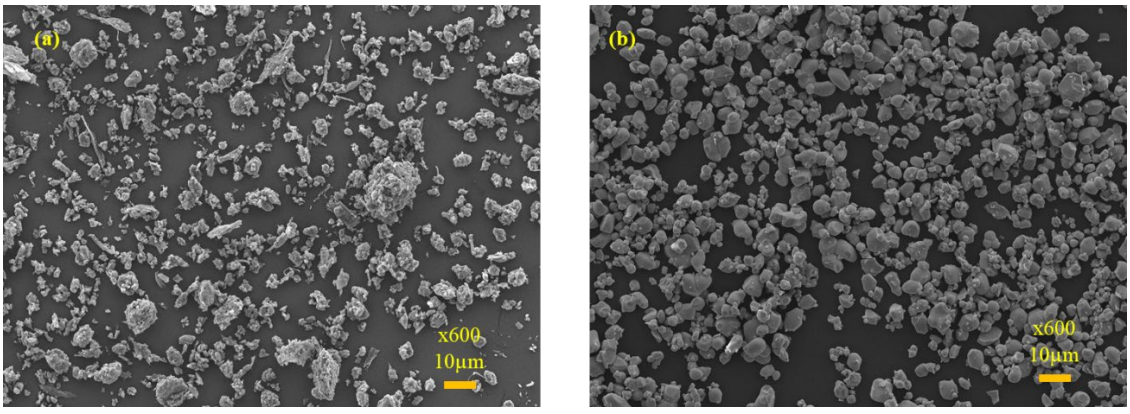

Fig. 5 SEM of (a) NDPP and (b) $NTiO_2P$.

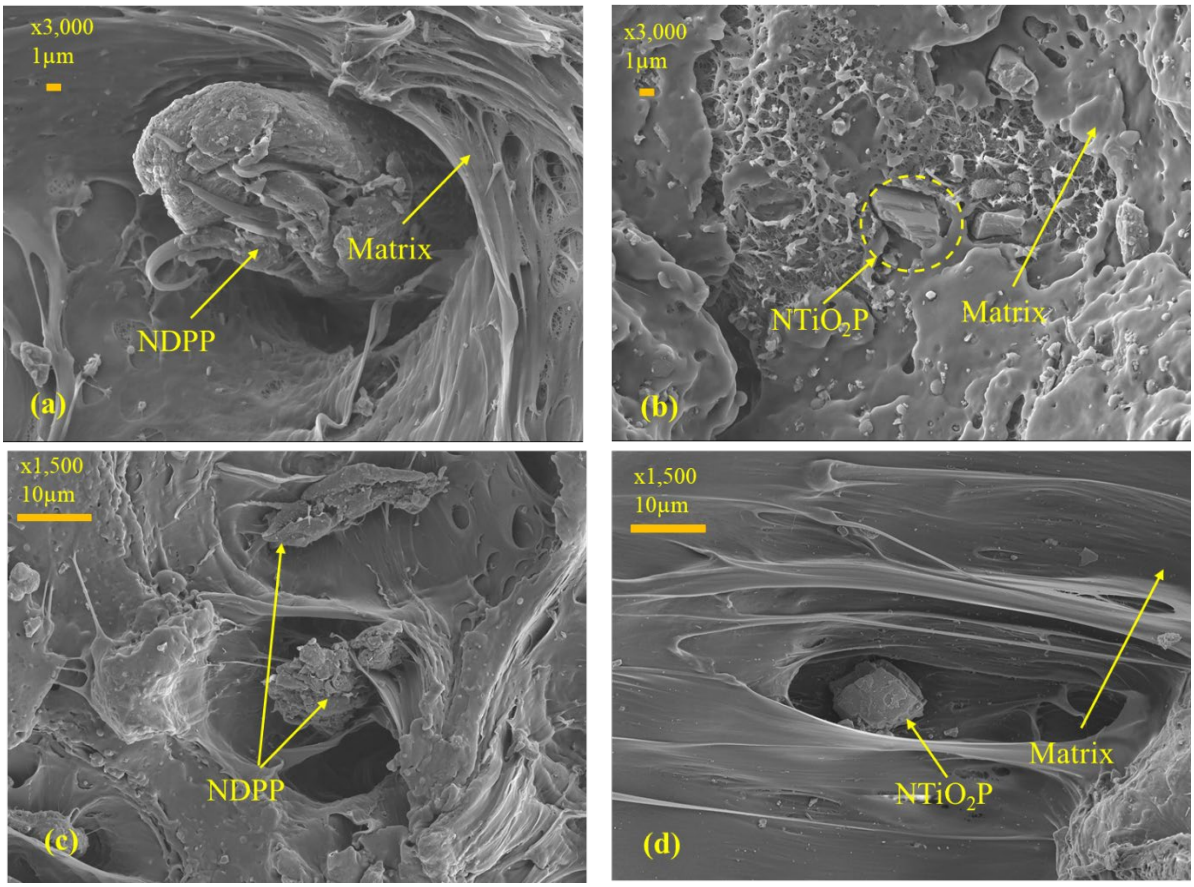

Fig. 6 SEM of (a) 3%wt. NDPC, (b) 6% wt. NTiC, (c) 10%wt. NDPC and (d) 7%wt. NTiC

4.2 Mechanical properties

4.2.1 Tensile strength

The mechanical characteristics of nanocomposites are determined by the type and filler percentage weight, the matrix properties, the nano filler-matrix interface, and the distribution of fillers within matrix. Fig. 7 shows that the tensile strength of the nanocomposites has been improved over the neat rPP in all cases. This is due to the high surface area of Nano particles [37], the strong interfacial bonding and the good particle distribution inside the matrix [40] which could contribute to the creation of a uniform stress distribution.

The slight degradation in tensile strength of the NDPC with 5% wt. and further reduction at 10% wt. is attributed to agglomeration of NDPP as supported by SEM in Fig. 6(c). Similar observation can be made for NTiC after increasing the $NTiO_2P$ content in the matrix with less degradation compared to NDPC. As confirmed by TEM (Fig. 4), the difference in results of both composites could be attributed to the fact that the particle size of $NTiO_2P$ is half size of the NDPP which provides more interlocking with the molecular chains of rPP. A similar conclusion can be made about the elongation at break as shown in Fig. 8. In addition, both optimum Nano particles content provides a higher elongation at break (%) than pure rPP, indicating that the NDPC and NTiC have better ductility, as confirmed by Fig. 8.

An analogous conclusion can be obtained from Fig. 9, which shows that rPP matrix with incorporation of 3% of NDPP and 6% of $NTiO_2P$ in the composites contributed to the greatest increases in Young's modulus (7.1%) and (10%), respectively. A higher level of interaction with the polymer chains and strong interfacial adhesion between NDPP and $NTiO_2P$ with the rPP matrix have been associated with this rise.

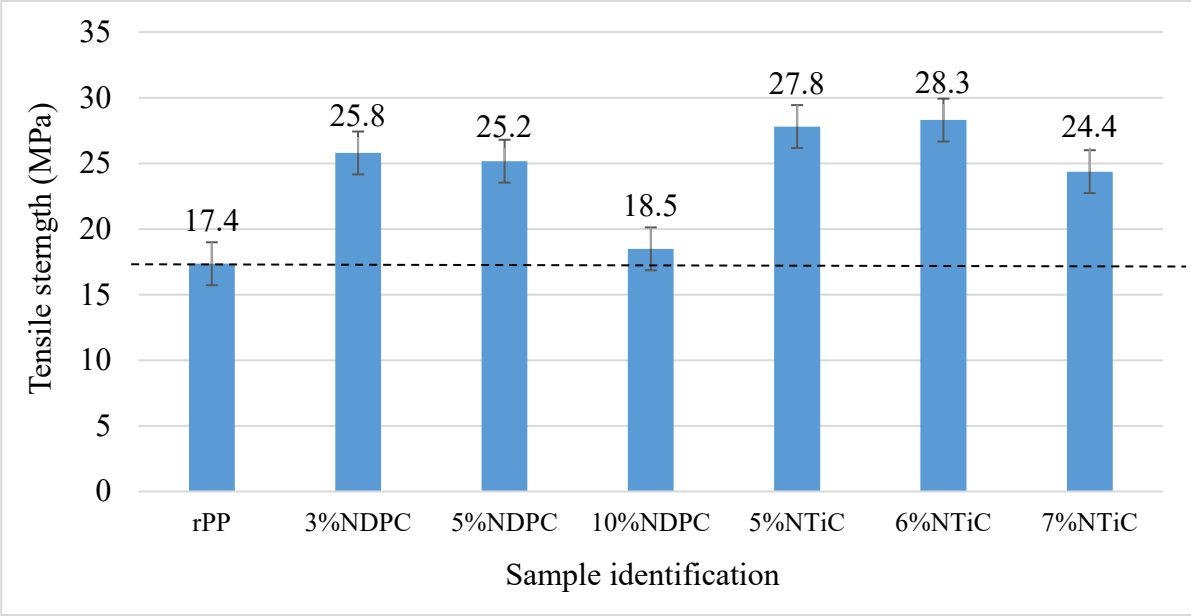

Fig. 7 Tensile strength of nanocomposites.

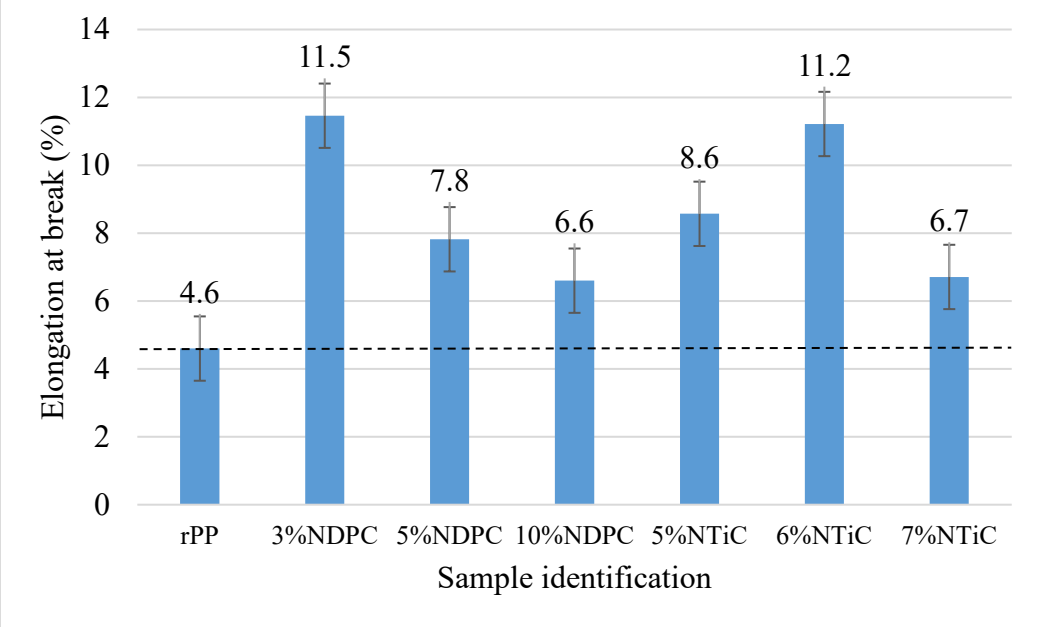

Fig. 8 Elongation at break of nanocomposites.

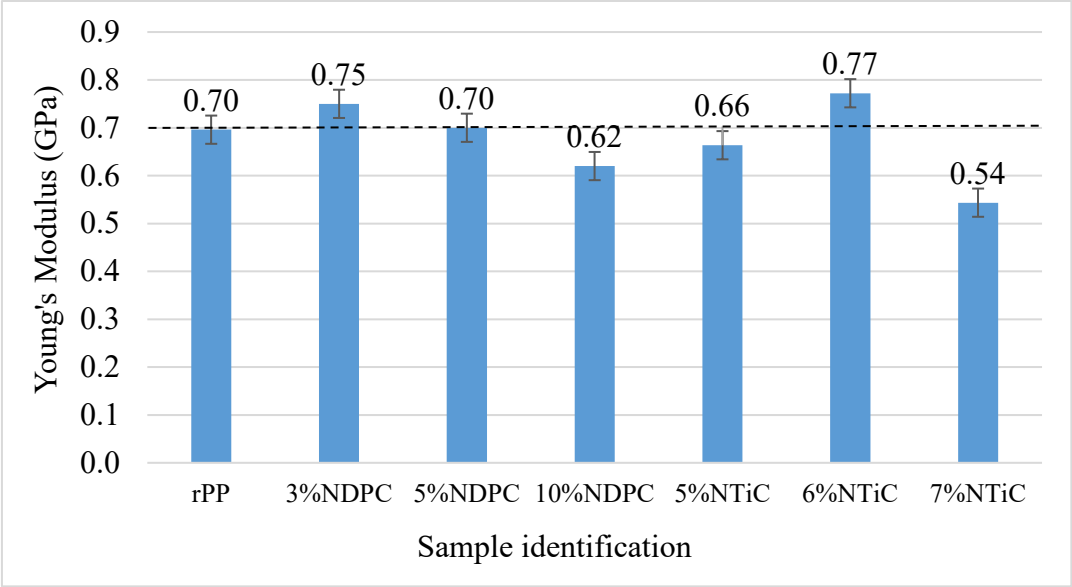

Fig. 9 Young's Modulus of nanocomposites.

To further examine the mechanical properties of the developed nanocomposites, stress-strain diagrams are presented in Fig. 10. It is clearly confirmed that the developed nanocomposites exhibited improved both strength and ductility over the neat polymer. As the content of NDPP increases, mechanical performance is degraded due to the issue of agglomeration. However, NTiC outperformed NDPC owing to the characteristics of the reinforcement.

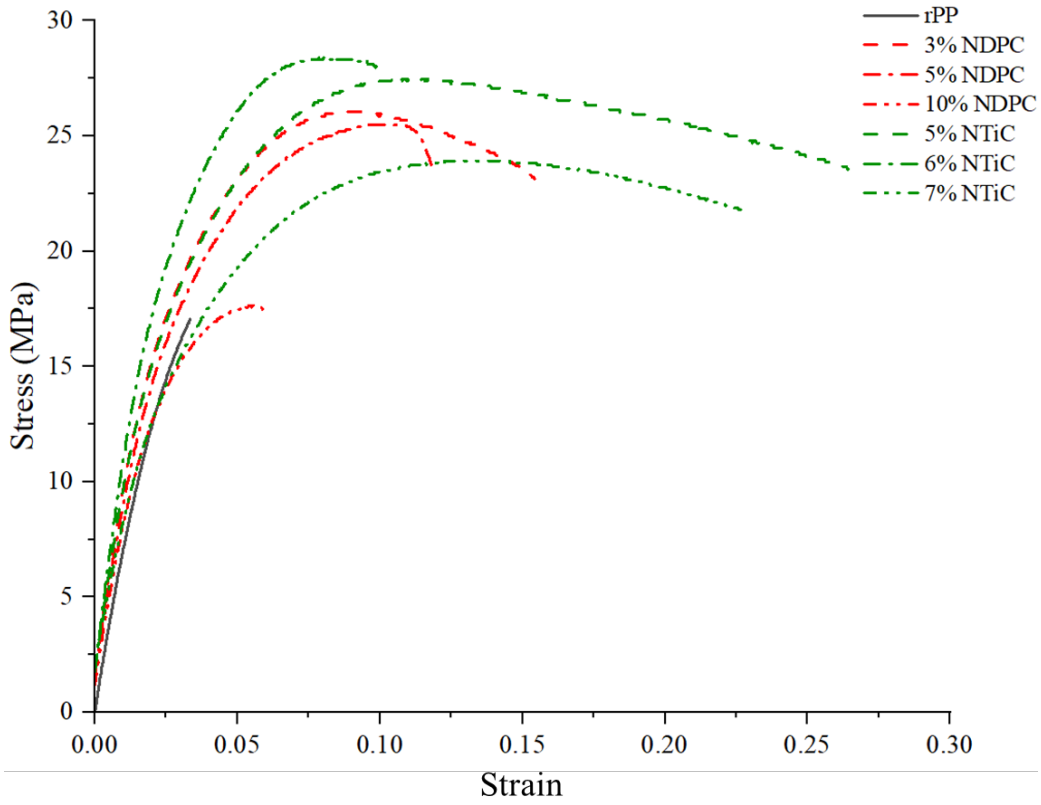

Fig. 10 Tensile stress-strain relationship of nanocomposites.

4.2.2 Flexural strength

Clearly, mixing Nano particles with rPP-powder demonstrated improved flexural strength of the nanocomposites as illustrated in Fig. 11. The highest flexural strength is observed in the case of 3%NDPP and 6% $NTiO_2P$, which is due to the good dispersion of both NDPP and $NTiO_2P$ with the matrix (as supported by the SEM images in Fig. 6). As particle concentration increases, samples show

a slight degradation in the flexural strength because of the higher chances of Nano particles accumulation within the samples. A similar trend of the flexural modulus of the nanocomposites prevails, as shown in Fig. 12. From the obtained results, the 6% wt. NTiC and 3% wt. NDPC exhibited optimal mechanical properties compared to other nanocomposites with different particle concentrations.

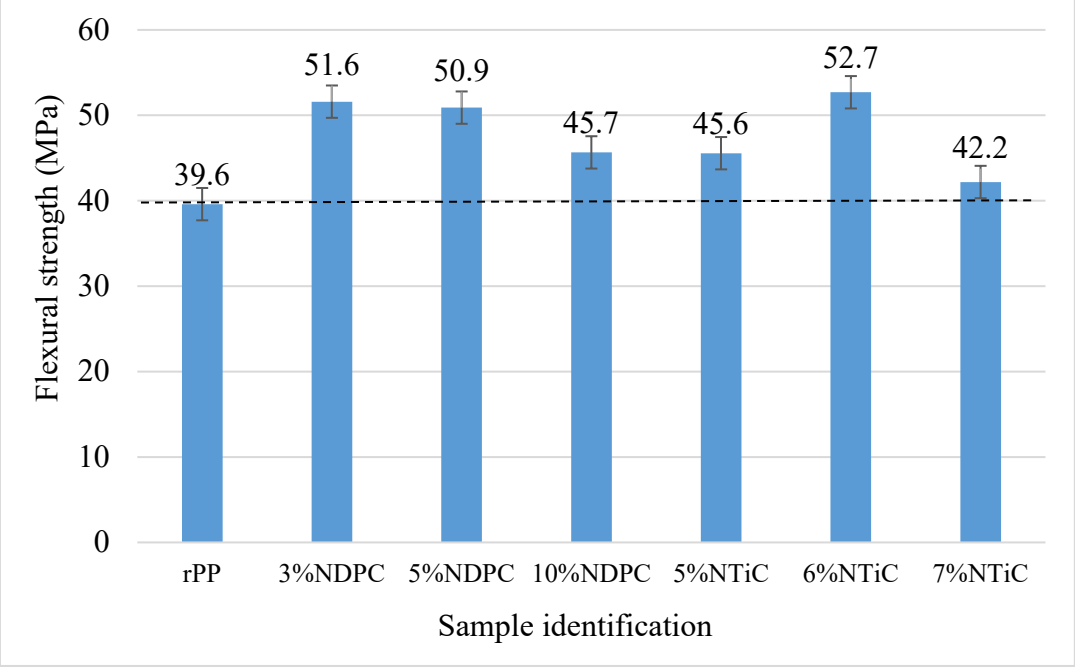

Fig. 11 Flexural strength of nanocomposites.

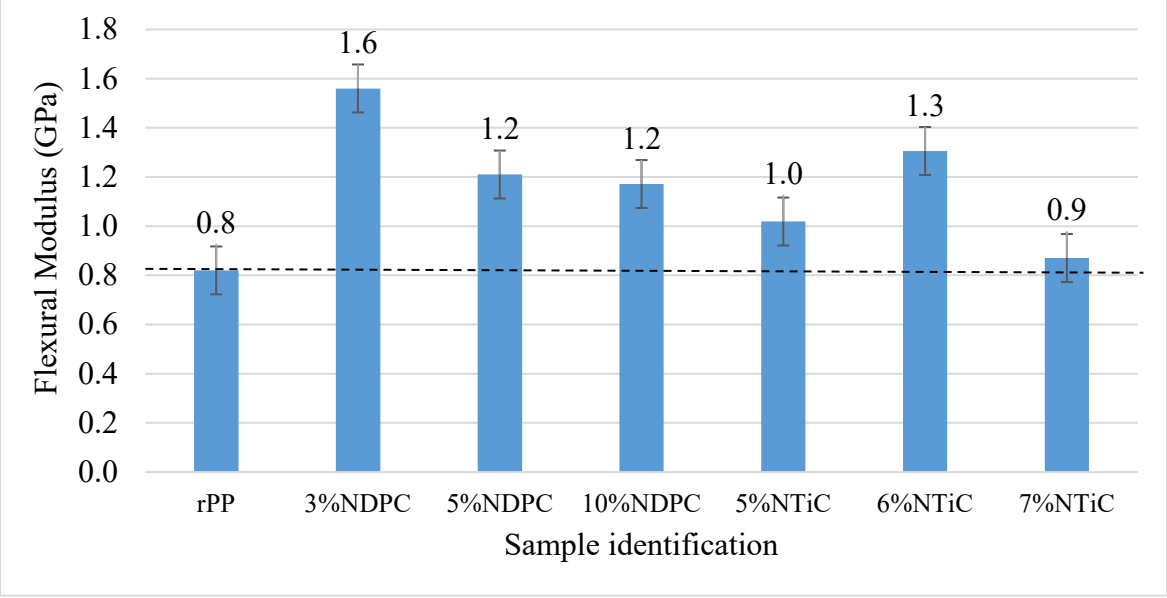

Fig. 13 Flexural Modulus of nanocomposites.

4.2.3 Melt flow index.

The results of the MFI experiments as shown in Fig. 13 clearly reveal that the MFI of NDPC is lower than that of NTiC. It implies that the addition of NDPP to rPP increased the viscosity of the polymer and decreased the flowability of nanocomposite (10%NDPC) to 2.66 g/10 min which is consistent with the results reported by [41]. It is obvious that when the content of both fillers increases, the MFI of the composite material decreases. A similar trend is obtained in [42]. In specific, the addition of $NTiO_2P$ up to 7%wt. reduced the MFI to 2.04 g/10min of the NTiC and thus

increased the viscosity of the nanocomposite compared to the neat rPP. The NDPC likewise follows a similar trend. Melt flow rate is an indirect indicator of molecular weight, with low molecular weight is counterpart to high MFI.

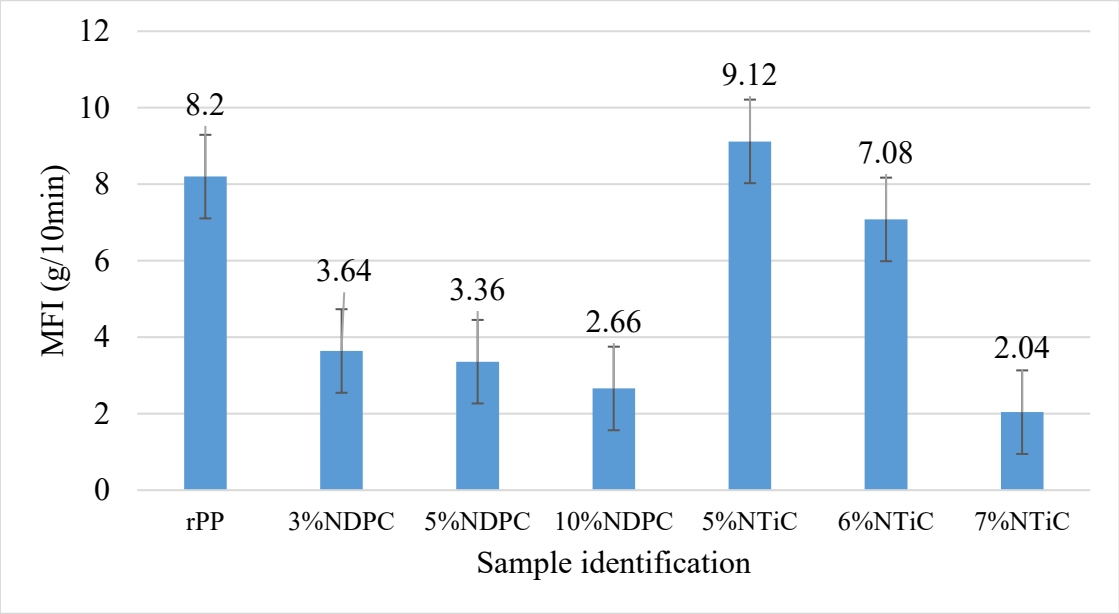

Fig. 13 MFI results of nanocomposites.

4.2.4 Density

In fact, the density of NDPC is lower than the density of NTiC and the neat rPP, thereby at 3% NDPP the density of NDPC was decreased as shown in Fig. 14. The addition of hard and stiff NDPP up to 10% wt. and NTiO2P up to 7% wt. increases the viscosity of both nanocomposites. As expected, the density slightly increased to 0.927 and 0.966 g/cm3 for 10%NDPC and 7%NTiC, respectively. As a similar trend was reported by [43] and supported by MFI values of both composites as well in Fig. 13. Additionally, the lower particle size of $NTiO_2P$ with good distribution inside matrix gives less voids inside NTiC compared with NDPC, as illustrated in TEM Fig. 4. In conclusion, the density values for each nanocomposite are slightly increased than the density value of the rPP matrix. This could be attributed to the fact that the density of the NDPP and $NTiO_2P$ are higher than rPP polymer [44].

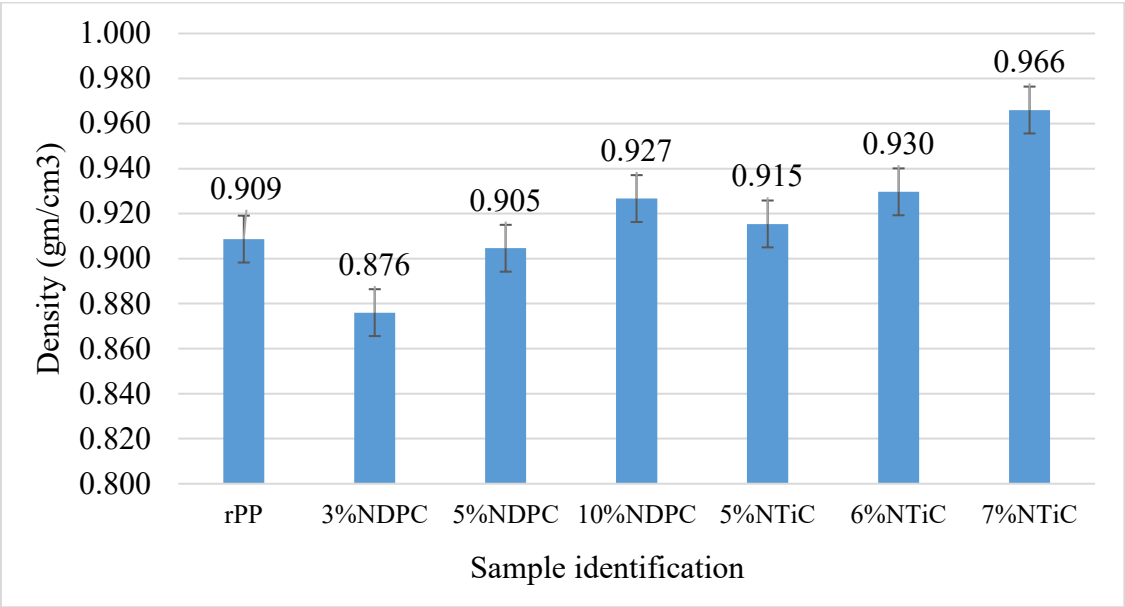

Fig. 14 Density of nanocomposites.

5. Conclusion

Nanocomposite materials made from agricultural waste and recycled thermoplastics provide a viable alternative to synthetic fiber-based composites to design products. This study aimed to explore the potential use of nanoparticles extracted from palm tree agro-residues and Titanium Oxides as reinforcing elements in rPP polymers to improve their performance and broaden their potential applications. Experimental characterizations have demonstrated that all mechanical properties of the developed nanocomposites were improved in reference to the neat rPP except the modulus of elasticity which was slightly decreased. The agglomeration of nanoparticles is responsible for decreasing mechanical properties as their concentration in the polymer grows. In contrast, density of nanocomposites increases for the same reason. Overall, the tensile properties of NTiC are higher than NDDP while the opposite is true for the flexural properties. Therefore, this confirms that the newly developed nanocomposite has a high potential for further development. In future, coupling agents and appropriate modification processes will be applied to enhance the attributes of the developed nanocomposite materials.

Acknowledgement

The authors would like to acknowledge the research internal grant No. IG/ENG/MIED/23/02 provided by Sultan Qaboos University (SQU) through Deanship of Research.

References

[1] M.M.A. Nassar, K.I. Alzebdeh, N. Al-Hinai, and M. Al Safy, "Enhancing mechanical performance of polypropylene bio-based composites using chemically treated date palm filler," *Ind. Crops Prod.*, vol. 220, p. 119237, 2024, doi: https://doi.org/10.1016/j.indcrop.2024.119237.

[2] O.Y. Alothman, H.M. Shaikh, B. A. Alshammari, and M. Jawaid, "Structural, Morphological and Thermal Properties of Nano Filler Produced from Date Palm-Based Micro Fibers (Phoenix dactylifera L.)," *J. Polym. Environ.*, 2021, doi: 10.1007/s10924-021-02224-0.

[3] T. Gurunathan, S. Mohanty, and S. K. Nayak, "A review of the recent developments in biocomposites based on natural fibres and their application perspectives," *Compos. Part A Appl. Sci. Manuf.*, vol. 77, pp. 1–25, 2015, doi: 10.1016/j.compositesa.2015.06.007.

[4] K.I. Alzebdeh and M.M.A. Nassar, "An integrated approach to evaluate mechanical performance of date palm filler reinforced polypropylene," *Mater. Today Commun.*, vol. 35, p. 105583, 2023, doi: 10.1016/j.mtcomm.2023.105583.

[5] A.N. Anyakora, "Investigation of Impact Strength Properties of Oil and Date Palm Frond Fiber Reinforced Polyester Composites," *Int. J. Curr. Eng. Technol.*, vol. 3, no. 2, pp. 493–497, 2013.

[6] K.I. Alzebdeh, M. M. A. Nassar, S. A. Awad, and E.-S. I. El-Shafey, "New click chemistry scheme towards improvement of filler/polymer crosslinking in bio-based polymer composites," *Polym. Technol. Mater.*, pp. 1–14, 2024, doi: 10.1080/25740881.2024.2376206.

[7] L. A. Elseify, M. Midani, L. A. Shihata, and H. El-Mously, "Review on cellulosic fibers extracted from date palms (Phoenix Dactylifera L.) and their applications," *Cellulose*, vol. 26, no. 4, pp. 2209–2232, 2019, doi: 10.1007/s10570-019-02259-6.

[8] M.M.A. Nassar, K.I. Alzebdeh, T. Pervez, N. Al-Hinai, and A. Munam, "Progress and challenges in sustainability, compatibility, and production of eco-composites: A state-of-art review," in *Journal of Applied Polymer Science*, 2021, vol. 138, no. 43, pp. 1–31. doi: 10.1002/app.51284.

[9] K. Almi, S. Lakel, a. Benchabane, and a. Kriker, "Characterization of Date Palm Wood Used as Composites Reinforcement," *Acta Phys. Pol. A*, vol. 127, no. 4, pp. 1072–1074, 2015, doi: 10.12693/APhysPolA.127.1072.

[10] S. Amroune *et al.*, "Tensile Mechanical Properties and Surface Chemical Sensitivity of Technical Fibers From Date Palm Fruit Branches (Phoenix Dactylifera L.)," *Compos. Part A Appl. Sci. Manuf.*, vol. 71, pp. 98–106, 2015, doi: 10.1016/j.compositesa.2014.12.011.

[11] M.M.A. Nassar, K. I. Alzebdeh, M. M. M. Alsafy, and S. Piya, "Optimizing drilling parameters for minimizing delamination in polypropylene-date palm fiber bio-composite materials," *J. Brazilian Soc. Mech. Sci. Eng.*, vol. 45, no. 11, 2023, doi: 10.1007/s40430-023-04528-9.

[12] N.F. Nabila Farhana binti Abdul Khalil, "Mechanical Properties of Low-Density Polyethylene/Recycled Poly (ethylene Terephthalate)(LDPE/r-PET) Microfibrillar Composite," 2011.

[13] H.P.S.A. Khalil, M.A. Tehrani, Y. Davoudpour, A. H. Bhat, M. Jawaid, and A. Hassan, "Natural fiber reinforced poly (vinyl chloride) composites: A review," *J. Reinf. Plast. Compos.*, vol. 32, no. 5, pp. 330–356, 2013.

[14] Z. Chen, H.Y. Xie, Y.J. Li, G.E. Chen, S.J. Xu, and Z.L. Xu, "Smart light responsive polypropylene membrane switching reversibly between hydrophobicity and hydrophilicity for oily water separation," *J. Memb. Sci.*, vol. 638, no. June, p. 119704, 2021, doi: 10.1016/j.memsci.2021.119704.

[15] G. K. Sathishkumar *et al.*, "Synthesis and Mechanical Properties of Natural Fiber Reinforced Epoxy/Polyester/Polypropylene Composites: A Review," *J. Nat. Fibers*, vol. 19, no. 10, pp. 3718–3741, 2022, doi: 10.1080/15440478.2020.1848723.

[16] B. A. Salazar-Cruz, M. Y. Chávez-Cinco, A. B. Morales-Cepeda, C. E. Ramos-Galván, and J. L. Rivera-Armenta, "Evaluation of Thermal Properties of Composites Prepared from Pistachio Shell Particles Treated Chemically and Polypropylene," *Molecules*, vol. 27, no. 2, 2022, doi: 10.3390/molecules27020426.

[17] J. Ahmad and Z. Zhou, "Mechanical properties of natural as well as synthetic fiber reinforced concrete: a review," *Constr. Build. Mater.*, vol. 333, p. 127353, 2022.

[18] W. Tang *et al.*, "Rheological behavior and mechanical properties of ultra-high-filled wood fiber/polypropylene composites using waste wood sawdust and recycled polypropylene as raw materials," *Constr. Build. Mater.*, vol. 351, no. June, p. 128977, 2022, doi: 10.1016/j.conbuildmat.2022.128977.

[19] B.O. Orji and A.G. McDonald, "Evaluation of the mechanical, thermal and rheological properties of recycled polyolefins rice-hull composites," *Materials (Basel).*, vol. 13, no. 3, 2020, doi: 10.3390/ma13030667.

[20] C. Wang, J. Mei, and L. Zhang, "High-added-value biomass-derived composites by chemically coupling post-consumer plastics with agricultural and forestry wastes," *J. Clean. Prod.*, vol. 284, p. 124768, 2021, doi: 10.1016/j.jclepro.2020.124768.

[21] K. I. Alzebdeh, M. M. A. Nassar, and N. Al-Hinai, "Development of New Eco-Composites From Natural Agro-Residues and Recycled Polymers," *ASME 2020 International Mechanical Engineering Congress and Exposition*. Nov. 16, 2020. doi: 10.1115/IMECE2020-23536.

[22] I. O. Oladele, A. A. Adediran, A. D. Akinwekomi, M. H. Adegun, O. O. Olumakinde, and O. O. Daramola, "Development of Ecofriendly Snail Shell Particulate-Reinforced Recycled Waste Plastic Composites for Automobile Application," *Sci. World J.*, vol. 2020, 2020, doi: 10.1155/2020/7462758.

[23] S. Nikmatin, A. Syafiuddin, A. B. Hong Kueh, and A. Maddu, "Physical, thermal, and mechanical properties of polypropylene composites filled with rattan nanoparticles," *J. Appl. Res. Technol.*, vol. 15, no. 4, pp. 386–395, 2017, doi: 10.1016/j.jart.2017.03.008.

[24] O.Y. Alothman, L.K. Kian, N. Saba, M. Jawaid, and R. Khiari, "Cellulose nanocrystal extracted from date palm fibre: Morphological, structural and thermal properties," *Ind. Crops Prod.*, vol. 159, no. June 2020, p. 113075, 2021, doi: 10.1016/j.indcrop.2020.113075.

[25] M.M.M. Alsafy, N. Al-Hinai, K.I. Alzebdeh, E.-S. I. El-Shafey, and M. M. A. Nassar, "Characterization of Extracted Bio-Nano Particles from Date Palm Agro-Residues," *J. Mater. Res. Technol.*, 2024, doi: https://doi.org/10.1016/j.jmrt.2024.04.222.

[26] E. S. Nascimento *et al.*, "All-cellulose nanocomposite films based on bacterial cellulose nanofibrils and nanocrystals," *Food Packag. Shelf Life*, vol. 29, p. 100715, 2021.

[27] S.M. Mousavi, O. Arjmand, M. R. Talaghat, M. Azizi, and H. Shooli, "Modifying the properties of polypropylene-wood composite by natural polymers and eggshell nano-particles," *Polym. from Renew. Resour.*, vol. 6, no. 4, pp. 157–174, 2015, doi: 10.1177/204124791500600403.

[28] S.A. Bello *et al.*, "Eggshell nanoparticle reinforced recycled low-density polyethylene: A new material for automobile application," *J. King Saud Univ. - Eng. Sci.*, no. xxxx, 2021, doi: 10.1016/j.jksues.2021.04.008.

[29] K. Zdiri, A. Elamri, M. Hamdaoui, O. Harzallah, N. Khenoussi, and J. Brendlé, "Elaboration and Characterization of Recycled PP/Clay Nanocomposites," vol. 2508, no. 8, pp. 2370–2378, 2018.

[30] M. Salavati and A. A. Yousefi, "Polypropylene–clay micro/nanocomposites as fused deposition modeling filament: effect of polypropylene-g-maleic anhydride and organo-nanoclay as chemical and physical compatibilizers," *Iran. Polym. J. (English Ed.*, vol. 28, no. 7, pp. 611–620, 2019, doi: 10.1007/s13726-019-00728-0.

[31] K. P. Srinivasa Perumal, R. Boopathi, P. Saravanan, and L. Selvarajan, "Effect of zircon and anatase titanium dioxide nanoparticles on glass fibre reinforced epoxy with mechanical and morphological studies," *Ceram. Int.*, vol. 49, no. 13, pp. 21667–21677, 2023, doi: 10.1016/j.ceramint.2023.03.304.

[32] M. D. Kiran, H. K. Govindaraju, and T. Jayaraju, "Evaluation of Mechanical Properties of Glass Fiber Reinforced Epoxy Polymer Composites with Alumina, Titanium dioxide and Silicon Carbide," *Mater. Today Proc.*, vol. 5, no. 10, pp. 22355–22361, 2018, doi: 10.1016/j.matpr.2018.06.602.

[33] R. K. Nayak, K. K. Mahato, and B. C. Ray, "Water absorption behavior, mechanical and thermal properties of nano TiO2 enhanced glass fiber reinforced polymer composites," *Compos. Part A Appl. Sci. Manuf.*, vol. 90, pp. 736–747, 2016, doi: 10.1016/j.compositesa. 2016.09.003.

[34] M. Alsafy, N. Al-Hinai, and K. Alzebdeh, "Production of Date Palm Nanoparticle Reinforced Composites and Characterization of Their Mechanical Properties," *ASME Int. Mech. Eng. Congr. Expo. Proc.*, vol. 3, pp. 2–9, 2022, doi: 10.1115/IMECE2022-95413.

[35] A. Hachaichi, B. Kouini, L. K. Kian, M. Asim, and M. Jawaid, "Extraction and Characterization of Microcrystalline Cellulose from Date Palm Fibers using Successive Chemical Treatments," *J. Polym. Environ.*, vol. 29, no. 6, pp. 1990–1999, 2021, doi: 10.1007/s10924-020-02012-2.

[36] M. D. Alotabi *et al.*, "Microcrystalline Cellulose from Fruit Bunch Stalk of Date Palm: Isolation and Characterization," *J. Polym. Environ.*, vol. 28, no. 6, pp. 1766–1775, 2020, doi: 10.1007/ s10924-020-01725-8.

[37] C. Shang, T. Liu, F. Zhang, and F. Chen, "Effect of network size on mechanical properties and wear resistance of titanium/nanodiamonds nanocomposites with network architecture," *Compos. Commun.*, vol. 19, no. September 2019, pp. 74–81, 2020, doi: 10.1016/j.coco.2020.03.002.

[38] V. G. Parale *et al.*, "Hydrophobic TiO2–SiO2 composite aerogels synthesized via in situ epoxy-ring opening polymerization and sol-gel process for enhanced degradation activity," *Ceram. Int.*, vol. 46, no. 4, pp. 4939–4946, 2020, doi: 10.1016/j.ceramint.2019.10.231.

[39] M. Karimi Sahnesarayi, H. Sarpoolaky, and S. Rastegari, "Effect of heat treatment temperature on the performance of nano-TiO2 coating in protecting 316L stainless steel against corrosion under UV illumination and dark conditions," *Surf. Coatings Technol.*, vol. 258, pp. 861–870, 2014, doi: 10.1016/j.surfcoat.2014.07.071.

[40] A. Zahrouni, A. Bendaoued, and R. Salhi, "Effect of sol-gel derived TiO2 nanopowders on the mechanical and structural properties of a polymer matrix nanocomposites developed by vacuum-assisted resin transfer molding (VARTM)," *Ceram. Int.*, vol. 47, no. 7, pp. 9755–9762, 2021, doi: 10.1016/j.ceramint.2020.12.115.

[41] S. Haq and R. Srivastava, "Wood Polypropylene (PP) Composites Manufactured by Mango Wood Waste with Virgin or Recycled PP: Mechanical, Morphology, Melt Flow Index and Crystalline Behaviour," *J. Polym. Environ.*, vol. 25, no. 3, pp. 640–648, 2017, doi:10.1007/ s10924-016-0845-9.

[42] V.A. Escócio, E.B.A.V. Pacheco, A.L.N. Da Silva, A.D.P. Cavalcante, and L.L.Y. Visconte, "Rheological Behavior of Renewable Polyethylene (HDPE) Composites and Sponge Gourd (Luffa cylindrica) Residue," *Int. J. Polym. Sci.*, vol. 2015, 2015, doi: 10.1155/2015/ 714352.

[43] P. Beesetty, A. kale, B. Patil, and M. Doddamani, "Mechanical behavior of additively manufactured nanoclay/HDPE nanocomposites," *Compos. Struct.*, vol. 247, no. April, p. 112442, 2020, doi: 10.1016/j.compstruct.2020.112442.

[44] B.A. Alshammari *et al.*, "Impact of Hybrid Fillers on the Properties of High Density Polyethylene Based Composites," *Polymers (Basel).*, vol. 14, no. 16, pp. 1–15, 2022, doi: 10.3390/polym14163427.

Published in: Materials Science Forum
ISSN: 1662-9752, Vol. 1126, pp 77-87
doi:10.4028/p-fb6OQW

Submitted: 2024-01-31
Revised: 2024-03-15
Accepted: 2024-03-26
Online: 2024-09-27

Evaluation of Fungal Decay and Biodegradation of Thermoplastic Composites Reinforced with Date Palm Fibres

Said Awad[1,a*], Tamer Hamouda[2,b], Ahmed Mohareb[3,c], Mohamad Midani[4,d], Menna Badawy[1,e]

[1]Valorizen Research and Innovation Center, Cairo, Egypt

[2]Textile Research Division, National Research Centre, Cairo 12622, Egypt

[3]Department of Forestry and Wood Technology, Faculty of Agriculture, 21545-El-Shatby, Alexandria University, Alexandria, Egypt

[4]Wilson College of Textiles, NC State University, Raleigh, United States

[a]said.awad@valorizen.com, [b]tehamoud@ncsu.edu, [c]ahmed_mohareb@yahoo.com, [d]msmidani@ncsu.edu, [e]menna.badawy@valorizen.com

*Corresponding author during all stages of refereeing and publication
*Post-publication corresponding author

Keywords: PLA; RPVC; Date palm fibres; Biodegradable composites; Fungal resistance; Biodegradation.

Abstract: Growing interest in utilizing and processing natural fibres (NF) to create biodegradable and sustainable composites as environmental concerns upsurge globally. Date palm trees (DPT) account for more than 4.5 million tons of waste annually worldwide, making it one of the most abundant agricultural biomass waste in the MENA region. This study evaluated the biological resistance of thermoplastic composites developed from polylactic acid (PLA) and recycled polyvinyl chloride (RPVC) reinforced with date palm fibre (DPF) at different contents (10, 20, 30, 40 wt.%) and fibre size (250 – 500 μm and ≥1,000 μm). Composites where exposed to the brown-rot fungus; Irpex lacteus, and white-rot fungus; Tyromyces palustris, to evaluate its resistance to biodegradation. Results showed that composites developed using PLA had higher weight loss (%) when compared to the same samples but reinforced with RPVC. Composites with higher DPF content showed high rates of decay when used with different polymer matrix. Also, DPF length had a significant effect on the disintegration of the composites. DPF/PLA reinforced with 40 wt.% DPF showed the highest weight loss (WL%) reaching 5.61% and 5.46% when exposed to Tyromyces palustris and Irpex lacteus respectively. On the other hand, the biodegradation had a direct impact on the disintegration of the composites developed where the WL%, of PLA composites developed with 40 wt.% DPF showed 61.40%.
Abbreviations: DPF, date palm fibre; natural fibre composite; fibre; DPT, date palm tree; DPFRC, date palm fibre reinforced composite.
Funding Sources: This research did not receive any specific grant from funding agencies in the public, commercial, or not-for-profit sectors.

1 Introduction

The increasing global environmental concerns and awareness along with the shortage of natural resources have urged the investigations on developing biodegradable composites as a substitute for non-biodegradable and petroleum based composites [1–3]. Their low cost, low density and biodegradable characteristics shed the light on natural fibre composites as a substitute to synthetic polymer composites. Due to the potential for the end products to be carbon negative and have biodegradable characteristics, composites reinforced with lignocellulosic fibre have gained high interest. The composite's durability, however, is significantly reduced by the hydrophilic nature of lignocellulosic fibres. Due to the ease of obtaining wood fibres, wood plastic composites (WPCs), which are lignocellulosic fibre composites made from a combination of wood-based materials and

polymer matrices, occupy a large portion of the lignocellulosic fibre composite market. However, due to the forestry regulations and legislations and alternative request was emerged [4–6].
Agricultural industries produce massive amounts of agro-waste each year. Lignocellulosic residues alone exceed 600 million tonnes per year globally, and they are poorly managed. Several factors, such as low cost, low density, biodegradability, availability, absence of associated health hazards, and they are relatively non-abrasive. Recycling of natural fibres (NF) by incorporating them into composites to manufacture renewable and biodegradable materials has drawn considerable attention as a biodegradable reinforcing material [6,7] and can help in waste reduction and reduce the cost of the composites developed [8]. It's possible that different types of plant fibres appeal to different regions thus numerous studies have been done on the use of various lignocellulosic materials in thermoplastic composites. In these investigations, thermoplastics were combined with a variety of materials, including wood, hemp, cotton, wheat straw, rice husk, leaf, oil palm, banana fibres, and many more. Date palm fibre (DPF) is one of the most abundant agricultural biomass waste in the MENA region, with over 2.8 million tons produced annually and 4.5 million tons produced globally. This waste is either incinerated or deposited into landfills causing serious environmental pollution as well as death of important soil microorganisms [1,9,10]. Several researchers have investigated an industrial application that can utilize this huge amount of biomass waste within the waste management scheme that are being implemented by most of the countries [5,11–17].
This study is considered as the first to be conducted on assessing the microorganism-based degradation of composites reinforced with DPF. This was achieved by utilizing two different types of fungus in this experimental work which are the brown-rot fungus, Irpex lacteus, and white-rot fungus, Tyromyces palustris. Understanding the durability of composites reinforced with DPF paves their way to its utilization in outdoor industrial applications, such as wood plastic composites (WPC) that undergoes different environmental conditions such as air, light, heat, or microorganism that affect their durability. The mechanical and physical strength of the composites evaluated in this study has been previously reported by the same research team [5,12].

2 Materials and Methods

2.1 Materials

Raw DPF surrounding the date palm stem, known as DPF sheath or mesh, were supplied by Valorizen Research and Innovation Centre, Egypt. DPF were washed with distilled water to remove dust and dirt from the fibres surface. The DPF were then dried in an oven at 60 ºC for 24 hours to ensure that the fibres have minimal moisture content. Fibres were then grinded using Retsch cutting mill (SM 100, Germany) equipped with a 2 mm sieve. The grinded DPF were sieved through several mesh sizes 1,000 µm, 500 µm, 250 µm where the fibres retained on each sieve mesh were preserved in sealed polythene bags to avoid any moisture absorption from the atmosphere. Furthermore, polymer matrices were obtained from Ecodeck Ltd, a UK leading composite manufacturing company, in pellet form. The pellets were dried in an oven at 60 ºC for 24 hours to ensure that the polymer have minimal moisture content.

2.2 Processing of DPF composite

The DPF and thermoplastic polymer matrix, PLA and RPVC, were processed in a Brabender Plastograph twin-screw mixer (with Cam blades for mixer type N50EHT) at 190 for RPVC and 170 ºC for PLA with screw speed of 50 rpm for 10 minutes for both polymer matrices. Samples with four different mass proportions (10, 20, 30, 40 Wt.%) and two different fibre diameter size (250 – 500 µm and ≥1000 µm) were produced. This was achieved by initially feeding into the mixer the required amount of polymer for each batch allowing it to completely melt for 3 minutes, and subsequently feeding in the DPF for 7 minutes to obtain a uniform mixture. Thus, the resulted mixture was grinded to pellets using Retsch cutting mill (SM 100, Germany) equipped with a 2 mm sieve. The grinded pellets were compression moulded into a 100 mm (L) x 100 mm (W) x 4 mm (T) mould using an electrically heated hydraulic press. Compression moulding procedure involved pre-heating

at 190 ºC and 170 ºC for RPVC and PLA respectively for 10 minutes without applied load followed by 5 minutes compressing at the same temperature under 10 MPa pressure, and subsequently cooling under load until the mould reached 35 ºC. The compression molded composite was cut using a band saw machine SEALEY SM1304 to achieve 20 mm (L) x 20 mm (W) x 4 mm (T) samples to be tested for biodegradation and disintegration. Tables 1 and 2 present the blend ratio, DPF diameter (µm) and code of each treatment. .

Table 1 Blend ratio, DPF diameter (µm) and sample code for DPF/PLA composites

Sample code	DPF size (µm)	Blend Ratio*	
		PLA (Wt.%)	DPF (Wt.%)
A	N/A	100	0
B	250 – 500	90	10
C	≥1000		
D	250 – 500	80	20
E	≥1000		
F	250 – 500	70	30
G	≥1000		
H	250 – 500	60	40
I	≥1000		

Table 2 Blend ratio, DPF diameter and sample code of DPF/RPVC composites

Sample code	DPF size (µm)	Blend Ratio*	
		RPVC (Wt.%)	DPF (Wt.%)
J	N/A	100	0
K	250 – 500	90	10
L	≥1000		
M	250 – 500	80	20
N	≥1000		
O	250 – 500	70	30
P	≥1000		
Q	250 – 500	60	40
R	≥1000		

2.3 Fungal biodegradation

A laboratory decay tests using mini block specimens 30 mm (L) x 10 mm (W) x 4 mm (T) were undertaken to assess biological resistance of the developed composites against *Pinus sylvestris* solid wood control samples. Sterile culture medium (20 ml), prepared from malt 40 grams and agar 20 grams in distilled water (1 L), was placed in 90 mm diameter Petri dish with a small piece of mycelium of a freshly grown culture of Tyromyces palustris (Berk. et Curt) Murr. as a brown rot fungus and Irpex lacteus HHB 7328 as a white rot fungus. The culture was incubated for 2 weeks at 27°C and 70% HR to allow full colonization of the medium by the mycelium. Samples were supported on sterile plastic mesh to prevent contact with culture medium [18]. All samples, previously oven dried at 60°C to constant weight, were sterilized with radiation and three blocks (two treated and one control) were placed in each Petri dish under sterile conditions, and all treatments were duplicated. Incubation was carried out for 8 weeks at 27°C under controlled humidity conditions of 70% RH in a climatic chamber WTB BINDER TYP KBF 240. At the end of the test period, 8 weeks, mycelia were removed, and all specimens were oven-dried to constant mass at 60°C and weighed. Weight loss (WL) was expressed as a percentage of the initial oven-dried weight of the samples according to equation 1:

$$\text{Weight loss (\%)} = \frac{M_0 - M_f}{M_0} \text{ x } 100 \quad \text{(Equation 1)}$$

Where M_0 is mass of oven-dried sample prior to the test, and M_f is mass of oven-dried sample after the test.

2.4 Disintegration analysis

The degradation test by composting was carried out according to ISO 20200 standard. The test determines the degree of disintegration of the materials when exposed to composting at laboratory conditions. For this test, previously dried and weighed 20 mm x 20 mm specimens were buried in a compost medium for 90 days. The sample weight in each reactor represents 5 % wt. of the total wet weight of compost. The compost medium consisted of 55 % wt. water and 45 % wt. of synthetic solid waste. The solid waste composition was 40 % wt. sawdust, 30 % wt. rabbit feed, 10 % wt. mature compost, 10 % corn starch, 5 % wt. saccharose, 4 % wt. cornseed oil, and 1 % wt. urea. Samples of each composition (by triplicate) were removed from reactors every 10 days, cleaned, and dried at 55 °C until constant weight. The biodegradation (degree of disintegration) was calculated with the equation 2:

$$\text{Weight loss (\%)} = \frac{W_0 - W_t}{W_0} \text{ x } 100 \quad \text{(Equation 2)}$$

Where W_t is the weight of the sample after certain time into the controlled compost soil and W_0 is the initial dry weight of the sample. All tests were triplicated to ensure reliability in results

2.5 Microstructure analysis

Scanning Electron Microscope (SEM), TESCAN-VEGA 3 (Czech Republic) field emission was used to examine the microstructure of the composites developed to ensure the homogeneous mixture between the DPFs and PLA. Also, samples were obtained by sticking the samples on a carbon adhesive tape. Afterwards, the samples were coated with a thin layer of gold film using Edwards S 150B sputter coater to provide electrical conductivity. Following coating, samples were observed and operated with 30 kV coupled with an Energy Dispersive X-rays (EDX) analyser unit.

3 Results

3.1 Fungal biodegradation

Decay resistance of mini blocks samples obtained from the modified composites panels and Pinus sylvestris wood control samples against Tyromyces palustris and Irpex lacteus is reported in Figures 1 and 2. After 8 weeks of fungal exposure, the results clearly demonstrate that the fungal activity of the test decay fungi was high enough under the test conditions, and this allowed us to compare the decay resistance (mean percent mass loss) for the composites panels. The mass losses caused by both tested fungi species were drastically decreased when compared with the control specimens. Slight mass loss of < 5 % was recorded with the modified composites against the brown rot fungus Tyromyces palustris while the percentage of mass loss in the control samples recorded approximate 30%. Meanwhile, the modified composites performed well against Irpex lacteus and sustained a mass loss of ≤ 5% while the control specimens suffered a mass loss of 28%. The present results strongly indicate that the modified composites exhibited a significant improvement in the decay-resistance when compared with the solid wood control samples. This can be attributed to the water-repellent effect of the used polymer, PLA and RPVC, which play an important role in preventing the wood based modified composites from absorbing moisture during fungal exposure leading to un-appropriate conditions for fungal decay. As expected, the pure thermoplastic specimens (PLA and RPVC) exhibited no fungal decay. Meanwhile, by adding the DPF with the rest of treatments, distinct mass losses were recorded. Most likely, small amount of DPF (probably on the surface) was biodegraded, but polymer matrix was intact.

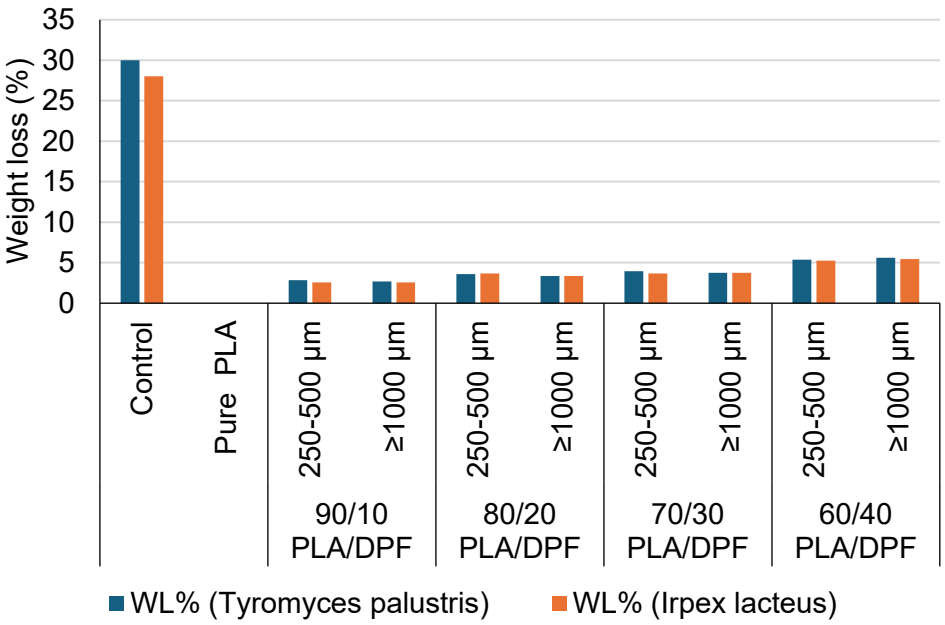

Fig. 1 Decay resistance of PLA/DPF composite and control solid wood samples (Pinus sylvestris) against Tyromyces palustris and Irpex lacteus.

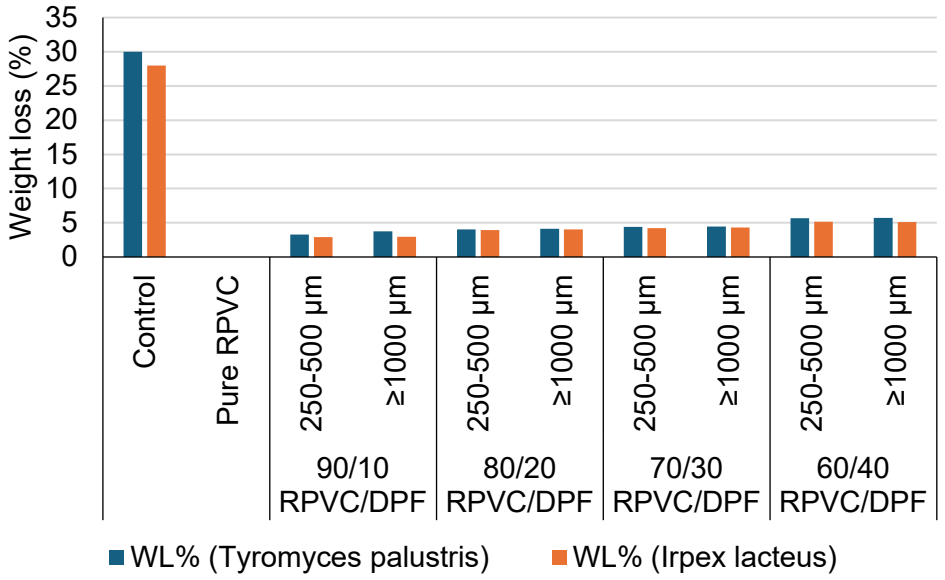

Fig. 2 Decay resistance of the RPVC/DPF composite and control solid wood samples (Pinus sylvestris) against Tyromyces palustris and Irpex lacteus.

These data indicated that all DPF modified composite samples showed significant resistance against both brown and white rot fungi used in this trial when compared to the control solid wood samples (Pinus sylvestris) Figures 3 and 4. The biodegradation rate (%) is drastically less than the control samples, although the wt.% of DPF is high (40%). Wt.% drop in control sample is 30%, while it is only 5% in sample with 40% DPF.

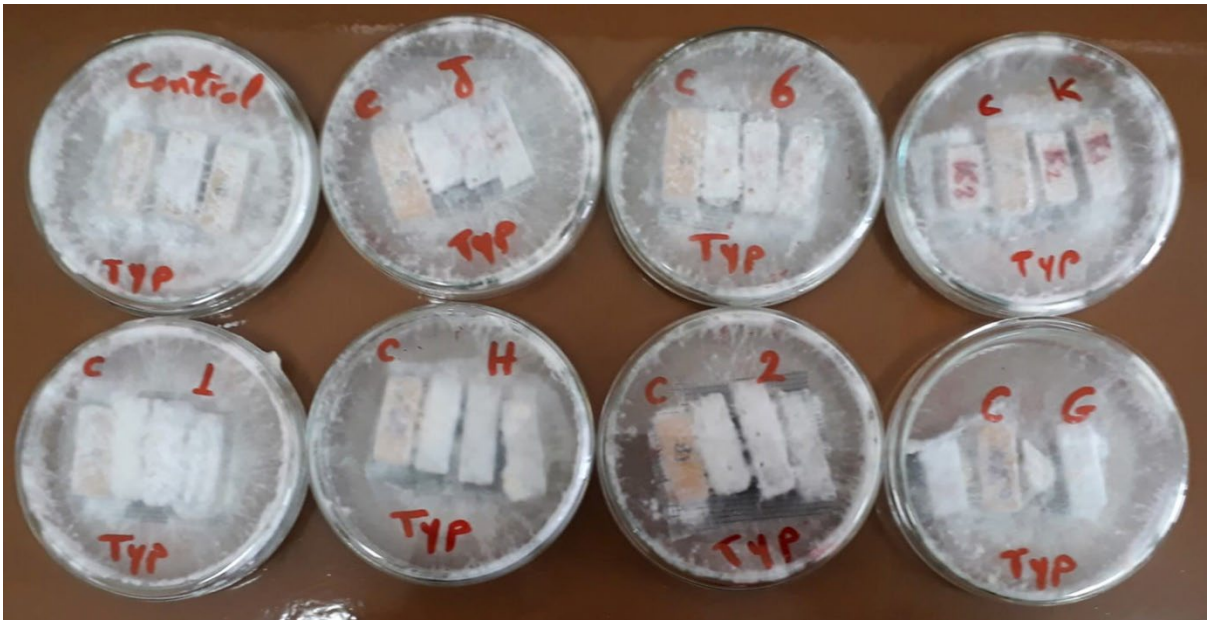

Fig. 3 Decay resistance of the modified DPF composite and control solid wood samples (Pinus sylvestris) against brown rot fungus Tyromyces palustris (TYP)

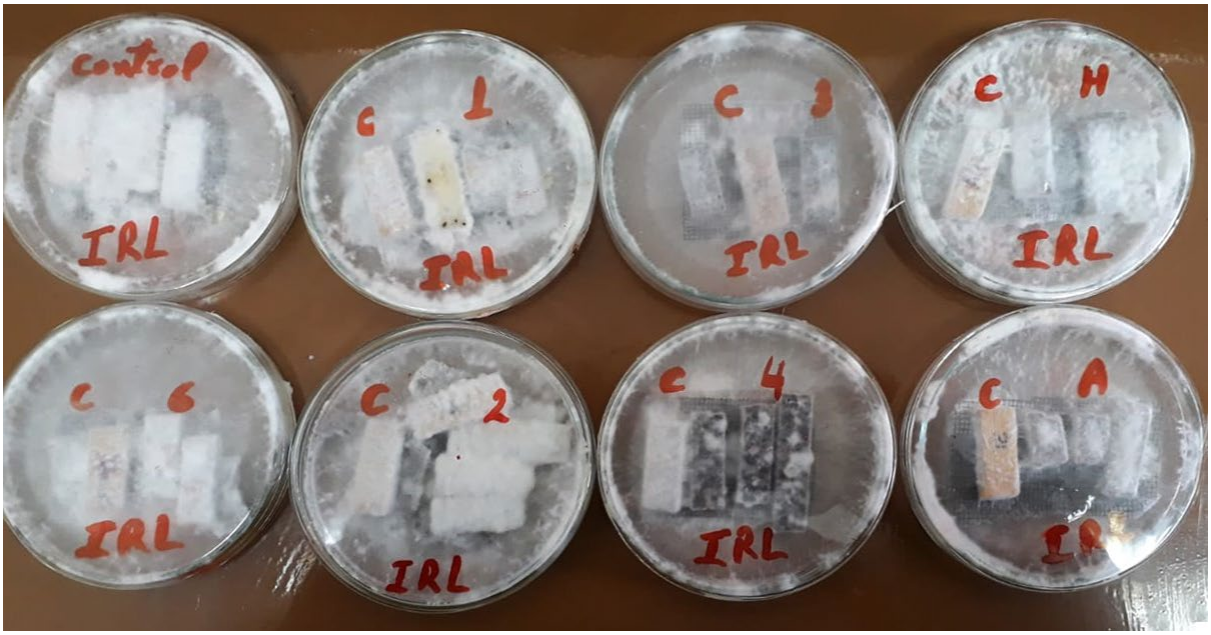

Fig. 4 Decay resistance of the modified DPF composite and control solid wood samples (Pinus sylvestris) against white rot fungus Irpex lacteus (IRL)

In this context, it seems that the DPF modified composites could be used as wood alternative in the above ground applications such as frames, outdoor decking, windows, and furniture. The obtained data revealed an increasing in the mass loss percentages by the addition of DPF. It seemed that the fungal durability of the produced biopolymer composites is governed by many factors like moisture absorption and biodegradability of natural fiber. Christian (2019) has stated that moisture absorption increases with increase in fiber volume fraction. Meanwhile, the biopolymer composites manufactured with hydrophobic biopolymers (like PLA and RPVC) show significant resistant against fungal degradation when compared to the control natural wood blocks [19]. These results were supported with those obtained by Bari et al. (2018) who stated that the natural fibers can be protected from fungal degradation by making them less hygroscopic and less susceptible to fungal enzymes. The gained fungal resistant was attributed to the surface modification of natural fibers by thermoplastic addition treatments and thereby reduces the moisture content below fungal requirement for growth [20]. The same behavior was noted by Mohareb et al. (2015) who found a considerable

fungal resistant for the reinforced biopolymer composites using thermoplastic polyester polymer with flax and jute fabrics [21]. Consequently, the noticeable fungal durability reported in this study with the produced biopolymer composites made them suitable for use in the above ground hazard 3 applications.

3.2 Disintegration

Figure 5 shows the results of the disintegration test which caried on pure PLA and PLA/DPF with different DPF content and fibre size. Results were calculated after duration of 90 days of exposing the samples to composting at laboratory conditions. Results show a significant weight loss which indicated disintegration for all samples. The amount of weight loss and disintegration are varied according to the DPF content and fiber size. In general, results indicate that as the DPF loading and size increased the disintegration of the composites material increased. Microorganisms attacked DPF which penetrated through the voids formed within the composite due to the processing technique and the weak interfacial bonding which led to void and crack formation within the samples. Which result in a disintegration to samples. This is clearly seen in the images of the samples, whereas samples turn to be very brittle and brakes easily. Therefore, the soil burial tests conducted with these produced composites showed that the microorganisms load in soil biodegrades and disintegrate the DPF and the PLA composites by creating holes, cracking over it and promote microorganisms' growth and thereby accelerated their degradation [22,23]. On the other hand, samples made of DPF/RPVC showed very low disintegration which can be considered neglected weight loss. The minimal weight loss occurring might be due to voids present by the processing technique which might have affected exposed DPF not RPVC. Figure 7 shows sample C before (to the left) and after (right) of the disintegration test. The image indicates the high disintegration of the sample by the microorganisms.

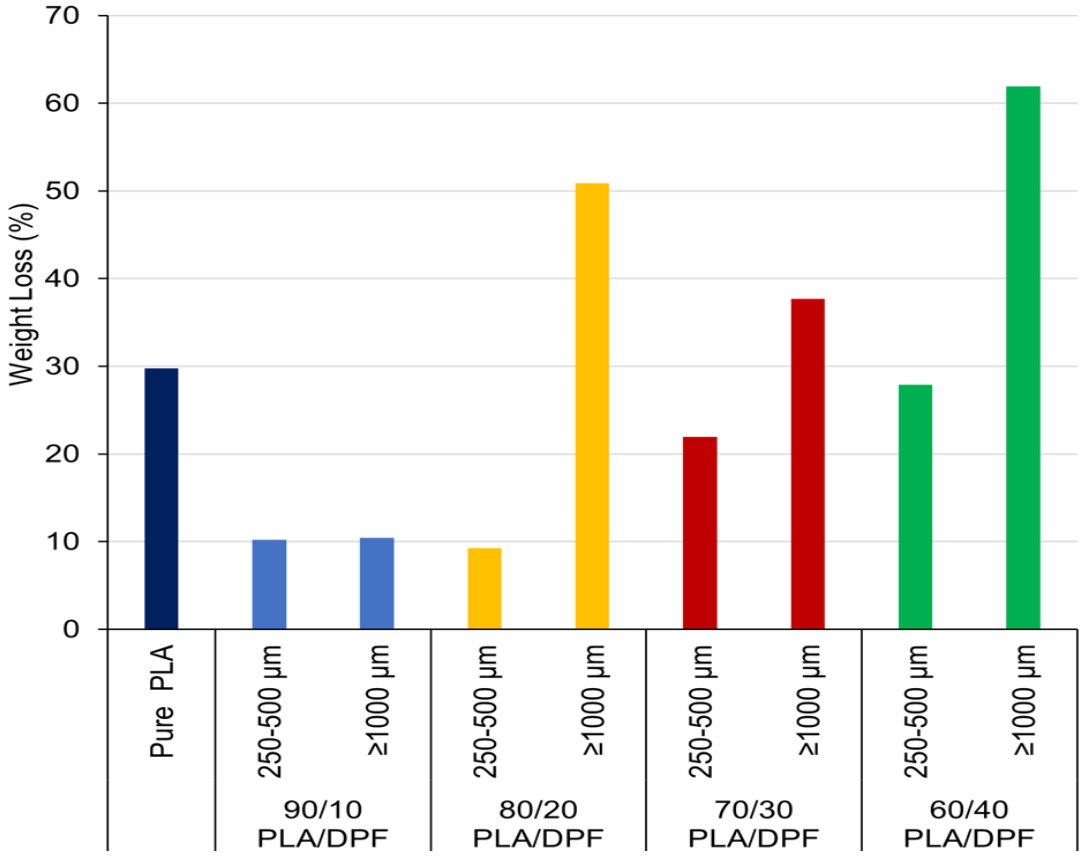

Fig. 5 Biodegradation of DPF/PLA composite with different DPF loading content and size

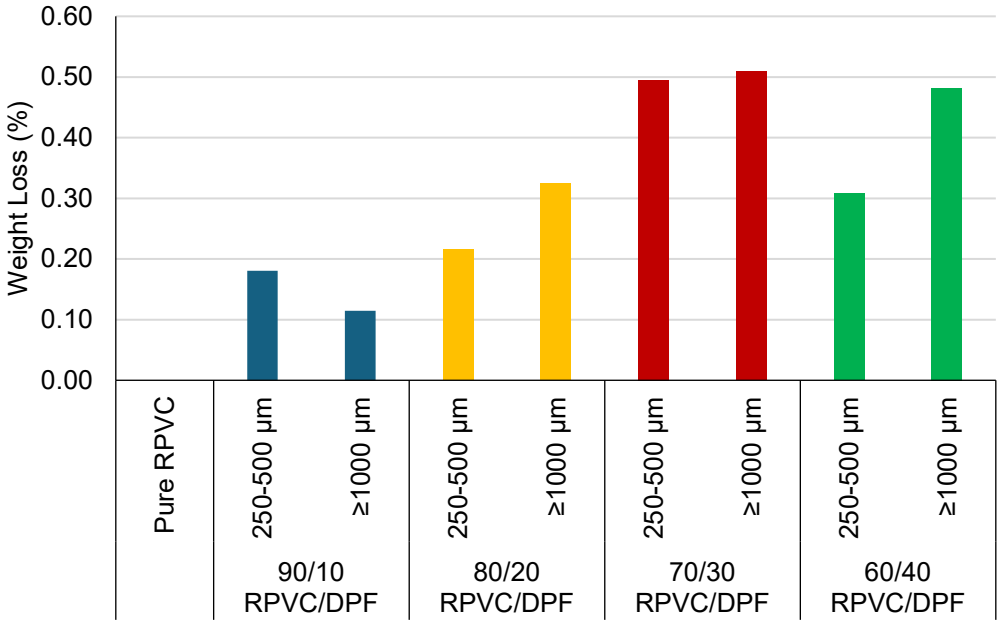

Fig. 6 Biodegradation of DPF/RPVC composite with different DPF loading content and size

Fig.7 DPF/PLA (90/10) composite with ≥ 1,000 µm before the test (top) and after the test (bottom)

3.3 Microstructural analysis

The microstructure of thermoplastic composites, DPF/PLA, developed with ≥ 1,000 µm DPF size and varying weight fractions contents (10, 20, and 30) wt.% is shown in Figure 8. It was observed that samples reinforced with 40 wt.% DPF content went under complete disintegration where it was very difficult to conduct the microstructure analysis. The presence of the voids within the microstructure of the composite was due to the weak interfacial bonding between the polymer matrix and the DPF which enhanced the biological attack leading to the degradation of DPF, thus disintegration of the matrix. As the size of the fibre increased, more voids were present which accelerated the biodegradation rate of the samples. It was noticed the fibre structure undergoes smudging. The fungal attack was randomly done where it was noticed that in Figure 8 (#C) the decay occurred longitudinally and split the DPF in the longitudinal direction, but in Figure 8 (#G) the decay occurred at the end or tip of the DPF.

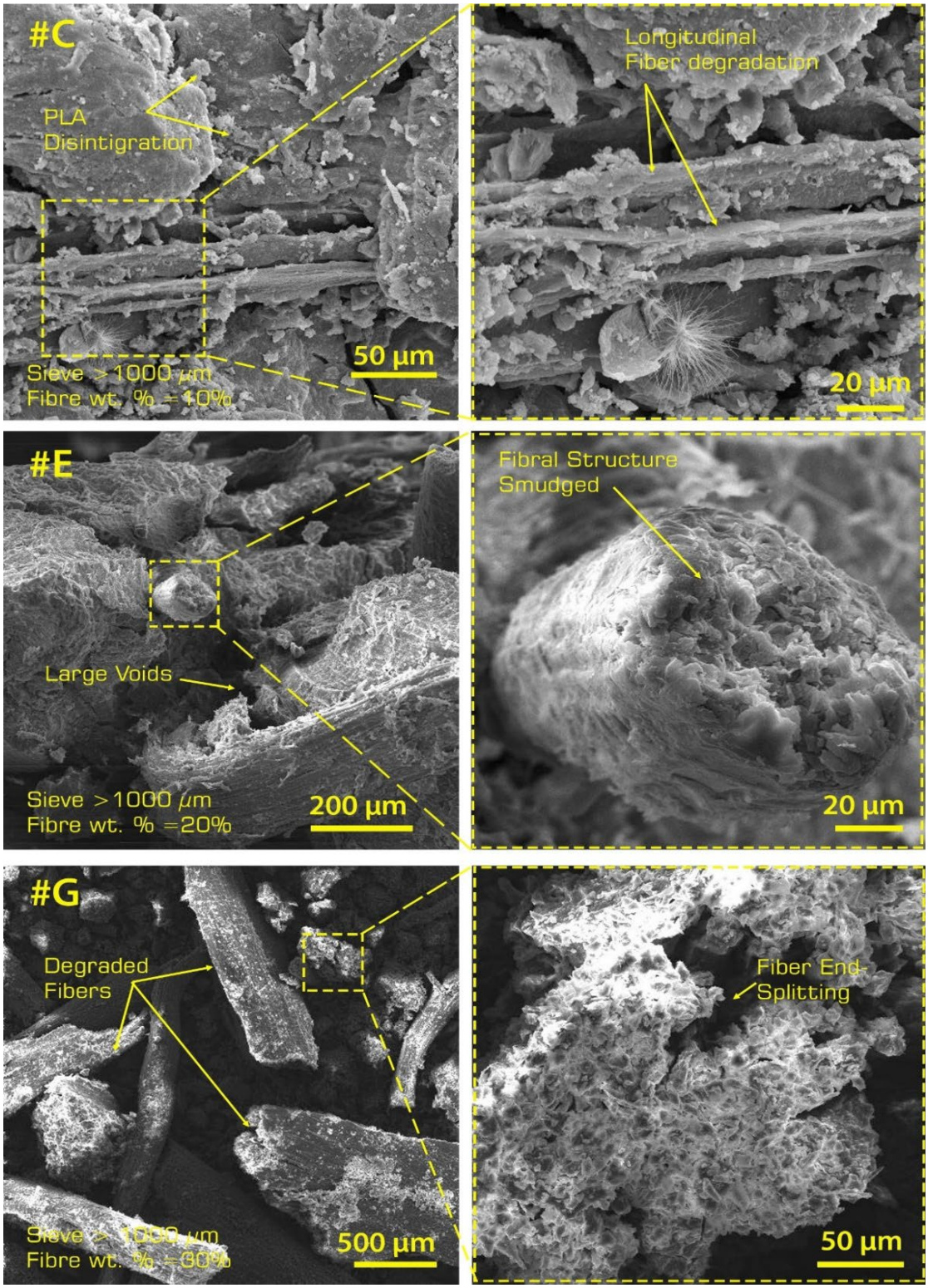

Fig. 8 SEM of DPF/PLA for sieve size ≥1,000 µm with different DPF contents

4 Conclusion

Due to its biodegradability, WPC production is continually subject to strict regulations and market restrictions, despite significant efforts to improve its mechanical and physical properties. Fungal attack and decay have an impact on the biodegradability, and texture of thermoplastic composites reinforced with DPF. Temperature, microorganisms, radiation, moisture, and other environmental factors all affect rate of disintegration and degradation. Therefore, this study paves the way for introducing 100% biodegradable WPC composite or utilizing recycled thermoplastic to produce WPC using DPF as a reinforcement. The mechanical and physical strength of the developed composites

DPF/PLA and DPF/RPVC met the requirements for production as WPC in earlier studies conducted by the same authors. Understanding the disposal and biodegradability resistance to microbial exposure is essential for WPC indoor and outdoor applications. Comparing DPF/PLA to DPF/RPVC composites, more significant disintegration results were shown. This is because RPVC does not have the same biodegradable properties as PLA. Results revealed that samples subjected to fungal decay and disintegration lost weight to a greater extent when the content of DPF was higher. When exposed to Tyromyces palustris and Irpex lacteus, respectively, the DPF/PLA composites with a 40-weight percent DPF showed the highest weight loss percentages, reaching 5.61% and 5.46%, respectively. On the other hand, the biodegradation had a greater effect on the disintegration of the composites created, with the weight loss caused by biodegradation in PLA composites made with 40 weight percent DPF showing a 61.40% rate.

References

[1] S. Awad, Y. Zhou, E. Katsou, Y. Li, M. Fan, A Critical Review on Date Palm Tree (Phoenix dactylifera L.) Fibres and Their Uses in Bio-composites, Springer Netherlands, 2020. https://doi.org/10.1007/s12649-020-01105-2.

[2] Y. Dong, A. Ghataura, H. Takagi, H.J. Haroosh, A.N. Nakagaito, K.T. Lau, Polylactic acid (PLA) biocomposites reinforced with coir fibres: Evaluation of mechanical performance and multifunctional properties, Compos Part A Appl Sci Manuf 63 (2014) 76–84. https://doi.org/10.1016/j.compositesa.2014.04.003.

[3] R. Siakeng, M. Jawaid, M. Asim, S. Siengchin, Accelerated weathering and soil burial effect on biodegradability, colour and textureof coir/pineapple leaf fibres/PLA biocomposites, Polymers (Basel) 12 (2020). https://doi.org/10.3390/polym12020458.

[4] S. Awad, Y. Zhou, E. Katsou, M. Fan, Polymer Matrix Systems Used for Date Palm Composite Reinforcement, in: M. Midani, N. Saba, O.Y. Alothman (Eds.), Date Palm Fiber Composite, Springer, Singapore, 2020: pp. 119–159. https://doi.org/https://doi.org/10.1007/978-981-15-9339-0_4.

[5] S. Awad, T. Hamouda, M. Midani, E. Katsou, M. Fan, Polylactic Acid (PLA) Reinforced with Date Palm Sheath Fiber Bio-Composites: Evaluation of Fiber Density, Geometry, and Content on the Physical and Mechanical Properties, Journal of Natural Fibers 00 (2022) 1–19. https://doi.org/10.1080/15440478.2022.2143979.

[6] T. Alsaeed, B.F. Yousif, H. Ku, The potential of using date palm fibres as reinforcement for polymeric composites, Mater Des 43 (2013) 177–184. https://doi.org/10.1016/j.matdes.2012.06.061.

[7] P.J. Herrera-Franco, A. Valadez-González, Mechanical properties of continuous natural fibre-reinforced polymer composites, Compos Part A Appl Sci Manuf 35 (2004) 339–345. https://doi.org/10.1016/j.compositesa.2003.09.012.

[8] M. V. Madurwar, R. V. Ralegaonkar, S.A. Mandavgane, Application of agro-waste for sustainable construction materials: A review, Constr Build Mater 38 (2013) 872–878. https://doi.org/10.1016/j.conbuildmat.2012.09.011.

[9] A. Alawar, A.M. Hamed, K. Al-Kaabi, Characterization of treated date palm tree fiber as composite reinforcement, Compos B Eng 40 (2009) 601–606. https://doi.org/10.1016/j.compositesb.2009.04.018.

[10] L.A. Elseify, M. Midani, L.A. Shihata, H. El-Mously, Review on cellulosic fibers extracted from date palms (Phoenix Dactylifera L.) and their applications, Cellulose 26 (2019) 2209–2232. https://doi.org/10.1007/s10570-019-02259-6.

[11] S. Abani, F. Hafsi, A. Kriker, A. Bali, Valorisation of Date Palm Fibres in Sahara Constructions, in: Energy Procedia, Elsevier Ltd, 2015: pp. 289–293. https://doi.org/10.1016/j.egypro.2015.07.608.

[12] S. Awad, T. Hamouda, M. Midani, Y. Zhou, E. Katsou, M. Fan, Date palm fibre geometry and its effect on the physical and mechanical properties of recycled polyvinyl chloride composite, Ind Crops Prod 174 (2021) 114172. https://doi.org/10.1016/j.indcrop.2021.114172.

[13] O. Benaimeche, A. Carpinteri, M. Mellas, C. Ronchei, D. Scorza, S. Vantadori, The influence of date palm mesh fibre reinforcement on flexural and fracture behaviour of a cement-based mortar, Compos B Eng 152 (2018) 292–299. https://doi.org/10.1016/j.compositesb.2018.07.017.

[14] H. Chaib, A. Kriker, A. Mekhermeche, Thermal Study of Earth Bricks Reinforced by Date palm Fibers, in: Energy Procedia, Elsevier Ltd, 2015: pp. 919–925. https://doi.org/10.1016/j.egypro.2015.07.827.

[15] T. Tioua, A. Kriker, G. Barluenga, I. Palomar, Influence of date palm fiber and shrinkage reducing admixture on self-compacting concrete performance at early age in hot-dry environment, Constr Build Mater 154 (2017) 721–733. https://doi.org/10.1016/j.conbuildmat.2017.07.229.

[16] A. Mekhermeche, A. Kriker, S. Dahmani, Contribution to the study of thermal properties of clay bricks reinforced by date palm fiber, in: AIP Conf Proc, American Institute of Physics Inc., 2016. https://doi.org/10.1063/1.4959400.

[17] K. Almi, A. Benchabane, S. Lakel, A. Kriker, Potential utilization of date palm wood as composite reinforcement, Journal of Reinforced Plastics and Composites 34 (2015) 1231–1240. https://doi.org/10.1177/0731684415588356.

[18] A. Mohareb, M.F. Thévenon, E. Wozniak, P. Gérardin, Effects of monoglycerides on leachability and efficacy of boron wood preservatives against decay and termites, Int Biodeterior Biodegradation 64 (2010) 135–138. https://doi.org/10.1016/j.ibiod.2009.12.004.

[19] S.J. Christian, Natural fibre-reinforced noncementitious composites (biocomposites), Elsevier Ltd, 2019. https://doi.org/10.1016/B978-0-08-102704-2.00008-1.

[20] E. Bari, J.J. Morrell, A. Sistani, Durability of natural/synthetic/biomass fiber-based polymeric composites: Laboratory and field tests, Durability and Life Prediction in Biocomposites, Fibre-Reinforced Composites and Hybrid Composites (2018) 15–26. https://doi.org/10.1016/B978-0-08-102290-0.00002-7.

[21] A.S.O. Mohareb, A.H. Hassanin, A.A. Badr, K.T.S. Hassan, R. Farag, Novel composite sandwich structure from green materials: Mechanical, physical, and biological evaluation, J Appl Polym Sci 132 (2015) 4–11. https://doi.org/10.1002/app.42253.

[22] V.A. Alvarez, R.A. Ruseckaite, A. Vázquez, Degradation of sisal fibre/Mater Bi-Y biocomposites buried in soil, Polym Degrad Stab 91 (2006) 3156–3162. https://doi.org/10.1016/j.polymdegradstab.2006.07.011.

[23] Z.N. Azwa, B.F. Yousif, A.C. Manalo, W. Karunasena, A review on the degradability of polymeric composites based on natural fibres, Mater Des 47 (2013) 424–442. https://doi.org/10.1016/j.matdes.2012.11.025.

Published in: Materials Science Forum
ISSN: 1662-9752, Vol. 1126, pp 89-108
doi:10.4028/p-ydFwb7

Submitted: 2024-02-05
Revised: 2024-03-04
Accepted: 2024-03-26
Online: 2024-09-27

Surface Modification Rout for Date Palm Fibers-Polymer Bio-Composites Towards Improved Interfacial Crosslinking

Khalid I. Alzebdeh[1,a,*] and Mahmoud M.A. Nassar[2,b]

[1]Department of Mechanical and Industrial Engineering, Sultan Qaboos University, P.O. Box 33, AlKhod 123, Sultanate of Oman. [*]E-mail: alzebdeh@squ.edu.om

[2]College of Applied Professions, Palestine Polytechnic University, Wadi Alhareya, Hebron P.O. Box 198, State of Palestine

[a]alzebdeh@squ.edu.om, [b]mnassar@ppu.edu

Keywords: Bio-composites; Chemical Treatment; Filler/Polymer Compatibility; Functionalization; Interfacial Crosslinking.

Abstract: Surface modifications of bio-filler and polymer matrix is critical in natural fiber reinforced composites to improve compatibility with the hosting polymer. The literature contains only a few studies on grafting bio-fillers to improve their reactivity with polymer matrix. This study focuses on introducing crosslinking between Date Palm Particles (DPP) and Polypropylene (PP) using new methods. The experimental setup starts with chemical modifications of PP that result in the formation of PP-g-mTMI. Following that, the two components are blended together, forming a urethane link between the filler and the polymer. Following the fabrication of bio-composite sheets based on the Taguchi design, various specimens were prepared and tested thoroughly to assess their chemical properties, thermal stability, and mechanical properties. The results of the experiments revealed an improvement in the interfacial adhesion of the filler/polymer, which was confirmed by experimental mechanical characterization and Scanning Electron Microscope (SEM) analysis. The new composite demonstrated improved strength, ductility, and overall durability, demonstrating its potential as a bio-based polymeric material.

1 Introduction

Modern bio-composites are comprised of plastic polymer matrix and agricultural waste serving as natural fillers. These materials remain a subject of significant research and development endeavors, as indicated by recent investigations [1, 2]. Recently, there has been an increasing interest in utilizing natural fillers to make bio-composites due to attractive attributes, such as cost-effectiveness and environmentally friendly nature [3]. The primary benefit of these composites is their capacity to enhance environmental sustainability through the utilization of biodegradable waste materials [4]. Nevertheless, the viability of incorporating natural fillers into composites is affected by multiple aspects, which impose constraints on their appropriateness for load-bearing purposes, hence impeding widespread commercial implementation [5, 6]. Among those, the uniform dispersion and orientation of fillers within the hosting polymer matrix, which have a substantial influence on the overall performance and crucial determinants of the quality of bio-composites [7, 8]. Natural fillers are commonly classified according to their botanical sources [9]. Perhaps, flax, hemp, palm, and jute are considered particularly the most significant ones due to their distinct strength, elasticity, and extensive availability. Additional fibers include kenaf bast, sisal leaf, henequen, pineapple leaves, cotton seeds, and coconut fruit [10, 11]. The utilization of bio-composites that integrate natural fillers has shown comparable performance to conventional composites made from glass or carbon fibers, indicating a significant advancement in the field of bio-composites [12, 13]. Consequently, a significant portion of bio-composites has been successfully commercialized across various industries. However, several issues related to sustainability and performance are still in the phase of research and development. These concerns encompass aspects such as fiber architecture, geometry, orientation, volume fraction, impregnation, matrix compatibility, and the necessary quantity of fibers to attain the desired mechanical properties [14, 15].

The interfacial bonding between the natural filler and surrounding matrix is primarily driven by chemical interaction, and mechanical interlocking. The inherent incongruity between hydrophilic plant fibers and hydrophobic polymers is essentially due to their distinct nature [16, 17]. Additionally, the existence of pectin and wax components, which form a defensive coating around the fiber, may impede the mechanical interlocking process with nonpolar polymer matrices. The presence of a large number of hydroxyl groups (OH) significantly increases their contact with the matrix [18, 19]. Hence, in order to attain maximum mechanical interlocking and bonding, it is imperative to chemically change both the natural filler and polymer matrix. This alteration boosts the capability of the reinforcing fillers to function as load-bearing components, so bestowing strength and stiffness upon the resultant bio-composites [20, 21]. Numerous studies in the field of chemistry and physics have been conducted with the aim of enhancing the adhesion between fillers and polymers [22, 23]. Bio-composites with enhanced compatibility, mechanical properties, water absorption, and thermal stability can be achieved through the chemical alteration of fibers and the irradiation of polymers [24–26].

This study presents a new route to functionalize PP to enhance the crosslinking in bio-composite by introducing a chemical linkage between filler and polymer. The process was analyzed utilizing the Taguchi statistical model to assess the impact of several parameters on its mechanical and physical characteristics. Following that, the efficacy of the developed bio-composite was evaluated using a series of physical and topographical investigations.

2 Materials and Methods

2.1 Chemicals and Modifiers

The current study utilizes various chemicals, including acetone as a solvent (99%, Sigma-Aldrich, USA), dicumyl peroxide (DCP, 98%, Fisher, USA) as an initiator, 3 Isopropenyl α, α Dimethylbenzyl Isocyanate (mTMI, 95%, Sigma-Aldrich) as a functional group, and styrene (St, 99%, Sigma Aldrich) as a copolymer. Scheme 1 illustrates the chemical configuration of the mTMI modifier used in this study. All chemicals were used in their original form, and the synthesis procedures involved a mixture of PP and solvent in a solid-state phase placed in a round bottom flask connected to a magnetic stirrer. Achieving a well-dispersed functional group distribution at the filler-polymer interface is crucial for an effective synthesis process.

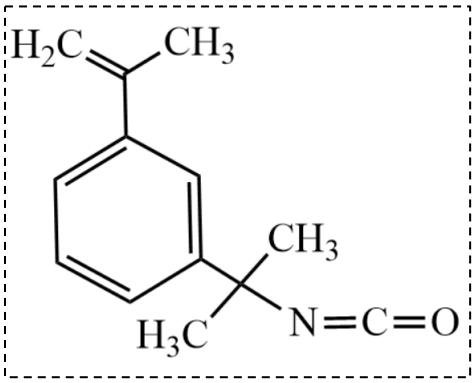

Scheme 1. Chemical structure and properties of mTMI.

The PP homopolymer powder, which was donated by INEOS, a company based in the United Kingdom, possesses a density of 0.905 g/cm^3 and a melt flow rate of 2.15 g/10 min under the conditions of 230 °C and 2.16 kg. In order to obtain natural fibers from date palm pedicles, a two-step process was employed. Initially, the pedicles were subjected to physical separation, resulting in the formation of small pieces. Subsequently, these pieces were ground using a cryogenic ball milling machine, followed by sieving through a 100-mesh sieve. In the instance of an additional collection of samples, the date palm powder denoted as DPP, underwent a new chemical processing procedure, as outlined in reference [27]. Figure 1 shows both untreated and treated DPP. The average density of the DPP was experimentally measured and determined to be 0.79 g/cm^3. F

(a) (b)

Fig. 1. Images of DPP (a) untreated, (b) treated.

2.2 Chemical Functionalization

PP is dipped in acetone to make a mixture, DCP as an initiator and mTMI as a functional group were blended to the mixture and then stirred at 60 °C for 15 min. In some cases, St was also added to the mixture before the addition of mTMI. The product was then cleansed with distilled water to remove unreacted chemicals. The functionalization conditions and used amounts of PP, DCP, St and mTMI are used as input parameters for statistical parametric analysis which will be discussed in Section 2.1. The reaction procedures for the coupling of polymer and filler are presented in Scheme 2 (a).

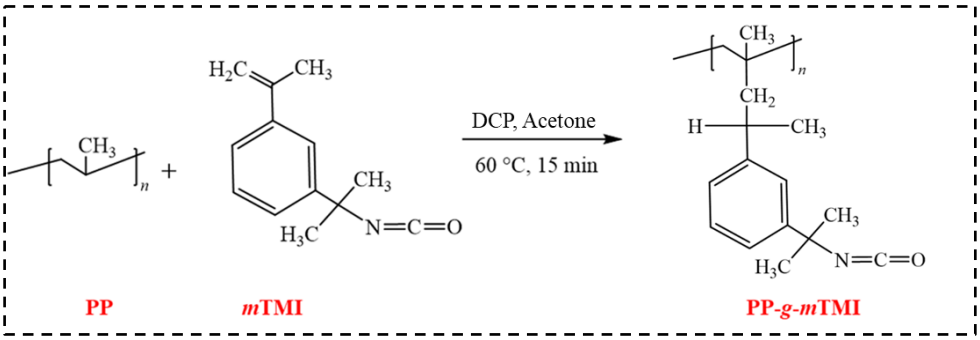

Scheme 2. Schematic representation for PP-g-mTMI formation.

2.3 Bio-Composite Fabrication

The initial phase of the production process encompasses a hot melt mixing procedure, in which dried filler and polymer materials are blended. The procedure commences by precisely measuring and amalgamating the constituents in predetermined ratios to generate a sheet using a mold with dimensions 270 mm × 270 mm × 3 mm. The blending procedure is conducted utilizing a laboratory-scale single screw extruder that is outfitted with two heating zones operating at temperatures of 175 °C and 185 °C, respectively. Furthermore, the screw of the extruder revolves at a velocity of 500 revolutions per minute. Following the extrusion process, the material undergoes a cooling phase until it reaches ambient temperature. Subsequently, it is manually divided into diminutive grains before the compression stage. In a second stage, the blend is subjected to compression molding in order to produce bio-composite sheets, which are utilized to fabricate test specimens. In order to effectively eliminate any moisture that has been adsorbed, the mixture is subjected to a drying process for a duration of 15 minutes within an electric oven set at a temperature of 105 °C. Afterwards, the mold is filled with the molten mixture, and compression is applied utilizing a molding machine operating at a temperature of 180 °C and a pressure of 40 MPa [28, 29]. The compression is sustained for a duration of 15 minutes prior to the cessation of the heating source, thereby facilitating the cooling process of the sheet. In order to finalize the procedure, the molded components undergo a curing process whereby tap water is applied to the outer surface of the heating plates within the compression

molding machine for a duration of 2 minutes. Scheme 3 depicts the coupling reactions of DPP/PP-g-mTMI, showcasing the incorporation of urethane groups.

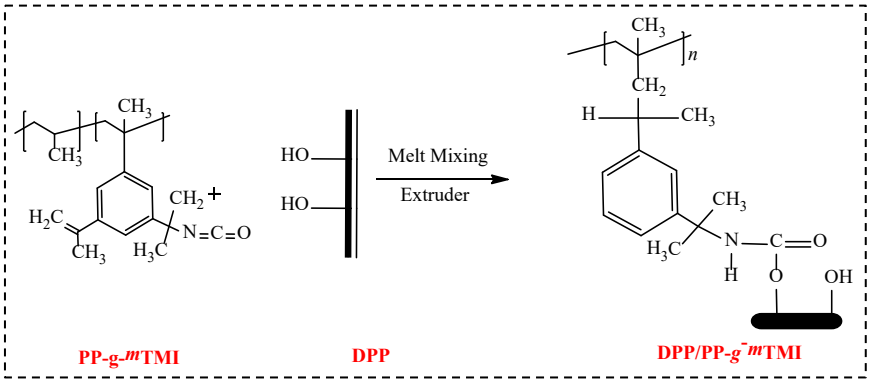

Scheme 3. The chemical reaction of DPP/PP-g-mTMI.

2.4 Bio-Composite Characterization

Fourier Transform Infrared Spectroscopy (FTIR) was employed to examine the chemical functional groups that are connected to the surface of the manufactured bio-composites. The examination was conducted utilizing a Cary 630 Fourier Transform Infrared (FTIR) spectrophotometer, which efficiently acquires comprehensive spectral data with high resolution throughout the whole spectrum. The device functions within a spectral range spanning from 650 to 4000 cm^{-1}, with a resolution of 16 cm^{-1} and performing 64 scans.

In order to examine the crosslinking between the filler and matrix at the interface of cracked specimens that have undergone tensile testing, a scanning electron microscope (SEM) of the JSM-7800F model manufactured by JEOL in Japan was utilized. In order to mitigate the interference caused by electrostatic charge during the inspection process, a procedure was employed wherein the broken sample's end is strategically laid on an aluminum stub and afterwards coated with a thin layer of gold.

The mechanical characteristics were evaluated using experimental setup as detailed in the ASTM D638 and ASTM D790 standards [30]. Five replicates of each test of the produced bio-composite have been evaluated to obtain the average values for statistical data including tensile and flexural strengths, tensile and flexural moduli and strain at break. These average values were then recorded.

In assessing the physical attributes, we measured two key characteristics: density, and water absorption. To determine the density of the tested specimens, a densitometer was employed. Each sample, weighing 2 grams, was submerged in distilled water at room temperature, and the change in water volume was measured. The average density, calculated from five replicates, was subsequently reported. Furthermore, we assessed water absorption following the ASTM D570 standard [31]. Five dried specimens were immersed in distilled water at room temperature for 24 hours. The proportion of water adsorbed by the bio-composite specimens was determined by evaluating the change in sample weight before and after placing in water.

In order to examine the thermal degradation of the bio-composites, Thermogravimetric Analysis (TGA) was accomplished and related Derivative Thermogravimetric (DTG) graphs were developed. The samples were enclosed in an aluminum container and exposed to a heating process, reaching a temperature of 600 °C. The heating rate was set at 10 °C per minute, and the entire process was conducted in an environment filled with nitrogen gas to prevent any reactions. Following that, the samples were further cooled to the ambient temperature.

3 Design of Experiment for Polymer Functionalization Parameters

In order to evaluate the performance of bio-composites using a functionalized polymer, we established four control factors (filler content, mTMI as grafted modifiers, DCP, and St) with three levels each. These levels were determined based on preliminary tests and existing literature sources

[32–35], as presented in Table 1. Optimization can be a time-consuming and costly process when employing a full factorial design involving four parameters, each with three levels, as it necessitates conducting a total of 81 experiments. Hence, Taguchi L_9 Orthogonal Array (OA) consisting of nine experimental runs was employed, as depicted in Table 2.

The aim of this analysis was to optimize the mechanical properties, specifically tensile and flexural properties, using a "larger is better" approach, while simultaneously minimizing water absorption using a "lower is better" approach. The Signal-to-Noise (S/N) ratio and Grey Relational Analysis (GRA) were utilized to evaluate the impact of process parameters on mechanical properties.

Table 1 Composite manufacturing parameters and their levels.

Factors	Levels		
	Lower	Center	Higher
Filler Content (v.%)	10	20	30
Grafted Modifiers (mTMI) (v.%)	1	5	10
DCP (v.%)	0.5	2	3
St (v.%)	0	1	2

Table 2 List of experimental runs based on Taguchi algorithm.

Identification	Experimental setup			
	Filler Content (v.%)	mTMI (v.%)	DCP (v.%)	St (v.%)
10 (a)	10	1	0.5	0
10 (b)	10	5	2	1
10 (c)	10	10	3	2
20 (a)	20	1	2	2
20 (b)	20	5	3	0
20 (c)	20	10	0.5	1
30 (a)	30	1	3	1
30 (b)	30	5	0.5	2
30 (c)	30	10	2	0

3.1 Taguchi Method

In the present study, Grey Relational Analysis (GRA) was employed to optimize various process parameters pertaining to distinct response variables. The General Rating Assessment (GRA) consolidates multiple variables into a single grey hierarchical grade. The feasibility of assigning equal weight to all GRA response variables may be called into question, as different applications may prioritize these variables in varying ways. Therefore, the utilization of the Analytic Hierarchy Process (AHP) and Taguchi-Grey approach was employed to determine the optimal process parameters to make composites with desired properties.

The AHP commences by establishing a hierarchical structure for the problem at hand and subsequently defining the criteria for evaluating the goals. The AHP method comprises the following steps:

Pairwise comparison

Within this context, the term "criteria" refers to the distinct set of outcomes that require optimization. After identification of these outcomes and structuring the problem, an assessment is conducted to determine their relative significance in attaining the overarching objective. In order to assess the significance of a particular matter, professionals are consulted in order to obtain their expert opinions and insights. The assessment provided by the experts is represented as a square matrix denoted as (V_l), where 'l' denotes each individual expert (l = 1, 2, ..., L). The dimensions of the matrix are n × n, where 'n' represents the number of responses being considered. Every element (a_{ijl}) in matrix V_l represents a numerical value that is assigned by the lth expert to compare the responses of i and j, according to the Saaty scale [36]. The scale is illustrated in Table 3. If the condition i equals j is satisfied, then the variable a_{ijl} is assigned a value of 1 in Eq. 1.

$$V_l = \begin{pmatrix} a_{11l} & a_{12l} & .. & a_{1nl} \\ a_{21l} & a_{22l} & .. & a_{2nl} \\ : & : & .. & : \\ a_{n1l} & a_{n2l} & .. & a_{nnl} \end{pmatrix} \quad (1)$$

where,

$a_{ijl} = 1/ a_{jil}$ and i = 1, . . ., n, j = 1, . . ., n, l = 1, . . ., L.

Table 3 Rank rules for pairwise comparison.

Value	Definition
1	'i' and 'j' are equally important
3	'i' is slightly more important than 'j'
5	'i' is important than 'j'
7	'i' is much important than 'j'
9	'i' is absolutely important than 'j'
2, 4, 6, 8	Intermediate values

Calculate the geometric mean of experts' opinion

In order to mitigate the potential influence of bias resulting from the excessive dominance of a singular expert perspective, it is common to request experts to deliver their viewpoints individually. In the subsequent stage, the experts' total rating is computed. The prevailing and extensively utilized approach for this computation is the utilization of the geometric mean, as demonstrated in Eq. 2. Equation 3 represents the collective scoring matrix.

$$b_{ij} = \sqrt[L]{\prod_{i=1}^{n} a_{ajl}} \qquad \forall i, j \text{ and } i, j \quad (2)$$

$$V = \begin{pmatrix} b_{11} & b_{12} & .. & b_{1n} \\ b_{21} & b_{22} & .. & b_{2n} \\ : & : & .. & : \\ b_{n1} & b_{n2} & .. & b_{nn} \end{pmatrix} \quad (3)$$

Normalize the aggregate score matrix

Using the geometric mean, the individual scores obtained are then normalized based on Eq. 4. Equation 5 illustrates a depiction of the standardized matrix.

$$p_{ij} = \frac{b_{ij}}{\sqrt{\sum_{i=1}^{n} b_{ij}^2}} \quad \forall i, j \quad (4)$$

$$W = \begin{pmatrix} p_{11} & p_{12} & .. & p_{1n} \\ p_{21} & p_{22} & .. & p_{2n} \\ : & : & .. & : \\ p_{n1} & p_{n2} & .. & p_{nn} \end{pmatrix} \quad (5)$$

Calculate the weight of response variables

Finally, Eq. 6 is utilized to establish the weights allocated to the response variables. These weights convey the relative significance of one response compared to others, such as the importance of factors like tensile strength, flexural strength, and water absorption in enhancing the material performance.

$$w_i = \frac{\sum_{i=1}^{n} p_{ij}}{\sum_{i=1}^{n}\sum_{i=1}^{n} p_{ij}} \quad \forall i \in j \qquad i= 1, 2\ldots, n \quad (6)$$

Consistency Check

A matrix that possesses a Consistency Ratio (CR) value below 0.1 is designated as a consistency matrix. A CR score exceeding 0.1 indicates the presence of a discrepancy in the pairwise

comparison. The inconsistency matrix is in violation of the concept of transitivity. Hence, it is imperative to amend the pairwise comparison matrix in the event of an inconsistency.

$$CR = \frac{CI}{RI} \tag{7}$$

where,

$$CI = \frac{\lambda_{max} - n}{n-1} \tag{8}$$

The Random Inconsistency Index (RI) in Eq. 7 denotes the average Consistency Index (CI) for a specific criterion, n. This CI is calculated by considering different entries inside the reciprocal matrix of the same order. The major eigenvalue of the pairwise comparison matrix, V, of order n, is denoted as λ_{max} in Eq. 8. Equation 9 can be utilized to calculate λ_{max}.

$$\lambda_{max} = \frac{\sum_{i=1}^{n} b_{ij}}{w_i} \tag{9}$$

Taguchi-Grey Relational Analysis (Taguchi-GRA)

In order to calculate the Global Relative Gain (GRG) using the Taguchi-Graphical Representation of Analysis (Taguchi-GRA) technique, the following steps are implemented:

Calculate S/N ratio for response variables

Taguchi categorizes the response characteristic into three types based on the Signal-to-Noise (S/N) ratio: "bigger-the-better", "smaller-the-better", and "nominal-the-better". Each of these types employs a distinct equation to transform the response function into the S/N ratio. In this research, since both maximizing and minimizing responses are under consideration, Eq. 10 and Eq. 11 will be employed to calculate the S/N ratio for the respective objectives.

$$x_k^0(i) = -10log_{10}\left(\frac{1}{n}\sum_{k=1}^{n}\frac{1}{y_k^2(i)}\right) \tag{10}$$

$$\mathrm{x_k^0(i)} = -10\log_{10}\left(\frac{1}{n}\sum_{k=1}^{n}\mathrm{y_k^2(i)}\right) \tag{11}$$

Where, 'n' denotes the overall count of experimental runs, 'y_k (i)' signifies the observed value for response variable 'i' (where 'i' ranges from 1 to 'h') derived from experiment 'k' (where 'k' ranges from 1 to 'h').

Normalize the value

To integrate these units into a unified value, the normalized Signal-to-Noise (S/N) ratio offers a dimensionless measure for response variables. The calculation of the normalized value depends on whether the objective is maximization or minimization, and this is accomplished through Eq. 12 and Eq. 13, respectively.

$$\mathrm{x_k^*(i)} = \frac{\mathrm{x_k^0(i) - \min x_k^0(i)}}{\mathrm{\max x_k^0(i) - \min x_k^0(i)}} \tag{12}$$

$$\mathrm{x_k^*(i)} = \frac{\mathrm{\max x_k^0(i) - x_k^0(i)}}{\mathrm{\max x_k^0(i) - \min x_k^0(i)}} \tag{13}$$

Calculate the grey relational coefficient (GRC)

The Grey Relational Grade (GRC) is employed to elucidate the connection among normalized data when the optimal result is achieved. This relationship is expressed using Eq. 14.

$$\gamma_k(i) = \frac{\Delta_{min} + \zeta\Delta_{max}}{\Delta_k(i) + \zeta\Delta_{max}} \tag{14}$$

Where, ζ is a coefficient with a distinct value that ranges from 0 to 1. A value of $\zeta = 0.5$ is chosen in situations where there is a requirement to decrease certain parameters while simultaneously optimizing others. This decision prioritizes the equitable consideration of both maximizing and decreasing absolute deviations. The symbol $\Delta_k(i)$ in Eq. 15 represents the discrepancy between the normalized value and the reference sequence for the i^{th} answer. The symbols Δ_{max} and Δ_{min} are used to denote the highest and lowest values of $\Delta_k(i)$, correspondingly.

$$\Delta_k(i) = |x_0^*(i) - x_k^*(i)| \quad (15)$$

Where, x_0^* is the maximum value of $x_0^*(i)$ and it represents the reference sequence.
Calculate grey relational grade (GRG)

The GRG for all response variables is determined by computing a weighted average GRC value, as described in Eq. 16.

$$\delta_k = \sum_{i=1}^{h} w_i y_k(i) \quad (16)$$

In Eq. 16, w_i is the weight of the response vector derived from the AHP.
The predicted GRG is eventually determined using Eq. 17 as follows:

$$\delta_{pre} = \delta_{tot} + \sum_{i=1}^{n} (\delta_{opt} - \delta_{tot}) \quad (17)$$

Where,

δ_{tot}: the total mean of GRG;
δ_{opt}: the average of GRG at the optimal level of each process factor;
n: the total number of parameters.

4 Results and Discussion

4.1 Chemical Attributes

PP-g-mTMI and PP-g-(St-mTMI) FTIR display absorption at 2253 cm^{-1} due to N=C=O stretching, absorption at 1755 cm^{-1} due to the C=O group. While the band at 1602 cm^{-1} is tracked to the stretching frequency of C=C aromatic from the mTMI group as shown in Fig. 2. This indicates that the functionalization is accomplished, and that the NCO group is grafted onto the PP surface using peroxide or peroxide with styrene. After mixing, the NCO absorption band disappears and a new absorption band appears at 1739 cm^{-1} which confirms the reaction between the NCO and OH groups on the polymer and filler surfaces, respectively. In comparison, the FTIR spectra of DPP/PP-g-mTMI shows absorption at 1657 cm^{-1}, which is related to the stretching frequency of the C=O group and the C=C aromatic stretching at 1576 cm^{-1}.

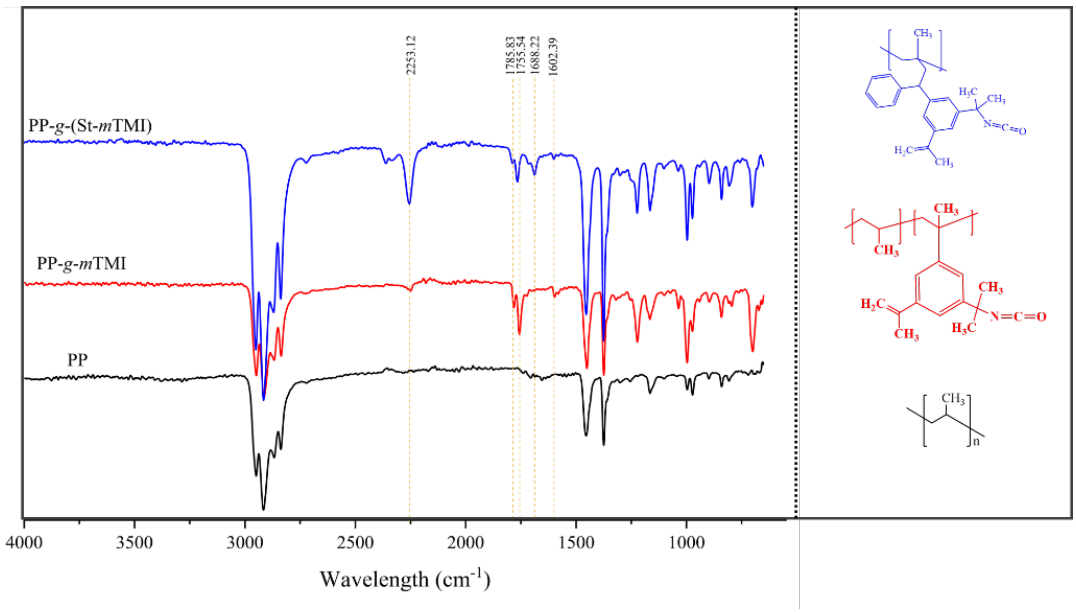

Fig. 2. FTIR spectra of PP, PP-g-mTMI, and PP-g-(St-mTMI).

A noticeable change in the infrared spectrum was observed during the melt mixing procedure of DPP and PP-g-mTMI. The distinctive peak observed at a wavenumber of 2255 cm^{-1}, which is associated with the N=C=O functional group, was no longer present in the subsequent product. A visible enhancement in the strength of the C=O signal at 1736 cm^{-1} was found, suggesting the occurrence of urethane (–NH-C(O)=O) bond formation [37, 38]. Moreover, upon the polymer's

mixing with the filler, a prominent broad peak emerges at 3350 cm^{-1}, signifying the presence of OH groups associated with the filler biomass. The aforementioned conversion presents irrefutable proof of a chemical reaction occurring between the functionalized polymer and the filler, as illustrated in Fig. 3. Figure 3 presents the FTIR spectrum of the developed coupled bio-composite, together with the unfunctionalized form, for the purpose of comparison.

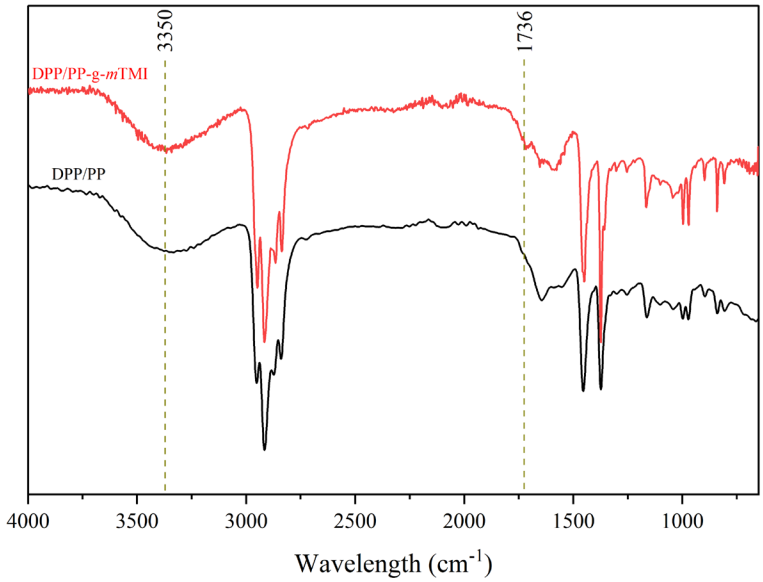

Fig. 3. FTIR spectra of the base and crosslinked bio-composites.

4.2 Mechanical Properties

4.2.1 Tensile Properties

The mechanical performance of bio-composite materials is influenced by various attributes, such as the bond at interfacial zone between the polymer matrix and the filler, as well as the mechanical properties exhibited by both the resin and fiber. The efficacy of stress transmission between the matrix and fillers in bio-composites composed of pure polymer is contingent upon several factors, including particle shape and size, dispersion condition, surface area, and particle content. In order to enhance the load transfer occurring at the interface between fibers and polymers, coupling agents are utilized to treat fillers and modify the surfaces of both fibers and polymers.

Enhanced interfacial adhesion between the polymer matrix and fillers is realized through the application of chemical treatment and modification, which contributes to the superior surface features of the fillers. This, in turn, contributes to an expansion in tensile strength. It is important to acknowledge that the tensile strength is subject to variation based on factors such as filler loading, treatment process, and coupling agent. Fig. 4 (a-c) displays the experimental outcomes pertaining to the tensile strength of bio-composites, taking into account the treated filler and functionalized polymer employed in the study.

The enhanced performance of functionalized polymer-based bio-composites in terms of tensile characteristics is illustrated in Fig. 4 (a), when compared to DPP/PP bio-composite. The improvement is especially notable in samples containing 10% and 20% filler content, particularly when incorporating functionalized PP with the isocyanate functional group. This observation implies that the presence of the isocyanate group facilitates profound connection between the filler and the PP matrix, hence enhancing their compatibility.

The inclusion of stiff particulate fillers into a polymer matrix can boost Young's modulus by virtue of the amplified surface area of these particles engaging with the polymer matrix. The Young's modulus of the developed bio-composites has a comparable pattern to the tensile strength, as depicted in Fig. 4 (b). Nevertheless, it is worth noting that the Young's modulus has exhibited considerable enhancements in each of the three-fiber loading (10%, 20%, 30%). The most substantial increase has been recorded in the case of DPP/PP-g-mTMI when contrasted to the pure polymer. The observed increase in Young's modulus in treated filler bio-composites can be attributed to the elimination of

non-cellulosic constituents that are originally present on the surface of individual fibers. In addition, it is worth noting that coupling agents have a crucial role in improving the ability to transfer loads and boost stiffness, as can be observed from the Young's modulus values.

The experimental findings demonstrate that the incorporation of 10% DPP into the coupling agents develops a substantial enhancement in the tensile properties of PP. Furthermore, the tensile strength of the bio-composites undergoes significant improvement as a result of the suggested chemical crosslinking process. In general, the incorporation of chemical crosslinking serves to enhance the tensile properties of bio-composites, with the exception of bio-composites formed from PP-g-mTMI. The increase in filler content is associated with a deterioration in mechanical performance, which can be attributed to the heightened micro-agglomeration of particle fillers at higher loading rates.

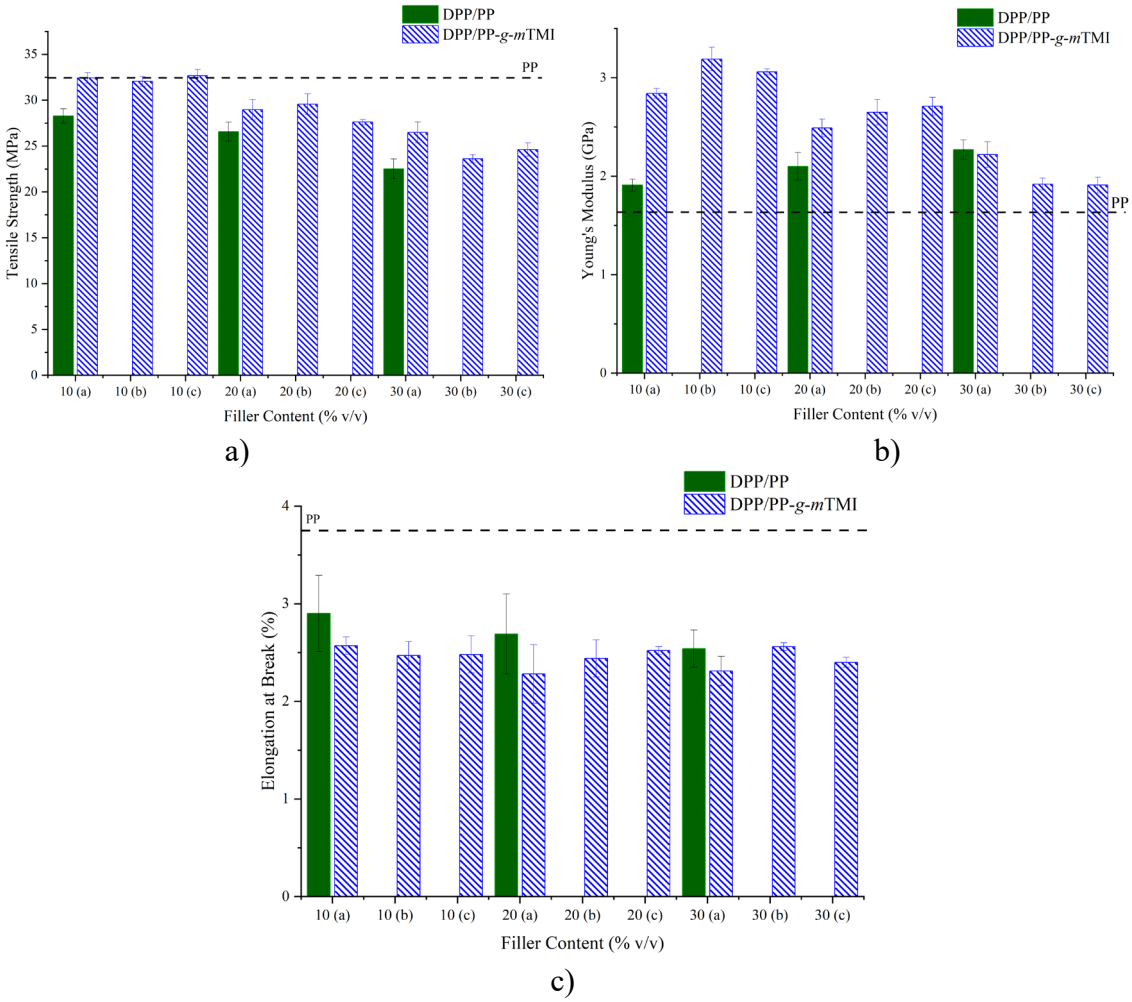

Fig. 4. Tensile characteristics of the produced bio-composites; a) Tensile strength, b), Young's modulus, and c) Elongation at break (The dashed line represents the neat polymer value).

4.2.2 Flexural Properties

The visual representation of the experimental results pertaining to the flexural strength and modulus of bio-composites is depicted in Fig. 5 (a) and (b), respectively. These findings are based on the application of a treated filler and a functionalized polymer. Significantly, when a filler loading of 10% was employed, the flexural characteristics demonstrated their peak values, and discernible enhancements were observed in the majority of instances with the utilization of functionalized polymer. This implies that the filler efficiently redistributes the load as a result of its heightened contact with the functionalized polymer.

The flexural strength values, which are influenced by the functionalization process, exhibit similar tendencies to those reported in the tensile strength. The flexural strength of a material generally exhibits a decline as the loading of fillers increases. However, it constantly remains higher

than the highest strength of the polymer without fillers in the majority of instances. The efficacy of the suggested techniques for compatibilization has been demonstrated by the enhancement of the bonding between the filler and polymer. This is supported by the observed increase in the levels of flexural stress that the bio-composites can withstand.

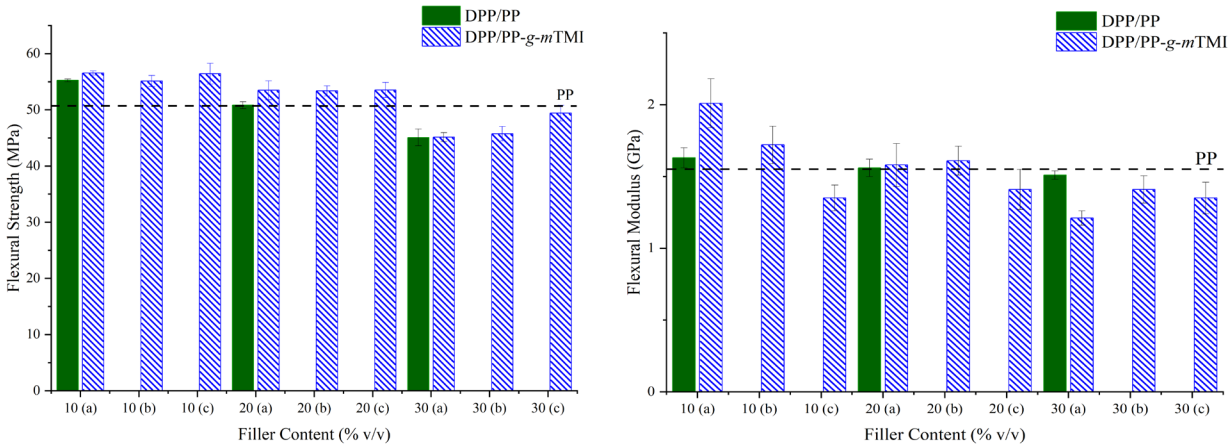

a) b)

Fig. 5. Flexural characteristics of the produced bio-composites; a) Flexural strength and b) Flexural modulus.

4.3 Morphological Analysis

Figure 6 depicts the morphology of shattered surfaces of functionalized polymer-based bio-composites in comparison to DPP/PP bio-composites. The compatibility between the surface of the polymer and the filler surface is clearly demonstrated, as it is influenced by both chemical bonding and mechanical interlocking mechanisms. The filler's rough texture is of significant importance in permitting enhanced polymer penetration onto the filler surface during the mixing procedure, thereby establishing a robust mechanical interlock between the filler and the polymer. Additionally, the process of functionalization serves to improve the interfacial adhesion between the filler material and the polymer. This is demonstrated by the strong adhesion seen between the two components, as well as the lack of fiber pull-out from the polypropylene matrix. It is worth noting that chemical bonding plays a critical role in facilitating the penetration of the polymer into the interfacial regions. This is attributed to the beneficial interaction that occurs between the surfaces of the filler and the polymer. As a result, the efficient transfer of load takes place in both the filler and the polymer matrix, leading to anticipated enhancements in the physical and mechanical characteristics of the bio-composites.

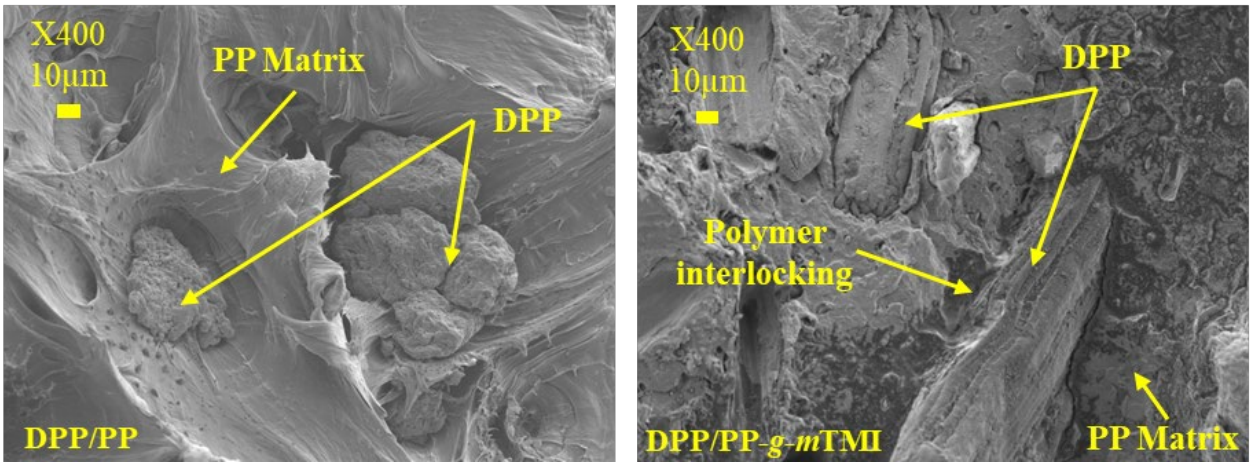

Fig. 6. SEM micrographs at fractured regions of tensile specimens of the developed bio-composites.

4.4 Physical Properties

4.4.1 Density

The density of bio-composites is a vital characteristic that significantly influences their appropriateness for various industrial applications. It frequently serves as a viable substitute for pure polymers or synthetic filler-reinforced polymers. In general, a rise in filler content is associated with a decrease in density. The observed result can be ascribed to the decreased density of the fibers in comparison to the pure PP, as depicted in Fig. 7. In the context of DPP/PP, it can be observed that the composite material demonstrates the lowest density. Subsequently, the bio-composites that include functionalized polymers have a somewhat higher density. Notably, the incorporation of isocyanate groups is emphasized in these bio-composites. The growth in density seen in the bio-composites based on functionalized polymers can be ascribed to the combined impacts of chemical treatment, functionalization, and bonding mechanisms.

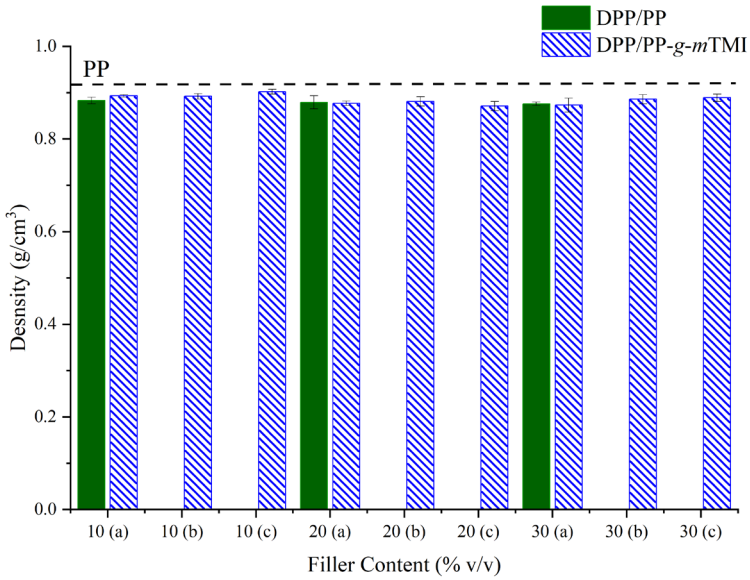

Fig. 7. Experimental densities of the developed bio-composites.

4.4.2 Water Absorption

Comparison of water absorption values of the developed functionalized polymer-based bio-composites at different volume fractions of fillers are presented in Fig. 8. Generally, it is found that the water absorption increases with the increase in filler content. Generally, it is shown that the DPP-g-mTMI based bio-composites exhibit the minimum water absorption capacity when compared with DPP/PP bio-composite. This might be an attribute of the higher hydrophobicity of the filler/polymer bonding in case of DPP-g-mTMI. In addition, results indicate that water intake of DPP/PP bio-composites are higher than other types of developed bio-composites due to the absence of chemical bonding. It can be stated with confidence that the bio-composites incorporating polymer functionalization are better in terms of water absorption reduction compared to DPP/PP, and hence increase the durability/stability of the date palm plastic bio-composites.

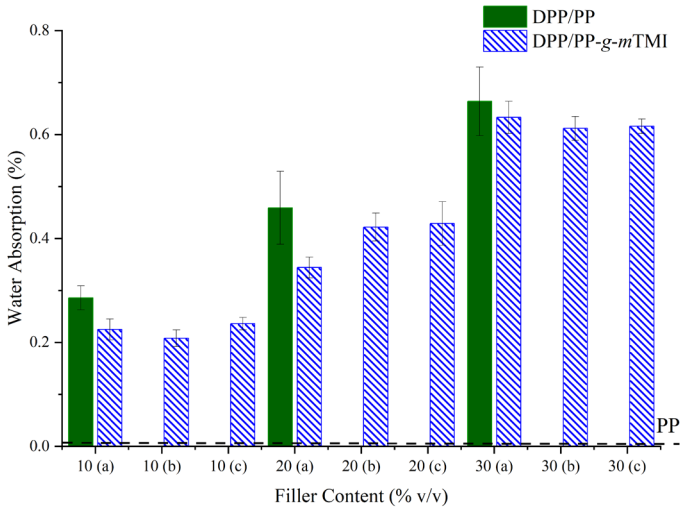

Fig. 8. Water absorption of the developed bio-composites

4.5 Thermal Degradation

The thermal behavior of functionalized polymer-based bio-composites compared to neat polymers, and the DPP with unfunctionalized polymer is analyzed using DTG tests as shown in Fig. 9 (a and b). An insignificant weight loss between 100 and 170 °C relative to the filler content is noticed. This is probably corresponding to water disappearance which is present in the form of inner moisture in the filler. After that, the degradation occurred in two phases. The first phase, between 225 and 340 °C, is related to thermal ruin of hemicellulose and lignin in the filler. The second phase suggests that the decomposition temperature of polymer matrix with the filler residue start at 350 °C. Above 490 °C, the filler and polymer were entirely decomposed with only residues of the bio-composite because of the filler ash. However, it is perceived that the temperature at largest rate of decomposition accelerates with the rise in the filler content except for the case of unfunctionalized polymer-based bio-composite. On the other hand, it is found that chemical crosslinking effectively facilitated the thermal stability of the developed materials. Overall, DTG characteristics showed good thermal stability after the filler addition, and it is improved potentially in case of using coupling agents.

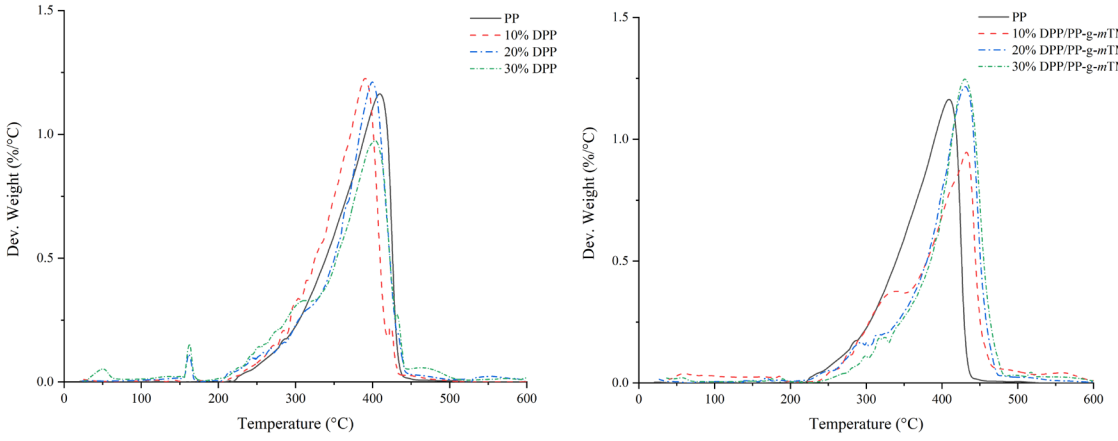

a) b)

Fig. 9. DTG curves of the developed bio-composites, a) DPP/PP, and b) DPP/PP-g-mTMI.

4.6 Statistical Analysis and Optimization

Experts' opinion

In addition to the selection and determination of variables (input and response), the expert opinion was evaluated to rate the response in terms of their value with the weight of each response. The key goal is to improve the performance of bio-composites on the basis of coupling agents and

their amounts in high-performance applications. A total of five experts in the field of composites were asked to compare the value of one parameter to the others on a basis of scale of importance as described in Table 3. The weighted matrices established by the experts were then combined using the geometric mean method. The unified mass matrix is shown in Table 4. It is then normalized, and the response variables were ranked based on the weights they achieved. The ranking and weight of the variables are shown in Table 5. The accuracy of the pairwise comparison received from the experts in Table 4 is also evaluated. It has been observed that λ_{max} is 6.5 and CI is 0.1. IR for n = 6 is 1.28. Accordingly, from Eq. 7, CR is equal to 0.079, which is smaller than the threshold value of 0.1. The pairwise comparison among response variables collected from experts is therefore authentic. As a consequence, it is obvious from Table 5 that the most critical material properties of the bio-composites is water absorption, followed by flexural strength, tensile strength, flexural modulus, and Young's modulus and elongation at break.

Table 4 Experts' unified pairwise comparison matrix.

Dimension	1	2	3	4	5	6
Tensile Strength (MPA)	-	6.30	5.69	0.44	4.74	0.54
Young's Modulus (GPa)	0.16	-	1.57	0.18	1.24	0.13
Elongation at Break (%)	0.18	0.64	-	0.22	1.03	0.19
Flexural Strength (MPa)	2.28	1.93	4.58	-	7.64	0.56
Flexural Modulus (GPa)	0.37	0.80	0.97	0.30	-	0.24
Water Absorption (%)	1.86	7.54	6.59	1.78	5.14	-

Table 5 Weight of response variables and their ranking.

Dimension	Weight	Rank
Tensile Strength (MPa)	0.22	3
Young's Modulus (GPa)	0.05	5
Elongation at Break (%)	0.05	6
Flexural Strength (MPa)	0.26	2
Flexural Modulus (GPa)	0.06	4
Water Absorption (%)	0.35	1

Taguchi analysis based on AHP and GRA

The obtained response variables are shown in Table 6. Also, Table 7 shows the S/N ratio and the normalized values of all response variables. The grey shaded cells denote the best and worst experimental runs based on S/N ratio and normalization.

Table 6 Taguchi experimental setup and obtained response variables of the developed Bio-composite.

Identification	Factors				Responses					
	Filler Content (v.%)	mTMI (v.%)	DCP (v.%)	St (v.%)	TS	YM	EB	FS	FM	WA
10 (a)	10	1	0.5	0	32.44	2.84	2.57	56.56	2.01	0.225
10 (b)	10	5	2	1	32.07	3.19	2.47	55.12	1.72	0.208
10 (c)	10	10	3	2	32.67	3.06	2.48	56.43	1.35	0.236
20 (a)	20	1	2	2	28.96	2.49	2.28	53.47	1.58	0.344
20 (b)	20	5	3	0	29.56	2.65	2.44	53.37	1.61	0.422
20 (c)	20	10	0.5	1	27.61	2.71	2.52	53.53	1.41	0.429
30 (a)	30	1	3	1	26.48	2.22	2.31	45.15	1.21	0.633
30 (b)	30	5	0.5	2	23.61	1.92	2.56	45.74	1.41	0.612
30 (c)	30	10	2	0	24.62	1.91	2.4	49.41	1.35	0.616

Table 7 S/N ratio and the normalized value of the response variable of the developed Bio-composite

Identification	S/N						Normalized value					
	TS	YM	EB	FS	FM	WA	TS	YM	EB	FS	FM	WA
10 (a)	30.22	9.07	8.2	35.05	6.06	12.96	0.979	0.774	1	1	1	0.93
10 (b)	30.12	10.08	7.85	34.83	4.71	13.64	0.943	1	0.663	0.888	0.693	1
10 (c)	30.28	9.71	7.89	35.03	2.61	12.54	1	0.917	0.702	0.99	0.216	0.886
20 (a)	29.24	7.92	7.16	34.56	3.97	9.27	0.631	0.516	0	0.75	0.525	0.548
20 (b)	29.41	8.46	7.75	34.55	4.14	7.49	0.691	0.637	0.567	0.745	0.564	0.364
20 (c)	28.82	8.66	8.03	34.57	2.98	7.35	0.482	0.682	0.837	0.755	0.3	0.35
30 (a)	28.46	6.93	7.27	33.09	1.66	3.97	0.355	0.294	0.106	0	0	0
30 (b)	27.46	5.67	8.16	33.21	2.98	4.26	0	0.011	0.962	0.061	0.3	0.03
30 (c)	27.83	5.62	7.6	33.88	2.61	4.21	0.131	0	0.423	0.403	0.216	0.025

Table 8 shows the rank of all nine experiments based on obtained GRG and GRC calculations. The findings reveal that experiment number 10 (a) reflects the best optimized mixture (10 v.% Filler content, 1 v.% mTMI, 0.5 v.% DCP without St) as the GRG value is closer to 1.0. While the lowest GRG value is obtained for the experimental run 30 (a) (30 v.% Filler content, 1 v.% mTMI, 3 v.% DCP, and 1 v.% St).

Table 8 Ranking of experiments of the developed bio-composite.

Identification	Grey Relational Coefficient (GRC)						GRG	Rank
	TS	YM	EB	FS	FM	WA		
10 (a)	0.96	0.689	1	1	1	0.877	0.933	1
10 (b)	0.898	1	0.597	0.817	0.62	1	0.886	2
10 (c)	1	0.858	0.627	0.98	0.389	0.814	0.865	3
20 (a)	0.575	0.508	0.333	0.667	0.513	0.525	0.562	4
20 (b)	0.618	0.579	0.536	0.662	0.534	0.44	0.556	5
20 (c)	0.491	0.611	0.754	0.671	0.417	0.435	0.534	6
30 (a)	0.437	0.415	0.359	0.333	0.333	0.333	0.362	9
30 (b)	0.333	0.336	0.929	0.347	0.417	0.34	0.376	8
30 (c)	0.365	0.333	0.464	0.456	0.389	0.339	0.385	7

Significant Process Parameter of the developed Bio-composite

The mean response value at different levels of input parameters is shown in the interaction plot (Fig. 10). From the interaction plot, it can be found that the optimal value of the process parameters is reached when the process parameters are at 10 v.% filler content, 10 v.% mTMI, 1 v.% DCP without St. Based on the average response GRG in Table 9, the parameters significance is ranked as follow: filler content, St, mTMI and DCP.

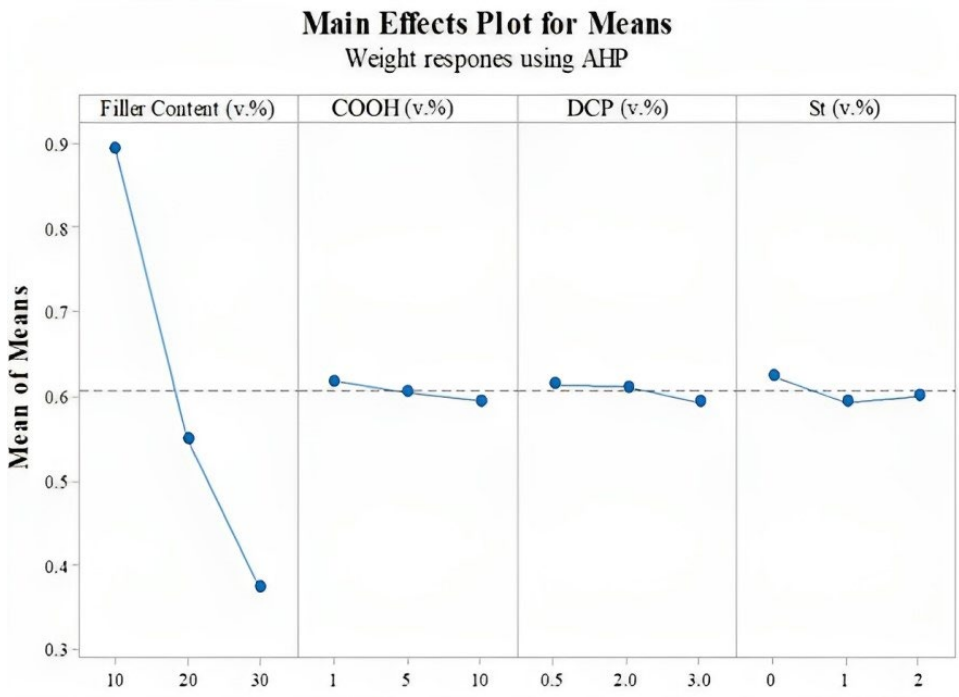

Fig. 10. Optimal parameters using GRG for DPP/PP-g-mTMI based composite.

Table 9 Response significance of the developed bio-composite.

	Level 1	Level 2	Level 3	Optimal Condition	Max-Min	Significance
Filler Content (v.%)	**0.895**	0.550	0.374	Level 1	0.520	1
mTMI (v.%)	**0.619**	0.606	0.595	Level 1	0.024	3
Peroxide (v.%)	**0.614**	0.611	0.594	Level 1	0.020	4
Styrene (v.%)	**0.625**	0.594	0.601	Level 1	0.031	2

Confirmation Experiment

The output of the validation test using the optimal process parameters is calculated by the AHP-GRA tool as reported in Table 10. The GRG for the validation test is found to be 0.94, which indicates an increase of about 0.74% over the original optimal setting.

Table 10 Confirmation Experiment.

	Initial setting (Best Run)	Prediction (Optimal Conditions)	Experimental (Confirmation)
Tensile Strength	32.44	-	33.1
Young's Modulus	2.84	-	2.44
Elongation at Break	2.57	-	2.72
Flexural Strength	56.56	-	56.73
Flexural Modulus	2.01	-	1.97
Water Absorption	0.225	-	0.231
Grey Relational Grade	0.933	0.9	0.94
Percentage Improvement in GRG			0.74%

5 Conclusion

This article presents a novel surface modification approach utilizing mTMI compatibilizer to boost the reactivity of polypropylene (PP) with natural date palm fillers, thereby making functional bio-composites. Through Taguchi design methodology, nine distinct specimens were fabricated from bio-composite sheets and subjected to comprehensive mechanical, chemical, and physical property testing, alongside thermal stability assessments. Key input parameters, including filler, mTMI, peroxide, and styrene contents, were systematically varied to optimize the urethane reaction, predominantly influencing mechanical properties and water absorption. Design of Experiment techniques enabled the determination of optimized parameter values leading to optimal responses. FTIR spectra analysis confirmed the presence of grafted functional groups and chemical crosslinking between filler and matrix. Enhanced mechanical performance of the bio-composites, compared to base counterpart composites and neat PP in some instances, was observed due to the introduced urethane reaction between functionalized PP and treated date palm fibers. The drop in strain at failure indicated a decrease in ductility of the bio-composites. SEM images supported visual confirmation of achieved filler/polymer compatibility, attributing rough surfaces of treated date palm fibers to mechanical linking crucial for enhanced bio-composite performance. DTG analysis revealed a slight improvement in thermal stability attributed to chemical crosslinking, where compatibilizers facilitated enhanced mixing efficiency during manufacturing, irrespective of surface compatibility between filler and matrix.

Additional research may be performed to explore the application of such grafting routes to other types of natural fillers and polymers to make a better breed of bio-composites. Optimum compatibilizers should be targeted, assessed, and properly incorporated into hybrid bio- and nanocomposites.

Acknowledgment

The authors would like to extend their sincere appreciation to INEOS, UK for their gracious contribution of virgin polypropylene. Furthermore, we would like to express our gratitude to the Nano-Technology Research Center and Surface Science Lab at Sultan Qaboos University for their significant support in obtaining Scanning Electron Microscopy (SEM) images.

Funding

The authors declare that no funds, grants, or other support were received during the preparation of this manuscript.

Declaration

Competing Interests

The authors have no relevant financial or non-financial interests to disclose.

Author Contributions

Both authors contributed to the study's conception and design. Material preparation, data collection and analysis were performed by Mahmoud Nassar and Khalid Alzebdeh. The first draft of the manuscript was written by Mahmoud Nassar and both authors commented on previous versions of the manuscript. All authors read and approved the final manuscript.

Data Availability

Data sharing is not applicable to this article as no datasets were generated or analyzed during the current study.

References

[1] Abdur Rahman, M., Haque, S., Athikesavan, M.M., Kamaludeen, M.B.: A Review of Environmental Friendly Green Composites: Production Methods, Current Progresses, and Challenges. Environ. Sci. Pollut. Res. 30, 16905–16929 (2023). https://doi.org/10.1007/s11356-022-24879-5

[2] Alzebdeh, K., Hinai, N. Al, Safy, M. Al, Nassar, M.: Recycled Polymer Bio-based : A Review of Compatibility and Performance Issues. (2023)

[3] Kumar, V., Chakraborty, P., Janghu, P., Umesh, M., Sarojini, S., Nandhagopal, M., Madhavan, A.: Potential of Banana Based Cellulose Materials for Advanced Applications: A Review on Properties and Technical Challenges. Carbohydr. Polym. Technol. Appl. 6, 100366 (2023). https://doi.org/10.1016/j.carpta.2023.100366

[4] Balart, R., Montanes, N., Dominici, F., Boronat, T., Torres-Giner, S.: Environmentally Friendly Polymers and Polymer Composites. Materials (Basel). 13, 1–6 (2020). https://doi.org/10.3390/ma13214892

[5] Jawaid, M., Mohd Sapuan Salit, Othman Y. Alothman: Green Energy and Technology. (2017)

[6] Phiri, R., Mavinkere Rangappa, S., Siengchin, S., Oladijo, O.P., Dhakal, H.N.: Development of Sustainable Biopolymer-Based Composites for Lightweight Applications from Agricultural Waste Biomass: A Review. Adv. Ind. Eng. Polym. Res. 6, 436–450 (2023). https://doi.org/10.1016/j.aiepr.2023.04.004

[7] Valente, M., Rossitti, I., Sambucci, M.: Different Production Processes for Thermoplastic Composite Materials: Sustainability versus Mechanical Properties and Processes Parameter. Polymers (Basel). 15, (2023). https://doi.org/10.3390/polym15010242

[8] Nagabushanam, M., Devade, K., Aravind Reddy, G., Nagaraj Goud, B., Sayed, R.M., Sood, S., Sonia, P.: Advance Biomedical Engineering – A Fundamental Review of Composite Materials and Its Applications. Mater. Today Proc. (2023). https://doi.org/10.1016/j.matpr.2023.08.216

[9] Müller, K., Bugnicourt, E., Latorre, M., Jorda, M., Sanz, Y.E., Lagaron, J.M., Miesbauer, O., Bianchin, A., Hankin, S., Bölz, U., Pérez, G., Jesdinszki, M., Lindner, M., Scheuerer, Z., Castelló, S., Schmid, M.: Review on the Processing and Properties of Polymer Nanocomposites and Nanocoatings and their Applications in the Packaging, Automotive and Solar Energy Fields. Nanomaterials. 7, (2017). https://doi.org/10.3390/nano7040074

[10] Asyraf, M.R.M., Syamsir, A., Ishak, M.R., Sapuan, S.M., Nurazzi, N.M., Norrrahim, M.N.F., Ilyas, R.A., Khan, T., Rashid, M.Z.A.: Mechanical Properties of Hybrid Lignocellulosic Fiber-Reinforced Biopolymer Green Composites: A Review. Fibers Polym. 24, 337–353 (2023). https://doi.org/10.1007/s12221-023-00034-w

[11] Elfaleh, I., Abbassi, F., Habibi, M., Ahmad, F., Guedri, M., Nasri, M., Garnier, C.: A Comprehensive Review of Natural Fibers and their Composites: An Eco-Friendly Alternative to Conventional Materials. Results Eng. 19, 101271 (2023). https://doi.org/10.1016/j.rineng.2023.101271

[12] Girijappa, Y.G.T., Mavinkere Rangappa, S., Parameswaranpillai, J., Siengchin, S.: Natural Fibers as Sustainable and Renewable Resource for Development of Eco-Friendly Composites: A Comprehensive Review. Front. Mater. 6, (2019). https://doi.org/10.3389/fmats.2019.00226

[13] Chandgude, S., Salunkhe, S.: In State of Art: Mechanical Behavior of Natural Fiber-Based Hybrid Polymeric Composites for Application of Automobile Components. Polym. Compos. 42, 2678–2703 (2021). https://doi.org/10.1002/pc.26045

[14] Rajak, D.K., Pagar, D.D., Menezes, P.L., Linul, E.: Fiber-Reinforced Polymer Composites: Manufacturing, Properties, and Applications. Polymers (Basel). 11, (2019). https://doi.org/10.3390/polym11101667

[15] Nassar, M.M.A., Alzebdeh, K.I., Pervez, T., Al-Hinai, N., Munam, A.: Progress and Challenges in Sustainability, Compatibility, and Production of Eco-Composites: A State-of-Art Review. J. Appl. Polym. Sci. 138, (2021). https://doi.org/10.1002/app.51284

[16] Maurya, A.K., Manik, G.: Advances Towards Development of Industrially Relevant Short Natural Fiber Reinforced and Hybridized Polypropylene Composites for Various Industrial Applications: A Review. J. Polym. Res. 30,(2023).https://doi.org/10.1007/s10965-022-03413-8

[17] Nassar, M.M.A., Abu Tarboush, B.J., Alzebdeh, K.I., Al-Hinai, N., Pervez, T.: New Synthesis Routes toward Improvement of Natural Filler/Synthetic Polymer Interfacial Crosslinking. Polymers (Basel). 14, (2022). https://doi.org/10.3390/polym14030629

[18] Zhou, Y., Fan, M., Chen, L.: Interface and Bonding Mechanisms of Plant Fibre Composites: An Overview. Elsevier Ltd (2016)

[19] Sari, P.S., Thomas, S., Spatenka, P., Ghanam, Z., Jenikova, Z.: Effect of Plasma Modification of Polyethylene on Natural Fibre Composites Prepared Via Rotational Moulding. Compos. Part B Eng. 177, 107344 (2019). https://doi.org/10.1016/j.compositesb.2019.107344

[20] Nassar, M., Munam, A., Alzebdeh, K.I., Al Fahdi, R., Abu Tarboush, B.J.: Efficient Methods of Surface Functionalization of Lignocellulosic Waste Toward Surface Clickability Enhancement. Compos. Interfaces. 29, 79–95 (2021). https://doi.org/10.1080/09276440.2021.1897924

[21] Lee, C.H., Khalina, A., Lee, S.H.: Importance of Interfacial Adhesion Condition on Characterization of Plant-Fiber-Reinforced Polymer Composites: A Review. Polymers (Basel). 13, 1–22 (2021). https://doi.org/10.3390/polym13030438

[22] Nasihatgozar, M., Daghigh, V., Lacy, T.E., Daghigh, H., Nikbin, K., Simoneau, A.: Mechanical Characterization of Novel Latania Natural Fiber Reinforced PP/EPDM Composites. Polym. Test. 56, 321–328 (2016). https://doi.org/10.1016/j.polymertesting.2016.10.016

[23] Martins, A.B., Santana, R.M.C.: Effect of Carboxylic Acids as Compatibilizer Agent on Mechanical Properties of Thermoplastic Starch and Polypropylene Blends. Carbohydr. Polym. 135, 79–85 (2016). https://doi.org/10.1016/j.carbpol.2015.08.074

[24] Lazim, N.H., Samat, N.: The Influence of Irradiated Recycled Polypropylene Compatibilizer on the Impact Fracture Behavior of Recycled Polypropylene/Microcrystalline Cellulose Composites. Polym. Compos. 40, E24–E34 (2019). https://doi.org/10.1002/pc.24430

[25] EL-Zayat, M.M., Abdel-Hakim, A., Mohamed, M.A.: Effect of Gamma Radiation on the Physico Mechanical Properties of Recycled HDPE/Modified Sugarcane Bagasse Composite. J. Macromol. Sci. Part A Pure Appl. Chem. 56, 127–135 (2019). https://doi.org/10.1080/10601325.2018.1549949

[26] Mohammed, M., Jawad, A.J. afar M., Mohammed, A.M., Oleiwi, J.K., Adam, T., Osman, A.F., Dahham, O.S., Betar, B.O., Gopinath, S.C.B., Jaafar, M.: Challenges and Advancement in Water Absorption of Natural Fiber-Reinforced Polymer Composites. Polym. Test. 124, 108083 (2023). https://doi.org/10.1016/j.polymertesting.2023.108083

[27] Nassar, M.M.A., Alzebdeh, K.I., Al-hinai, N., Pervez, T., Nassar, M.M.A., Alzebdeh, K.I., Al-hinai, N., Nassar, M.M.A., Alzebdeh, K.I.: A New Multistep Chemical Treatment Method for High Performance Natural Fibers Extraction A New Multistep Chemical Treatment Method for High Performance Natural Fibers Extraction. J. Nat. Fibers. 20, 1–17 (2023). https://doi.org/10.1080/15440478.2022.2150922

[28] San, F.G.B., Tekin, G.: A Review of Thermoplastic Composites for Bipolar Plate Applications. Int. J. Energy Res. 37, 383–309 (2013). https://doi.org/10.1002/er

[29] Pickering, K.L., Efendy, M.G.A., Le, T.M.: A Review of Recent Developments in Natural Fibre Composites and Their Mechanical Performance. Compos. Part A. 83, 98–112 (2016). https://doi.org/10.1016/j.compositesa.2015.08.038

[30] Alzebdeh, K.I., Nassar, M., Arunachalam, R.: Effect of Fabrication Parameters on Strength of Natural Fiber Polypropylene Composites: Statistical Assessment. Measurement. 146, 195–207 (2019). https://doi.org/10.1016/j.measurement.2019.06.012

[31] Protzek, G.R., Magalhães, W.L.E., Bittencourt, P.R.S., Neto, S.C., Villanova, R.L., Azevedo, E.C.: The Influence of Fiber Size on the Behavior of the Araucaria Pine Nut Shell/PU Composite. Polimeros. 29, 1–9 (2019). https://doi.org/10.1590/0104-1428.01218

[32] Ma, P., Jiang, L., Ye, T., Dong, W., Chen, M.: Melt Free-Radical Grafting of Maleic Anhydride onto Biodegradable Poly(Lactic Acid) by Using Styrene as a Comonomer. Polymers (Basel). 6, 1528–1543 (2014)

[33] Zhang, L., Lv, S., Sun, C., Wan, L., Tan, H., Zhang, Y.: Effect of MAH-g-PLA on the Properties of Wood Fiber/Polylactic Acid Composites. Polymers (Basel). 9, 5–8 (2017). https://doi.org/10.3390/polym9110591

[34] Aggarwal, P.K., Raghu, N., Karmarkar, A., Chuahan, S.: Jute-Polypropylene Composites Using m-TMI-Grafted-Polypropylene as a Coupling Agent. Mater. Des. 43, 112–117 (2013). https://doi.org/10.1016/j.matdes.2012.06.026

[35] Hejna, A., Przybysz-Romatowska, M., Kosmela, P., Zedler, Ł., Korol, J., Formela, K.: Recent Advances in Compatibilization Strategies of Wood-Polymer Composites by Isocyanates. Wood Sci. Technol. 54, 1091–1119 (2020). https://doi.org/10.1007/s00226-020-01203-3

[36] Arunachalam, R., Piya, S., Krishnan, P.K., Muraliraja, R., Christy, J.V., Mourad, A.H.I., Al-Maharbi, M.: Optimization of Stir–Squeeze Casting Parameters for Production of Metal Matrix Composites Using a Hybrid Analytical Hierarchy Process–Taguchi-Grey Approach. Eng. Optim. 52, 1166–1183 (2020). https://doi.org/10.1080/0305215X.2019.1639693

[37] Chauhan, S., Aggarwal, P., Karmarkar, A.: The Effectiveness of m-TMI-grafted-PP as a Coupling Agent for Wood Polymer Composites. J. Compos. Mater. 50, 3515–3524 (2016). https://doi.org/10.1177/0021998315622050

[38] Karmarkar, A., Chauhan, S.S., Modak, J.M., Chanda, M.: Mechanical Properties of Wood-Fiber Reinforced Polypropylene Composites: Effect of A Novel Compatibilizer with Isocyanate Functional Group. Compos. Part A Appl. Sci. Manuf. 38, 227–233 (2007). https://doi.org/10.1016/j.compositesa.2006.05.005

Published in: Key Engineering Materials
ISSN: 1662-9795, Vol. 985, pp 33-41
doi:10.4028/p-h3uRIh

Submitted: 2024-01-28
Revised: 2024-04-18
Accepted: 2024-04-21
Online: 2024-08-27

Investigation on the Processability and Thermal Aspects of Date Palm Nanofiller/Polypropylene Biocomposites Processed via Melt Cast Film Extrusion

Hamid M. Shaikh[1,a*], Othman Y. Alothman[2,b], Basheer A. Alshammari[3,c], Abdullah Alhamidi[1,c] and Mohammad Jawaid[4,d]

[1]SABIC Polymer Research Centre, Department of Chemical Engineering, King Saud University, P.O. Box 800, Riyadh 11421, Saudi Arabia

[2]Department of Chemical Engineering, College of Engineering, King Saud University, P.O. Box 800, Riyadh 11421, Saudi Arabia

[3]National Center for Petrochemicals, Materials Science Institute, King Abdulaziz City for Science and Technology, Riyadh, Saudi Arabia

[4]Department of Biocomposite Technology, Institute of Tropical Forestry and Forest Products (INTROP), University Putra Malaysia, Serdang, Selangor, Malaysia

[a]hamshaikh@ksu.edu.sa, [b]othman@ksu.edu.sa, [c]shammari@kacst.edu.sa, [c]444105905@student.ksu.edu.sa, [d]jawaid@upm.edu.my

Keywords: Polypropylene, Nanofillers, Date palm, Melt cast extrusion, Thermal analysis.

Abstract. To preserve the environment and its resources for future generations, research must focus on alternate methods of producing materials that begin with an environmentally friendly and sustainable source. In view of this, nanosize reinforcing fillers were obtained from date palm agricultural waste without use of any toxic chemicals. Date nanofillers (DNF) with typical filler sizes ranging from 30-110 nm in width and 1-10 mm in length were obtained using rotary mechanical ball milling methods. This filler was then dry blended with the polypropylene (PP) to make a biocomposites thin film to study processability characteristics of this fillers. The loading of this filler was kept in the range of 1-5wt. % and film were melted cast through a slit height of 0.6mm. The resulting PP/DNF biocomposites films were subsequently analyzed by various analytical techniques to established structure property relationship. The change in thermal properties with loading of this filler was investigated using thermogravimetric analysis (TGA) and differential scanning calorimetry (DSC). TGA study showed that the thermal stability of film samples improved up to 20 ℃ when compared to the neat PP, representing an 8% enhancement. While the DSC measurement indicated that the crystallinity of the highest filler loading sample reduced from 52.89% to 41.79% in comparison to the PP sample. The surface morphology of some samples shows the compact and smooth feature, indicating the incorporation of fiber fillers could improve the structure of polymer. Therefore, study gave some insight into the processing behavior of such composites, which may be useful in some packaging applications.

Introduction

In numerous industrial applications, a wide range of agrowaste residue of lignocellulosic fibers or fillers are being investigated as naturally occurring reinforced materials for polymer-based composites. An enormous amount of residues derived from bio-mass, and food crops available in nature to be used as sustainable source for formulation of variety of bio composites that the composite material sectors looking for desirable properties, like low-cost cost, eco-friendliness, and renewability. The strategy for using these plant-based fillers could be viewed as a type of eco-system support that offers socioeconomic innovation for local agriculture [1]. Nonetheless, due to laws and regulations concerning sustainability and environmental impact, the development of biocomposites that utilize natural fillers and polymers has progressed considerably in recent time [2].

Similarly, nanofillers, be it in the form of particles or fibers, organic or inorganic can dry melt blended with different polymer matrices. Moreover, nanofillers has large surface area, and high aspect ratio that improve physical, mechanical, and chemical properties of the matrix relatively at low loading and thus making them useful reinforcing additives for a wide range of engineering composite fabrication [3]. Natural filler can be made in a variety of sizes, shape and often free of defects and therefore has the possibility to overcome the limits of conventional micrometer-scaled material. The uniform distribution of nanoparticles, which provides the mechanical, thermal, and molecular mobility as well as the change in relaxation behavior, is responsible of the higher interfacial interactions between the matrix and filler materials [4]. However, micro accumulation of particles from nanoscale filler materials leads to plastic zone deformation and this will improve the brittle, mechanical, and fracture properties of the materials. Filler materials that have a larger to smaller geometrical ratio are of greater interest and are therefore more suitable for use as reinforcements in the formulation of nanocomposite. [5]

These naturally occurring fillers, which are derived from lignocellulosic materials, are classified as supramolecules and consist of polymers such as lignin, cellulose and hemicellulose moieties arranged in a three-dimensional structure. Lignocellulose nanofillers are a form of nanoscale cellulose fibril that contains lignin and can be obtained from plants, wood, agricultural and forest residue [6]. In particular, film based lignocellulosic nanofillers show higher antioxidant properties and superior thermomechanical abilities when compared to pure cellulose nanofibrils. The presence of aromatic phenylpropanoid unit in lignin is attributed to the UV-blocking abilities and thus making these nanofillers suitable for food related applications [7,8].

In the past, some researcher has already tried to extract date palm nanofillers. For example, Mahmoud Al-Safy et al. used mechanical ball milling to produce a nano-sized lignocellulosic filler from date palm microfibers. In this work, high-speed cycles of ball milling are carried out at different intervals, and the particles with sizes ranging from 27 to 122 nm were reported to be obtained [9]. Similar to this, a rigorous mechanical ball milling procedure was used in another investigation to produce nano and microfiber from the date palm lignocellulose. After conducting 99 cycles of 15 minutes each, the authors reported obtaining irregularly shaped nanofibers with diameters ranging from 1 to 10 mm in length and 30 to 110 nm in width [10].

The impact of reinforcing natural fillers on the thermal properties of polymer matrix composite material is demonstrated by various literature. Numerous study analyzes the thermal impacts of several types of reinforcement with varying ratios and sizes. Thermogravimetric analysis (TGA) is a technique that analyse changes in weight in relation to temperature and time using an extremely sensitive microbalance. This instrument is very sensitive and accurate in recording weight and temperature. Most often, weight loss occurs as the temperature rises because different components are progressively eliminated from the matrix. Moreover, the ratio of a polymer matrix's constituent parts and particular filler directly influences the processing conditions and determine how effective or inefficient for a particular composite system. Similarly, natural filler reinforced composites' thermal stability is an important factor to take into account because the processing temperature is vital to the composites' formulation.

The thermal, mechanical and other properties of the composite alter with temperature due to the degradation of the natural fillers components, namely cellulose, hemicellulose, and lignin [11]. However, extensive research into new natural fillers/fibers, their physical treatment and chemical modification, and hybridization have all advanced recently to address some of the drawbacks of natural filler reinforced composites melt processability. In general, the use of nanoscale fillers at low concentrations of reinforcement (often less than 10% weight percent) can generally result in better thermal characteristics. In our previous work, it was demonstrated that the dimensional stability of injection molded composites of polypropylene reinforced with date palm nanofiller has a low coefficient of thermal expansion (CTE) [12].

Similarly, in another work, polypropylene biocomposites with lemon leaves and fig leaves with loadings ranging from 20 wt% to 40 wt% were produced using an injection molding procedure. It has been shown that these fillers exhibited good thermal stability. The maximal decomposition

temperature for lemon and fig leaves was 305°C and 320°C, with residue remaining after 500°C being 26.5 and 29.7, respectively [13]. Thus, a large filler loading of up to 40 weight percent or more is needed to obtain satisfactory thermal characteristics from these natural fillers based polymer composite. Moreover, due to higher processing temperature the thermal degradation of the fillers is obvious. Therefore, the novelty of this study consists of the casting of composite thin film under precise and appropriate processing conditions, with minimum filler degradation in the molten state of the chosen polymer. Thus, in this work, a thin film of polypropylene with a comparatively low filler loading (1–5%wt%) was obtained using nanosized natural fillers from the waste date palm by simple ball milling techniques. The thermal properties of this film, including stability, mass loss, and surface morphology have been carefully studied.

Materials and Methods

Melt casting of composite thin film: The biocomposites thin film was formulated using polypropylene homopolymer (PP 3030) with a density of 0.9 g/cm^3 and melt flow index (MFI) of 3 g/10) which was obtained from the National Industrialization Company (TASNEE) Saudi Arabia. Moreover, waste fiber portion of the trunk of a fully grown date palm *(Phoenix dactylifera L.*) tree, located in a King Saud University campus in the Riyadh region of Saudi Arabia was used to production of the lignocellulosic nanosize fillers (NF). These fillers finally used as a reinforcement additive for composite film of the PP. Initially, a mixture grinder was used for crushing waste fibers into small particles, and a series of selected ASTM E11 standard sieves were used for dry sieving. These sieves having a serial number 14050979 and 12020883 corresponding to aperture size of 63(μm) and 38(μm) respectively. They were arranged in descending order with a vertical vibration sieve shaker (ELE Sieve Shaker, UK) and fine powder was collected. Finally, this powder was subjected to ball milled treatment using a planetary ball mill (Pulverisette 7 Premium, Fritsch Co. Germany) to obtained nanoscale fillers. These fillers were found to be between 1 and 10 mm in length and 30 to 50 nm in diameter on average. Their morphological details and image have been given in our earlier work [10]. A micro-compounder (Xplore15 cm^3, The Netherlands) was used to dry melt oven-dried nanofillers in the 1–5% weight loading range and PP with the addition of PP based compatibilizer (PRIEX 25097: Maleic anhydride modified polypropylene (PP-g-MA), having 0.45 % of grafting). A melting temperature of 180°C, a screw speed of 100 rpm, and a mixing period of 10 minutes were maintained in a speed-controlled mode. The molten material was thereafter fed through a film device with a 0.6 mm slit height and a 65 mm wide film die. This film device also equipped with the air knife, speed and torque controlled roller and parameter controlled unit. Table 1 shows the formulation of these composite films, and Figure 1 depicts a digital image of such a films.

Table 1. List of biocomposites film produced in this work.

Sample ID.	Composition of DNF (wt. %)
Film 1	PP (98) + PRIEX (2)
Film 2	1% (NF) + PP (97) + PRIEX (2)
Film 3	2% (NF) + PP (96) + PRIEX (2)
Film 4	3% (NF) + PP (95) + PRIEX (2)
Film 5	4% (NF) + PP (94) + PRIEX (2)
Film 6	5% (NF) + PP (93) + PRIEX (2)

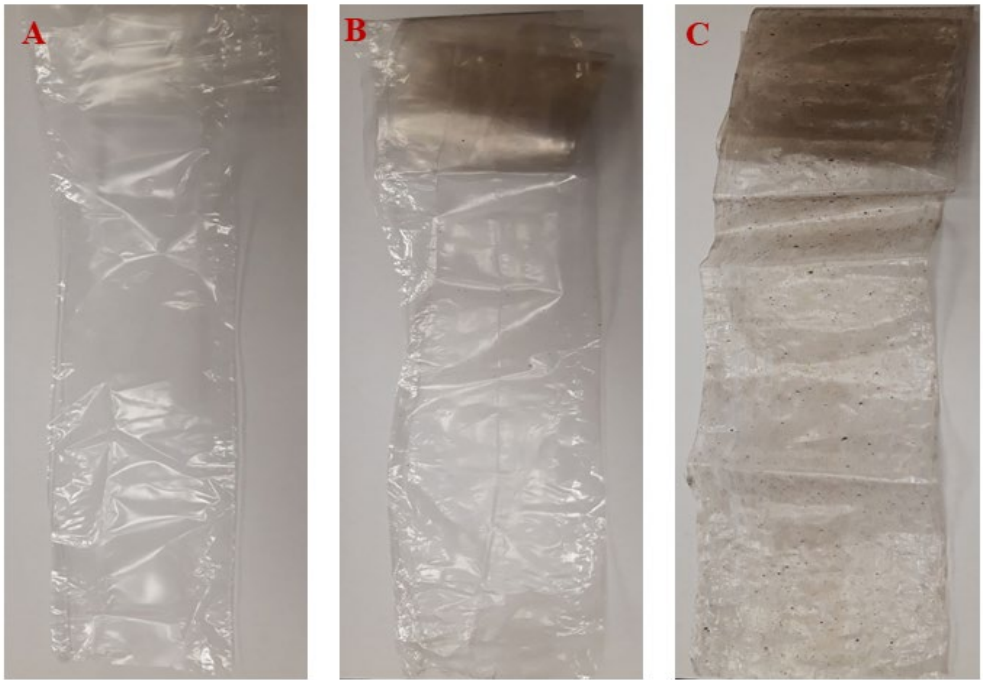

Fig. 1. Digital images of PP films, A) Neat PP, B) Film 2(1% (NF), and C) Film 6 (5 % (NF).

Analysis of functional group:

Fourier transform infrared spectroscopy (ATR-FTIR) analysis was carried out using a (Thermo Scientific, Winsford, UK) Nicolet iN10 FTIR microscope having a germanium microtip. The analysis was carried out in the wavenumber range of 650–4000 at a resolution of 6 cm^{-1} over 16 scans.

Thermal Analysis

Thermogravimetric analysis (TGA) was performed using Shimadzu thermal analyzer (Model: DTG-60H). The alumina pan was filled with ~ 10-15 mg of the sample. Subsequently, the samples were heated from room temperature to 900°C at heating rate of 20°C/minutes. The analysis was done under a nitrogen atmosphere with a flow rate of (50 cm^3/min) and accordingly, the corresponding weight loss was recorded. In order to study the thermo-molecular behavior of fillers, a differential scanning calorimetry (DSC) (Shimadzu DSC-60, Japan) was used. These film samples were heated from room temperature to 250 °C at a rate of 10 °C/minutes. The average of three readings were recorded and the degree of crystallinity (Xc) was calculated by using below equation,

$$X_c(\%) = \frac{\Delta H_m}{(1-\Phi)\Delta H_0} \times 100$$

where ΔHm is the calculated enthalpy of melting for the composite, Φ is the weight fraction of PP and ΔH_0 is the theoretical enthalpy of melting for 100% crystalline PP which is reported to be 209 J/g[13].

Analysis of Mechanical Properties

The tensile properties of the composite samples films were determined using a Hounsfield H100 KS series tensile testing machine (Salfords, UK) at a rate of 10 mm/min crosshead speed. The PP composite films were cut into a rectangular shape of 40 mm X 5 mm X 0.5 mm and at least five measurements were taken for each specimen, and the mean values were reported.

Morphological Analysis

Scanning electron microscopy (SEM, JSM-6360A, JEOL, Japan) was used to analyze the morphological properties of these composite films. This analysis was carried out on the neat PP and composites film samples. A small portion of the sample was placed directly on the conductive carbon tape and gold sputtered before analysis.

Results and Discussion

FTIR analysis was utilized to examine the variations in the functional groups of the filler and the matrix composition with processing conditions. The FTIR measurement indicated that the functional groups of the filler and matrix maintained their intensity. FTIR spectra of film samples are presented in Fig. 2. The film 1 sample showed significant peaks at 2851 cm^{-1} and 2922 cm^{-1}, which corresponded to the C-H stretching of polymeric molecular chains of the PP. The intensity of these peak increases in rest of the samples due to contribution of C-H functional group of cellulose, lignin and hemicellulose components of the lignocellulosic nanofiller. Similarly, another prominent peak appears at 1732 cm^{-1} due to the presence of C=O from the maleic anhydride and lignin. In addition, the peaks at 1219 cm^{-1}, 1371 cm^{-1}, and 1438 cm^{-1}, were assigned to the C-C bending of polymer backbone structure [14].

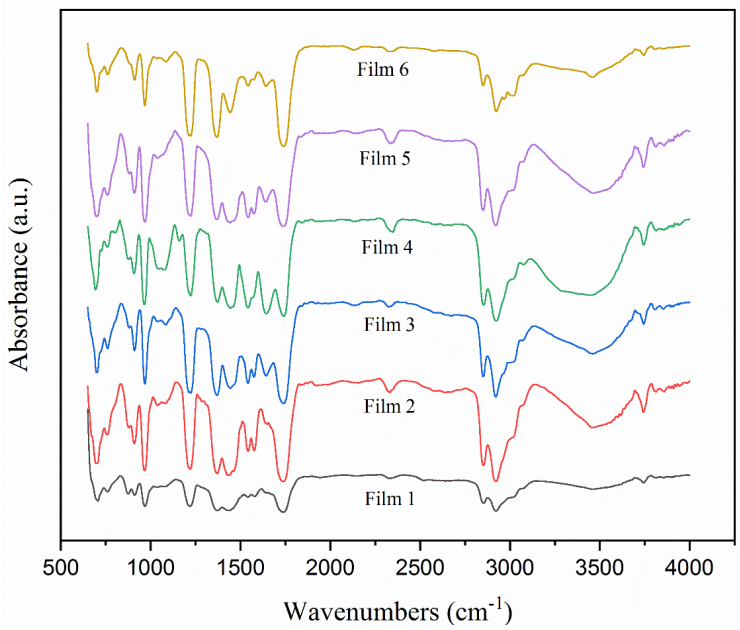

Fig. 2. FTIR spectra of film samples.

Furthermore, the =C-H bending vibration is associated to the 968 cm^{-1} peak, and the CH_2 rocking vibration is assigned to the 704 cm^{-1} peak. Similarly, for the film samples, the broad peak of the O-H group vibration also presents at approximately 3452 cm^{-1}. It should be noted that the addition of fillers caused a gradual change in the peaks' intensities because of their functional groups. These findings are consistent with the previously reported analysis [15].

Similarly, TGA curves of film samples are presented in Fig. 3a. It was observed that the neat PP shows single stages degradation behavior capered to the film samples. It is due to fact that all lignocellulosic biomass inherently hygroscopic in nature and contain about 5-6% of moisture. This fact was also observed in our previous study, wherein this nanofillers evaporates the moisture in the range of 70°C-130°C. However, overall the thermal stability of these nanofillers is considerably superior than that of microsize fibers at the processing temperature employed. [10]. In the case of composite film samples, the initial decomposition temperature for both the films i.e., Film 3 and Film 4 is found to be 281.9°C and 279.5°C, respectively. These values were higher than the samples of Film 2 and Film 1, which is found to be around 261.6°C and 276.5°C, respectively.

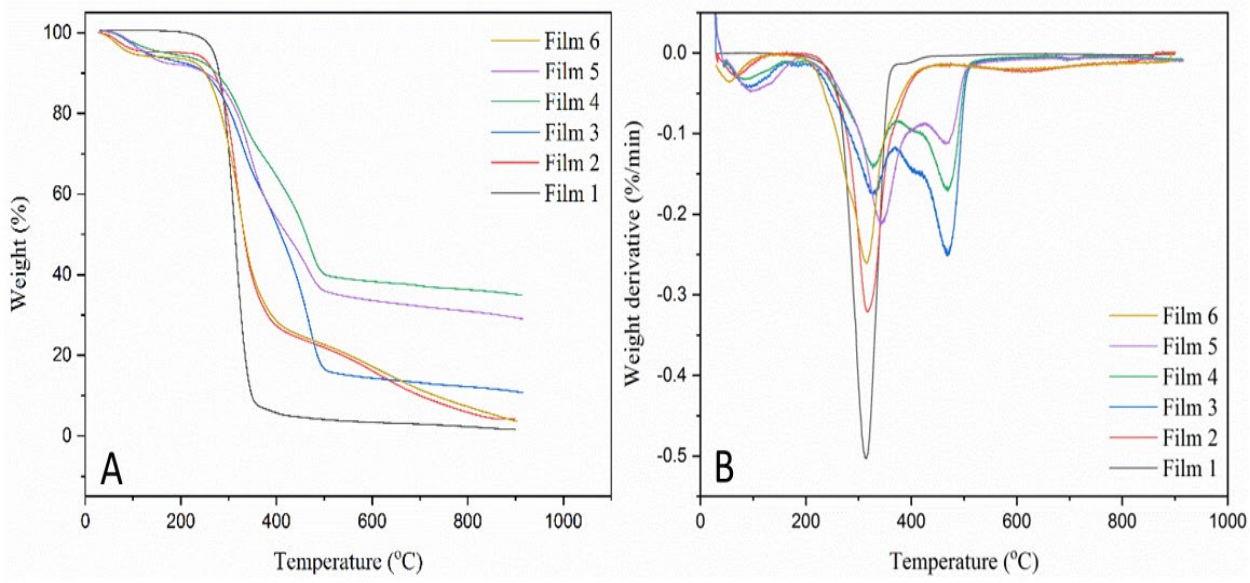

Fig. 3. TGA (a) and DTG (b) curves of film samples.

It was probably due to the good componential interaction in film composite, contributing to the stable thermal degradation behavior with improved heat resistance. In addition, the weight loss behavior of both film composites is consistent with that of the film 2 sample, suggesting that their biocomponents interacted well with one another and can be clearly seen in DTG curves (Fig. 3b) On the other hand, film 4 and film 5 exhibited higher peak decomposition temperatures of 320.7°C and 318.6°C, respectively, compared to film 2 at 315.7°C and film 1 at 316.0°C. These thermal results demonstrated that the developed composite film has excellent thermal stability and may be employed in a variety of packaging applications capable of withstanding high temperatures.

Similarly, Fig. 4 shows the dynamic thermogram (heating and cooling), and Table 2 summarizes the details of the analysis of the neat PP and the film composites. It is observed that the composite films have been shown to have nearly constant melting temperatures (Tm), but their crystallization temperatures (Tc) were found to be higher than those of the virgin PP. This suggests that the filler particle addition has a greater impact on Tc, yet total crystallinity is observed to be somewhat lower than that of PP. This could be due to the large amount of fillers that may limit the mobility of the polymer chain, and hinder crystal growth development, and thereby induce a decrease in crystallinity. Furthermore, the decrease in the enthalpy of melting implies that the polymer chain's mobility is reduced. The polymer chain may be interrupted by these stiff filler particles, preventing the chain from reassembling in an orderly manner. This might be because of the fillers' poor or negligible nucleating ability. These results are consistent with previously reported work [16].

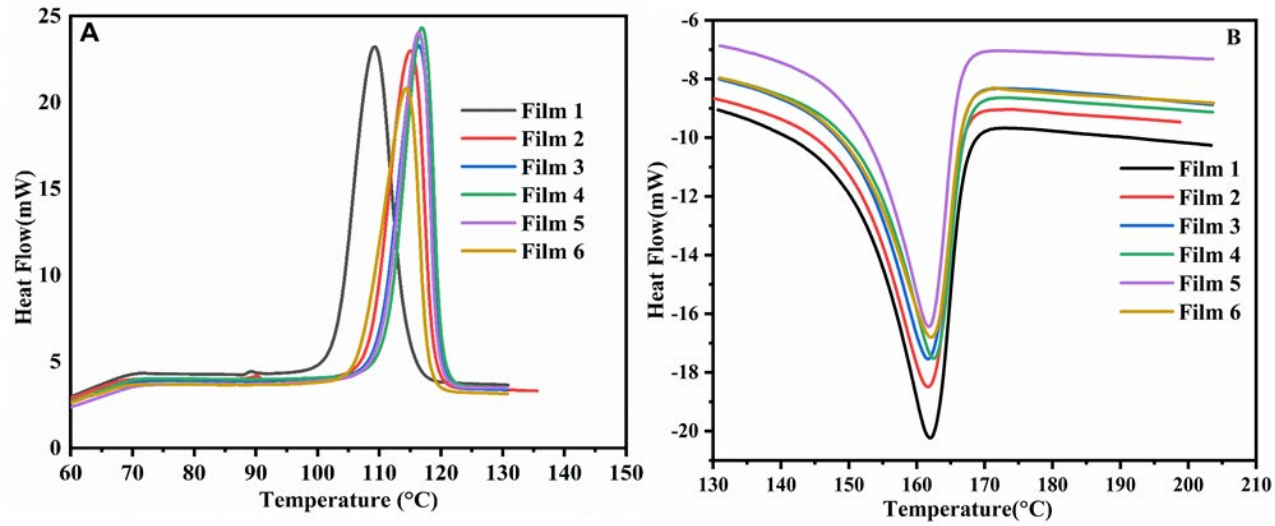

Fig. 4. DSC thermogram of samples A) Crystallization peaks B) Melting peaks of the samples.

Table 2. DSC characteristic of the film composite samples.

Samples	Tc °C	T_m °C	ΔT_m (J/g)	X_c (%)
Film 1	109.51(±0.50)	162.81(±0.40)	111.75(±3.17)	51.90(±4.28)
Film 2	114.62(0.87)	161.74(±1.08)	95.23(±4.75)	46.72(±5.67)
Film 3	116.85(±0.57)	162.20(±0.60)	87.13(±4.02)	43.99(±4.17)
Film 4	117.63(±0.67)	162.45(±1.32)	87.27(±5.50)	42.42(±3.41)
Film 5	118.06(±1.08)	163.96(±0.85)	83.49(±6.30)	40.72(±1.75)
Film 6	119.05(±0.87)	164.85(±0.50)	80.89(±8.47)	40.43(±2.46)

Mechanical characteristic of the polymer cpmposite film can alter by a variety of factors, including the types and particle size of the renforcing addtives, loading percentage, particle–matrix adhesion and processing condtions used to make such composites. The effective stress transfer between the filler particles and matrix determines the maximum strength that nano composites film sustained under uniaxial tensile loading. Table 3 highlights the key mechanical parameters of these films. It is observed that both the tensile strength and elongation at yield slightly increase or remain constant in the samples having less fillers loading i.e film 1 and 2 which having filler loading 1% and 3% respectively. This could be attributed to the good dispersion of the filler and adhesion with the matrix. Similar fact was also reported in various cellulose reinforced polypropylene system [17]. On the other hand, higher loading amount of the filler leads to decrease in this properties compared to the neat PP. This reduction can be attributed to the PP chains' limited mobility a result of the addition of high filler amount which may be beyond the percolation threshold of the composites system, and rigidity of the filler. These results are in good accordance with the previously reported studies [18,19].

Table 3. Mechanical characteristics of film composite samples.

Samples	Tensile Strength at Yield (MPa)	Elongation at Yield (%)
Film 1	32.03 (±1.40)	10.36 (±1.01)
Film 2	34.86 (±1.12)	11.67 (±1.06)
Film 3	34.22 (±2.05)	10.26 (±0.63)
Film 4	32.98 (±0.88)	9.98 (±0.87)
Film 5	30.96 (±1.08)	8.71 (±0.68)
Film 6	30.28(±1.61)	8.03 (±0.50)

Analysis of surface morphology

Fig. 5 displays the SEM image of Film samples mixed with different amount of fiber fillers. From Fig. 5A, the sample of Film 1 had flat surface morphology with wrinkle-like and protuberant features. This was because the asymmerical interaction between polymeric chains. When mixed with fiber fillers, the morphology had changed for Film samples, and the apparent feature had become compact and smooth, indicating the incorporation of fiber fillers unformaly distributed and could improve the filler-matrix adhesion. Howeve, at higher filler laoding, filler pull out and the agglomeration effect and void are also observed.

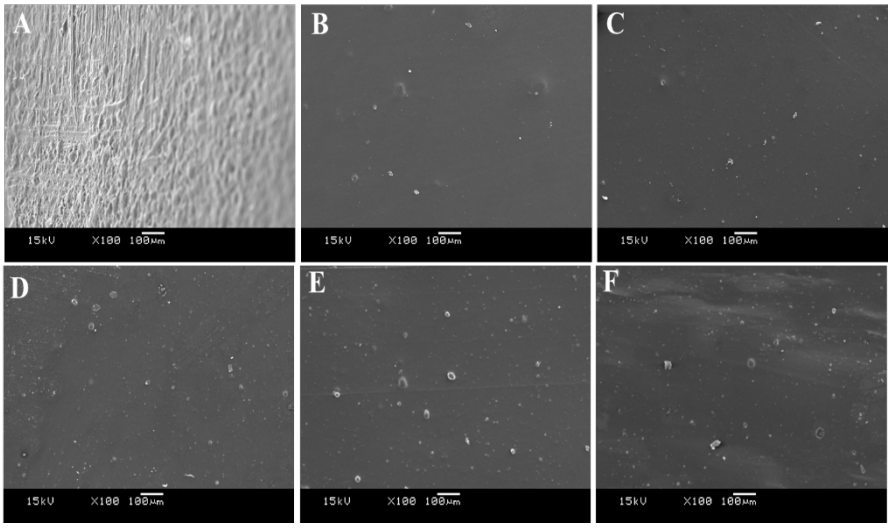

Fig. 5. Scanning Electron Microscopy images of A) Neat PP, B) Film 2(1% NF), C) Film 3 (2% NF), D) Film 4 (3% NF), E) Film 5 (4 % NF), and F) Film 6 (5% NF).

Conclusion

In this work, nanofillers from the waste lignocellulosic biomass of date palm was utilized to formulate PP based thin film. This filler was employed as such without any chemical modifications with attempt to use industrial viable melt process, and formulated successfully. The uniform and flexible composite film with the average thickness of 0.25mm was casted by controlling various processing parameters. The functional analysis shows presence of both the filler and matrix. The thermal stability of theses composite films was found to be good enough while the crystallization behavior of the composite indicated that the crystallinity of the composites film was lower than that of the neat PP due to the nanofillers' low or non-nucleating ability. The crystallinity of the neat PP is about 51.90% which is reduced to 40.43% for the highest loading of the nanofillers composite sample (Film6). The tensile strength of the films having 1wt.% and 2wt.% loading of the fillers displays tensile strength of 34.86 MPa and 34.22 MPa, which are higher that the neat PP. Similarly, the surface morphology indicates uniform distribution of the nanofillers. The lack of oxidation of the filler and good thermal stability suggest that such composites film are suitable for room temperature packaging applications.

Acknowledgements

The project was supported by the National Plan for Science, Technology, and Innovation (MAARIFAH), King Abdulaziz City for Science and Technology, Kingdom of Saudi Arabia, Award Number (2-17-02-001-0061).

References

[1]. C.M.P. Kumar, B, A.R. Kumar,Natural nano-fillers materials for the Bio-composites: A review. Journal of the Indian Chemical Society. 99 (2022) 100715.

[2]. M.M.A. Nassar, B.J.A. Tarboush, K.I. Alzebdeh, N. Al-Hinai, T. Pervez, New Synthesis Routes toward Improvement of Natural Filler/Synthetic Polymer Interfacial Crosslinking. Polymers. 14 (2022) 629.

[3]. R. Yadav, M. Singh, D. Shekhawat, S. Y.Lee, S.J. Park, The role of fillers to enhance the mechanical, thermal, and wear characteristics of polymer composite materials: A review. Composites Part A: Applied Science and Manufacturing. 175 (2023) 107775.

[4]. De Azeredo, H.M. Nanocomposites for food packaging applications. Food research international. 42 (2009), 1240-1253.

[5]. D. Wong, M. Anwar, S. Debnath, A. Hamid, S. A. Izman, Review: Recent Development of Natural Fiber-Reinforced Polymer Nanocomposites. JOM.73 (2021) 2504-2515.

[6]. E.Amini, I. Hafez, M, Tajvidi, D.W. Bousfield, D. Cellulose and lignocellulose nanofibril suspensions and films: A comparison. Carbohydrate Polymers. 250 (2020)117011.

[7]. Anushikha, K.K.Gaikwad, Lignin as a UV blocking, antioxidant, and antimicrobial agent for food packaging applications. Published in Biomass Conversion and Biorefinery (2023).

[8]. J. Trifol, R. Moriana, Barrier packaging solutions from residual biomass: Synergetic properties of CNF and LCNF in films. Industrial Crops and Products. 177 (2022) 114493.

[9]. M. Al-Safy, N. Al Hinai, K. Alzebdeh, Production of Date Palm Nanoparticle Reinforced Composites and Characterization of Their Mechanical Properties. Proceedings of the ASME 2022 International Mechanical Engineering Congress and Exposition. Volume 3: Advanced Materials: Design, Processing, Characterization and Applications; Advances in Aerospace Technology. Columbus, Ohio, USA. October 30–November 3, (2022) V003T03A032. ASME.

[10]. O.Y. Alothman, H.H. Shaikh, B.A.Alshammari, M.Jawaid. Structural, Morphological and Thermal Properties of Nano Filler Produced from Date Palm-Based Micro Fibers (Phoenix dactylifera L.). J Polym Environ. 30 (2022) 622–630.

[11]. J.S.S.Neto, H.F.M. de Queiroz, R.A.A. Aguiar, M.D. Banea, A Review on the Thermal Characterisation of Natural and Hybrid Fiber Composites. Polymers. 13 (2021) 4425.

[12]. H. Shaikh, O.Y. Alothman, B.A. Alshammari, M.Jawaid, Dynamic and thermo-mechanical properties of polypropylene reinforced with date palm nano filler. Journal of King Saud University –Science. 35 (2023) 102561.

[13]. F.M. Al-Oqla, M.T. Hayajneh, M.M. Al-Shrida, Thermal stability analysis and mechanical performance of Mediterranean lignocellulosic fiber reinforced polypropylene sustainable composites. Journal of Industrial and Engineering Chemistry. 134 (2024) 231-243.

[14]. H.M. Shaikh, Effect of carbon fiber as secondary filler on the electrical, thermal and rheological properties of carbon fiber/polypropylene composites. Journal of Polymer Engineering. 38 (2018) 545-553.

[15]. C. Campanale, I. Savino, C. Massarelli,V.F. Uricchio, Fourier Transform Infrared Spectroscopy to Assess the Degree of Alteration of Artificially Aged and Environmentally Weathered Microplastics. Polymers. 15 (2023) 15 911.

[16]. B.A. Alshammari, O.Y. Alothman, A. Alhamidi, M. Jawaid, H.M. Shaikh, Effect of Accelerated Weathering on the Thermal, Tensile, and Morphological Characteristics of Polypropylene/Date Nanofiller Composites. Materials. 15 (2022) 6053.

[17]. S. Mustapha, J. Lease, K. Eksiler, S.T. Sim, H. Ariffin, Y. Andou, Facile Preparation of Cellulose Fiber Reinforced Polypropylene Using Hybrid Filler Method. Polymers. 14 (2022) 1630.

[18]. O. Das, N.K. Kim, M.S. Hedenqvist, An Attempt to Find a Suitable Biomass for Biochar-Based Polypropylene Biocomposites. Environmental Management, 62 (2018) 403–413.

[19]. A.Y. Elnour, A.A. Alghyamah, H.M. Shaikh, A.M. Poulose, S.M. Al-Zahrani, A. Anis, A M.I. Al-Wabel, Effect of Pyrolysis Temperature on Biochar Microstructural Evolution, Physicochemical Characteristics, and Its Influence on Biochar/Polypropylene Composites. Appl. Sci. 9 (2019) 1149.

Published in: Key Engineering Materials
ISSN: 1662-9795, Vol. 985, pp 95-112
doi:10.4028/p-6p7TFu

Submitted: 2023-11-29
Revised: 2024-03-19
Accepted: 2024-03-26
Online: 2024-08-27

Design, Processing, Testing and Characterizing for Orthodontics Material of Palm-Fibres Based Bio-Nanocomposite

R. EL-Sheikhy[1*], A. AlKhuraif [2]

[1,2]Professors, Dental Health Department, College of Applied Medical Sciences, King Saud University, Saudi Arabia.

*Corresponding author: [a]relsheikhy@ksu.edu.sa, [b]aalkhuraif@ksu.edu.sa

Keywords: Dental biomaterials; Bio-CPNC bio-nanocomposite; layered nanocomposites; palm tree fibers; orthodontics.

Abstract. Current research is carried out for newly developed of Bio-CPNC biomaterial nanocomposite for dentistry applications. The developed Bio-CPNC is invented of clay-based polymer CPNC and palm-tree micro-fibers, where CPNC is composed by nanotechnology of HDPE and MMT nanoclay. The research contains the methodology of design, processing, testing and characterization mainly focusing on mechanical and fracture properties, microstructure morphology and testing of thermal effect changes due to surrounding temperature changes. The necessity for finding new biomaterials and new techniques for dental materials for restoration and orthodontics with high biocompatibility with human bones and tissue are the aim for developing this natural bio-nanocomposites to be instead of using ceramics and metals like titanium. The new developed bio-CPNC dental material have special mechanical, thermal and fracture properties to resist the effects of occlusal loads of mastication with sustainability without expecting bad effects with orofacial esthetics and normal lingual ability because it is green. It can be applied for different types of orthodontics like crowns, bridges and dental implants. The study included processing, design, testing and characterization of different properties. The testing included detailed fundamental experimental work for investigation of the changes of mechanical and fracture properties based on fracture mechanics science. The results and comparison are promising where they are showing large enhancement of the mechanical, fracture and thermal properties of Bio-CPNC in comparison to the polymer material which encourage the researchers, dentists, and dental-companies for extra research to stabilize these natural green Bio-CPNC nanocomposite for dental applications with reducing the cost where all materials components are available locally in comparison to use of conventional ceramics materials or expensive zirconia composites.

Introduction

It is known that polymers suffer from degradation phenomena. These result in materials with low tensile strength, low toughness, and poor physical properties, leading to material deterioration, fracture, cracking, and failure. There are several types of degradation process, for example, thermal degradation, chemical degradation, environmental stress cracking, environmental stress fracture, stress corrosion of polymers, hydrogen embrittlement, biological degradation, thermal de-polymerization, uv degradation and oxidation of polymers . Thermal degradation occurs by de-polymerization, and side-group elimination. Polymer thermal degradation has certain mechanism for initiation then propagation, bifurcation and failure [1-32]. There are several methods of polymer stabilization to reduce degradation like using additives such as anti-oxidants, anti-ozonants, and uv absorbers. Degradation of polymeric materials leads to changes in properties such as mechanical properties, for example, tensile strength, and physical properties, for example, color and shape. These are caused by environmental factors such as exposure to high temperatures or direct sunlight, and contact with chemicals. The main result of these processes is crack formation in polymers and polymer-based materials [1-32]. Thermal degradation of polymeric materials is caused by molecular deterioration. High temperatures cause the molecules in long polymer chains to separate and react again with other molecules; this weakens the material as well as causing cracks [1-22]. As the polymer degradation instability and fracture mean deterioration of the polymer properties and appearance, the

degradation has main several reasons such as heat effects (thermal degradation and thermal oxidative degradation when in the presence of Oxygen), light (photo-degradation), uv degradation, mechanical energy, radiation, ozone, etc. The different types of polymer degradation (thermal, mechanical, chemical and biological) have various serious reactions undergone by polymers such as de-polymerization, cross-linking, side group elimination, substitution and reaction of side group among themselves [1-22]. In addition to the effects of reducing the mechanical and fracture properties of the polymers, chalking, color changes, cracking initiation and propagation. The degradation in majority cases has similar mechanism. As in the case of thermal degradation , the initiation process start in general by oxidation in addition to thermal stresses on the polymers, then it can propagate following by branching , bifurcation and finally termination and separation producing total failure [1-32]. Saudi Arabia is one of the major producers of plastic in the world. It can be easily imagined how much money can be saved from recycling the plastics especially if we used in this purpose low cost domestic green material for changing it to useful high functional nanocomposites or nano-micro-composites with enhanced new advanced properties such as mechanical properties, thermal properties, fracture and degradation properties. To manufacture sustainable polymers many researchers have conducted research projects where they depended on adding anti-oxidants and stabilizers to the polymers for enhancement of the polymer properties [1-20]. They realized some results for producing stabilization for the polymers while the degradation could not be prevented. The polymers suffer from oxidation process which can be happened during any period of lifetime of the polymers starting from manufacturing stage to storage stage and use stage. Oxidation badly affects the mechanical properties of the polymers such as reducing the tensile strength, harming the impact capacity and deteriorating the toughness rather than the fracture resistance. In addition, it can deteriorate the thermal properties of the polymers, color and appearance and changing the molecular weight of the polymers. On the other hand, based on the detailed structure of the mouth and teeth, detailed applied loads of teeth occlusal and masications, problems of fracture and failure, problems of bond, problems of thermal effects, heavy weight, short lifetime, high cost, and problems of implementations of previous materials of ceramics and metals for dental applications, the current developed bionanocomposite is useful for solving the dentistry problems. The developed bio-nanocomposite pplications in the field of dental biomaterials include the dental crowns of all types and design, dental bridges of all types geometry, dimensions and design based on the patient age and orofacial anatomy, dimensions and structure as shown in figures (1, 2). The developed bionanocomposite is also can be applied for design and implementation of partial denture and complete dentures as shown in figure (3). This applications are very important due to the unique properties of developed bionanocomposites from both engineering side and medical side. Thses are because of the suitable special properties for orthodontics like high strength, high mechanica properties, light weight, ease of implemenation, high thermal resistant, high fracture resistant, safe contact to mouth tissue, ease of cleaning, ease of design, low cost, and compatiblity with tissue. Therefore, current study is devoted to the investigation of engineering side and engineering properties where they are the main task of any dental biomaterials for any orthodontics applications.

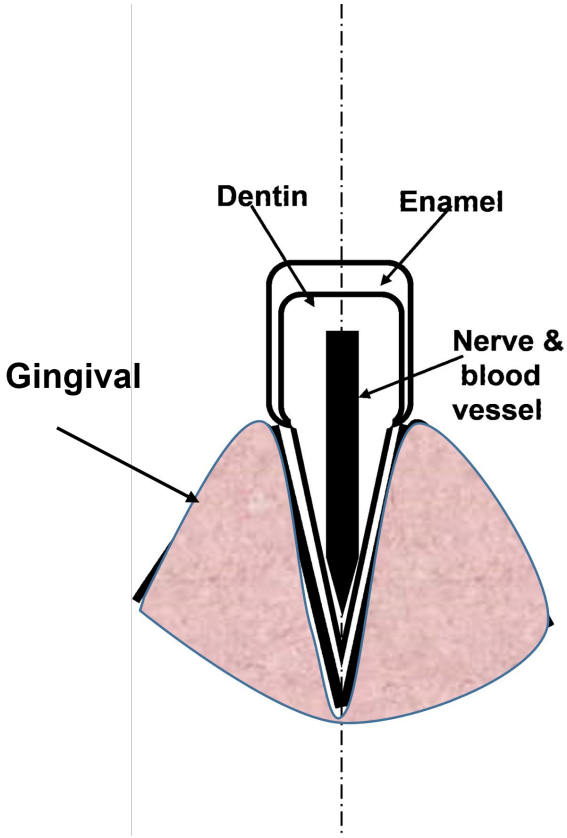

Fig. 1 Main structure of the tooth

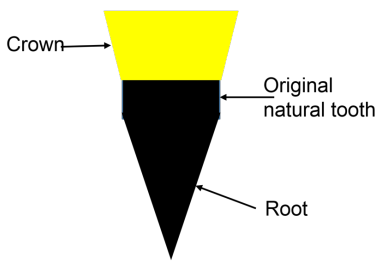

(a) some types of crowns

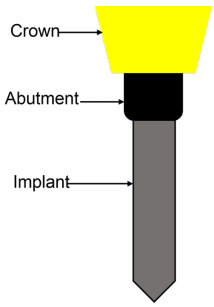

(b) some types of implants

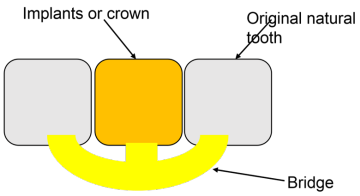

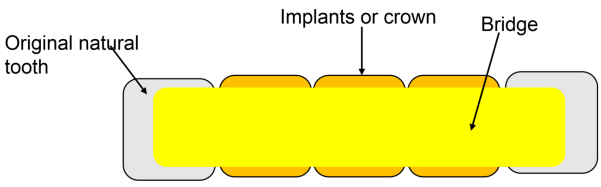

(C) some types of dental bridges for fixing some types of crowns by resin or mechanically

Fig. 2 Orthodontics of (a) some types of crowns , (b) some types of implants, (C) some types of dental bridges for fixing some types of crowns by resin or mechanically

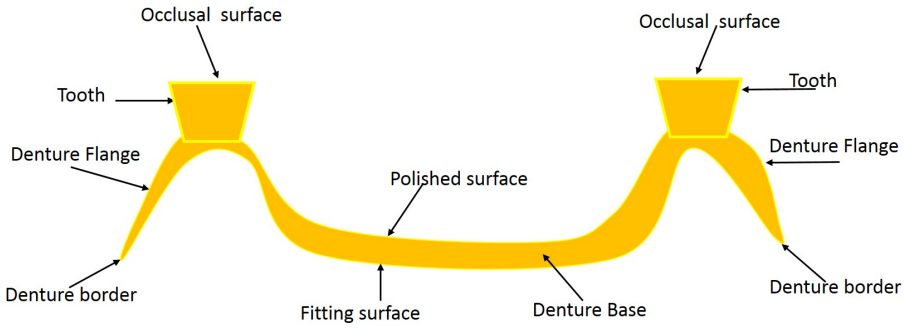

Fig. 3 Main elements and components of structure of complete denture

Experimental Work Method

The study purposes include reducing environmental pollution by reducing polymer degradation, Producing new, low-cost, nano–micro, green, highly functional materials, producing long-life orthodontic material for safe dentures with low thermal conductivity and good mechanical and fracture properties, controlling the degradation and failure of polymer products, and use of domestic materials for producing advanced, highly functional, green materials**.** The research can also use waste polyolefin compounds and pre-used polyolefin systems which mechanical, chemical, and thermal properties, have been previously affected due to environmental conditions, where it is known that prolonged exposure of polymers to thermal effects, especially sunlight, reduces their mechanical and thermal properties, resulting in degradation, fracture and failure. This causes environmental pollution and has adverse effects on human health and the economy. To solve these problems by reducing pollution and thereby protecting health and saving money, new composites made of polyolefin matrix, using a special method, with nanoclay and palm tree microfibers are produced. These waste materials are a source of serious environmental pollution, and this adversely affects health and quality of life. Then, it can be recycled to produce highly functional green nanocomposites using green nanoclay particles and palm tree microfibers fillers. These nanocomposites can be applied to produce dental biomaterials which enhance mechanical and fracture properties and reduce thermal effects of temperature. Processing consists of several steps like mixing, extruding, and pelletizing. The melted polymers are mixed at certain stages with nanoclay and palm tree microfibers. These new nano–micro composites will incorporate mainly domestic materials. They are highly functional materials with modified mechanical and thermal properties and degradation, and fracture resistant. Detailed characterizations of thermal, mechanical, and fracture properties are predicted. Saudi Arabia is one of the major producers of plastic in the world. Thus there is a huge waste stream creating a big environmental problem. It can be easily imagined how much money can be saved from using these huge amount of plastic wastes. If we used low cost domestic green material as nanoclay and palm tree fibres for changing the polymers to useful high functional nanocomposites or nano-micro-composites with new enhanced advanced properties such as mechanical properties, thermal properties, fracture and degradation properties. Polymers also suffer from thermal degradation, fracture, thermal cracking and these lead to failure after a short period of time. This affects the quality and has an adverse effect on health. Degradation of polymer products also causes environmental pollution and can be occurs despite the addition of chemical stabilizers during polymer processing to reduce or prevent this phenomenon. As the polymer degradation instability and fracture mean deterioration of the polymer properties and appearance, the degradation has main several reasons such as heat effects, light, uv de-gradation, radiation, etc. The different types of polymer degradation (thermal, mechanical, chemical and biological) have various serious reactions undergone by polymers such as random chain scission, de-polymerization, cross-linking, side group elimination, substitution and reaction of side group among themselves. In addition to the effects of reducing of the mechanical and fracture properties of the polymers, chalking, color changes, cracking initiation and propagation, general reduction in most of other desirable physical properties have dangrous effects. The procedure would reduce environmental pollution, control the degradation process, modify the mechanical and

thermal properties of polymers, and make it safe for human consumption. The results of tests are promising as shown in figures (10-13) for thermal effects while figures (6, 7, 8, 9, 15) show mechanical and fracture mechanics tests on pre-cracked sample ofmade of bionanocomposites. The bionanocomposites tests made of HDPE and LLDPE (50% -50%), nanoclay layer and palm date fiber layer. We mixed polymers with both nanoclay and palm tree fibers producing nanocomposite to be used in production of bionanocomposites. The proposed procedure would solve these problems by mixing nano- and microscale domestic natural green materials with polymeric materials. In current research, the authors are aiming to share in solving the existing problem of degradation without using chemical stabilizers or antioxidants. It is through changing the polymers to nanocomposite with enhanced mechanical, fracture and thermal properties which can make it more durable and fracture–resistant by adding green nature nano and micro particles of Montmorillonite clay MMT and palm trees micro fibers. The authors expect better results than the antioxidants applications which may be registered as a patent. In another research phase, the authors may use an oxidants and stabilizers in addition to the domestic green natural material to check the differences. The research proposes nanocomposites of nanoclay and palm fobers based polymer nanocomposites using a melt-processing method with the addition of specified ratios of nanoclay particles and palm tree microfibers by mixing them using a twin extruder and high shear mixer as shown in Figs (4, 5). This method helps to prevent environmental pollution and will benefit the economy, as well as reducing degradation problems and solving the problems associated with traditional polymer composites. The bionanocomposites are made of the new nanoclay–palm tree microfiber / polymer nanocomposites. The research is experimentally. Characterizations and testing of the materials are carried out in the laboratory and in the field. The main techniques used for characterization depend on scanning electron microscope SEM, and tests are performed for mechanical and fracture properties in addition to checkingof the thermal effects. Additives of antioxidants and stabilizers can represent some type of contamination but it is known that antioxidants and stabilizers represent very few amount which their effect can be ignored and accepted in the polymers without affecting the final product. For the same reason, additional antioxidant and stabilizers may be not added to the polymer during process to minimize the effect of these additives on the mechanical and fracture properties of the final product. But anyway, adding it to the polymer matrix has no bad effect since it is very small ratio. In case of using wastes or recycled polymers, for avoiding any deterioration of mechanical and fracture properties mainly or any other property of the final product of HDPE, LLDPE and HDPE/LLDPE, due to excess of antioxidants or stabilizers additives, we minimized it or preventing it at all in some samples for checking and testing purposes. The solid and liquid contaminations should be removed easily while melted contamination will make a big problem for removing by methods such as the sink and float method. The liquids or the contaminations which can be melted in water such as dust, soil, ink, or others can be removed by the washing. The antioxidants and stabilizers used in the current research are CESA Antioxidant PA-31 and CESA uv stabilizer PA-788-51 produced by CLARIANT. The structure of the Montimorillonite MMT type consisting of two layers of tetrahedral atoms of silicon sandwiching one layer of octahedral atoms of aluminum. It is known that anti-oxidants and stabilizers represent very few amount which their effect can be ignored and neglected and can be accepted in the polymers without badly affecting the final product. For the same reason, additional antioxidant and stabilizers may be not added to the polymer during process to minimize the effect of these additives on the mechanical and fracture properties of manufactured nanocomposites.

Materials

The main materials used in the research are polymer systems (HDPE), nanoclay of montimorillonite type MMT, and palm date fibers.

1. Polymers

The polymer systems are HDPE. They are collected and classified, then granulated and grained to powder. Then, they are extruded with adding nano clay (5%) to enhance both of the mechanical,

thermal properties and fracture properties. Adding palm tree fibers (5%) to the polymers only or to the nanoclay and polymers will enhance the thermal properties.

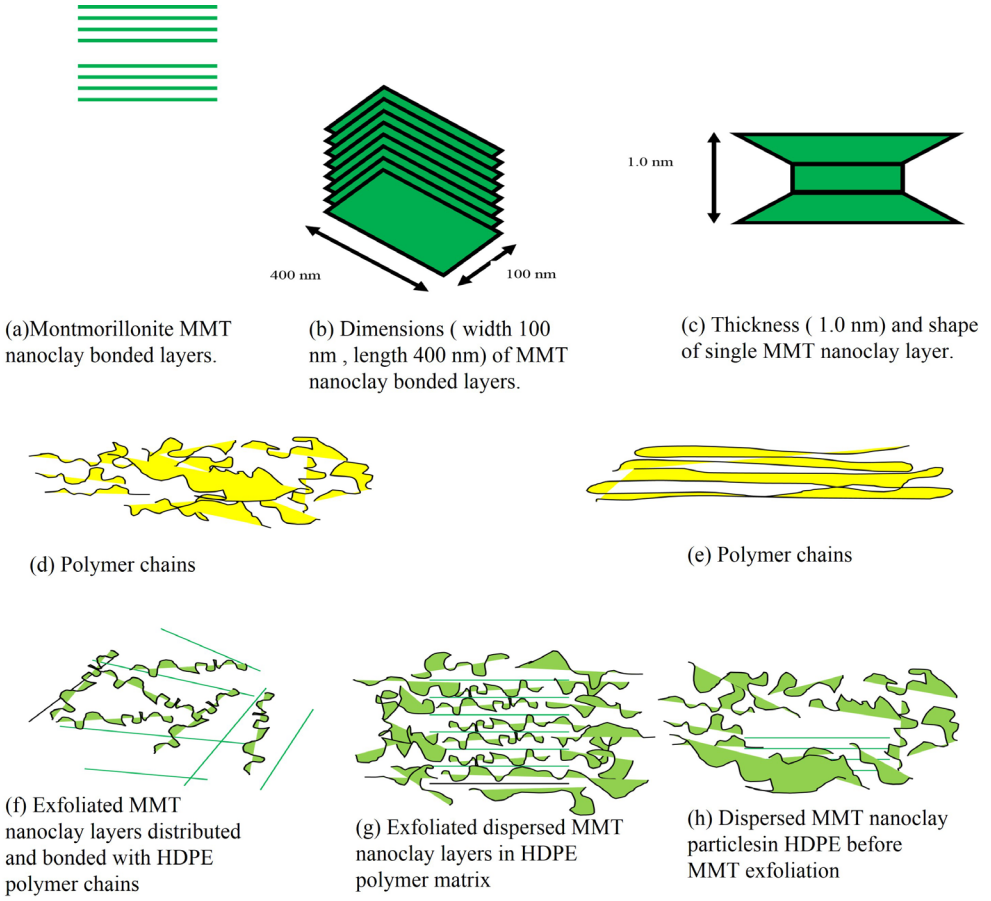

Fig. 4 Nanoclay layers, agglomerated nanoclay particle, nanocly layer, HDPE exfoliated nanoclay, Intercalated nanoclay dispersed in the polymer matrix, and agglomerated nanocly.

2.Nano clay

Structure of MMT consists of as shown in Figs. (4). MMT particle consists of one aluminum sheet sandwiched between two silicon sheets, as shown in Fig. (4). Clay sheets are bonded together in agglomerated particles by the effect of moisture or wetting from any source since it is strongly hydrophilic material. Clay can just be exfoliated to layers of (1.0 nm) thickness if it is mixed with high shear mix process by using device like co-rotating or counter co-rotating twin screw extruder or roll mill. The nano composite made of polymer and nanoclay can only be made if the clay particles are separated in layers with insertion of the nanoclay layers in the polymer and in the same time intercalation of polymers between the nanoclay layers.

3.Palm tree fibers

Palm tree fibers is produced by collecting the fibers leaves and fronds fibers of the palm tree which are available in all areas of Saudi Arabia. Then it will go through some steps of preparation until producing it in final form of micro and nano fibers. It is collected from the palm trees fronds as dry or green. Then the green palm tree fronds are left in the sun until drying naturally then it is washed and cleaned. All of them are dried in an oven with low temperature. Then it is grinded using grinding machine. Then it is sieved to pass through sieve # (400) of size < 38 microns. The passing material is used in the composite by mixing it to the polymer through the twin screw extruder through adding it mechanically by putting it in the side feeder while the polymers are in the main feeder (Fig. 5). The extruder and feeders are under computer control, as shown in the figure (5). The non passed fibers through the sieve are grinded once again for the same use.

Fig. 5 Computerized lab station operating co-rotating twin screw extruder, and CPNC nanocomposite samples

4.Clay polymer nanocomposite and palm tree fiber

The product material of the extruder is in the form of grains or powder. Then the powder is used in the casting and molding of the bionanocomposite sheets and plates for testing of mechanical fracture and thermal properties. The bionanocomposite samples include layered and non layered bionanocomposites to simulate the dental biomaterials for different orthodontics applications like crowns, bridges and complete dentures. It also is checked under variable and constant temperatures. The materials also are tested for each of mechanical and fracture properties in addition to the microstructure investigation. We do not add other additives like stabilizers or antioxidants for uv or others because adding more antioxidants or stabilizers may badly affect the mechanical properties or other properties like producing cracks and fractures.

Preparation Steps of Bio-CPNC

The preparation of the polymers go through several steps before preparation for extruding to prosuce the bionanocomposites. These steps include each of collecting of the polymers with Identification and classification of the polymer, preparation for grinding to grains or pellets with collecting the grinded materials and then producing it in the shape of powder, preparation of nanoclay, preparation of palm tree fibers, extruding with mixing the nanoclay, extruding with mixing the palm tree fibers, extruding with mixing of both nanoclay and palm tree fibers. Then , it is followed by re-extruding of the nanoclaypolymer composite with adding the palm tree fibers, some cases are extruded for producing sheets and plates which are made to test the mechanical, fracture and thermal properties, sample are designed as layered nanocomposite and tested to check the effect on temperature changes. Some samples are tested under variable cyclic tempreature degree as shown in figures (10-12), while others are tested under effect of constant temperature degree as shown in figure (13). The main equipment and devices for processing, characterizations, processing and testing include computerized twin screw extruder with (L/D = 40) where (L) is length of each screw and (D) is the diameter of each screw, with five temperature zones, computerized granulator, computerized mixer, and pelletizer as shown in figure (5). The characterization and testing equipment include mainly scanning electron microscope SEM and displacement control Universal testing machine for mechanical and fracture properties testing.

Testing, Results, Analysis and Characterization

The research procedures and techniques include the experimental work, characterization and testing. The experimental program included each of procurement of clays and polymers, materials preparation, and processing of the nanocomposites, using a twin extruder, mixer, water bath and granulator. The characterizations will include analyses using of SEM microscope. The tests include mechanical properties testing, fracture properties testing, and thermal properties testing. Mechanical properties testing and results are shown in figures (6, 7, 8,) and table (1). Also, testing of fracture properties as fracture toughness is carried out as shown in figures (9, 10, 11) and table (2). In addition, testing of thermal effects are checked as shown in figure (12,13), while microstructure morphology is shown in figure (14) for each of HDPE, MMT nanoclay, micro fibers of palm tree, CPNC and bio-CPNC.

1.Mechanical properties

Testing method and details are introduced for investigating of mechanical, fracture and thermal properties. The testings are carried based on the ASTM international standard specifications for plastics testing for each of testing of Mechanical properties as mainly tensile strength. The mechanical properties testings are based on ASTM D638 standards for testing of tensile strength using dumbbell-shaped specimens as shown in Figs. (6, 7, 8) and table (1). The mechanical properties test investigated that the results of bio-CPNC are enhanced better than the original pue polymers with large ratio of about (70%), as shown in the figures of stress-strain relations and table (1) indicating the enhancement and change ratios of the results which are included in the table (1) and calculated based on the equation (1).

$$Enhancement\ (change) ratio\ = [\frac{BioCPNC\ result - Original\ HDPE\ result}{Original\ HDPE\ result}]\% \quad (1)$$

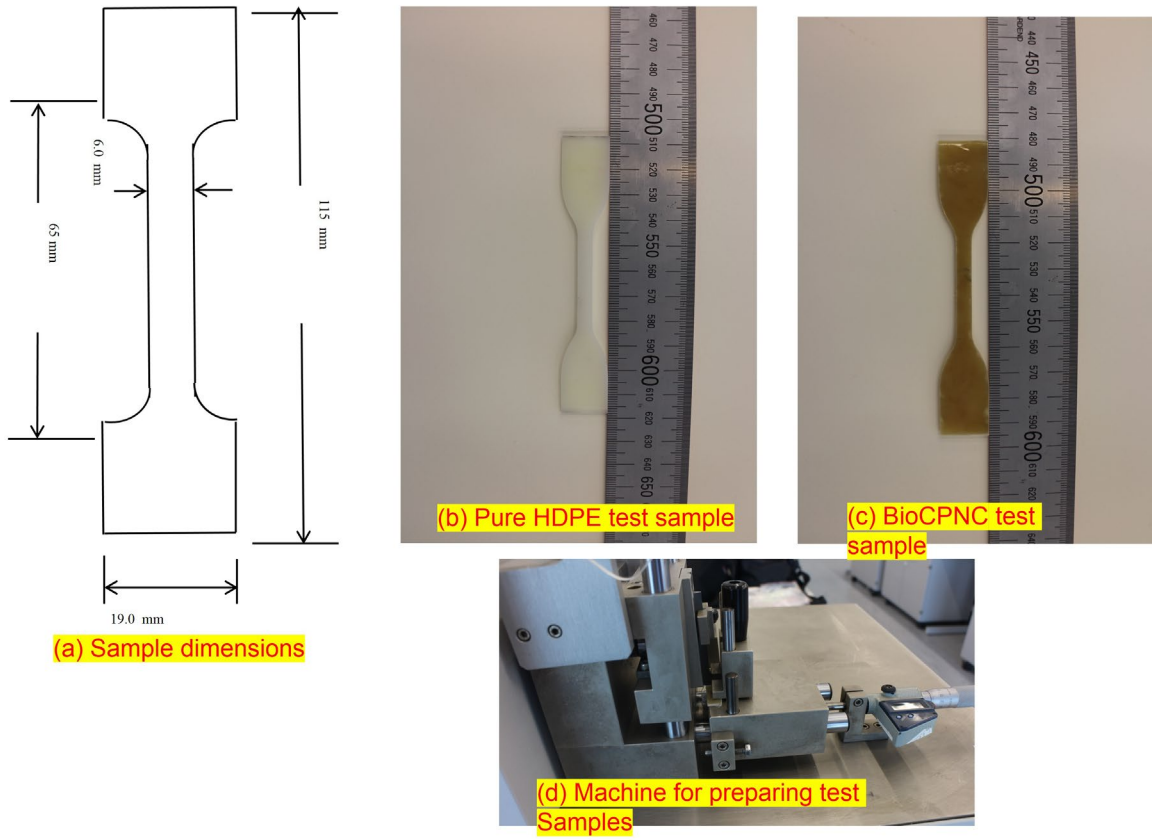

Fig. 6 Dumbbell-shaped specimen for tensile test ASTM D638: (a) sample dimensions based on ASTM standard, (b) Test sample for pure HDPE, (c) Test sample for pure BioCPNC , (d) machine for cutting the test sample based on ASTM D 638 standard

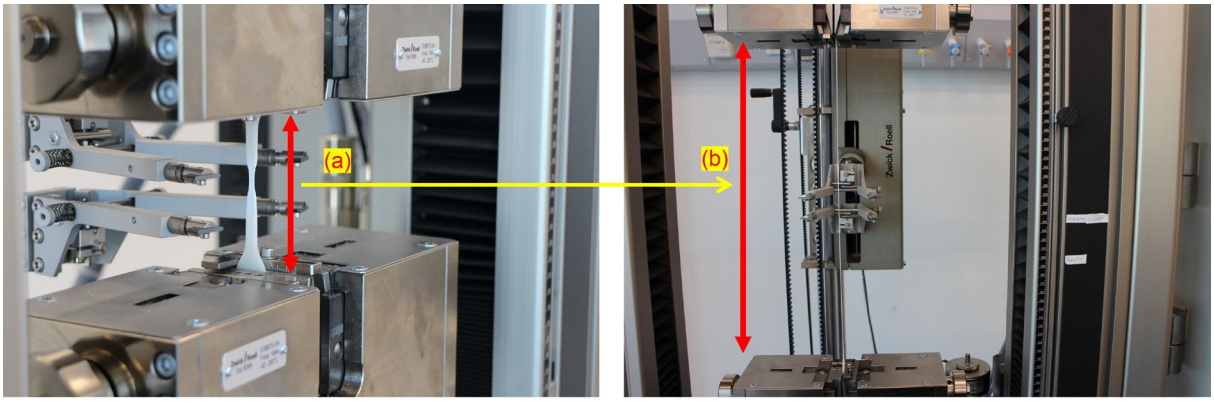

Fig. 7 Tested sample of pure HDPE under tension load showing the deformation and elongation during testing

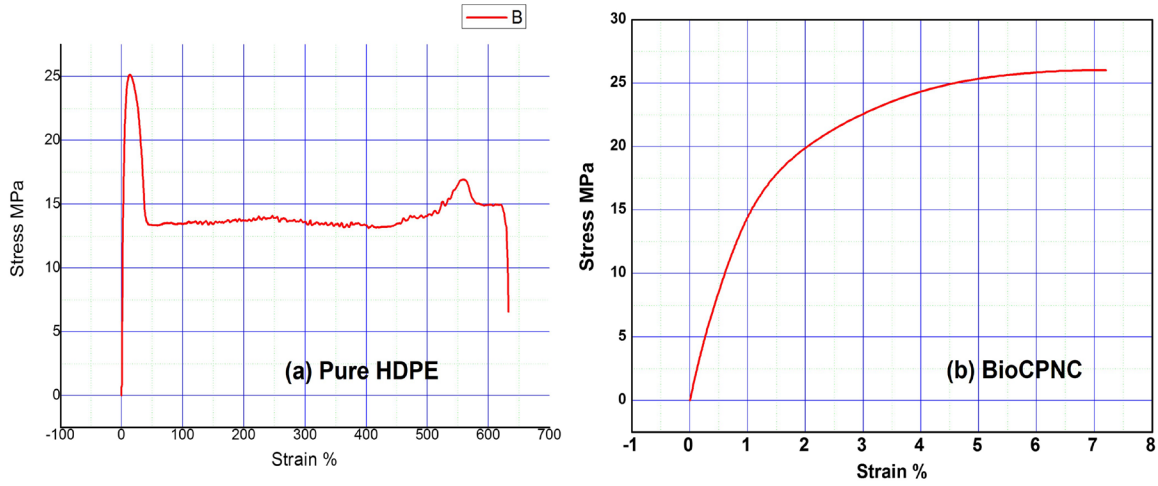

(a) Stress-strain of tensile for pure HDPE (b) Stress-strain of tensile for BioCPNC

Fig. 8 Stress-Strain curves for tested samples of: (a) pure HDPE and, (b) BioCPNC for tensile test based on (ASTM D638)

Table 1 Mechanical properties testing showing the enhancement of bio-CPNC properties in comparison to pure HDPE properties.

Property	Pure (High density polyethylene) HDPE Polymer matrix	bio-CPNC Bionanocomposite made of (95%(HDPE)Polymer + 3% MMT nanoclay + 2%(palm tree micro fibers)	Enhancement (Change) ratio% as Eq. (1) $Enhancement\ (change) ratio = = [\frac{BioCPNC\ - Original\ HDPE}{Original\ HDPE}]\%$
Tensile strength at break (Mpa)	15.5	26.5	$[\frac{26.5-15.5}{15.5}]\% = 70\%$ (Large increase of tensile strength)
Elongation ratio %	630	7.4	$[\frac{7.4-630}{630}]\% = -98\%$ (Large Decrease of elongation)
Young's modulus of elasticity (E)	1188	1959	$[\frac{1959-1188}{1188}]\% = 65\%$ (increase of Modulus of elasticity)

2.Fracture properties

Fracture properties testing are carried out based on ASTM D 5045 testing of fracture toughness based on using single edge notched specimens tested under 3-point load, shown in Fig.(9). Testing of fracture behavior of inclined cracks (mixed modes) based on the International specification and stress intensity factors with comparing it to result of Mode I specimens and non cracked specimens as shown in Figs. (9, 10, 11). The results of the fracture mechanics tests indicated that the fracture behavior is completely changed from to linear elastic fracture mechanics and elastic-plastic fracture mechanics EPFM where some cases can be considered as LEFM similar to brittle materials. The results are concluded and shown in table(2) and figures (9, 10, 11). The test was carried out for mode I crack to check the critical stress intensity factor at the crack tips due to the concentration of stresses under loading which may also called as fracture toughness K_{Ic}, as indicated by the equations (2, 3).

$$K_{Ic} = \sigma_{\chi} (\pi a)^{0.5} (F) \quad (2)$$

$$F= [1.07 (1 +3.03 a/b)] / [2 (3.14 a/b)^{0.5} (1-(a/b))^{1.5}] , \quad (3)$$

Where, (F) is correction factor for edge cracks in finite sheet under uniform tensile stress, (a) = half crack length, (b) = sample width, (σ_c) = critical stress at fracture. The sample dimensions are 120 mm length, 12 mm width and 2.0 mm thickness, half crack length (a) = 2.0 mm. The test for mixed mode cracks was carried out under the condition of plan stress fracture mechanics since the samples were made of thin sheets of thin thickness. Some samples were pre-cracked at the middle at the edge from just one side to be cracked with single edge crack of length a = 2.0 mm and crack width of about 0.3 mm. The elastic fracture energy G_f is calculated through equations (4, 5), for elastic energy release rate for plane stress condition.

$$G_f = (K_{Ic})^2/E \quad (4)$$

Where, G_f = Elastic energy release rate, K_{Ic} =Fracture toughness which equals critical stress intensity factor for mode I crack.

$$K_{Ic} = \sigma (3.14 a)^{0.5} \ [MPa (mm)^{0.5}/mm^2] \quad (5)$$

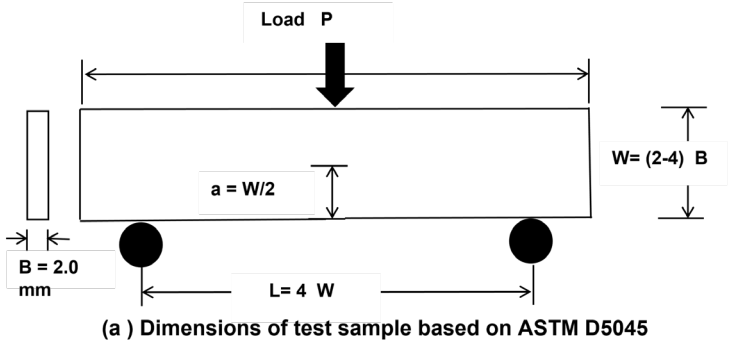

(a) Dimensions of test sample based on ASTM D5045

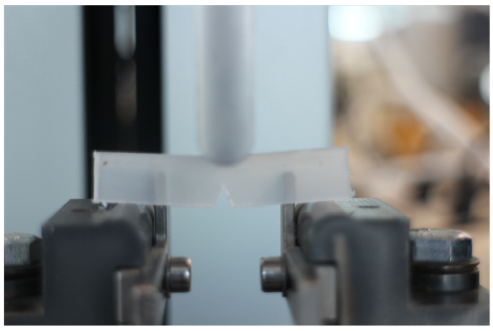

(b) Pure HDPE test sample under testing operation

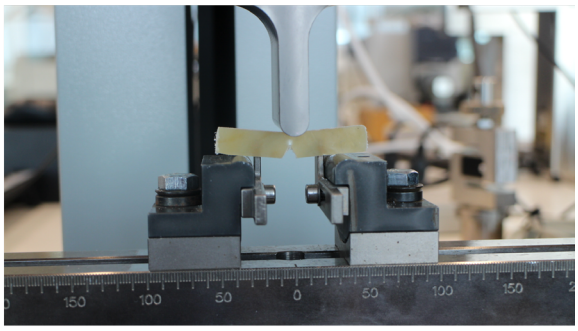

(c) BioCPNC test sample under testing operation

Fig. 9 Single Edge notch beam (Single edge crack) SENB test specimens for fracture toughness testing based on ASTM D5045 : (a) Standard specimen dimensions based on ASTM D 5045, (b) Specimen of pure HDPE under testing, (c) Specimen of BioCPNC under testing

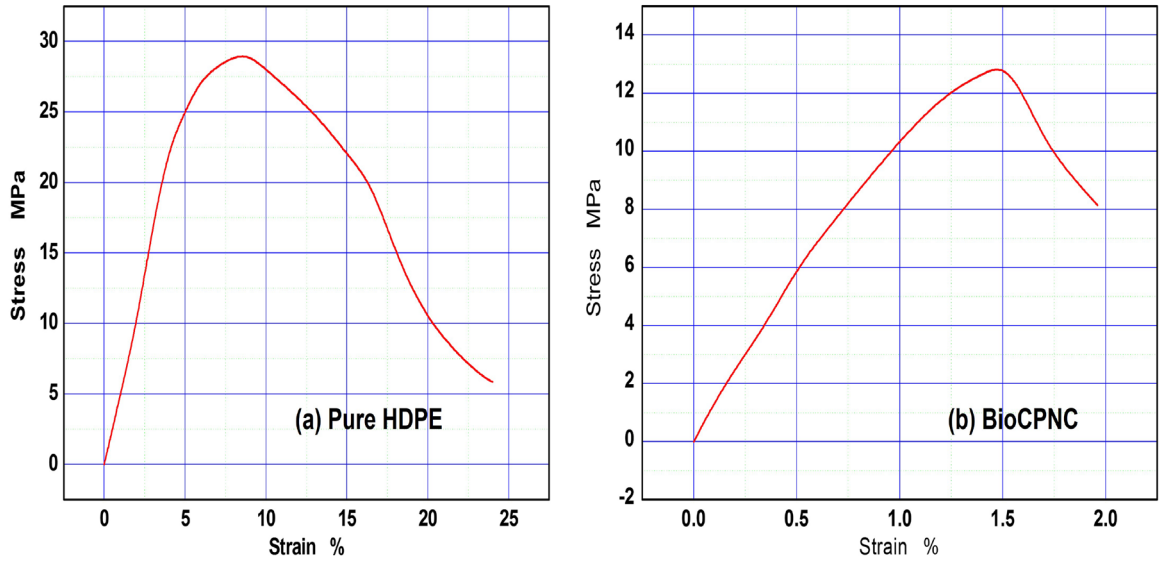

Fig. 10 Single Edge notch beam (Single edge crack) SENB test specimens for fracture toughness testing based on ASTM D5045 : (a)Specimen of pure HDPE under testing, (b) Specimen of BioCPNC under testing

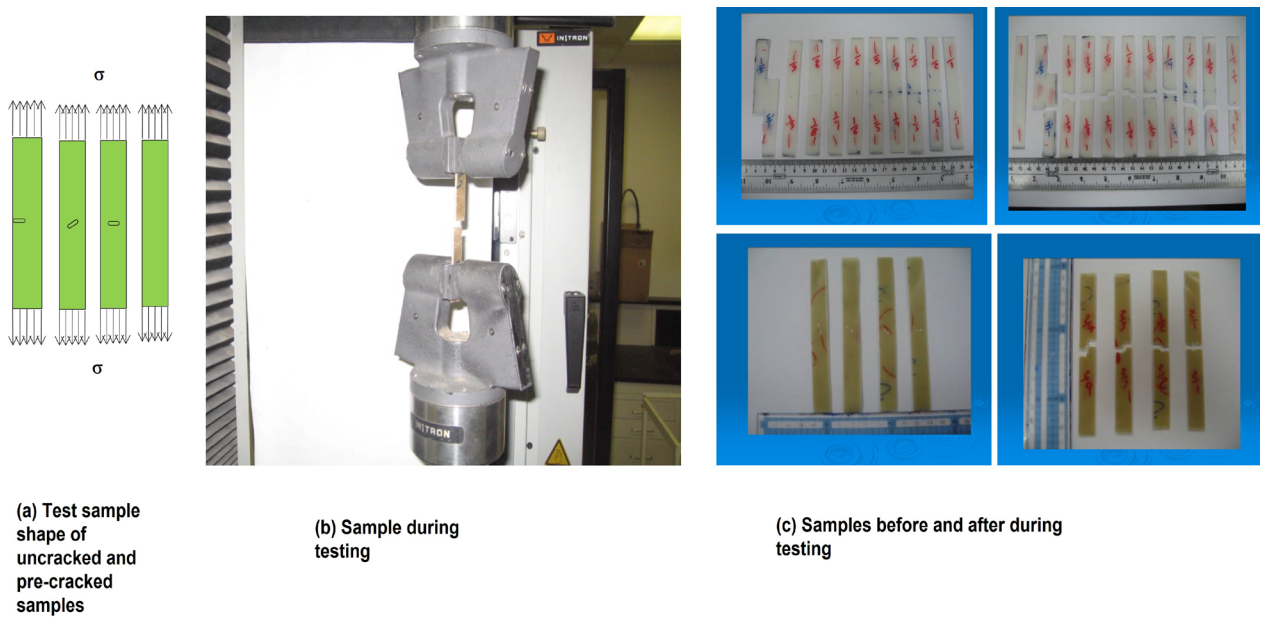

Fig. 11 Test specimens of modeI, mixed modes fracture for internal and edge cracks in addition to testing of uncracked specimen of pure HDPE and BioCPNC: (a) Test speciments shape, (b) test specimen under testing operation, (C) tested specimen before and after testing

As shown in Figure (11) , it is presenting the dteailed fracture test procedures for mixed mode cracks under tension and samples of pre-cracked pure HDPE and Clay-Palm tree fibers-HDPE BioCPNC nanocomposite, Pure HDPE pre-cracked samples before testing, during testing and after testing.

Table 2 Fracture properties testing showing enhancement of bio-CPNC properties in comparison to pure HDPE.

Property	Pure (High density polyethylene) HDPE Polymer matrix	bio-CPNC Bionanocomposite made of (95%(HDPE)Polymer + 3% MMT nanoclay + 2%(palm tree micro fibers)	Enhancement (Change) ratio% $Enhancement\ (change) ratio = = [\frac{BioCPNC\ - Original\ HDPE}{Original\ HDPE}]\%$
Fracture toughness (K_I) (Mpa. $(mm)^{0.5}$	54	62	$[\frac{62-54}{54}]\% = 15\%$ (increase of fracture toughness)
Elastic Fracture Energy (G_f) (Mpa.mm)	3.72	10.33	$[\frac{10.33-3.72}{3.72}]\% = 177\%$ (Large increase in fracture energy)

3.Thermal properties

Thermal properties Testing include testing of the thermal behavior of the layered bionanocomoosite under cyclic variable heating-cooling and constant temperature degrees for the samples designed and produced of composed layers of bio-CPNC made of HDPE, MMT nanoclay and palm tree mico fibers as shown in the model in Fig. (12) layered cross section of bionanocomposite of polymer matrix, palm-tree fibers and nanoclay particles, where figures (13 a, 13b, 13c) show the results of the tests. Regarding the quality of product lifetime, thermal, mechanical and fracture properties are studied in addition to the characterization of microstructure morphology of the hogenity, distribution showing the well distribution and bonding. Filler of nanoclay particles will enhance mechanical, fracture and thermal properties while palm tree micro fibers will enhance additionally the thermal properties of the polymer matrix. The exfoliated Nanoclay layers will intercalate and strengthen the polymer matrix by connecting between the polymer chains as reinforcement layers. It can reduce the possibility of crack nucleation by closing the cracks produced during manufacturing stage. It can close the pre-existing internal cracks by interlocking between the crack surfaces. Therefore, nanoclay helps in enhancement of mechanical and fracture properties. This result will enhance the lifetime of the nanocomposite making it longer than the lifetime of pure polymer matrix. Results of cyclic tests of thermal effect on bio-CPNC bionanocomposite made of polymers matrix and MMT nanoclay-palm tree fibers indicate that when the teprature degree of the surrounding climate was about (32) ^oC degree, the bio-CPNC can reduce it to be between (15 to 18) ^oC degrees only, as shown in figures (13a, 13b, 13c). Under cyclic thermal changes when the climate temperature degree was between (3 to 4)^oC degrees, the bio-CPNC containing nanoclay and palm tree fibers could change the temperature effect to be about (13-14) ^oC degrees as shown in figures (13a, 13b, 13c). These reseults of cuclic tests show that the bio-CPNC can control and prevent the temperature effect to be almost constant temperature suitable for human use and for keeping the dental materials of orthodontics, crowns, bridges and implanes safe from severe temperature changes and make the human teeth and human health safe. Regarding the tests under constant temperature as shown in figure (13), it shown that the bio-CPNC material could control the temperature changing to reach at (37) ^oC degrees after (72) hours exposure to effect of constant temprature of (40) ^oC degrees, while the normal polymer material of HDPE and LLDPE reached the (37) ^oC degrees temperature after just (4) hours exposure to thae same degree under same conditions. The tests under both cyclic or constant temperature degree show thae big difference between Bio-CPNC and other materials for controlling the temperature effects.

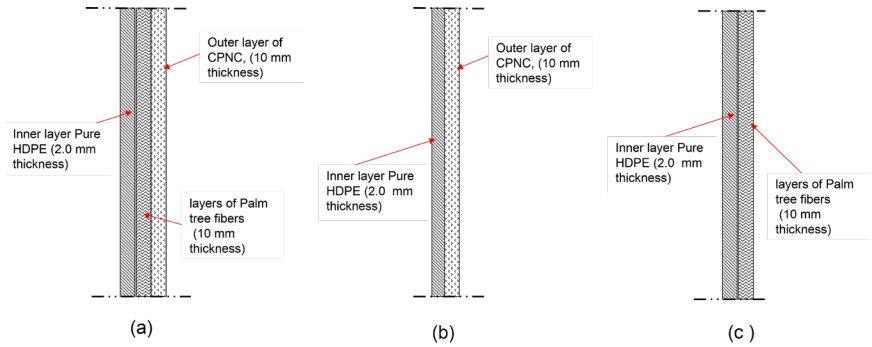

Fig. 12 Critical cases of designed layered-BioCPNC samples of BioCPNC of HDPE polymer matrix, palm-tree fibers and MMT nanoclay particles, which tested for thermal properties examination.

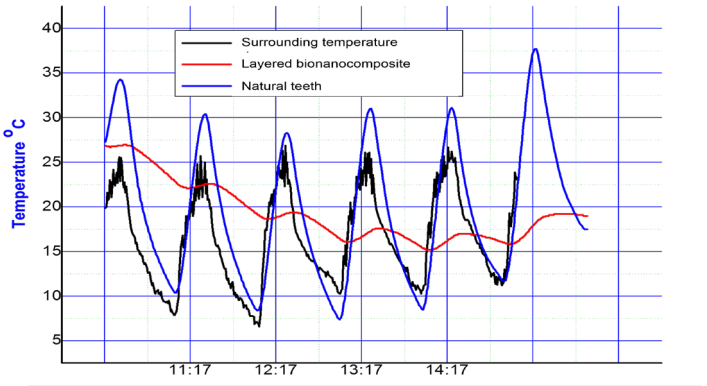

(a)

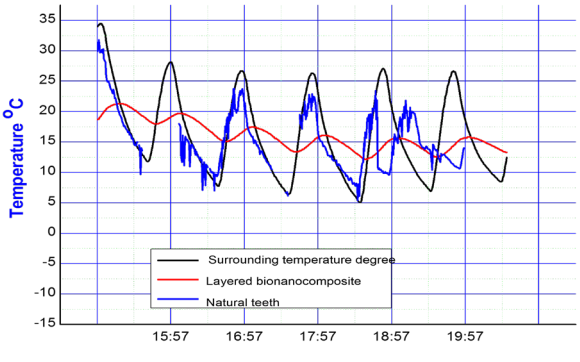

(b),

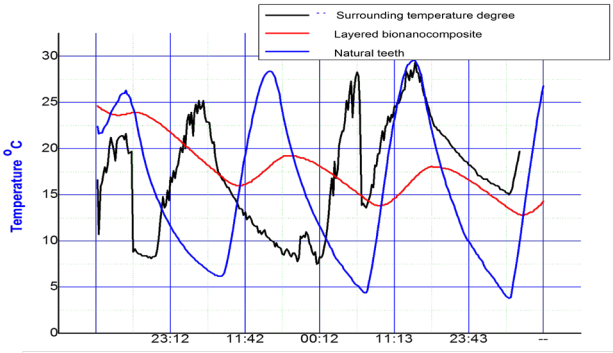

(c)

Fig. 13 Thermal test results: (a) Results of palm tree fibers thermal effect tests on temperature effect, (b) Results of Nanoclay thermal effect tests on temperature changes, and (c) Results of Nanoclay-palm tree fibers thermal effect tests on temperature changes under variable temperature degrees showing the relations between temperature degree (^{o}C) and time (hrs)

4. Microstructure Characterization using SEM

The microstructure morphology of each of HDPE, MMT-nanoclay, palm-tree fibers CPNC and Bio-CPNC made of HDPE-MMT- palm tree fibers are examined as shown in Fig. (14) included the clear difference between particles types, size and dimensions, bond between particles without defects or cracks which proove the development and enhancement of the mechanical and fracture properties whown in tables (1, 2) and relations between stres and strains of tested samples. HDPE powder (SEM), Melt HDPE (SEM), Clay/polymer nanocomposite, Clay/polymer nanocomposite (SEM), MMT Nanocly layers (SEM), MMT nanoclay layers (SEM), Palm tree fibers microstructure , and Palm tree fibers (SEM) shown in Fig. (14) are showing new results of processing of the natural nanomaterials to develope green bio-nanocomposite. Regarding the materials, the main materials which used in the research are polymer systems HDPE, nanoclay (Montimorillonite type MMT) and palm date fibers (micro fibers of size less than 38 micron). The polymers include the most famous types and applied which are HDPE. The materials are collected and classified and grained to powder. Then they are extruded with adding nano clay (5%) to enhance both of the mechanical and thermal properties in addition to enhancing of the fracture properties. Adding palm tree fibers (5%) to the polymers only or to the nanoclay and polymers will enhance the thermal properties.

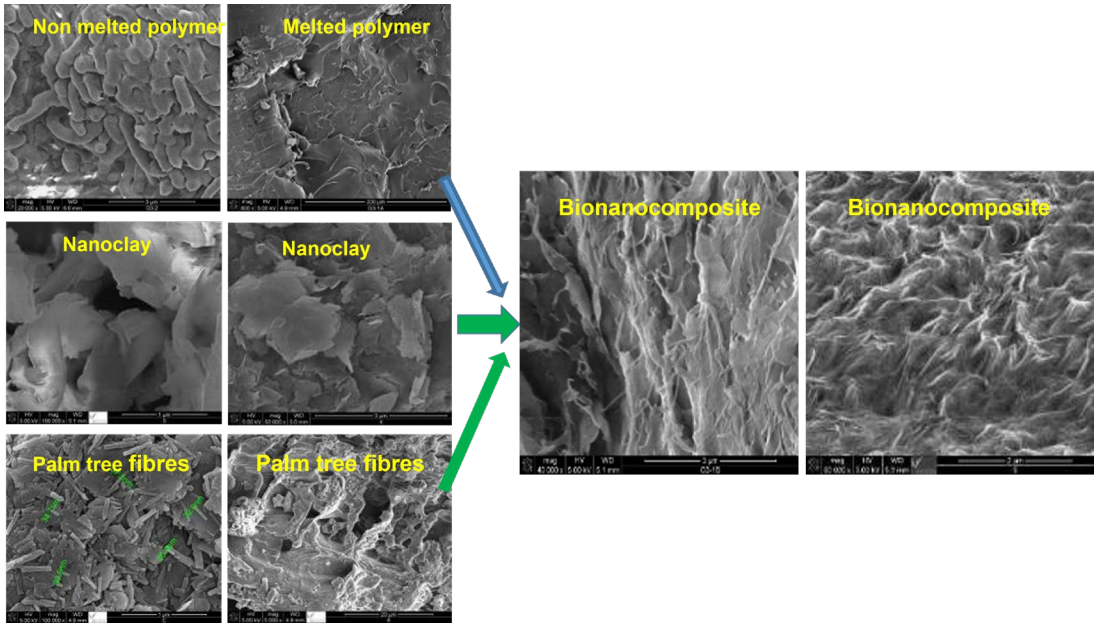

Fig. 14 HDPE powder (SEM), Melt HDPE (SEM), Clay/polymer nanocomposite, Clay/polymer nanocomposite (SEM), MMT Nanocly layers (SEM), MMT nanoclay layers (SEM), Palm tree fibers microstructure , and Palm tree fibers (SEM).

Discussion

Regarding nanoclay, MMT nanoclay particles structure consists multi-layered particles bonded to each others where MMT clay particle consists of one aluminum sheet sandwiched between two silicon sheets, as shown in Fig. (4). Clay sheets are bonded together in agglomerated particles by the effect of moisture or wetting from any source since it is strongly hydrophilic material. Clay can just be exfoliated to layers of 1.0 nm thickness if it is mixed with high shear mix process by using device like twin screw extruder or 2 or 3 roll mill. The nano composite made of polymer and nanoclay can only be made if the clay particles are separated in layers with insertion of the nano clay layers in the polymer and in the same time intercalation of polymers between the nano clay layers. Therefore the nano clay layers should be exfoliated by the method of high shear mix through the extruder as shown in the figure (5). We have a new advanced and computerized twin screw extruder of L/D= 40 screws and five zones of temperature with advanced data acquisition system as shown in the Fig. (5). Nanoclay is natural or synthesized material in the powder shape with particle thickness is one nanometer. It has very special and unique properties in several aspects such as unique structure, high aspect ratio, large surface area, mechanical and thermal properties. These unique properties make it

convenient for manufacturing advanced green nanocomposite. Clay layers can be exfoliated or delaminated to separate platelets as shown in Figs (4). The properties of these platelets include geometry with dimensions of thickness = (1 nm), Width = 100 nm, length=400 nm, aspect ratio (width/thickness - length/thickness) = 100 – 400, surface area = 700 – 800 m^2/g, coefficient of linear thermal expansion= 5.9 (10^{-6} m/m.K), specific heat capacity=920 (J. $kg^{-1}.K^{-1}$), and thermal conductivity factor=0.15 (W/m.K). It is applied in many fields of advanced technologies and industries such as automobiles, aerospace, electronics, electrical devices, constructions, packaging, coating, medicine, biomedical engineering, ….etc. The production of nanocomposite material goes through several stages of preparation, mixing and processing. There are several methods for the processing such as mixing the nanoclay during polymerization process, Sol-Gel method and melt processing method. The most suitable method of processing for polymers is melt processing technique. The main general approach to produce clay/ polymer nanocomposites is to disperse exfoliated nanoclay layers (filler) in the polymer (matrix), as shown in figure (4). Palm tree fibers are produced by collecting the fibers leaves and fronds fibers of the palm tree. Then it will go through some steps of preparation until producing it in final form of micro and nano fibers. It is collected from the palm trees as dry or green. Then the green fronds are left in the sun until drying naturally then it is washed and cleaned. All of them are dried in an oven with low temperature. Then it is grinded using grinding machine. Then it is sieved to pass through sieve # (400) of size < 38 Micrometer. The passing material are used in the composite by mixing it to the polymer through the twin screw extruder through adding it mechanically by putting it in the side feeder while the polymers are in the main feeder. The extruder and feeders are under computer control, as shown in the figure (5). The non passed fibers through the sieve are grinded again for the same use. The effect of each of nanoclay and palm tree fibers on the polymers in the developed bionanocomposites in the tested samples for temperature effects was checked by using layered system of nanoclay and palm date fiber separately and together. The presults are shown in the figures (10-13). In current paper, the materials are very cheap since we are using polymers and natural green Saudi materials of nanoclay and palm tree fibers. In addition it can be used in many applications since it enhance not only the thermal properties but also the mechanical and fracture properties. The main properties of the palm dates fibers areincluding each of coefficient of linear thermal expansion= 3.7- 5.4 (10^{-6} m/m.K), specific heat capacity=1800 ($J.kg^{-1}. K^{-1}$), thermal conductivity factor = 0.17 (W/m.K). The effect of fibers on the thermal behavior is shown in Figs. (12, 13). The produced Bio-CPNC material of the extruder is in the form of grains or powder. Then the powder is used in the casting and molding of the test samples. The samplesy are composed of several layers. Then, the samples are tested to check the thermal properties effect of temperature changes under both variale and constant temperature degrees.. It also is checked under constant temperature in the lab in special control room. The materials also are tested for each of mechanical and fracture properties in addition to the microstructure investigation. Regarding the steps of the study, polymers went through several steps before preparation for extruding and graiding as collecting of the polymers, identification and classification. Collecting the grinded materials and then producing it in the shape of powder. Then, the other steps include each of preparation of nanoclay, preparation of palm tree fibers, and then extruding with mixing both of the nanoclay, and palm tree fibers. Extruding with mixing both of nanoclay and palm tree fibers (re-extruding of the nanoclay polymer composite with adding the palm tree fibers, Then, sheets and plates of bio nanocomposites are made to test the mechanical, fracture and thermal properties, as shown in figure (12,13). Sample are made for characterization of microstructure morphology , homogenity, distribution and bond. Some samples are tested to check the effect of temperature changes under both variable and constant temperature degrees, as shown in figures (12, 13). Some cases are produced using nano clay and palm tree fibers without surfactants while other cases will produced using surfactant of octadecylamine. The surfactant of the nanoclay is organic material. Since the nanoclay and palm tree fibers are hydrophilic and thermosetting material while polymer systems are hydrophobic and thermoplastic the nanoclay and palm tree fibers are better to be surface modified by surfactant for bonding reason to the polymers. It is usually known that the degradation of polymers accelerates the failure process of the final product. Therefore, the polymers are reinforced with nanoclay sheets to reduce the fracture and degradation. It will make bond to the polymer through the surfactant layer of the nanoclay. The

nanoclay layers are modified by surfactant organic layers of Octadecylamine [my paper] which facilitate the bond with the HDPE. It will reduce or prevent the cracks and increase the mechanical (such as tensile strength, hardness), fracture properties (such as fracture toughness, crack propagation, crack initiation, crack branching,…) and thermal properties (such as linear thermal expansion factor, thermal conductivity factor, and specific heat capacity). Some test samples are designed as layered composite where the samples layers made of bionanocomposite as shown in figure (12). Some samples were tested under constant temperature degree, while the others are tested under effect of variable temperature degree as shown in figures (12, 13). The results show the effects of nanoclay and palm tree figers on the changes of the temprature where the bionanocomposite materials are reinforced by nanoclay and palm tree fibers with very small ratios as shown in Figs.(12, 13). Nanoclay is added as (5%) by weight. Also, different ratios of palm tree fibers have been added such as 5-20%. The research work is using mainly of the recycling of clean polymers. For avoiding any bad effect of possible presence of contaminations on the mixing process or product of bionanocopmpsite, the research took into consideration polymers without contaminations. Any contaminations presence in the polymers will produce weak points and cause stress concentration which will produce plastic zones and fracture when the stresses reaches the critical value at the vicinities of the defects. This means it will produce fracture process and failure. It also represents the main cause of the deterioration of the mechanical properties in addition to the fracture properties. The most common method of the separation is the float-sink method. Any contaminations are removed if it found by identification, classification and then removal, cleaning, washing and drying steps can be done for the polymers. Removal of possible contamination is very important for purity of the final product. For checking the thermal properties effects of each of nanoclay and palm tree fibers in order to be sure that the results of the research are promising for both of thermal insulation effects and cracking resistance effects, two simple experiments were done. First test for checking the fracture mechanics resistance by comparing between samples made of pure polymers and others made of CPNC made of HDPE mixed with (5%) nanoclay and palm-tree fibers. For testing the thermal effects of nano clay and palm tree fibers, samples are made to check the effect of each of nanoclay and palm tree fibers on temperature as shown in figures (12, 13). As a test example, temperature decrease from 32 ^{o}C to be 18 ^{o}C and keep it at 14 ^{o}C when surrounding temperature is at 3 ^{o}C. This phenomenon is clear in the figures (12,13). Adding 5% of nanoclay to the polymer systems HDPE can enhance the mechanical and thermal properties by about (70%). Adding the same ratio of palm tree fiber can enhance the thermal properties. Therefore we made layers composed of NC only to enhance the mechanical properties. In the same time we made another layers made of Polymer and nanoclay and palm tree fibers and make a layered composite of these two systems. The polymers are HDPE by different ratios to enhance the ductility of HDPE producing brittle-ductile nanocomposite. Usually polymers like HDPE include antioxidants and stabilizers, therefore we did not add stabilizers or antioxidants because it can cause deterioration of the properties. Effects of contaminations on the nanocomposite processing of HDPE, will produce defects. Therefore, polymers should be free of contaminations where the contaminations presence produces weak points and causes stress concentrations which produce fracture and failure. It also represents the main cause of the deterioration of the mechanical and fracture properties. Therefore it must be avoided in processing of nanoclay-palm tree fibers bionanocomposite. The enhancements of the thermal and mechanical properties of polymers are described by some experiments which are made for this aim mainly during the last months to check its ability. Regarding the test of mechanical properties as shown in figures (7, 8, 9) and table (1). It is proved that mechanical properties are enhanced wherethe tensile strength at break is enhanced from (15.5 Mpa) to (26.8 Mpa), Young's modulus is changed from (1188 Mpa) to (1959 Mpa), and the ultimate elongation is changed from (560%) to (28%). Regarding the fracture properties tests as shown in figures (8, 9, 15) and table(1), it is shown that the fracture toughnes; critical stress intensity factor (K_{Ic}); is changed from (54 Mpa $(mm)^{0.5}$) to (62 Mpa $(mm)^{0.5}$) while the elastic fracture energy (G_f) is changed from (3.72 Mpa .mm) to (10.72 Mpa .mm). The microstructure investigations for morphology, homogenty, distribution, bond between particles, it is shown from the results in fuger (14). Regarding the microstructure morphplogy of the raw materials and nanocomposite products as shown in figure (14). It is investigated by scanning emession

microscope SEM. The figure (14) includes each of microstructure morphology, homogenty, distribution, bond between particles and there are no defects or cracks. It is showing the converting of the polymers, nanoclay and palm tree fibers powders to homogenous bio-nanocomposite. The bio-nanocomposite has uniform distribution of theparticles of nanoclay and palm tree fibers within the melted particles of polymers. It proves the the well despersion and bonding.

Conclusion

Through the methodology of the idea of manufacturing new bionanocomposite material for mainly denestry applications and results of each of the mechanical, fracture and thermal properties the research, it is proved that the current new bionanocomposites is promising for dental applications including different types. In addition to the main aim of bionanocomposite made of palm-tree fibers, nanoclay and polymers for the denestiry applications of orthodontics like crowns, bridges, implantes and complete denture, the nanocomposite products of the research can be applied in many fields like thermal insulators, packaging, wires and rods, textiles and threads, sheets and plates, tents , cover of computers, 3-D printers, and many other applications The results of this research are very important because the results will have a significant impact on the denestiry fields, medical fields and environment with providing new job opportunities for assisting the economy. They adversely affect health by solving the important dental, meciacl and environmental problems for practically protecting human health through using new technologies and domestic materials of polymers, nanoclay, and palm tree microfibers, to produce stable, highly functional nanocomposites with good mechanical fracture and thermal properties for orthodontics..

Authors statement

Both of the two authors R. El-Sheikhy and A. Alkhuraif participated with same role in all aspects of the manuscript.

Acknowledgments

The authors extend their thanks to Researchers supporting project number (RSP2024R31), King Saud university, Riyadh, Saudi Arabia.

Declaration of interests

The authors declare that they have no known competing financial interests or personal relationships that could have appeared to influence the work reported in this paper.

References

[1] T. Shigemori, M. Okamoto, S. Yamasaki, H. Hayami, Direct melt neutrization and nano-structure of polyethylene monomer-based nano-composites, Composites: Part A, 39, 1924-1929 (2008)

[2] N. Sheng, et. al., “Multiscale micromechanical modeling of polymer/clay nanocomposites and the effective clay particle” polymer 45, 487-506, (2004).

[3] J. Woe, H. Sue, “Effects of clay orientation and aspect ratio on mechanical behavior of nylon-6 nanocomposite”, Polymer 46, 6235-6334, (2005).

[4] Refat El-Sheikhy, Abdulaziz Alkuraif, Mosleh Al-Shamrani, “Converting polymer wastes to nanocomposites”, Vacuum, Vol. 217 (2023).

[5] Refat El-Sheikhy, Exploring of new natural Saudi Nanoparticles, Nature: Scientific Reports, Vol., 10, p. 1-12, 2020.

[6] T. Saito, M. Okamoto, R. Hiroi, M. Yamamoto, T. Shiroi, "Poly (p-phenylenesulfide)-based nano-composite formation: Delamination of organically modified layered filled via solid-state processing"; Polymer, 48, 4143-4151(2007)

[7] N. Sheng, et. al, " Multiscale micromechanical modeling of polymer/clay nanocomposites and the effective clay particle", Polymer 45 , 487-506, (2004).

[8] Q. H. Zheng, et. al, " Clay –based polymer nanocomposites: Research and commercial Development", Journal of nanoscience and nanotechnology, Vol. 5, 1574-1592, (2005).

[9] Refat El-Sheikhy, "Resisting of environmental pollution diseases", Scientific Reports, Vol., 13, pp.1-27, 2023.

[10] Sheng, et. al., "Multiscale micromechanical modeling of polymer/clay nanocomposites and the effective clay particle" polymer 45, 487-506, (2004).

[11] K. Nogi, et. al, " Handbook of nanoparticles", JWRI, Osaka Univ., Osaka, Japan, (2007).

[12] Q. H. Zheng, et. al, " Clay –based polymer nanocomposites: Research and commercial Development", Journal of nanoscience and nanotechnology, Vol. 5, 1574-1592, 82005).

[13] El-Sheikhy, R.., Al-Shamrani M. Interfacial bond Assessment of Clay-Polyolefin Nanocomposites (CPNC). J Advanced Powder Technology APT. 28, 983-992 (2017)

[14] H. Zhang, et. al. "Fracture behavior of in situ Silica nanoparticle-filled epoxy at different temperature", Polymer 49, 3816-3825, (2008).

[15] X. F. Yao, D. Zhou, H. Y. Yeh, "Macro/microscopic fracture characterizations of SiO2/epoxy nanocomposites", aerospace science and technology 12, 223- 230, (2008).

[16] Z. Wang, et. al., "Fabrication and mechanical properties of exfoliated clay-CNTs /epoxy nanocomposites", Materials science and engineering A 490, 481-487, (2008).

[17] R. El-Sheikhy, A new treatment of fracture in uniaxial fields, 5th Int. Conf. on multiaxial Fatigue and Fracture, Cracow, Poland, 1997, pp. 657-672.20.

[18] R. El-Sheikhy and M. Al-Shamrani, on the processing and properties of clay/polymer nanocomposites, Lat. Am. j. solids struct. vol.12 no.2, 2015.

[19] ASTM D638, for tensile strength testing.

[20] ASTM D 5045, for fracture toughness testing.

[21] R. El-Sheikhy, N. Nishimura, Comparison among directional fracture theories, Journal of Osaka university scientific reports, Vol. pp. ,1999,

[22] Lee JJW, et. al., Properties ofTooth Enamel in Great Apes. Acta biomater. (2010) 6:4560-4565.

[23] Meckel AH, Griebstein WJ, Neal RJ (1965) Structure of Mature Human Dental Enamelas Observed by Electron Microscopy. Arch. oral biol. 10:775-783. Epub 1965/09/01.

[24] Xu HH, et al. (1998), Indentation Damage and Mechanical Properties of Human Enamel and Dentin. J. dent.res. 77: 472-480. Epub 1998/03/13.

[25] He LH, Swain MV (2008) Understanding the Mechanical Behaviour of Human Enamelfrom its Structural and Compositional Characteristics. J. mech. behav. biomed. mater.1:18-29. Epub 2008/01/01.

[26] Deng Y, Lawn BR, Lloyd IK, Characterization of Damage Modes in Dental Ceramic Bilayer Structures. J. biomed. mater. res. (2002) 63:137-145.

[27] Fradeani M, Aquilano A, Clinical Experience with Empress Crowns. Inter. j.prosthet. 10:241-247, (1997)

[28] Rhee YW, et. al., Brittle Fracture versus Quasi Plasticity in Ceramics: A Simple Predictive Index. J. amer. cer. soc. (2001) 84:561-565.

[29] MATSUZAKI, et. al., Translucency and flexural strength of monolithic translucent zirconia and porcelain-layered zirconia, Fumiyori, *Dental Materials Journal 2015; 34(6): 910–917*

[30] Yoshiki ISHIDA and Taira MIYASAKA, Dimensional accuracy of dental casting patterns created by 3D printers, *Dental Materials Journal 2016; 35(2): 250–256*

[31] Akimasa TSUJIMOTO, et. al., Mechanical properties, volumetric shrinkage and depth of cure of short fiber reinforced resin composite, *Dental Materials Journal 2016; 35(3): 418–424*

[32] Lawn BR, et. al., Predicting Failure in MammalianEnamel. J. mech. behav. biomed. mater., (2009) 2:33-42

CHAPTER 2:

Production and Industrial Application of Biomass-Based Materials

Published in: Key Engineering Materials
ISSN: 1662-9795, Vol. 985, pp 43-51
doi:10.4028/p-1rt2Ck

Submitted: 2024-01-31
Revised: 2024-04-21
Accepted: 2024-04-21
Online: 2024-08-27

Analyzing the Impact of Annealed Steel Sludge Doses on the Physicochemical Properties of Biochar Obtained from Waste Date Palm Frond

Hana Mohammed Almarri[1,2,a], Saleh M. Alluqmani[4,b], Moudhi Alshammary[2,3,c], Sana Alenzi[2,3,d], Nadiyah M. Alabdallah[2,3,e]

[1]Department of Physics, College of Science, Imam Abdulrahman Bin Faisal University, P.O. Box 1982, Dammam, 31441, Saudi Arabia

[2]Basic and Applied Scientific Research Center- College of Science -Imam Abdulrahman Bin Faisal Abdulrahman Bin Faisal University, P.O. Box 1982, Dammam, 31441, Saudi Arabia

[3]Department of Biology, College of Science, Imam Abdulrahman Bin Faisal University, P.O. Box 1982, 31441, Dammam, Saudi Arabia

[4]Department of Physics, College of Science, Umm Al-Qura University, P.O. Box 715, Makkah 24382, Saudi Arabia

[a]*Corresponding author: hmalmarri@iau.edu.sa

[b]smluqmani@uqu.edu.sa, [c]moudhi.1257@gmail.com, [d]smsalenzi@iau.edu.sa, [e]nmalabdallah@iau.edu.sa

Keywords: Valorization of Waste, Date Palm, Biochar, Low Pyrolysis, Steel sludge, Ball-Milling, Magnetic Composite

Abstract Large quantities of date palm frond waste generated from the pruning process are accumulated or burned in burn barrels, harming the environment and having very little economic value. However, because of the lack of data revealing the characteristic magnetic properties of biochar derived from date palm fronds, further research on low-cost and sustainable strategies could offer a new composite material and serve to extend the way for novel applications. In this study, we prepared biochar derived from palm fronds via pyrolysis under a limited-oxygen atmosphere at a lower temperature of 300 °C for 2 h. We introduced a facile strategy for the production of magnetic biochar with various doses of annealed steel sludge material via ball milling. Various amounts of annealed steel sludge material (5%, 15%, and 25% w) were added to date palm frond biochar, and the obtained product was fabricated by ball milling. The physicochemical characteristics of the magnetic biochar composite were subsequently analyzed using scanning electron microscopy (SEM), energy-dispersive X-ray spectroscopy (EDS), X-ray diffraction (XRD), Fourier-transform infrared spectroscopy (FTIR) spectroscopy, and UV-vis spectroscopy. Our findings showed that the ball milling method is a successful step for producing date palm fronds with magnetic biochar material possessing rough and packed pores, as shown by SEM. XRD patterns assumed the existence of magnetic phases of iron oxide (magnetite (Fe_3O_4), hematite (α-Fe_2O_3), and maghemite (γ-Fe_2O_3) at different generated peaks. FTIR outputs exhibited the abundant presence of various oxygen-containing functional groups (- COOH and -OH) on the surface of magnetic biochar material, which help to create chemically reactive sites to adsorb potential surrounding species. The UV spectra showed a noticeable enhancement of the optical properties of the magnetic biochar with an increase in the sludge dose for light absorption in the visible region from wavelengths of 400 – 700 nm . This result signifies the synthetic optimization and potential application of magnetic biochar materials for composites that could be employed in targeted uses including soil amendment, water remediation and energy applications.

1. Introduction

Cultivation of palm trees is an old practice that has been used for thousands of years in the arid regions of the Middle East, the Arabian Peninsula, and North Africa. The importance of palm trees as a direct source of nutrients and materials, such as for building, fabrication, and furnishings, has sustained the human population in desert regions and has expanded cultivation to other countries with appropriate environmental conditions. (Chao & Krueger, 2007). Date palm tree agriculture in the Kingdom of Saudi Arabia is one of the largest vendors in the global market, with an estimated 1,565,830 tons produced in 2021 and grown within an area of 152,734 ha (FAO, 2023). Over the productive life span of a date palm, which may extend for up to 50 years, farmers usually trim tree branches and fronds throughout this period of life. One date palm produces approximately 20 kg of litter annually from the removal of the branch and annual removal of any dead or damaged fronds (Faiad et al., 2022). Large volumes of date palm trash are produced by the pruning process. Once gathered, the majority of this waste is often eliminated, either by incineration or landfilling, causing environmental damage and low economic value (Abdulrazzaq et al., 2014).

Recent research on the sustainable management of biowaste could offer new composite materials for environmental and agricultural applications. Magnetic biochar is an advanced material that can be developed from date palm frond waste and is composed of a highly porous, carbon-rich substance that is produced by the thermochemical conversion of biomass under anaerobic conditions (Khan et al., 2022). Typically, the characteristics and properties of biochar govern its application. Physicochemical characteristics, performance, manufacturing procedures, and economic variables are among the most essential elements that influence biochar. Its physical and chemical qualities are determined by the synthesis technique and carbon source (Chen et al., 2022).

Magnetic biochar is an important component for green advanced technologies and the sustainable future (Zhao, et. al., 2021). The development of magnetic biochar has been applied in water purification from pollutants (Wang et. al., 2015) and used as excellent electrodes for supercapacitors (Du, et. al., 2022). Although various technologies are used to prepare magnetic biochar including thermal treatment, microwave heating, co-precipitation, and calcination (Zhao, et. al., 2021), further work is required to explore preparing tuned properties of magnetic biochar by the ball-milling method.

steel sludge material is a common by-product generated from the iron and steel industry. It is considered as is a fine solid material obtained after wet cleaning and scrubbing during the manufacturing of steel (scrubber sludge). Fine particles of steel sludge emerge in the form of iron oxides and calcium carbonate (calcite) (Andrade, et. al., 2006 Roslan, at. Al., 2016). In general, the resulting chemical composition is composed mostly of oxides and silicates generated by the oxidation of different additives in steel-making residue (Saeedi, et. al., 2023, Yousef Malkawi, 2003). To enhance the physicochemical properties, adsorption capacity, and recovery of biochar, its magnetic properties were combined by adding iron oxides derived from steel-making byproducts steel slag (Kim et al., 2021). It has been reported to be utilized as a sorbent for wastewater treatment, removing organic pollutants (B. Chen et al., 2011), dyes (Shin et al., 2021; Theydan & Ahmed, 2012), and heavy metals such as arsenic (Wang, Gao, Zimmerman, et al., 2015), lead (Wang, Gao, Li, et al., 2015). However, because of the need for data revealing the characteristic magnetic material of date palm frond biochar derived from date palm fronds, further research on low-cost and sustainable strategies could offer new beneficial composite materials and serve to extend the way for novel applications.

In this preliminary study, we aimed to optimize the conditions and produce magnetic biochar by mixing various doses of annealed steel sludge with date palm frond biochar by ball milling method under ambient conditions. The detection of the obtained product was carried out by several analytical techniques, including SEM, EDS, FTIR, XRD, and UV methods, revealing the physicochemical characteristics of the magnetic biochar with different doses of annealed steel sludge and exploring the effect of the annealed sludge dose on the product properties.

2. Material and Methods

2.1 Materials:

The date palm fronds (Phoenix dactylifera) used in this study were obtained from local farmers in the eastern province of Saudi Arabia. Sludge steel waste was collected in powder form from the Al Rajhi factory for iron and steel production in Jeddah, Saudi Arabia.

2.2 Preparation of thermally modified steel sludge material

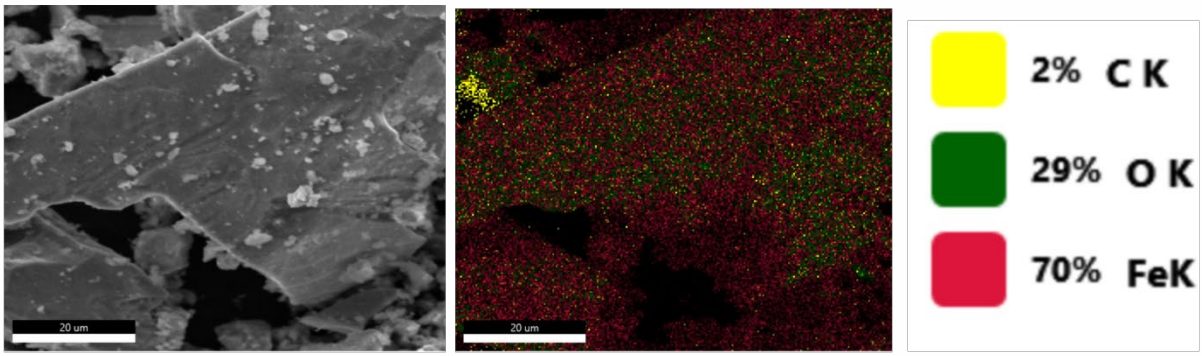

Fig. 1. Elemental analysis of the annealed steel sludge material (wt%)

The as-received steel sludge powder samples were treated using the same strategy as described in our previous work reported elsewhere (Saeedi et al., 2023). Briefly, a ground soft powder (50 g) was prepared using a mortar and then sieved through a 1 mm sieve to remove large fragments and solid clusters. The powder sample was thermally heated to 900 °C in a conventional furnace under ambient pressure at a rate of 5 °C/min for two hours. The elemental dispersive X-ray (EDX) output of the thermally modified steel sludge is shown in Figure.1 It was observed that the heated steel sludge exhibited a higher total iron content (70%), which can be better interpreted because of the high temperature of 900 °C, which tends to influence the magnetic phases of iron oxide structures in the steel slag material (Saeedi et al., 2023). It is also seen that the oxygen percentage is 29% and the lower amount of carbon is 2%. Figure 2. shows a simple test of the successful attraction of the steel sludge material by a magnet, indicating the magnetic enrichment of the as-received sludge powder.

Fig. 2. Magnetic response of steel sludge material to the magnet

2.3 Preparation of date palm frond Biochar:

To create graphitic biochar, we subjected the palm fronds to pyrolysis under a limited oxygen atmosphere at a lower temperature of 300 °C for 2 h. The elemental dispersive X-ray (EDX) output

of the thermally modified steel biochar is shown in Figure 2. The carbon content was dominant at approximately 74%, oxygen percentage at 29%, and lower amount of iron at 1%.

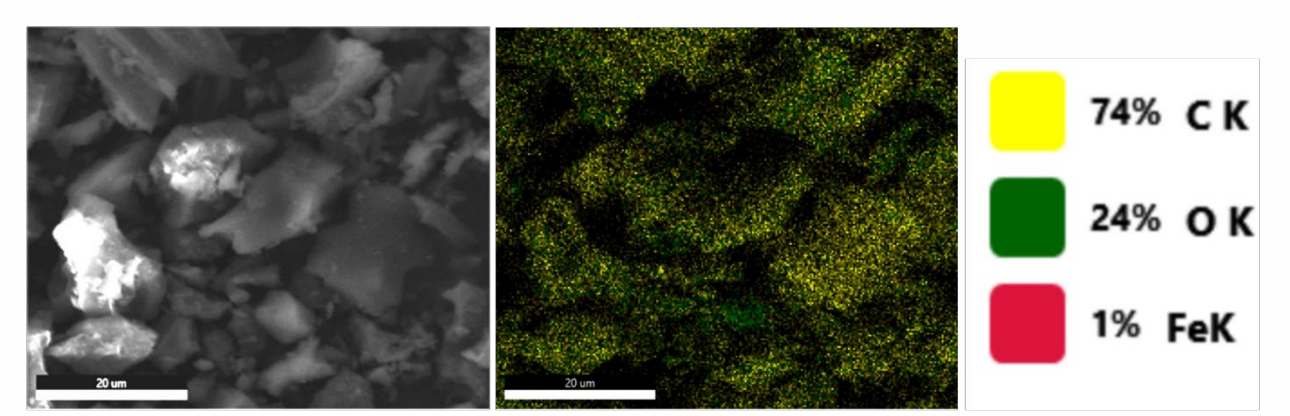

Fig. 3. Elemental analysis of the biochar of date palm frond material (wt%)

2.4 Preparation of date palm frond magnetic biochar by the ball-milling method

We introduced various amounts of steel sludge material (5%, 15%, and 25% w) to the biochar and magnetic mixture through a facile route utilizing ball-milling technology for 2 h. This technique is an inexpensive, simple, eco-friendly, and scalable tool [Alluqmani et. Al., 2021]. The experimental setup for magnetic biochar production is shown in Figure. 3.

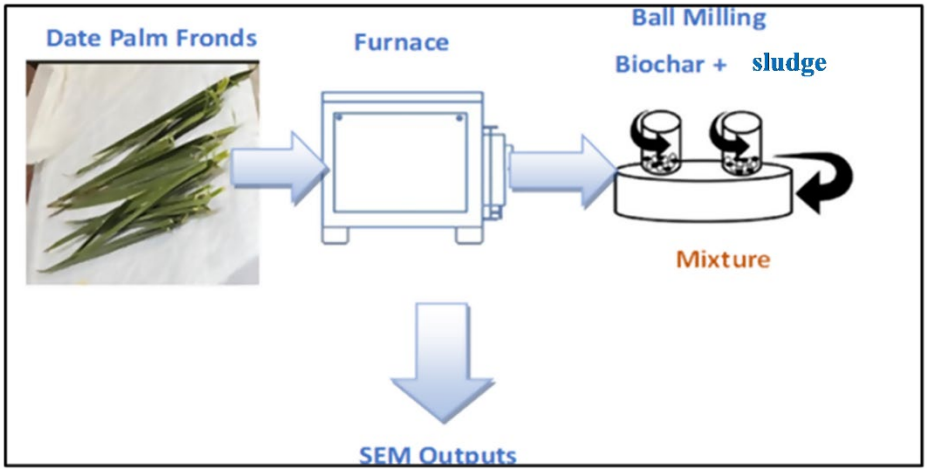

Fig. 4. Experimental setup for the magnetic biochar preparation

2.2 Characterization Methods:

To assess the physicochemical properties of the magnetic biochar composites, we conducted a range of tests. These include scanning electron microscopy (SEM), energy-dispersive X-ray spectroscopy (EDS), Fourier-transform infrared spectroscopy (FTIR), X-ray diffraction (XRD), and UV-vis spectroscopy.

3. Result and Discussion

3.1 Morphological analysis

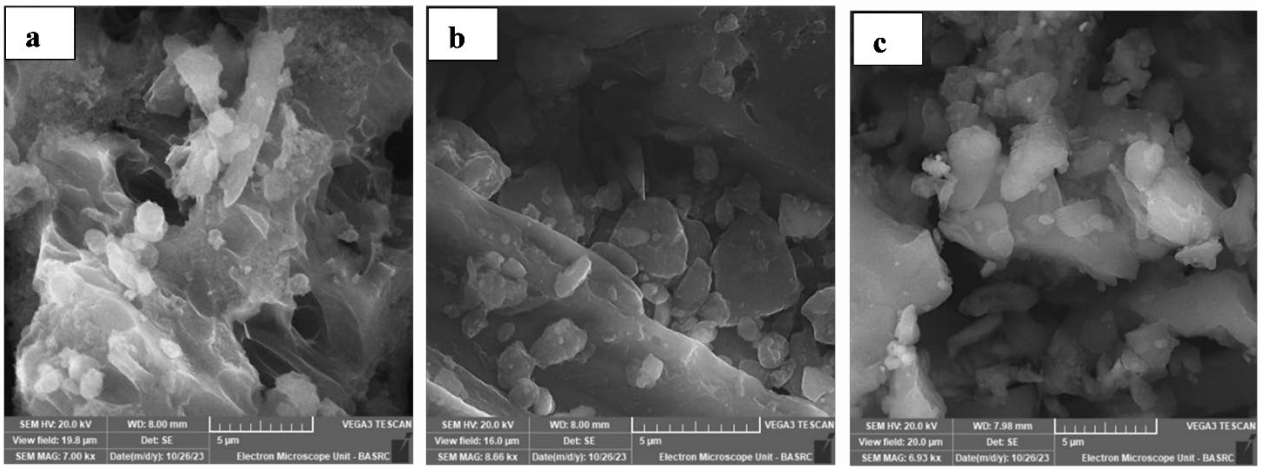

Fig. 5. Surface morphology of magnetic biochar at sludge doses of 5% **(a)**, 15% **(b)** and 25% **(c),** respectively.

The morphological properties of the surface of the date palm frond biochar at steel sludge doses of 5, 15%, and 15% were investigated using SEM analysis. Figure. 5 (a–c) shows a rough and porous channel surface. These channels of biochar surfaces were gradually packed because of the incorporation and accumulation of small steel sludge particles doses during the ball milling process. These observations have led to the development of biochar surface as a magnetic biochar, providing areas for the binding effect (Oyekanmi et. Al., 2024; Vijayaraghavan, 2021). Our new strategy can open up a potential use for date palm frond magnetic biochar as an important tool in soil amendment, water treatment, and energy harvesting.

3.2 Surface functional groups

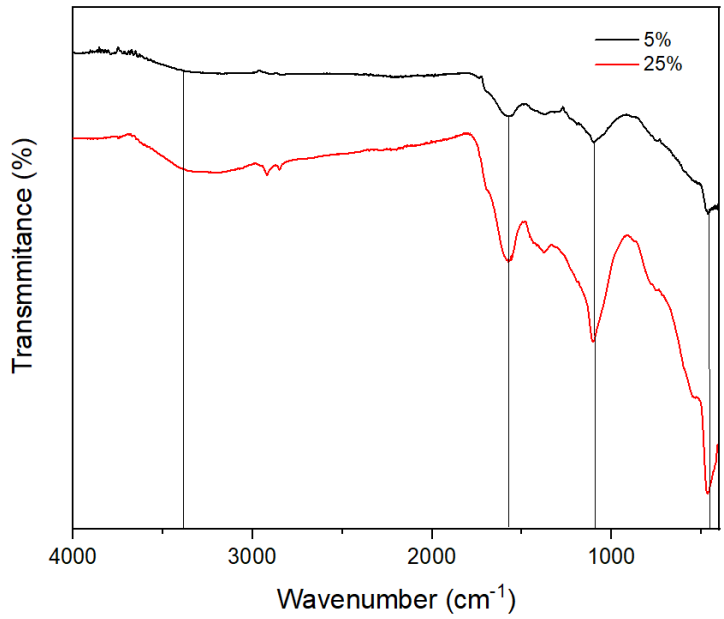

Fig. 6. Surface functional groups on magnetic biochar at sludge doses of 5% and 25

The surface properties were revealed by assessing the functional oxygen-containing groups of date palm frond magnetic biochar at steel sludge doses of 5, 15%, and 25% via FTIR spectroscopy. As shown in Figure. 6, functional groups including Fe-O, C-O, C=O, and –OH were detected in the obtained samples at 5% and 25% of steel sludge for the curve clarity. A characteristic peak around

448 cm^{-1} typically introduces Fe–O, assigning a modification to the structures of iron oxide (Feng et. al., 2023).The peak at 1090 cm^{-1} was attributed to the C-O group. The wide peaks around 3385 cm^{-1} can be assigned to the vibration of the –OH groups, and the peak centered around 1568 cm^{-1} was attributed to C=O stretching due to the presence of carboxyl groups (Oyekanmi et. Al., 2024; Son et al., 2021).Thus, FTIR outputs exhibited the abundant presence of various oxygen-containing functional groups (- COOH and -OH) on the surface of magnetic biochar material, which help to create chemically reactive sites to adsorb potential surrounding specious.

3.3 Magnetic biochar structure

The crystalline structures of the magnetic date palm frond biochar were evaluated using XRD. The XRD patterns of the steel sludge steel incorporated into the biochar by ball milling at 5, 15, and 25% w were in the range of 10–80°, as illustrated in Figure. 7. The XRD spectra of the magnetic biochar assumed the existence of magnetic phases of iron oxide (magnetite (Fe_3O_4), hematite (α-Fe_2O_3), and maghemite (γ-Fe_2O_3). The generated diffraction peaks of the magnetic biochar were observed at 21.56°, 23.7°, 33.18°, 34.6°, 39.3°, 49.48°, 50. 44°, 54.64°, 68° and 74.05°, which were closer to those observed in the published work by (Oyekanmi et. Al., 2024, Son et. al., 2021). This observation indicates the successful optimization of date palm magnetic biochar using a ball-milling strategy for targeted applications. Further work is required to study the magnetic biochar patterns developed by steel sludge particles using a ball-mailing technology.

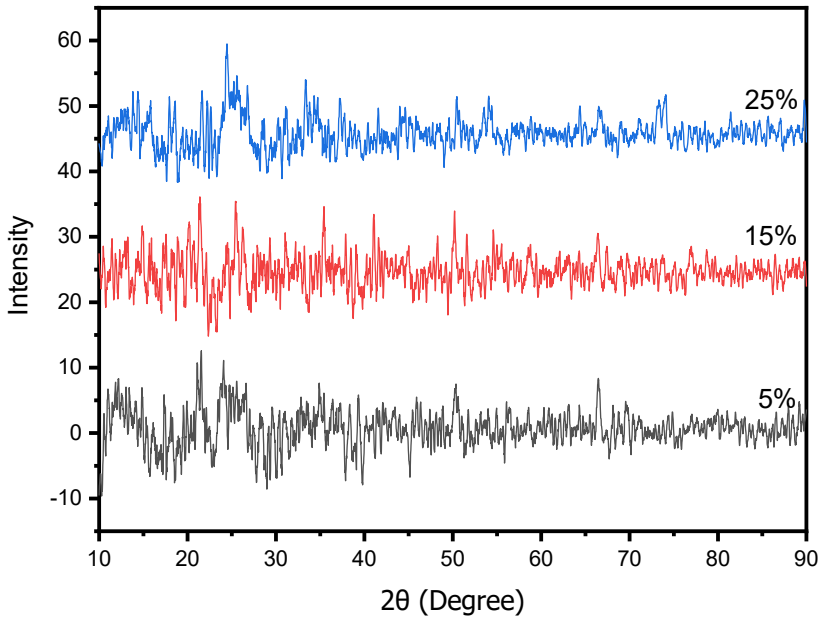

Fig. 7. X-ray diffraction (XRD) analysis of magnetic biochar at sludge doses of 5%, 15%, and 25%

3.4 Optical properties

Figure. 8 depicts the UV–VIS absorption spectra of the date palm frond magnetic biochar at various doses of steel sludge (5, 15%, and 25%). The spectra revealed that an increase in the steel sludge dose led to a noticeable enhancement in the visible light absorption ranging from 400 to 700 nm. This wide peak is indicative of the electronic transition, which is associated with the high intensity, indicating a high concentration of 3d (Fe^{+}) depending on the elemental content of C, O, and Fe in the produced sample [Gherca, et. al., 2022; Wu, et. al., 2023; Saeedi et. al., 2023]. This observation agrees with the morphological properties observed in the representative SEM analysis shown in Figure. 5 (a–d).

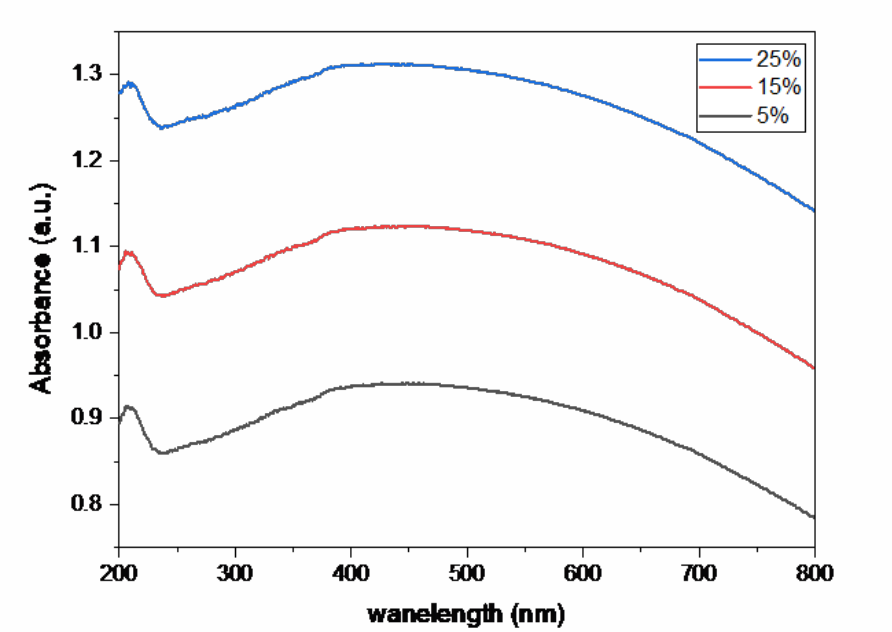

Fig. 8. UV–VIS absorption spectra of magnetic biochar samples at different sludge doses at 5%, 15% and 5%.

4. Conclusion

In this preliminary study, a facile and sustainable model for the production of date palm frond magnetic biochar based on the addition of annealed steel sludge doses using the ball-milling method was developed. SEM analysis proved that the cavities at the biochar surface were filled by annealed steel sludge particles with an increase in the dose from 5% to 25%. The structural properties of the obtained samples were investigated, and the presence of magnetic iron oxide was confirmed by XRD and FTIR studies. The optical properties of magnetic biochar can be controlled by varying the steel sludge dose. It was shown that the light adsorption detected by UV spectroscopy appeared in the visible region, thereby allowing the produced samples to serve as potential precursors for the engineering of advanced composites. Our findings pave the way for an innovative strategy for converting waste into important products for soil amendment, water treatment and energy harvesting.

References

[1] Quah, R. V., Tan, Y. H., Mubarak, N. M., Kansedo, J., Khalid, M., Abdullah, E. C., & Abdullah, M. O. (2020). Magnetic biochar derived from waste palm kernel shell for biodiesel production via sulfonation. Waste Management, 118, 626-636.

[2] Bhatia, S. K., Palai, A. K., Kumar, A., Bhatia, R. K., Patel, A. K., Thakur, V. K., & Yang, Y. H. (2021). Trends in renewable energy production employing biomass-based biochar. Bioresource Technology, 340, 125644.

[3] Abdulrazzaq, H., Jol, H., Husni, A., & Abu-Bakr, R. (2014). Biochar analysis. In *BioResources* (Vol. 9, Issue 2).

[4] Chao, C. T., & Krueger, R. R. (2007). The date palm (Phoenix dactylifera L.) : Overview of biology, uses, and cultivation. *Hortscience*, *42*, 1077–1082. https://api.semanticscholar.org/CorpusID:85796808

[5] Chen, B., Chen, Z., & Lv, S. (2011). A novel magnetic biochar efficiently sorbs organic pollutants and phosphate. *Bioresource Technology*, *102*(2), 716–723. https://doi.org/https://doi.org/10.1016/j.biortech.2010.08.067

[6] Chen, X., Lin, J., Su, Y., & Tang, S. (2022). One-Step Carbonization Synthesis of Magnetic Biochar with 3D Network Structure and Its Application in Organic Pollutant Control. *International Journal of Molecular Sciences*, *23*(20). https://doi.org/10.3390/ijms232012579

[7] Faiad, A., Alsmari, M., Ahmed, M. M. Z., Bouazizi, M. L., Alzahrani, B., & Alrobei, H. (2022). Date Palm Tree Waste Recycling: Treatment and Processing for Potential Engineering Applications. In *Sustainability (Switzerland)* (Vol. 14, Issue 3). MDPI. https://doi.org/10.3390/su14031134

[8] FAO. (2023). *Crops and livestock products- Production*.

[9] Khan, K., Aziz, M. A., Zubair, M., & Amin, M. N. (2022). Biochar Produced from Saudi Agriculture Waste as a Cement Additive for Improved Mechanical and Durability Properties—SWOT Analysis and Techno-Economic Assessment. *Materials*, *15*(15). https://doi.org/10.3390/ma15155345

[10] Zhao, Q., Xu, T., Song, X., Nie, S., Choi, S., Si, C. (2021). Preparation and Application in Water Treatment of Magnetic Biochar. Frontiers in Bioengineering and Biotechnology, 9, 769667.

[11] Du, H., Zhang, M., Liu, K., Parit, M., Jiang, Z., Zhang, X., et al. (2022). Conductive PEDOT:PSS/cellulose Nanofibril Paper Electrodes for Flexible Supercapacitors with superior Areal Capacitance and Cycling Stability. Chem. Eng. J. 428, 131994. https://doi:10.1016/j.cej.2021.12199410.1016/j.cej.2021.131994

[12] Andrade, P. M., Vieira, C. M. F., Monteiro, S.M., Venilli, J.F. (2006) Recycling of steel sludge into red ceramic, Mater. Sci. Forum 544–549.

[13] Roslan, N, H., Ismail, M., Abdul-Majid, Z., Ghoreishiamiri, S., Muhammad, B. (2016) Performance of steel slag and steel sludge in concrete. Construction and Building Materials 104. 16–24 (2016).

[14] Kim, G., Kim, Y. M., Kim, S. M., Cho, H. U., & Park, J. M. (2021). Magnetic steel slag biochar for ammonium nitrogen removal from aqueous solution. *Energies*, *14*(9). https://doi.org/10.3390/en14092682

[15] Shin, J., Bae, S., & Chon, K. (2021). Fenton oxidation of synthetic food dyes by Fe-embedded coffee biochar catalysts prepared at different pyrolysis temperatures: A mechanism study. *Chemical Engineering Journal*, *421*, 129943. https://doi.org/https://doi.org/10.1016/j.cej.2021.129943

[16] Theydan, S. K., & Ahmed, M. J. (2012). Adsorption of methylene blue onto biomass-based activated carbon by FeCl3 activation: Equilibrium, kinetics, and thermodynamic studies. *Journal of Analytical and Applied Pyrolysis*, *97*, 116–122. https://api.semanticscholar.org/CorpusID:98508107

[17] Wang, S., Gao, B., Li, Y., Mosa, A., Zimmerman, A. R., Ma, L. Q., Harris, W. G., & Migliaccio, K. W. (2015). Manganese oxide-modified biochars: Preparation, characterization, and sorption of arsenate and lead. *Bioresource Technology*, *181*, 13–17. https://doi.org/https://doi.org/10.1016/j.biortech.2015.01.044

[18] Wang, S., Gao, B., Zimmerman, A. R., Li, Y., Ma, L., Harris, W. G., & Migliaccio, K. W. (2015). Removal of arsenic by magnetic biochar prepared from pinewood and natural hematite. *Bioresource Technology*, *175*, 391–395. https://doi.org/https://doi.org/10.1016/j.biortech.2014.10.104

[19] Yousef Malkawi, H. (2003). *Review of steel slag utilization in Saudi Arabia*. The 6th Saudi Engineering Conference, KFUPM, Dhahran, Saudi Arabia, 14–17 December 2002.

[20] Alluqmani, S. M. et. al. (2021). Elaboration of TiO2/carbon of oil fly ash nanocomposite as an eco-friendly photocatalytic thin-film material, Ceram Int. ;47:13544–51.

[21] A. M. Saeedi, H. M. Almarri, N. M. Alabdallah, M. A. Alamri, H. S. Albaqawi, A. R. Algamdi, F. A. Alfayez, S. M. Alluqmani, Morphological, Structural, and Optical Features of Thermally Annealed Slag Powders Generated from the Iron and Steel Industry: A Source of Disordered Iron Oxide Composites. Crystals 2023, 13, 1601.

[22] K. Vijayaraghavan, The importance of mineral ingredients in biochar production, properties, and applications. Critical Reviews in Environmental Science and Technology (2021), VOL. 51, NO. 2, 113–139

[23] Oyekanmi, et al. A novel oil palm frond magnetic biochar for the efficient adsorption of crystal violet and sunset yellow dyes from aqueous solution: synthesis, kinetics, isotherm, mechanism and reusability studies. Applied Water Science (2024) 14:13.

[24] E. Son, K. Poo, J. Chang, K. Chae. Heavy metal removal from aqueous solutions using engineered magnetic biochar derived from waste marine macro-algal biomass. Science of the Total Environment 615 (2018) 161–168.

[25] C. Feng, M. Huang, C-P Huang, Specific chemical adsorption of selected divalent heavy metal ions onto hydrous γ-Fe2O3-biochar from dilute aqueous solutions with pH as a master variable. Chem. Eng. J. 451 (2023) 138921.

[26] Gherca, D.; Borhan, A.I.; Mihai, M.M.; Herea, D.-D.; Stoian, G.; Roman, T.; Chiriac, H.; Lupu, N.; Buema, G. Magnetite-induced topological transformation of 3D hierarchical MgAl layered double hydroxides to highly dispersed 2D magnetic hetero-nanosheets for effective removal of cadmium ions from aqueous solutions. Mater. Chem. Phys. 2022, 284, 126047.

[27] Wu, K.; Nie, F.; Zhao, H.; Qi, X.; Li, P.;Wu, M. Morphology-dependent catalysis on nanostructures Fe2O3@MWCNT as Pt-free counter electrode for dye-sensitized solar cells. Int. J. Hydrogen Energy 2023, 48, 33571–33579.

Published in: Key Engineering Materials
ISSN: 1662-9795, Vol. 985, pp 53-74
doi:10.4028/p-U5s41d

Submitted: 2023-12-31
Revised: 2024-04-09
Accepted: 2024-04-14
Online: 2024-08-27

Sustainable Approaches for the Fabrication of Nanocellulose-Polyamide Membrane Based on Waste Date Palm Leaves for Water Treatment

Seham S. Alterary[1,a*], Ahmed A. Alshahrani[2,b], Athar Elhadi[1,c], Maha F. El-Tohamy[1,d]

[1]Department of Chemistry, College of Science, King Saud University, Riyadh, P.O. Box 11495, Saudi Arabi

[2]Nuclear Technologies Institute, King Abdul Aziz City for Science and Technology, Riyadh, 11442, Saudi Arabia

[*a]salterary@ksu.edu.sa, [b]ashahrni@kacst.edu.sa, [c]athorh1994@gmail.com, [d]moraby@ksu.edu.sa

Keyword: Crystalline nanocellulose; Date palm; Polysulphone; Polyamide; Membranes; water treatment.

Graphical Abstract

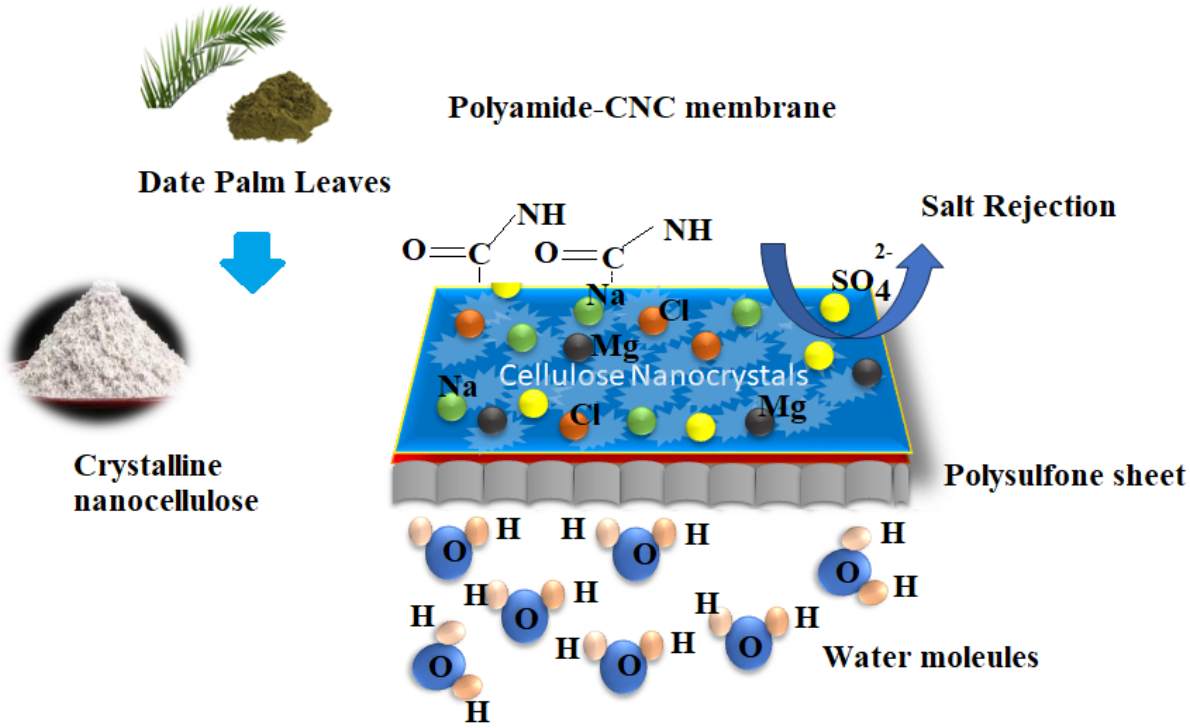

Abstract. A vast amount of agricultural waste, such as dried leaves, stems, pits, seeds, etc., are produced by date palm trees in Saudi Arabia each year. This waste is an excellent source of degradable biomass suitable for many uses. Crystalline nanocellulose (CNC) is one of the most important nanomaterials that can be used in various applications. Due to its unique properties, which include biorenewability, optical transparency, high mechanical strengths, and sustainability, nanocrystalline cellulose has become a significant nanomaterial in recent years. In this study, CNC was isolated from the waste date palm leaves and used for the production of PA-modified membranes for water treatment by reverse osmosis membrane technology. The membranes were prepared by surface polymerization with the polyamide as a selective layer on the polysulfone support film. Three membranes were produced, two with 0.01% and 0.02% (w/v) CNC and the third with PA-free CNC for comparison. Each membrane produced was tested using different characterization techniques. The polyamide membrane with 0.01% w/v CNC had a higher water permeability of 43.25 L/m^2 h bar than the membranes with 0% w/v CNC (36.25 L/m^2 h) and 0.02% w/v CNC (42.85 L/m^2 h bar). Under the same conditions, salt retention was also found to be above 98% for both NaCl and $MgSO_4$ for the two modified membranes. The contact angle was

found to be 68.04±3.7, 72.83±0.8, and 63.76±5.5 for PA(0%CNC), PA-CNC (0.01% w/v), and PA-CNC (0.02% w/v), respectively. The 0.01% PA-CNC membrane exhibited a higher water contact angle, greater hydrophobicity and lower surface roughness. As a result, the isolated CNC might be appropriate for use as a modifier agent for membrane fabrication and water treatment.

1. Introduction

Water resources occupy a unique position compared to other natural resources. As the main element of the environment and a necessary component of human life, water is the basis of life as we know it. Furthermore, water is essential for maintaining a high standard of living and for social and economic progress. Human health is strongly influenced by water. Diseases, natural disasters and environmental damage can be caused by contaminated water or by a surplus or shortage of water. Over the last 20 years, it has become clear that natural resources especially water resources are finite and should be used wisely to meet people's needs [1]. According to united nation water statistics, clean water accounts for about 2.5% of the earth's total water capacity. Water scarcity is the result of high demand compared to available supply and is caused by a number of factors. The physical environment can be altered by both human activities and natural processes that create some elements and leave others behind [2]. Due to urbanization, industrialization and overpopulation, global warming is affecting the availability of water resources. Numerous industries are emerging in an attempt to meet the challenges of a growing population; however, this places unsustainable demands on water resources, ultimately leading to their depletion [3].

The date palm (Phoenix dactylifera) is one of the most common agricultural crops in many countries [4]. This tree has always been essential for the beginning and development of civilizations in the arid parts of the Arab world [5]. The United Nations Educational, Scientific, and Cultural Organization has recently acknowledged date palm-related knowledge, customs, and practices as a component of the global intangible cultural heritage [6]. In addition, much work is being put into preserving the long-threatened crop, as it is an important symbol of the Arab world's prosperity [7]. The Arab world can benefit from date palms as they are remarkably resilient to harsh environments and require little care [8]. It is estimated that 2 million tons of dry palm fronds are produced annually during the date harvest. When the palms are seasonally pruned and grafted, large quantities of waste biomass are therefore produced [9]. According to estimates in Saudi Arabia, each palm produces between 20 and 35 kg of biomass waste each year, which amounts to a total of about 1 million metric tons of biowaste [10]. Date palm waste is usually burned on farms or disposed of in landfills, polluting the environment in date-growing countries. There are numerous thermal, biochemical and physico-chemical technologies for the sustainable use of date palm biomass. The date palm has a low moisture content and a high content of volatile components. Due to these properties, date palm residues are a large biomass resource in date growing countries [11].

Cellulose nanocrystals (CNCs) obtained from different parts of the date palm have been found to have different properties in terms of shape, surface morphology, degree of polymerization and surface characteristics. Date palm leaves were selected for the present study as it contains 60-75% cellulose [12]. CNC provides special uniqueness like non-toxicity, increased thermal stability, reduced cost, optical transparency, and biodegradability. However, because of its exceptional mechanical and thermal properties, CNC is frequently used as a reinforcing reagent in polymer composites [13]. Numerous techniques for separating cellulose from agricultural biomass resources and converting it into nanocellulose have been documented [14]. The most widely used techniques to produce nanocellulose include acid hydrolysis of accessible or semi-crystalline amorphous cellulose [15], the use of a combined nanomaterial containing polyvinyl alcohol and starch [16], and chlorine-free refining techniques to extract CNCs from date palm leaf sheaths, which are a by-product after harvesting [17]. In general, it is a laudable goal to seek alternative methods of converting by-product waste into a useful product in order to reduce the effort and cost associated with its disposal. This goal can be achieved by promoting research on this topic. In general, nations that have an agriculturally oriented economy generate a significant amount of waste through the agricultural sector. This would ultimately be bad for the environment and the economy because the

problem of global warming is so serious and so much waste is produced [18]. Massive amounts of waste are produced by date palm plants, most of which is burned and composted, degrading the environment. The palm industry, especially the date palm and oil palm sector, still lacks effective waste management [19]. Although numerous studies on the products and uses of palm trash have recently been published, proper industrial use of these applications is still in its infancy [20]. Therefore, in order to carry out a management plan of recycling such waste into useful products, a suitable and manageable method of waste extraction as well as beneficial product synthesis is required [21].

The utilization of cellulose-rich biomass waste from date palms can contribute to the overall expansion of biorefineries. Therefore, it is possible to utilize the various components of date palm waste to produce new, sustainable bioproducts such as cellulose [22]. In addition, there would be major financial and environmental benefits, and high-quality biomaterials with better chemical and physical properties would be produced. Cellulose is composed of crystalline and amorphous regions, whereby the proportion of the two regions varies depending on the cellulose source [23]. Nanocelluloses have become a viable substitute for traditional materials used in wastewater treatment. The literature survey addressed some reports described the use of CNC as filler in modified membrane technology for wastewater treatment. These include lignocellulosic biomass CNC [24], sustainable CNC composite for membrane production [25], nanocellulose based membrane for industrial wastewater treatment [26], etc. Because of their high aspect ratio, surface charge, surface area, and mechanical strength, they can help achieve this goal by offering highly effective materials for wastewater treatment. Materials used in wastewater treatment that are based on nanocelluloses, such as adsorbents, membranes, flocculants, photocatalysts, and disinfectants, must perform a variety of tasks. The ideal balance between porosity, high permeability, specific filtration mechanisms, durability, and selective binding must be maintained for nanocelluloses to perform their functions [27]. This study emphasizes on the use of date palm waste leaves as a ssustainable and potential source of CNC for the removal of hazardous contaminants and water treatment. These contaminants may be radioactive, chemical, biological or physical. "Water treatment" refers to all processes of an entity that uses procedures and other steps to remove hazardous contaminants. These pollutants can be radioactive, chemical, biological or physical. Membrane processes account for about 53% of applications in clean water production, wastewater treatment/purification and water recycling [28].

Membrane separation is one of the most efficient, useful and promising techniques for water treatment. The removal of pollutants from water is necessary for water treatment with membranes [29]. A pressure difference is the most common driving force in membrane separation. Reverse osmosis (RO), microfiltration, nanofiltration and ultrafiltration are membrane separation processes for water. Reverse osmosis (RO) is a more effective system that can perform several purification processes simultaneously. Salts and pollutants can be efficiently removed by RO membranes. Without phase shifting or heating, the water is extracted from dissolved substances in a pressurized salt solution using a membrane separation technique. In addition, the pH value of the product and the chemical transformations are only minimally affected [30].

Generally, phase inversion or the formation of a thin film systems can be used to create an asymmetric membrane structure utilizing various materials. Good chemical, thermal, and mechanical stability are features of many commercial polymeric membrane materials, including polyimide (PA), polysulfone (PS), Polyethersulfone (PES), polyvinylidene difluoride (PVDF), and polypropylene (PP) [31]. Due to their ability to reject salt and permit selective water permeation, polyamide (PA) membranes are frequently employed in the RO desalination process, which turns seawater into potable water. However, the polymer backbones, though, they typically lack reactive functional groups. As a result, membranes made of their materials must be altered to get rid of non-specific absorption and boost efficiency by using better adsorptive surfaces to enhance membrane separation [32].

The objective of this study is to develop sustainable technique to recycle the date palm waste and isolate the crystalline nanocellulose (CNC) for water treatment. The isolation technique was performed through three steps pulping, bleaching, and hydrolysis. The isolated CNC was used to fabricate three polyamide membranes with (0.0%, 0.01%, and 0.02% w/v) CNC. The salt rejection for sodium chloride (NaCl) and magnesium sulfate ($MgSO_4$) was investigated.

2. Materials and Methods

2.1. Materials

Pure grade of chemicals and reagents were used throughout this study. Polysulfone (PS-20) sheet was purchased from (Spero, California, United States). 1,3,5-benzenetricarbonyl trichloride (TMC, 98%),1,3-phenylenediamine (MPD, 99.5%) were provided by Merck (New Jersey, United States). Hexane (99%), absolute ethanol (97%), sodium chloride (NaCl, 99%), sulfuric acid (99.9%), sodium chlorite (99.9%), sodium hydroxide (99.9%), and anhydrous sodium carbonate (98%) were supplied by Sigma Aldrich (Hamburg, Germany). Milli-Q® water (Ω18.2) was used to prepare all solutions.

2.2. Collection of date palm leaves

Date palm leaves were collected from local farms in Riyadh, Saudi Arabia, and crushed to a size of about 2 cm using a pulverizer. The pulverized leaves were washed with distilled water to remove any adhering dust and then air dried and finely pulverized.

2.3. Isolation of crystalline nanocellulose from date palm leaves

The isolation of crystalline nanocellulose (CNC) was performed by alkali pulping, bleaching, and the acid hydrolysis processes (Scheme 1). By combining the palm leaves powder in a 1:20 ratio (g/ mL) with a 10 % sodium hydroxide solution, the lignin was removed during the digestion process. The mixture was then heated at 80 °C for three hours. Following pulping, the fiber was filtered out and washed with deionized water until the pH reached a neutral level. The pulped fiber was then bleached using a solution of sodium chlorite at pH 10 and a solid to liquid ratio of 1:20 (g/mL) for 3 h in order to remove dye and color. The pH was adjusted using concentrate sodium hydroxide solution. After bleaching, the fiber was washed with deionized water three times and the degreasing fiber was utilized for the isolation of CNCs. By hydrolyzing the fiber from bleached date palm leaves at 45 °C for 3 hours at a solid to liquid ratio of 1:10 (g/mL), in 200 mL of 64% sulfuric acid solution, the CNCs were obtained. Approximately, 400 mL of cool distilled water were used to stop the hydrolysis reaction. After centrifuging the diluted suspension for 10 minutes at 5,000 rpm to obtain the precipitate, distilled water was used to wash the mixture. Until the pH of the suspension was lowered to pH 5, this procedure was repeated. After washing the CNC precipitate, the sample was dialyzed by adding distilled water until a neutralized pH of 7 was reached. The dialysis tube was made of cellulose membrane, and both ends were tied with thread. The CNC was collected and dried at 50°C overnight. The dried CNC was stored in tight container for further uses.

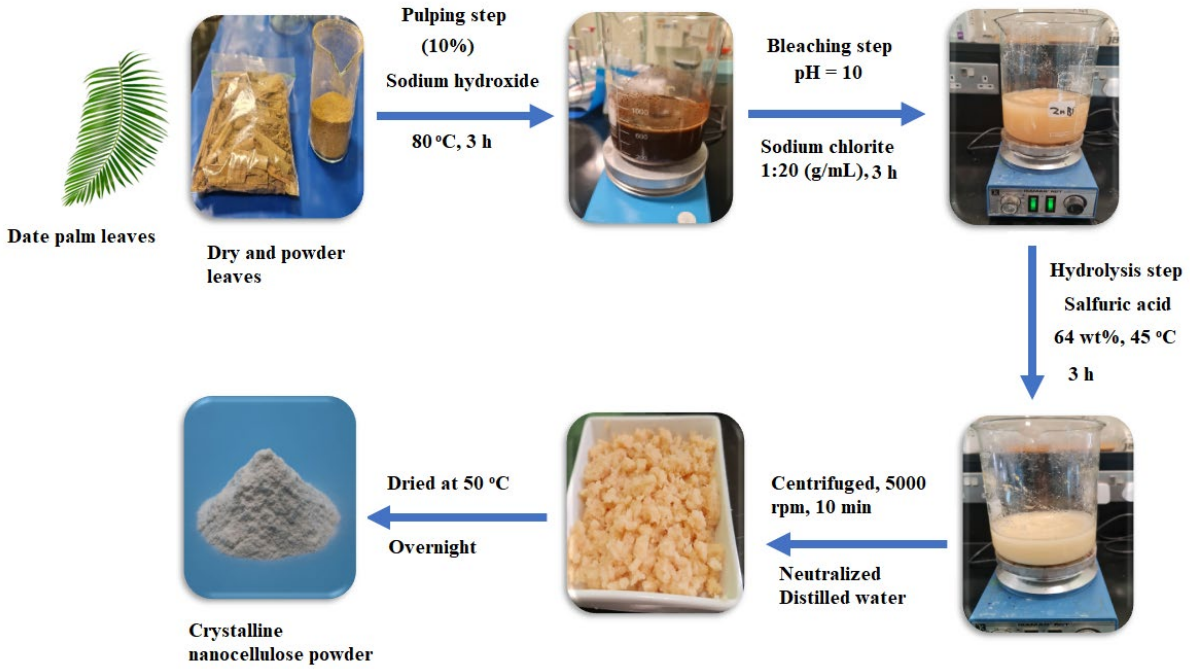

Scheme 1. Isolation of crystalline nanocellulose from date palm leaves through three steps (pulping, bleaching, and hydrolysis).

The yields of the isolated CNC during the three steps pulping, bleaching, and hydrolysis were calculated from the following equation:

$$\text{Yield}_{\text{pulping}}\,(\%) = \frac{\text{Weight of pulping sample}}{\text{Weight of the palm leaves}} \times 100 \quad (1)$$

$$\text{Yield}_{\text{bleaching}}\,(\%) = \frac{\text{Weight of bleaching sample}}{\text{Weight of the pulped sample}} \times 100 \quad (2)$$

$$\text{Yield}_{\text{CNCs}}\,(\%) = \frac{\text{Weight of CNCs}}{\text{Weight of the bleached sample}} \times 100 \quad (3)$$

2.5. Confirmation analysis

The morphological analysis of the isolated CNC was investigated using field emission scanning electron microscopy (FE-SEM, JEOL-JSM-7610F, Tokyo, Japan). Fourier transform infrared spectroscopy (FT-IR, Shimadzu, Kyoto, Japan) was used to identify the functional groups that can be observed on the surface of CNC during the isolation process. Farther, X-ray diffraction spectroscopy analysis (XRD, Shimadzu-6000, Kyoto, Japan). The thermal stability of the isolated CNC was evaluated using thermogravimetric and differential scanning calorimetry analysis (TGA/DSC, Mettler-Toledo, Colombus, United States).

2.6. Preparation of polyamide membrane

The RO membrane was produced in four steps (Scheme 2). In the first step, the support layer of the PS membrane was modified. In the second step of the process, a (2% w/v) MPD solution was prepared.

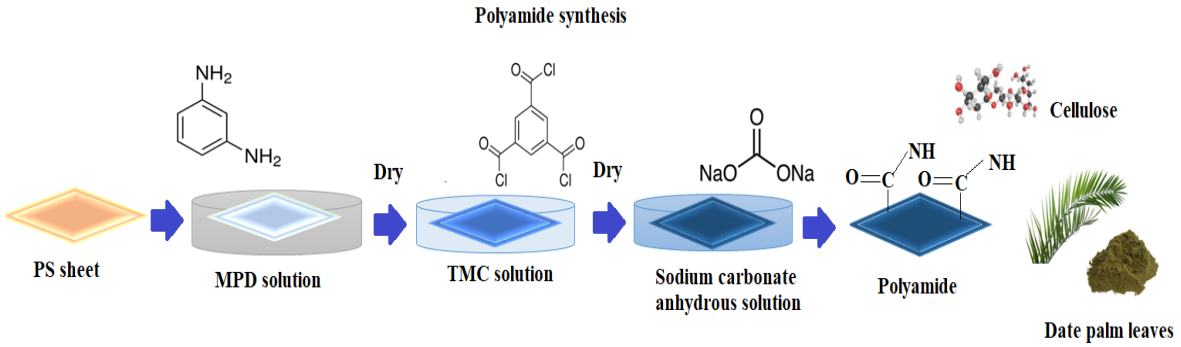

Scheme 1. Schematic diagram of polyamide membrane synthesis.

The preparation of a (0.1% w/v) TMC solution was the third step. The preparation of a (2% w/v) anhydrous sodium carbonate solution was the final step. To facilitate interfacial polymerization (IP) between the MPD and TMC support membranes, a polyamide layer was deposited on the PS. The PS support sheets were modified by soaking them in an aqueous solution at room temperature for a whole day before the process began. The PS sheet was then immersed in an aqueous MPD solution for two minutes. Excess MPD was removed with a rubber roller. After one minute in the TMC solution (0.1 % w/v), the substrate membranes were rolled over the support surface with a rubber roller. Finally, they were rinsed for ten minutes in distilled water with a 2% (w/v) anhydrous sodium carbonate solution [33].

2.7. Preparation of PA-Cellulose membranes

The process for producing PA-cellulose membranes is the same as that described in Section 2.5. Typically, PA-CNC dispersions were made by mixing 15 mL of MPD in an aqueous solution with CNC at (0.01%, w/v) and (0.02%, w/v). Sonication was used at different intervals to distribute the CNC throughout the solution in order to maximize dispersion for comparison PA-CNC free was also prepared. Using a 30 W power output and 0.5 second on/off pulses, sonication was performed. To lessen temperature swings while the sample vial was being sonicated, a water bath was utilized.

2.8. Zeta Potential (ZP)

Every membrane surface's zeta potential (ZP) was determined using the SurPASS electrokinetic analyzer (Graz, Austria). A 1 mM KCl supporting electrolyte solution was used to measure the zeta potentials of PA-CNC membranes at room temperature. The KCl solution was changed with a 0.05 M HCl solution, and the pH range (2.5–8) was established for each automated titration test.

2.9. Morphological analysis of PA-CNC membranes

Microscopic images of the three synthesized membranes surfaces were taken using a SEM. The samples of membranes were allowed to dry at room temperature for a full day, and then they were coated with gold to improve imaging and conductivity.

2.10. Contac angle

The contact angles were used to evaluate the hydrophilicity using a Data Physics SCA20 Goniometer attached to a camera.

2.11. Salt rejection of water

All membranes with a 40 cm^2 area were characterized by monitoring water flow and salt rejection. A salt solution with 2 g/L of magnesium sulfate and sodium chloride was used as the feed solution; each salt was tested separately. We looked at water fluxes and salt rejection at pressures (6–25 bar, pH 7). All data pertaining to water flow and salt rejection were collected after the device was compressed for 45 minutes at 28 bar pressure in order to achieve steady-state operation. At room temperature (21°C), Milli-Q® water was used for all tests.

Water flux was estimated using the following equation (4):

$$J = \frac{V}{A \times t'} \quad (4)$$

where water flux (J, L/m^2 h), permeate volume (V, L), membrane area (A, m^2), and treatment time (t, h), respectively.
The salt rejection (R) was calculated using equation (5):

$$R\% = \left(1 - \frac{C_p}{C_f}\right) \times 100 \quad (5)$$

where Cp and C_f represent the concentration of salt (NaCl and $MgSO_4$) in the permeate and feed streams, respectively.

3. Results and Discussion

3.1. Characterization of isolated CNC

The form of nanocellulose produced from date palm leaves biomass by acid hydrolysis is crystalline nanocellulose (CNC). In the current study, the morphological structure of the extracted cellulose specimen was investigated under SEM. Prior to SEM analysis, the specimen was coated with Au/C using a vacuum sputter coater to improve their conductivity and the quality of the images that was captured. It was evident that the appearance of CNC was impacted by the mechanical treatment procedure [34]. The acid hydrolysis process eliminated the amorphous components leaving only the CNC. The surface structure of the isolated CNC was investigated under SEM at 20,000x magnification and an accelerating voltage of 15 kV. The SEM image shows that the formed CNC exhibit a rod like shape with size 1µm (Figure 1a). Some nodular agglomerates have been observed on the surface of CNC isolated from date palm leaves biomass. This due to the surface was dominated with hemicellulose and lignin to form bundles [35]. The average length of the particles was 507±29 and diameter were found to be 70.02±2.
The chemical structure of CNC was ascertained through an analysis of FTIR characterization. Before being examined using FT-IR, the sample 5 mg was dried in an oven at 60 °C for an entire night. The ultrasonic homogenizing sample was recorded with a resolution of 4 cm^{-1} and a wavenumber between 500 to 4000 cm^{-1} and scanning rate 20 nm/s and 30 scans.

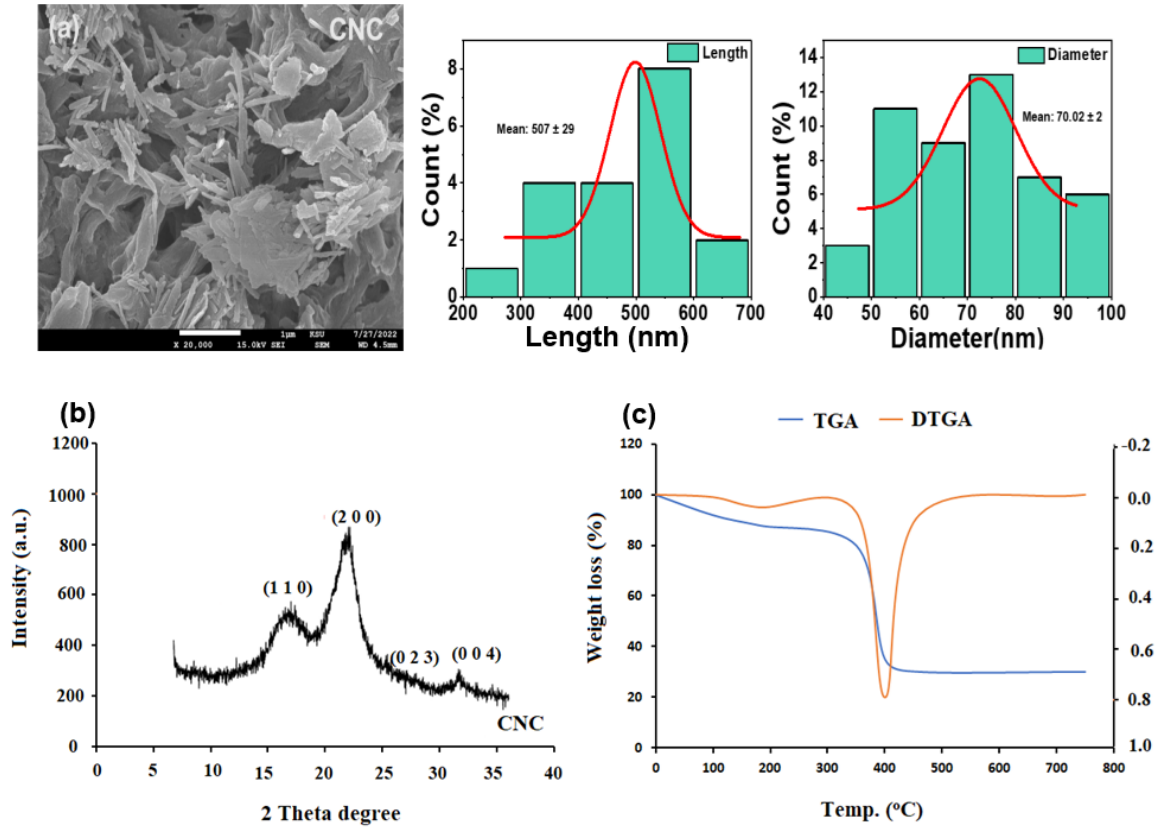

Fig. 1. (a) SEM images with particle size distribution, (b) XRD pattern, and (c) TGA and DTGA analysis of isolated CNC from date palm leaves.

XRD analysis is a useful tool to study the crystalline behavior of the isolated CNC sample. The analysis was performed under current flow 40 mA and operating voltage of 40 kV. The XRD device was set to scan at a rate of 4 s/step, with a step size of 0.05°/min, and scattering 2θ angles from 10 to 40° using a Cu-Kα radiation source (λ = 1.5406 Å). The observed peaks of CNC were appeared at 15.2° (1-1 0), 22.6° (1 1 0), 34.5° (0 2 0) cellulose crystallography planes of cellulose type II. According to the intensity of the diffraction peaks, it can be determined the degree of cellulose crystallinity. The percentage crystallinity index (CrI) of isolated CNC was calculated using the Segal equation (6). The CrI of CNC was 84.27%.

$$\text{CrI}\ (\%) = \frac{I_{2\,0\,0} - I_{am}}{I_{2\,0\,0}} \times 100 \qquad (6)$$

The thermogravimetric analyses (TGA) and derivative thermogravimetric analyses (DTGA) were used to perform thermal stability analyses of isolated CNC. It was found that below 200°C there was a weight loss of about 15%. This can be attributed to the evaporation of moisture, which is associated with weight loss due to the hydrophilicity of date palm leaves [36]. The maximum thermal degradation was found at 385°C with corresponding weight loss of 64.18% (Figure 1d).

The CNC that was separated from the waste date palm leaves biomass using sulfuric acid hydrolysis had the highest thermal stability, as evidenced by the lowest weight loss of CNCs that was achieved at a comparatively lower T_{max} temperature [37]. As a result of amorphous compounds being eliminated from the cellulose chain, CNC has improved thermal stability [38]. It can be explained that the carbonization of polysaccharide chains, which is started with the cleavage of C-H and C-C bonds, leveled off or gradually decreased over 400 °C. This was the case for CNC isolated from waste date palm leaves.

The electrostatic or charge attraction/repulsion between particles is quantified by the Zeta potential. It is among the basic variables that are known to have an impact on stability. Its measurement offers comprehensive information about the reasons behind flocculation, aggregation, and dispersion. The

isolated CNC Zeta potential analysis yielded a conductivity of 0.0248 mS/cm and a Zeta potential charge of -32.9 mV. Studies that have been reported state that the addition of sulfate groups to the cellulose surface during acid hydrolysis produces CNC with negative surface charge. This prevents the sedimentation and agglomeration of CNC in aqueous suspension by means of the esterification of surface hydroxyl groups, which produces sulfate groups [39]. The result is electrostatically stable colloidal aqueous suspensions. Based on the idea of electrostatic repulsion between the similar charge of the negative charge (anions), surface charge modification by the addition of sulfuric acid during acid hydrolysis (sulphate group) introduces anionic functionality to increase the defibrillation of cellulose. It is well known that negatively charged colloidal particles, or CNC can form extremely stable, surfactant-free substances [40].

3.2. SEM investigation of PA-CNC membranes

The fabricated PA-CNC membranes were examined under various magnifications using a SEM. The micrographic images of the blended PS and PA membranes (Figure 2a and 2b) show smooth surface with no significant pores. Because of the interaction between the CNC and the functional groups on the PA chain, SEM images of the surface PA-CNC (0.01% CNC w/v) and PA-CNC (0.02% CNC w/v) showed that they were more evenly distributed on PA (Figures 2c and 2d). Furthermore, CNC made PA membranes more hydrophilic. Comparing PA-CNC (0.01% CNC w/v) and PA-CNC (0.02% CNC w/v), it has been found that as CNC concentration increases, the mean pore size of the support decreases. More MPD solution is absorbed on the support when the pore size is large enough, which leads to more MPD diffusing into the hexane solution and reacting with TMC to form a "sheet-like" structure [41]. Figures 2e and 2f show the cross section of the formed modified) PA-CNC (0.01% CNC w/v) and PA-CNC (0.02% CNC w/v) membranes.

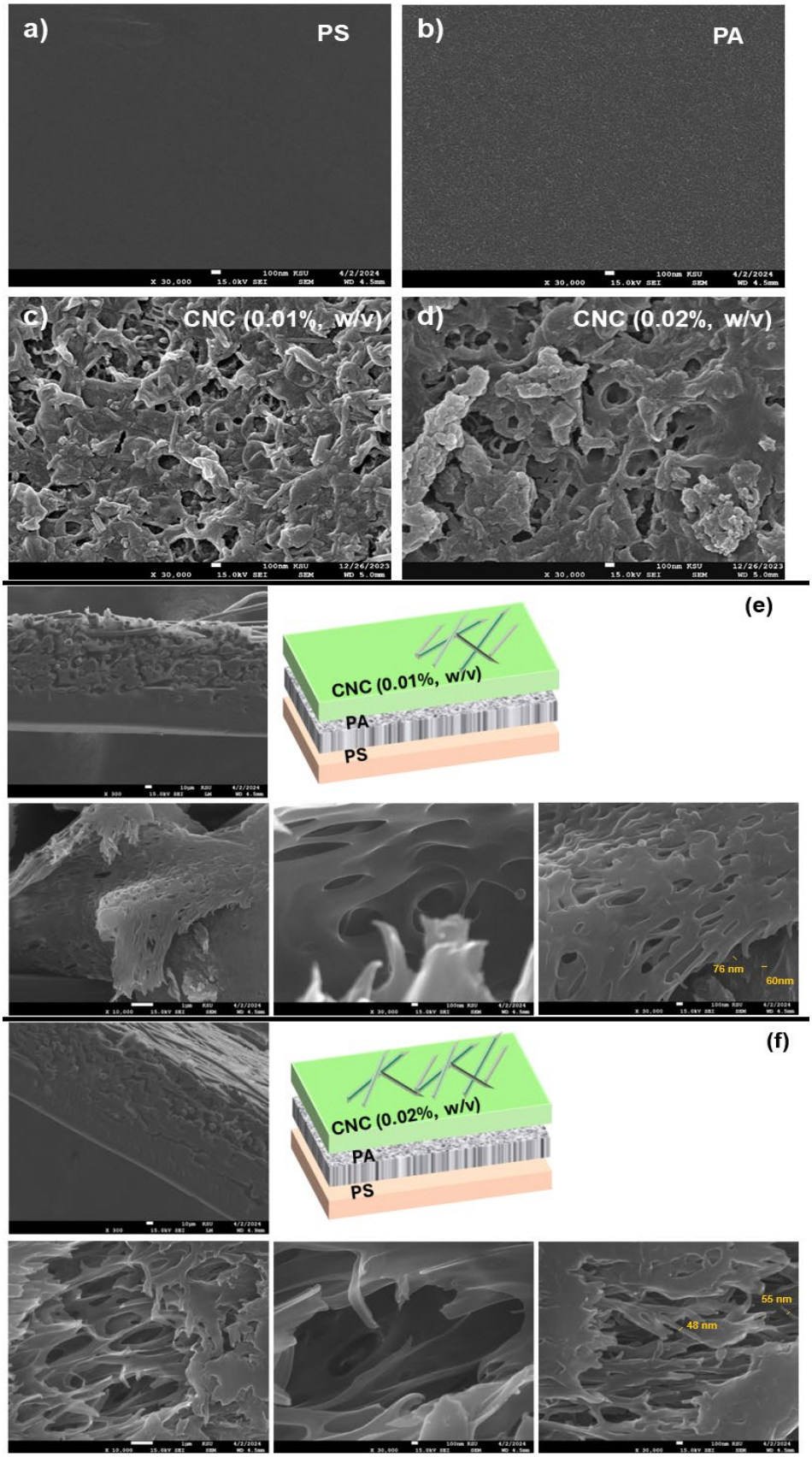

Fig. 2. SEM images of membrane top surface of (a)PS, (b) PA, (c) PA-CNC (0.01% CNC w/v), (d) PA-CNC (0.02% CNC w/v) and cross-section morphologies for (e) PA-CNC (0.01% CNC w/v), (f) PA-CNC (0.02% CNC w/v).

3.3. FT-IR of PA-CNC membranes

The FT-IR spectra of CNC, PA, PA-CNC (0.01%), and PA-CNC (0.02%) were analyzed in Figures 3a-3d. The FT-IR spectrum of CNC showed a significant absorption peak at 3417 cm^{-1}, which was due to the presence of H-bond stretching vibration of a hydroxyl group in cellulose. Another peak was observed at 2916 cm^{-1}, which was related to C-H stretching vibration of cellulose molecules [42]. C=O stretching of ester was found to be at 1728 cm^{-1}. The absence of the band at 1651 cm^{-1} was due to C=O stretch. The relative strength of the absorption was slightly reduced, confirming the removal of lignin and hemicellulose. The peak at 1581 cm^{-1} was related to the O-H bending vibration of absorption water molecules. The bands at 1157 cm^{-1}, which corresponded to the elongation of the ether C-O-C linkage, and 1435 cm^{-1}, which corresponded to aromatic ring vibrations or CH_3 of the acetyl group, were also linked to lignin. The band observed at 1056 cm^{-1} indicated the presence of strong C-O stretching of secondary alcohol.

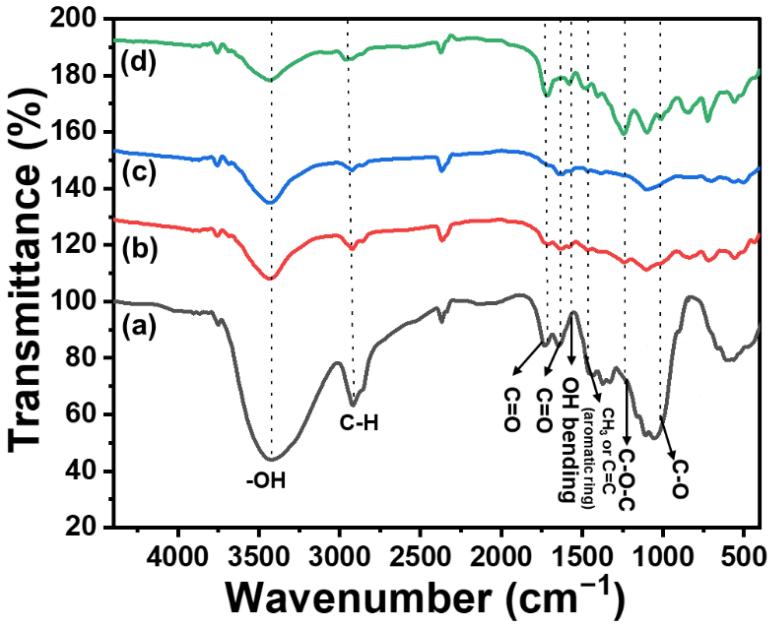

Fig. 3. FT-IR analysis of (a) CNC, (b) PA, (c) PA-CNC (0.01% CNC w/v), and (d) PA-CNC (0.02% CNC w/v) measured at wavenumber 500-4000 cm^{-1}.

3.4. Elemental analysis of PA-CNC membranes

An essential tool, energy dispersive spectroscopy (EDS) analyzes the X-rays produced by the electron beam of the scanning electron microscope (SEM) to determine the elements contained in a sample. The elemental composition of the fabricated PA-CNC membranes was performed with the use of a SEM connected to an EDX spectrometer. The obtained results shows that in PA (0% CNC) membrane the weight% of C and O were 42.94% and 57.06%, however the atomic% for the same elements were 50.06% and 49.94%, respectively (Figure 4a). In the fabricated PA-CNC membranes, for PA-CNC (0.01% w/v), the weight% of C, O, and S were 67.51%, 30.08%, and 2.41%, while the atomic % were 74.19%, 24.82%, 0.99% (Figure 4b). However, in the PA-CNC (0.02% w/v) the weight% were 71.72%, 21.45%, and 6.82%. However, the atomic% were 79.35%, 17.82%, and 2.83%, for C, O, and S, respectively (Figure 4c).

In addition, the X-rays are limited to the surface area excited by the tiny electron beam, so it is possible to obtain spectra of specific regions or particles. Hence, by scanning the beam, spectral information can be produced for the whole field of view, resulting in an elemental map. The collection and analysis of high-resolution data sets in minutes as opposed to days. Our clients can see the chemical landscape of their samples right away thanks to this elemental mapping technique. All elemental mapping images confirm the successful formation of modified membrane with CNC (Figures 5a-5c).

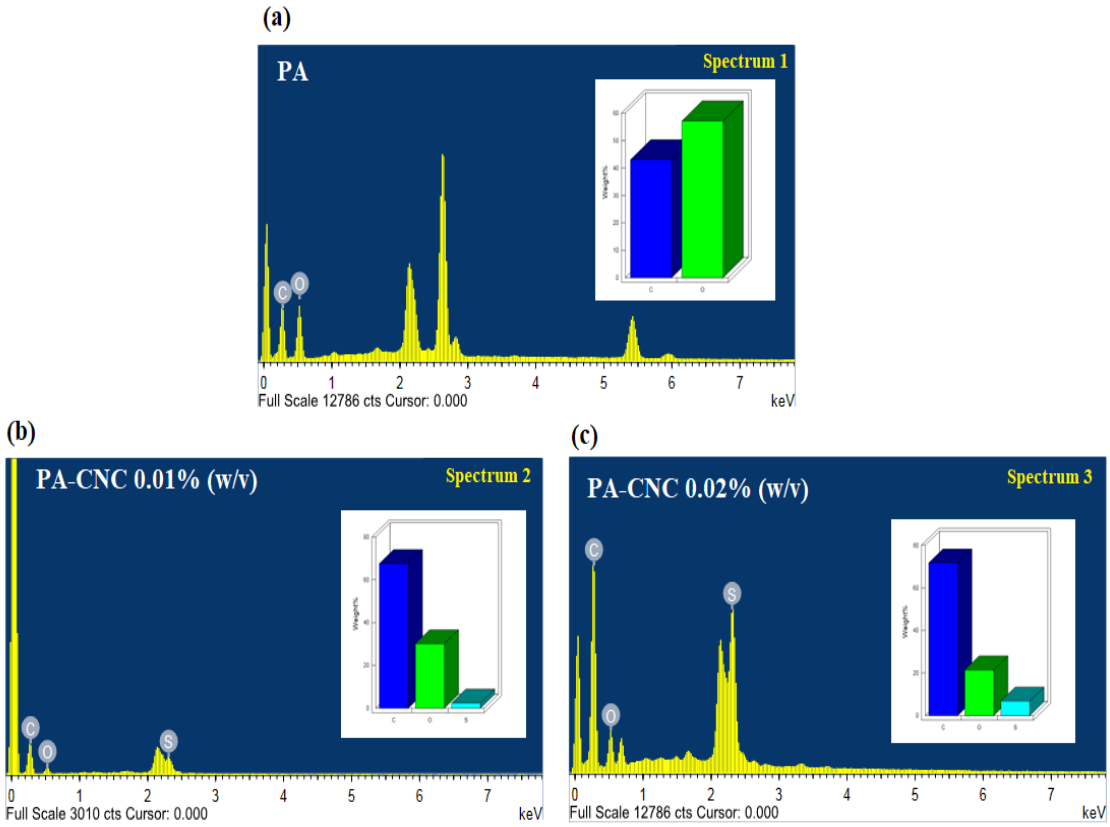

Fig. 4. EDX analysis of the fabricated (a) PA, (b) PA-CNC 0.01% (w/v), and (c) PA-CNC 0.02% (w/v) using CNC from date palm waste biomass.

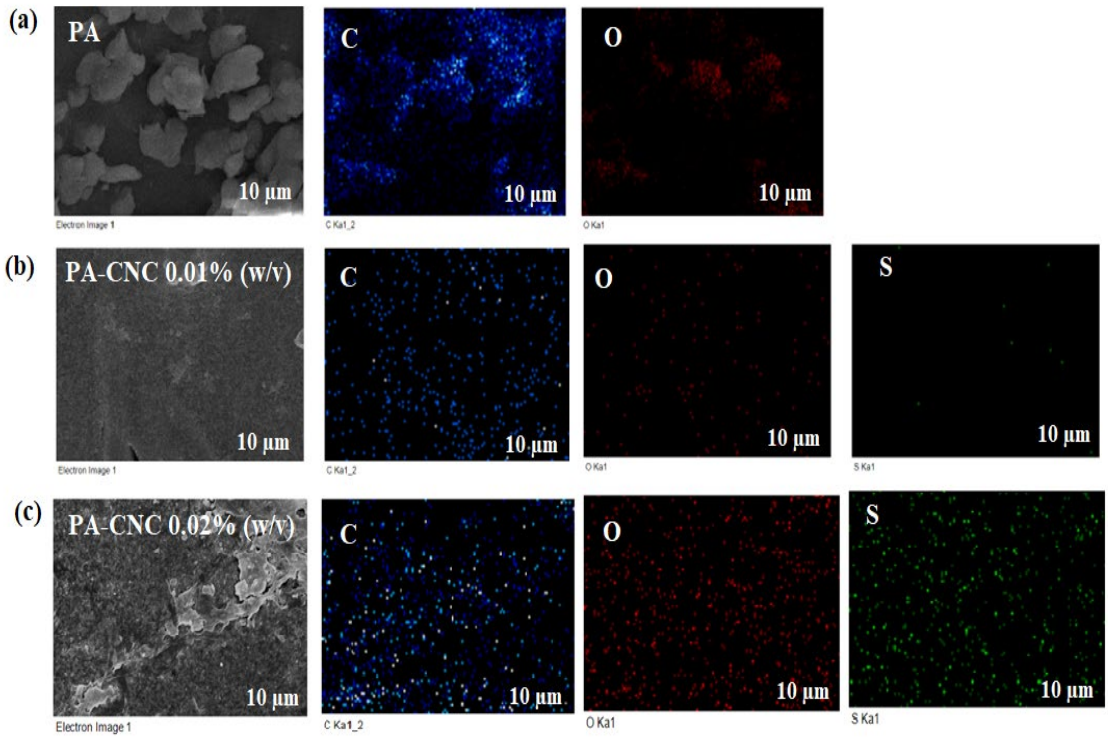

Fig. 5. Mapping images of the fabricated (a) PA, (b) PA-CNC 0.01% (w/v), and (c) PA-CNC 0.02% (w/v) using CNC from date palm waste biomass.

3.5. Thermogravimetric analysis of PA-CNC membranes

The thermal stability of the PA-CNC membranes produced was investigated using thermogravimetric analysis. It was found that the weight loss occurred in three successive stages. The first stage started at 425, 451, and 403 °C, and the weight loss was 3.5 %, 1.5 % and 5.2 % for

PA, PA-CNC 0.01 % (w/v) and PA-CNC 0.02 % (w/v), respectively. In the second stage, which started at 539, 556 and 506°C, the weight loss of the membranes was 69%, 56%, and 63% for the three membranes, respectively. However, in the third stage, a weight loss of 9.2%, 6.4%, and 8.6% was observed at 671, 696, and 659°C, respectively, for the three membranes mentioned above (Figures 6a-6c).

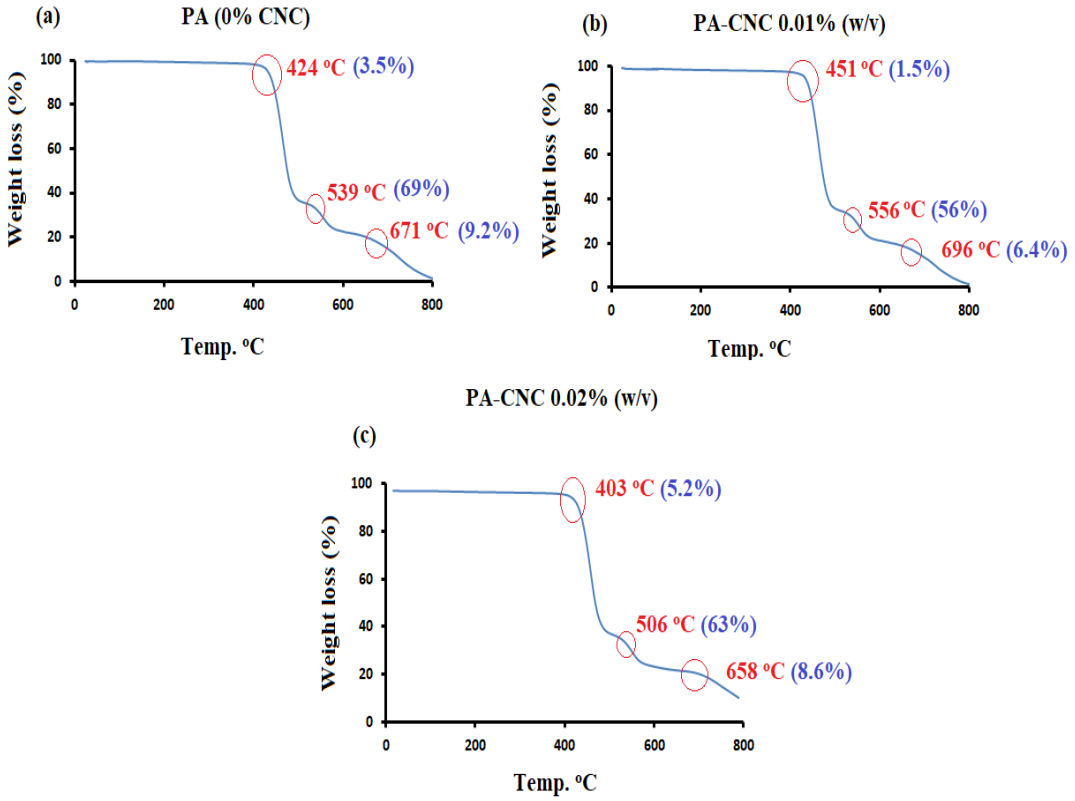

Fig. 6. Thermogravimetric analysis of (a) PA, (b) PA-CNC 0.01% (w/v), and (c) PA-CNC 0.02% (w/v).

3.6. Surface charge and Zeta potential of the PA-CNC membranes

As the pH deceased, the zeta potential becomes more negative, indicating an increase in surface charge. There are notable changes in zeta potential between pH 4.8 and 4.4, where the potential becomes less negative. At a pH 2.9, the zeta potential becomes positive, suggesting a shift from a negative charged surface to a positive charged one. The surface of materials often contains functional groups that can be ionized based on the pH of the surrounding solution. Common functional groups include carboxyl groups (-COOH) and amino groups ($-NH_2$). The ionization of these groups can influence the overall charge of the surface. Many functional groups are pH-sensitive, meaning their ionization state changes with the acidity or basicity of the solution. For example, carboxyl groups can become negatively charged (-COO-) at higher pH values and neutral (-COOH) at lower pH values. Amino groups, on the other hand, can become positively charged ($-NH^{3+}$) at lower pH values. In your specific case, the Zeta Potential becomes positive at a pH of 2.9. This may suggest that at lower pH values, certain functional groups on the material's surface are predominantly in their protonated (positively charged) form. This shift from a negatively charged surface to a positively charged one can have implications for the material's interactions with other charged particles, stability, and performance in various applications (Figure 7).

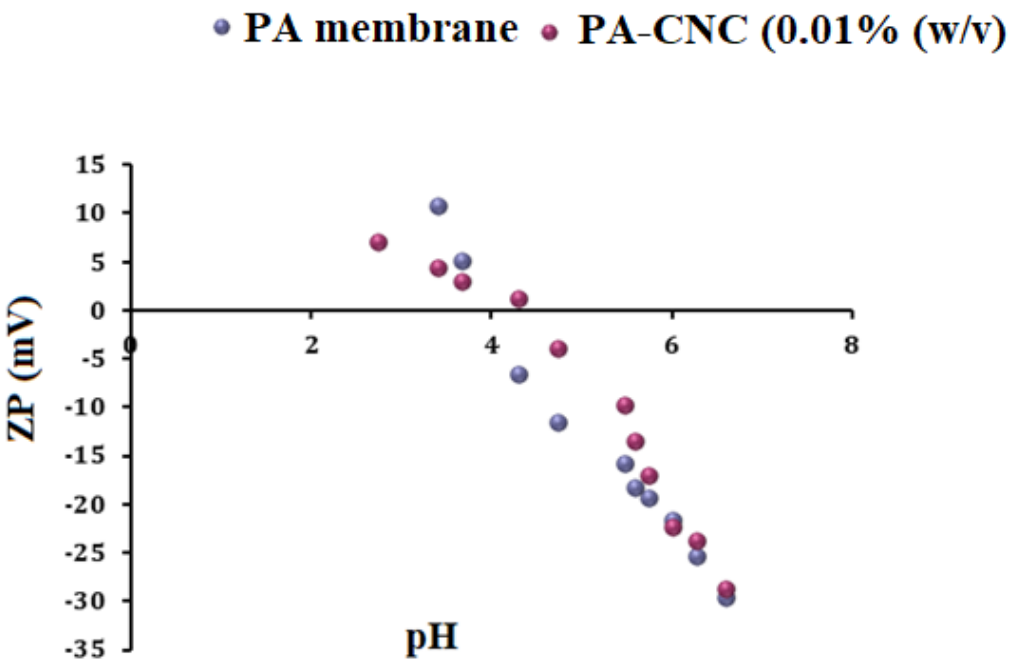

Fig. 7. Zeta potentials of PA membrane and modified PA-CNC 0.01% (w/v).

3.7. Mechanical properties of the PA modified membranes

In this work, interfacial polymerization was employed to create a thin layer of polyamide linked to the cellulose on the surface of a commercial polysulfone membrane, with the goal of increasing the membrane& surface characteristics to reject salts from aqueous solutions. The majority of the membrane is polysulfone, which is used as a support for the top thin layer (polyamide layer), which only makes up a small portion, determining its mechanical characteristics difficult. Furthermore, the mechanical characteristics of polysulfone were investigated in a number of studies, which revealed that it has high mechanical properties, high porosity, and is employed as a support layer owing to its unique mechanical properties [43-45].

Cellulose nanocrystals (CNCs) are cellulose-derived nanoparticles with great strength, stiffness, and biodegradability that can have a considerable impact on molecular motion, relaxation processes, and orientation in the polymer matrix [46, 47]. CNCs in polymer matrix can limit chain molecular motion due to physical entanglement, lowering total mobility and influencing characteristics like as flexibility and ductility. CNCs influence polymer matrix relaxation, which affects glass transition temperature and stiffness. They also have an impact on secondary relaxation processes, which alter the creep and stress relaxation characteristics of composite materials. CNCs align inside the polymer matrix during processing, giving anisotropic characteristics. Oriented CNCs improve mechanical qualities like as tensile strength and modulus according on processing conditions and shear pressures. Interfacial interactions between CNCs and polymer matrix significantly impact composite material performance, with strong adhesion improving load transfer and reducing stress concentrations. In summary, CNCs in polymer composites provide sophisticated materials for structural components and biomedical devices, but proper processing settings and interface engineering are required for maximum potential.

3.8. Contact angles

The flow and antifouling properties of a membrane are influenced by its hydrophilicity [48]. The hydrophilicity of the membranes was determined by measuring the contact angles of water droplets on the membrane surfaces with PA (0 % CNC), PA-CNC (0.01 % w/v) and PA-CNC (0.0 % w/v). The measured contact angles for the prepared membranes are displayed in Table 1 and Figure 8.

Table 1. The contact angles of water droplets on the surface of fabricated PA-CNC membranes.

Contact angle (°)	Membrane
68.04±3.7	PA (0% CNC)
72.83±0.8	PA-CNC (0.01%, w/v)
63.76±5.5	PA-CNC (0.02%, w/v)

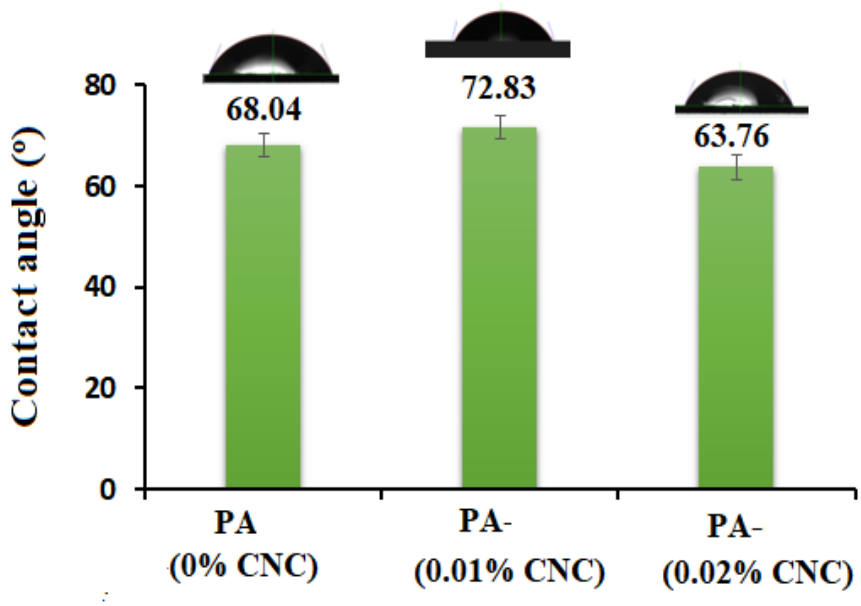

Fig. 8. Water droplets contact angles evaluated on the surface of PA-CNC membranes PA (0% CNC), PA-CNC (0.01% w/v), and PA-CNC (0.02 % w/v).

Their contact angle of less than ninety degrees indicates the hydrophilicity of the developed membranes and the decreased fouling during water treatment. The reason for this is that the water molecules coat the surface of the membrane, obstructing the contaminants from coming into direct contact with it. Because of its hydrophilicity, the surface attracts polar molecules like water, giving it a strong polarity. It doesn't take any more pressure to penetrate. All the modified PA-CNC membranes had reduced contact angles because the membrane surface contains a large number of hydrophilic groups that increase the membrane's hydrophilicity. This is because the hydrophilic groups effective surface area is decreased by the aggregation of PA-CNC and the hydrophobic nature of CNC [49]. Moreover, as CNC % increased, the contact angle values of PA-(0% CNC), PA-CNC (0.01% w/v), and PA-CNC (0.02% w/v) were (68.04°, 72.83°, and 63.76°, respectively), due to the hydrophobic nature of CNC nanopowder.

3.9. Water permeability

Chemical content, the membrane surface's charge, and its hydrophilicity all have a significant impact on the rate of water flow because they influence how the membrane surface interacts with the solution. This interaction can be mediated by secondary forces like dipole-dipole, electrostatic contact, hydrogen bonding, and van der Waals [50]. The permeate flow versus applied pressure for PA (0% w/v), PA-CNC (0.01% w/v), and PA-CNC (0.02% w/v) is displayed in Figure 9. The linear regression curves between the applied pressure and the flow rate were used to compute the permeability values. Water permeability at 30 bars were found to be 36.25, 43.25, and 42.85 $Lm^{-2}h^{-1}bar^{-1}$ for PA (0% w/v), PA-CNC (0.01% w/v), and PA-CNC (0.02% w/v), respectively. All membrane flow rates generally increased in tandem with pressure increases. This concentration will therefore be allowed. All membrane flux rates generally increased in tandem with pressure increases. This concentration will therefore be permitted (Table 2).

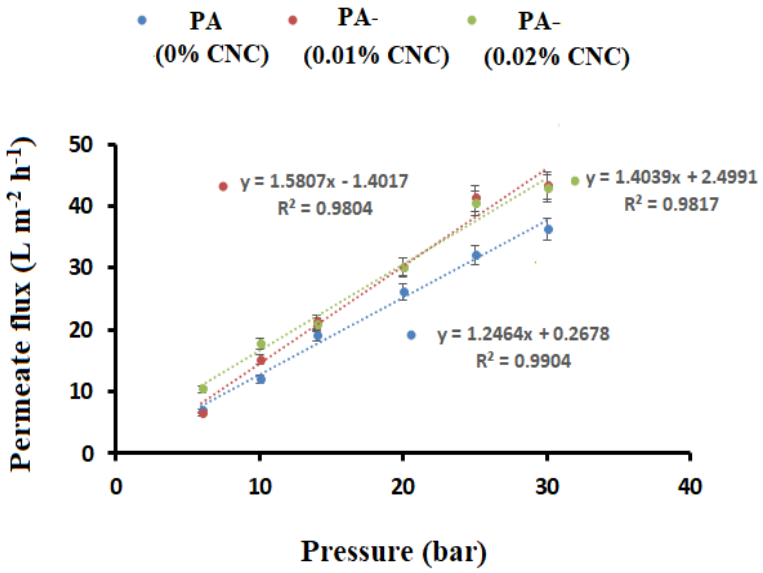

Fig. 9. Permeate flux rate of (a) PA (0% CNC), (b) PA-CNC (0.01%, w/v), and PA-CNC (0.02%, w/v) vs. transmembrane pressure.

Table 2. The data obtained for water permeability, salt rejection, and contact angle of all fabricated PA-CNC membranes.

Salt rejection (%) at 30 bar		Water permeability at 30 bar ($Lm^{-2}h^{-1}bar^{-1}$)	Contact angle (°)	Membrane
NaCl	$MgSO_4$			
99.23	98.89	36.25	68.04±3.7	PA (0% CNC)
98.21	98.85	43.25	71.00±0.8	PA-CNC (0.01%, w/v)
98.45	98.45	42.85	63.76±5.5	PA-CNC (0.02%, w/v)

3.10. Salt rejection

The salt-rejection potential of all fabricated PA-CNC membranes was investigated using a crossflow RO/NF system. The salt rejection of the membranes produced for PA (0% CNC), PA-CNC (0.01% w/v), and PA-CNC (0.02% w/v) is displayed in Figures 10a and 10b.

The salts that were rejected were NaCl and $MgSO_4$, each of which had two grams of salt per liter. All manufactured membranes typically had rejected ratios greater than 98%, indicating that modified membranes can be more effective. Poor CNC-polymer interfacial compatibility seems to have prevented CNC from being entrapped into the modified membrane matrix in the case of reduced rejection, leading to unselective voids. Moreover, a permeability trade-off was present, wherein the polymer matrix's hydrophilic CNC rejection was preferred over a greater pore size. Many studies have examined the impact of interfacial polymerization and PS pretreatment on the desalination characteristics of membranes based on TMC and MPD. Table 3 displays the comparison of the produced membranes' flow and salt retention characteristics with those of other membranes.

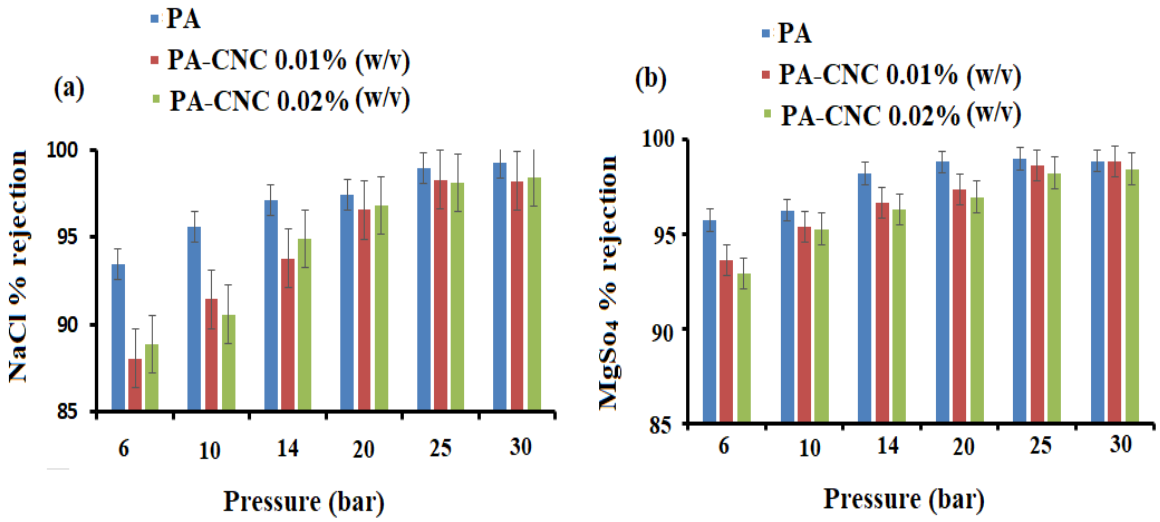

Fig. 10. Salt rejection of (a) NaCl and (b) $MgSO_4$ for PA, PA-CNC 0.01% (w/v), and PA-CNC 0.02% (w/v).

Table 3. Comparative results obtained from PA-CNC 0.01% and previously reported membranes.

Membrane	Conditions	Flux rate (L/m^2h)	NaCl salt rejection %	Reference
PA-NMP 82%	15 bar, 2000 ppm NaCl solution	36.0	95.0%	[51]
PA-DMF 12%	16 bar, 2000 ppm NaCl solution	3.98	98.8%	[52]
PASiO_2 1%	15bar, 2000 ppm NaCl solution	47.9	98.9%	[53]
PA-CNC 0.01%	30 bar, 2000 ppm NaCl solution	43.25	98.2%	Present study

4. Conclusion

In the current investigation, the acid hydrolysis method proved effective in separating CNC from waste date pale leaves biomass. According to the morphological analyses, the isolated CNC had a crystalline structure resembling a rode-like structure with length Mean about 507 ± 29 nm and a diameter of 70.02 ± 2 nm. According to the FTIR spectra analyses, the resulting CNC was identified as cellulose species. According to the XRD analyses, acid hydrolyses improved the percentage crystallinity index; the isolated CNC produced the highest percentage crystallinity index, which was 83.46. The CNC isolated from waste date palm leaves biomass exhibited good thermal stability, according to analyses of thermal stability, and they may be used modifier for polyamide modified membranes for water treatment. On the polysulfone support sheet, interfacial polymerization was used to produce polyamide-CNC membranes. It has been investigated how well the constructed polyamide membranes reject water and salt. SEM and water contact angle measurements revealed that the PA-CNC 0.01% membrane had a smoother surface with more hydrophobic. The results showed that the modified membranes performed better when CNC nanopowder was added. More than 98% of the penetration rejection of NaCl and $MgSO_4$ was shown by the water flow of a reverse osmosis membrane factionalized with 0.01% w/v CNC at pressure (30 bar). This is due to large pores and higher-value PA-CNC wettability, which influence how quickly water molecules pass through. The results showed that adding functionalized CNC powder increased the prepared membranes' efficiency.

Author Contributions

Conceptualization, supervision and funding acquisition, S.S.A.; Methodology, formal analysis, A.A.A.; Investigation, data curation; A.E.; data curation, formal analysis, M.F.E. This version of manuscript has been revised and approved by all authors.

Funding

This study was supported by Researchers Supporting Project (number RSP-2024/195) from King Saud University, Riyadh, Saudi Arabia.

Institutional Review Board Statement

Not applicable.

Informed Consent Statement

Not applicable.

Data Availability Statement

The outcomes of this study have been included within the text.

Acknowledgments

The authors are grateful for the Researchers Supporting Project (number RSP-2024/195) from King Saud University, Riyadh, Saudi Arabia.

Conflicts of Interest

The authors declare no conflict of interest.

References

[1] Uralovich, K.S., Toshmamatovich, T.U., Kubayevich, K.F., Sapaev, I.B., Saylaubaevna, S.S., Beknazarova, Z.F. and Khurramov, A.: A primary factor in sustainable development and environmental sustainability is environmental education. Caspian J. Environ. Sci. 21(4), 965-975 (2023).

[2] Mishra, R.K.: Fresh water availability and its global challenge. British J. Multidiscip. Adv. Studies 4(3), 1-78 (2023). https://doi.org/10.37745/bjmas.2022.0208

[3] Mumtaz, T., Cheema, A.T.: Causes and Effects of Water and Environmental Pollution: A Way Forward. J. Pol. Stud. 30, 83 (2023).

[4] Soomro, A.H., Marri, A. and Shaikh, N.: Date Palm (Phoenix dactylifera): A Review of Economic Potential, Industrial Valorization, Nutritional and Health Significance. Neglected Plant Foods Of South Asia: Exploring and valorizing nature to feed hunger, 319-350 (2023). https://doi.org/10.1007/978-3-031-37077-9_13

[5] Alotaibi, K.D., Alharbi, H.A., Yaish, M.W., Ahmed, I., Alharbi, S.A., Alotaibi, F., Kuzyakov, Y.: Date palm cultivation: A review of soil and environmental conditions and future challenges. Land Deg. Dev. 34(9), 2431-2444 (2023) https://doi.org/10.1002/ldr.4619

[6] Al-Awa, Z.F.A., Sangor, F.I.M.S., Babili, S.B., Saud, A., Saleem, H. Zaidi, S.J.: Effect of Leaf Powdering Technique on the Characteristics of Date Palm-Derived Cellulose. ACS Omega. (2023) https://doi.org/10.1021/acsomega.3c01222

[7] Aral, B.: Turkey's Voting Preferences in the UN General Assembly During the AK Party Era as a Counterchallenge to Its 'New'Foreign Policy. J. Balkan Near East. Stud. 25(3), 399-439 (2023). https://doi.org/10.1080/19448953.2022.2143852

[8] Sebastian, J.K., Nagella, P., Mukherjee, E., Dandin, V.S., Naik, P.M., Jain, S.M., Al-Khayri, J.M. Johnson, D.V.: Date Palm: Genomic Designing for Improved Nutritional Quality. ICompend. Crop Genome Design. Nutraceut. 1-64 (2023). Singapore: Springer Nature Singapore. https://doi.org/10.1007/978-981-19-3627-2_43-1

[9] Al-Mohamed, R., Majar, A., Fahed, K., Dagar, J.C. Sileshi, G.W.: Agroforestry for Plant Diversity and Livelihood Security in Southwest Asia. Agro. Sustain. Inten. Agr. Asia Afr. 387-428, (2023). Singapore: Springer Nature Singapore. https://doi.org/10.1007/978-981-19-4602-8_13

[10] Anvari, S., Aguado, R., Jurado, F., Fendri, M., Zaier, H., Larbi, A. Vera, D., 2024. Analysis of agricultural waste/byproduct biomass potential for bioenergy: The case of Tunisia. Energy Sustain. Dev. 78,101367 (2024). https://doi.org/10.1016/j.esd.2023.101367

[11] Rodríguez-Espinosa, T., Papamichael, I., Voukkali, I., Gimeno, A.P., Candel, M.B.A., Navarro-Pedreño, J., Zorpas, A.A. Lucas, I.G.: Nitrogen management in farming systems under the use of agricultural wastes and circular economy. Sci. Total Environ. 876,162666 (2023). https://doi.org/10.1016/j.scitotenv.2023.162666

[12] Raza, M., Abu-Jdayil, B., Banat, F. and Al-Marzouqi, A.H., 2022. Isolation and characterization of cellulose nanocrystals from date palm waste. ACS omega, 7(29), pp.25366-25379. https://doi.org/10.1021/acsomega.2c02333

[13] Raza, M., Abu-Jdayil, B., Banat, F. and Al-Marzouqi, A.H., 2022. Isolation and characterization of cellulose nanocrystals from date palm waste. ACS omega, 7(29), pp.25366-25379. https://doi.org/10.1021/acsomega.2c02333

[14] Saud, A., Saleem, H., Khan, A.W., Munira, N., Khan, M. and Zaidi, S.J., 2023. Date Palm Tree Leaf-Derived Cellulose Nanocrystal Incorporated Thin-Film Composite forward Osmosis Membranes for Produced Water Treatment. Membranes, 13(5), p.513. https://doi.org/10.3390/membranes13050513

[15] Gelaw, B.B., Kasaew, E., Belayneh, A., Tesfaw, D. and Tesfaye, T., 2023. Review of the sources, synthesis, and applications of nanocellulose materials. Polymer Bulletin, pp.1-23. https://doi.org/10.1007/s00289-023-05061-4

[16] Hashem, A.H., El-Naggar, M.E., Abdelaziz, A.M., Abdelbary, S., Hassan, Y.R. and Hasanin, M.S., 2023. Bio-based antimicrobial food packaging films based on hydroxypropyl starch/polyvinyl alcohol loaded with the biosynthesized zinc oxide nanoparticles. International Journal of Biological Macromolecules, 249, p.126011. https://doi.org/10.1016/j.ijbiomac.2023.126011

[17] Debnath, B., Haldar, D. and Purkait, M.K., 2021. A critical review on the techniques used for the synthesis and applications of crystalline cellulose derived from agricultural wastes and forest residues. Carbohydrate polymers, 273, p.118537. https://doi.org/10.1016/j.carbpol.2021.118537

[18] Sharma, S., Sharma, V., Chatterjee, S. Contribution of plastic and microplastic to global climate change and their conjoining impacts on the environment-A review. Sci. Total Environ. 875,162627 (2023). https://doi.org/10.1016/j.scitotenv.2023.162627

[19] Khoshnodifar, Z., Ataei, P. Karimi, H.: Recycling date palm waste for compost production: A study of sustainability behavior of date palm growers. Environ. Sustain. Ind. 20, 100300 (2023). https://doi.org/10.1016/j.indic.2023.100300

[20] Padha, B., Verma, S., Ahmed, A., Chavhan, M.P., Mahajan, P. Arya, S. From Trash to Treasure: Crafting electrochemical supercapacitors with recycled waste materials. Progress Energy (2023). https://doi.10.1088/2516-1083/ad139c

[21] Di Fraia, S., Sharmila, V.G., Banu, J.R. Massarotti, N. A comprehensive review on upscaling of food waste into value added products towards a circular economy: Holistic approaches and life cycle assessments. Trends Food Sci. Technol. 104288 (2023). https://doi.org/10.1016/j.tifs.2023.104288

[22] Boughezal, A., Ben Mya, O., Lanez, T. Fethiza Tedjani, C.: Extraction of pure cellulose from palm residues using alkaline treatment method and its performance in PVC polymer matrix composite. Biomass Conv. Bioref. 1-10 (2023). https://doi.org/10.1007/s13399-023-04927-x

[23] Ivbanikaro, A.E., Okonkwo, J.O., Sadiku, E.R. Maepa, C.E.: Recent development in the formation and surface modification of cellulose-bead nanocomposites as adsorbents for water purification: a comprehensive review. J. Polym. Eng. 43(8), 680-714 (2023). https://doi.org/10.1515/polyeng-2023-0056

[24] Sadare, O.O., Yoro, K.O., Moothi, K. Daramola, M.O.: Lignocellulosic biomass-derived nanocellulose crystals as fillers in membranes for water and wastewater treatment: a review. Membranes, 12(3), 320 (2022). https://doi.org/10.3390/membranes12030320

[25] Kian, L.K., Fouad, H., Jawaid, M. Karim, Z.: Crystalline nanocellulose based sustainable nanoscopic composite membrane production: removal of metal ions from water. Cellulose, 29(7), 3803-3816 (2022). https://doi.org/10.1007/s10570-022-04494-w

[26] Liu, Y., Liu, H. Shen, Z.: Nanocellulose based filtration membrane in industrial waste water treatment: A review. Materials, 14(18), 5398 (2021). https://doi.org/10.3390/ma14185398

[27] Salama, A., Abouzeid, R., Leong, W.S., Jeevanandam, J., Samyn, P., Dufresne, A., Bechelany, M. Barhoum, A.: Nanocellulose-based materials for water treatment: adsorption, photocatalytic degradation, disinfection, antifouling, and nanofiltration. Nanomaterials, 11(11), 3008 (2021). https://doi.org/10.3390/nano11113008

[28] Adegoke, K.A., Giwa, S.O., Adegoke, O.R. Maxakato, N.W.: Bibliometric evaluation of nanoadsorbents for wastewater treatment and way forward in nanotechnology for clean water sustainability. Sci. Afr. 21, e01753 (2023). https://doi.org/10.1016/j.sciaf.2023.e01753

[29] Davoodbeygi, Y., Askari, M., Salehi, E. Kheirieh, S.: A review on hybrid membrane-adsorption systems for intensified water and wastewater treatment: Process configurations, separation targets, and materials applied. J. Environ. Manag. 335, 117577 (2023). https://doi.org/10.1016/j.jenvman.2023.117577

[30] Demoulin, C., Dahdouh, L., Ricci, J., Ruiz, E., Delalonde, M. Wisniewski, C.: Synergistic effect of particle size, shear rate and driving-force during microfiltration of fruit juices: Toward a relevant choice of pretreatments and filtration conditions. Innov. Food Sci. Emerg. Technol. 84, 103247 (2023). https://doi.org/10.1016/j.ifset.2022.103247

[31] Tang, Q., An, X., Lan, H., Liu, H. Qu, J.: A homogeneous carbon nitride nanomodifier for promoting the water permeation of polyamide desalination membranes. Separation and Purification Technology, 127082 (2024). https://doi.org/10.1016/j.seppur.2024.127082

[32] Dai, B., Hu, Y., Ding, Y., Shen, L., Li, R., Zhao, D., Jiao, Y., Xu, Y., Lin, H. Innovative construction of nano-wrinkled polyamide membranes using covalent organic framework nanoflowers for efficient desalination and antibiotic removal. Desalination, 570, 117083 (2024). https://doi.org/10.1016/j.desal.2023.117083

[33] Liu, S., Yang, F., Zhou, J., Peng, Y., Wang, E., Song, J., Su, B.: Construction of highly permeable organic solvent nanofiltration membrane via β-cyclodextrin assisted interfacial polymerization. J. Membrane Sci. 687, 22052 (2023). https://doi.org/10.1016/j.memsci.2023.122052

[34] Al-Awa, Z.F.A., Sangor, F.I.M.S., Babili, S.B., Saud, A., Saleem, H. and Zaidi, S.J.: Effect of leaf powdering technique on the characteristics of date palm-derived cellulose. ACS omega, 8(21),18930-18939 (2023). https://doi.org/10.1021/acsomega.3c01222

[35] Alhamzani, A.G. and Habib, M.A., 2021. preparation of cellulose nanocrystals from date palm tree leaflets (phoenix dactylifera l.) Via repeated chemical treatments. Cellul. Chem. Technol, 55, 33-39 (2021).

[36] Huang, K., Maltais, A., Wang, Y.: Enhancing water resistance of regenerated cellulose films with organosilanes and cellulose nanocrystals for food packaging. Carbohyd. Polym Technol. Appl. 6,100391 (2023). https://doi.org/10.1016/j.carpta.2023.100391

[37] Benhamou, A.A., Kassab, Z., Boussetta, A., Salim, M.H., Ablouh, E.H., Nadifiyine, M., Moubarik, A., El Achaby, M.: Beneficiation of cactus fruit waste seeds for the production of ellulose nanostructures: extraction and properties. Int. J. Biol. Macromol. 203, 302-311 (2022).https://doi.org/10.1016/j.ijbiomac.2022.01.163

[38] D'Acierno, F., Hamad, W.Y., Michal, C.A. and MacLachlan, M.J.: Thermal degradation of cellulose filaments and nanocrystals. Biomacromolecules 21(8),3374-3386 (2020).https://doi.org/10.1021/acs.biomac.0c00805

[39] Shojaeiarani, J., Bajwa, D.S., Chanda, S.: Cellulose nanocrystal based composites: A review. Composites Part C: Open Access, 5,100164 (2021). https://doi.org/10.1016/j.jcomc.2021.100164

[40] Ramos, P.Z., Call, C.C., Simitz, L.V., Richards, J.J.: Evaluating the rheo-electric performance of aqueous suspensions of oxidized carbon black. J. Coll. Inter. Sci 634, 379-387(2023). https://doi.org/10.1016/j.jcis.2022.12.017

[41] Li, J.B., Zhu, C.Y., Guo, B.B., Liu, C., Xin, J.H., Zhang, C., Wu, J., Zhang, L., Yang, H.C., Xu, Z.K.: Ultrahigh-permeance polyamide thin-film composite membranes enabled by interfacial polymerization on a macro-porous substrate toward organic solvent nanofiltration. J. Membrane Sci. 122342 (2023). https://doi.org/10.1016/j.memsci.2023.122342

[42] Raza, M., Abu-Jdayil, B., Banat, F. and Al-Marzouqi, A.H.: Isolation and characterization of cellulose nanocrystals from date palm waste. ACS omega, 7(29), 25366-25379 (2022).

[43] Pouresmaeel-Selkjani, P., Jahanshahi, M., amp; Peyravi, M.: Mechanical, thermal, and morphological properties of nanoporous reinforced polysulfone membranes. High Performance Polymers, 29(7), 759-771 (2017).

[44] Ismail, N. M., Jakariah, N. R., Bolong, N., Anissuzaman, S. M., Nordin, N. A. H. M., & Razali, A. R.: Effect of polymer concentration on the morphology and mechanical properties of asymmetric polysulfone (PSf) membrane. Journal of Applied Membrane Science & Technology, 21(1), (2017).

[45] Yang, X., Liu, H., Zhao, Y., amp; Liu, L.: Preparation and characterization of polysulfone membrane incorporating cellulose nanocrystals extracted from corn husks. Fibers and Polymers, 17, 1820-1828 (2016).

[46] Masese, F.K., Njenga, P.K., Ndaya, D.M. and Kasi, R.M., 2023. Recent Advances and Opportunities for Cellulose Nanocrystal-Based Liquid Crystalline Polymer Hybrids and Composite Materials. Macromolecules, 56(17), pp.6567-6588. https://doi.org/10.1021/acs.macromol.3c00369

[47] Hynninen, V., Patrakka, J. Nonappa: Methylcellulose–cellulose nanocrystal composites for optomechanically tunable hydrogels and fibers. Materials, 14(18), 5137 (2021). https://doi.org/10.3390/ma14185137

[48] Li, J.B., Zhu, C.Y., Guo, B.B., Liu, C., Xin, J.H., Zhang, C., Wu, J., Zhang, L., Yang, H.C., Xu, Z.K.: Ultrahigh-permeance polyamide thin-film composite membranes enabled by interfacial polymerization on a macro-porous substrate toward organic solvent nanofiltration. J. Membrane Sci. 122342 (2023). https://doi.org/10.1016/j.memsci.2023.122342

[49] Abedi, F.: Thin Film Nanocomposite Membranes Using Cellulose Nanocrystals for Water Treatment (Doctoral dissertation, Université d'Ottawa/University of Ottawa) (2023). http://hdl.handle.net/10393/45239

[50] Cheng, X., Zhang, Y., Shao, S., Lai, C., Wu, D., Xu, J., Luo, X., Xu, D., Liang, H., Zhu, X.: Highly permeable positively charged nanofiltration membranes with multilayer structures for multiple heavy metal removals. Desalination 548, 116266 (2023). https://doi.org/10.1016/j.desal.2022.116266

[51] Hurwitz, G., Guillen, G.R., Hoek, E.M. Probing polyamide membrane surface charge, zeta potential, wettability, and hydrophilicity with contact angle measurements. J. Memb. Sci. 349, 349–357 (2010).

[52] Yan, W., Wang, Z., Wu, J., Zhao, S., Wang, J., Wang, S.: Enhancing the flux of brackish water TFC RO membrane by improving support surface porosity via a secondary pore-forming method. J. Memb. Sci. 498, 227–241 (2016).

[53] Wang, J., Xu, R., Yang, F., Kang, J., Cao, Y., Xiang, M.: Probing influences of support layer on the morphology of polyamide selective layer of thin film composite membrane. J. Memb. Sci. 556, 374–383 (2018).

Published in: Materials Science Forum
ISSN: 1662-9752, Vol. 1125, pp 53-63
doi:10.4028/p-ONoxF5

Submitted: 2023-09-29
Revised: 2024-03-20
Accepted: 2024-03-26
Online: 2024-09-23

Developing New Natural Surfactant from Date Seeds for Different Field Applications

Noah AlOtaibi[1,a], Moustafa Aly[2,b], Taha Moawad[1,c*]

[1]Department of Petroleum Engineering, King Saud University, Riyadh, Saudi Arabia

[2]Department of Energy and Petroleum Engineering, University of Wyoming, Laramie, WY 82071, United States

[a]438103133@student.ksu.edu.sa, [b]maly1@uwyo.edu, [c]tmoawad@ksu.edu.sa

Keywords: Crude Oil, Enhanced Oil Recovery, Green Surfactant, Date Seeds.

Abstract. The increase in using natural surfactants for enhanced oil recovery (EOR) purposes in recent years is mainly attributed to the widespread global awareness of the environmental effects the oil and gas industry causes. In accordance with KSA Vision 2030 and the corresponding global direction, the purpose of this study is to discover a cost effective, readily available, environmentally friendly, and locally sourced surfactant. This surfactant will help reduce the interfacial tension (IFT) between reservoir liquids to enhance the reservoir's productivity and increase its ultimate recovery.
In this study, date seeds have been chosen as the green surfactant source due to the abundance of such seeds. Al-Khalas, which is a well-known palm tree that grows in Qassim, Al-Kharj, and Al-Ahsa provinces in KSA was chosen. Properties such as surface tension (ST), IFT, pH, and density were measured to evaluate the effectiveness of date seeds as a natural surfactant.
ST results showed a reduction from 72 mN/m (of distilled water) to 43 mN/m using the new surfactant in formation water at 10 wt% comprising a 40% reduction. Moreover, IFT of the new surfactant with Saudi medium oil (26 API) was 10 mN/m compared to 18 mN/m of a formation water-oil system which represents a 49% reduction in interfacial tension.
Overall, the novel surfactant studied in this research shows great promise in being an effective EOR agent in addition to eliminating the negative impacts of regular surfactants on the environment.

Introduction

Crude oil remains a necessity to meet growing energy demands despite a decline in the discovery of new oil reserves on a worldwide scale [1,2]. Alternative energy sources, while promising, have continued to fall short of satisfying the world's expanding energy demands. As a result, the energy requirement is satisfied by a combination of crude oil and alternative energy sources [3]. According to chronological order, the process of recovering oil from a reservoir can be divided into three stages: primary, secondary, and tertiary oil recovery [4]. To reduce the quantity of trapped oil in the pore space of matrix rock, surfactant flooding is an essential method for improving oil recovery. By reducing the interfacial tension between oil and water and/or by changing the wettability from oil-wet to water-wet, surfactants are injected to mobilize leftover oil. Numerous cationic, anionic, non-ionic, and amphoteric surfactants have been studied in the lab under various temperature and salinity circumstances. Several screening approaches must be used to analyze surfactants in order to select the best surfactant [5].

The primary objectives of surfactant addition in different petroleum processes include converting the reservoir's unfavorable behaviors to more favorable ones to improve hydrocarbon recovery. It was found that the characteristics of the reservoir rock (rock type, pore shape, and size), fluid properties, reservoir heterogeneities, and the initial wetting condition of the reservoir rock all influence the recovery factor in water flooding [6]. As a result, several tertiary recovery techniques, such as polymer flooding, miscible gas injection, surfactant flooding, and microbial EOR, have been developed. Therefore, the capacity of a surfactant to alter wettability and enhance water absorption would be an excellent technique for enhancing oil recovery [7–10].

Numerous studies on surfactant flooding for EOR in hydrocarbon reservoirs have been conducted in recent years. These studies are based on mechanisms, measurements, and the influencing factors of surfactant retention on rocks [11–23]. As an example, Chen and Schechter studied how to best select a surfactant for wettability alteration. They found that increased levels of surfactants lead to greater reductions in interfacial tension (IFT) and decreased contact angles. A relatively elevated concentration is required to transition the rock into the water-wet zone. Additionally, the recovery factor of oil in spontaneous imbibition experiments rises as surfactant concentration increases. The brine's salinity affects both rock wettability and surfactant effectiveness, leading to reduced interfacial tension (IFT) and increased contact angles (CA) compared to distilled water. Moreover, the cloud point of nonionic surfactants rises with higher salinity levels [24]. Furthermore, additional research has focused on the impact of surfactant concentration, salinity, temperature, and pH on surfactant adsorption, but they were only able to examine the effects of these factors in the majority of conventional reservoirs [21].

Natural surfactants, also known as polar lipids, are obtained from renewable sources such as plants or animals [25,26]. Sen (2008) noted that some of the typical bio surfactants employed in EOR include microorganisms like Rhodococcus, Rhamnolipid, Pseudomonas, and Trehalose lipids [27]. However, due to unpredictable performance, challenges with achieving standardized engineering designs by microbial processes, low oil recovery, and challenges with handling live bacterial procedures, these bio-surfactants are only rarely used in EOR processes [28]. When Kumar et al. (2017) performed a core flooding experiment on three distinct sand pack media with surfactant concentrations of 0.8, 1, and 1.2 wt%, the results gave additional recoveries over water flooding of 24.7%, 25.8%, and 27.6%, respectively, for original oil in place (OOIP) [29]. The recovery rate of methyl ester sulfonate (MES) derived from Jatropha oil was at 32.07%, 31.00%, and 29.18%, respectively, for dodecane, heptane, and decane, in a sand pack experiment using distinct alkanes (dodecane, heptane, and decane) as the oil phase [30].

The most promising production method in reservoir rocks with low permeability was found to be changing wettability from oil-wet to intermediate/water-wet conditions. With capillary forces controlling the recovery mechanism, this approach promotes spontaneous imbibition [31].

Currently, the use of non-biodegradable and toxic compounds are not permitted, which has led to the abandonment of several surfactants in the United States and Europe. These surfactants include dialkyl quats, linear alkylbenzene sulfonates, and alkylphenol ethoxylates. Hence, finding a superior surfactant with good surface characteristics from biomass sources to replace the current surfactants has been the focus of recent studies [26,32–35]. Surfactants should also be thermally stable and have a good tolerance for the salinity and hardness of brine [36].

Harsh reservoirs condition of high salinity and temperature should be taken into considerations in surfactant applications. Because it can reduce the chemical stability of the solution by accelerating breakdown, temperature has significant effects on the performance of surfactant solutions, especially under reservoir conditions [37]. On the other hand, high temperature has the opposite effect and speeds up the hydrolysis of surfactants, especially anionic surfactants like sulfates [5]. Cloud point is a common approximation for thermal stability during the screening stage. In some nonionic surfactant systems, careful temperature management might result in the desired type of microemulsion because nonionic surfactant solubility in brine decreases with rising temperature [38,39]. Nonionic surfactants lose their solubility at their cloud point or phase inversion temperature, unlike chemical EOR techniques where high-temperature reservoirs provide a substantial difficulty [40].

The date palm (*Phoenix dactylifera*) is a species of flowering plant in the Aceraceae family of palms that is grown for its edible fruit known as dates. The species is widely grown in South Asia, the Middle East, and northern Africa. It has also become naturalized in many tropical and subtropical areas around the world [37]. The Kingdom of Saudi Arabia is currently the third-largest producer in the world. The type of the date kernel that been used in this experimental work is from

the Al-Khalas which is a variety of date that is well-known in the Saudi Arabian provinces of Qassim, Al-Kharj, and Al-Ahsa. In addition to the surfactant that can be extracted, it was found that the solid waste can actually be used a fracture sealing-material in drilling operations [41]s. This means that date seeds are an exceptionally attractive choice to solve problems in both EOR and drilling sectors.

The goal of this work is to study the date seed's efficacy as a surfactant source under high salinity/high temperature (HS/HT) conditions of Saudi reservoirs. The primary goal of this study is to develop a novel, affordable, readily available, locally sourced natural surfactant that is environmentally friendly for use in different oil fields, especially EOR applications. This is to be achieved through the evaluation of this natural surfactant for Saudi reservoirs in HS/HT environments. To further support this, the new surfactant will be extracted using water with different salinity values resembling formation brine and sea water in addition to distilled water to decide which salinity is best suited for this process.

Materials and Methods

Date Seed Preparation

The date type used in this experiment is the Al-Khalas Dates native to the Qassim, Al-Kharj, and Al-Ahsa regions in the Kingdom of Saudi Arabia. To prepare the date seeds for the extraction of the surfactant, the seeds were placed in a Memmert convection oven (Grainger®, USA) at 70 ºC for 24 hours for drying (Fig. 1). After that, a high-speed blender (Homeelec®) was used to grind the seeds into a fine powder which was then sieved using a 150-mesh size sieve to obtain the right sized particles.

Fig. 1. Drying date seeds in oven at 70ºC.

Surfactant Extraction

To determine the effect of salinity on the extraction of the surfactant, three types of water were used: formation brine, sea water, and distilled water.

To prepare formation water, NaCl, $CaCl_2$, $MgCl_2$, and $NaHCO_3$ (as outlined in Table 1) were dissolved in 1L of distilled water using a magnetic stirrer in a 2L flask. After the salts were completely dissolved, water was added to reach the 2L mark finalizing a solution of 168,000 ppm. The formation water had been selected based on Saudi Khafji field formation water [42].

Table 1. Formation water composition for a 2L solution.

Component	Mass [g]
NaCl	257.3
$CaCl_2$	56.56
$MgCl_2$	14.8
$NaHCO_3$	1.64

In order to prepare sea water, 500 g of the formation water prepared earlier was diluted with 1,722.2 g of distilled water to get a solution of 37,000 ppm. The extraction of the surfactant was carried out using three date seed concentrations (1, 5, and 10 wt%) in formation brine, sea water, and distilled water at room temperature (23 ºC) and 70 ºC. As an example, 10 g of date seeds were added to 190 g of distilled water at 70 ºC and stirred for 24 hours to extract a 5% surfactant solution with distilled water base. A summary of all the solutions can be found in Table 2.

Table 2. Summary of surfactant extraction solutions.

Temperature	Water	Surfactant Concentration [wt%]
23 ºC	Distilled Water	1
		5
		10
	Formation Brine	1
		5
		10
	Sea Water	1
		5
		10
70 ºC	Distilled Water	1
		5
		10
	Formation Brine	1
		5
		10
	Sea Water	1
		5
		10

After the seed grinds have been stirred in the solution, air vacuum system was built and utilized in order to filter the suspension and remove any solid materials. This process was done using Whatman® filter papers with 25 µm mesh size which is suitable for core flooding in next studies. With this, the extraction of the surfactant was completed, and the solutions were ready for testing.

Surface/Interfacial Tension Measurement

A Du-Nouy tensiometer (K9 by Kruss®, Germany) was used to measure the surface/interfacial tension of the different fluids in this study. As a standard, the surface tension of distilled water and toluene were measured before any of the study fluids as references to make sure that the equipment is calibrated and measurements are accurate. Interfacial tension between the different surfactant solutions and Saudi medium crude oil was measured to determine the optimum concentration of both brine and surfactant.

Saudi Medium Crude Oil

Saudi medium crude oil of 26 API was used in this study to measure the IFT.

pH and Density Measurement

The pH of the different samples was measured using a Fischer Scientific® Benchtop pH meter. The meter was calibrated using stock solutions of pH 7 and pH 4 before conducting the measurements of the surfactant solutions.

As for density, the DMA 5000 density meter by Anton Paar (USA) was used to conduct measurements at 25 and 70 ºC.

Results and Discussion

Table 3 displays the amount of date seeds retained after drying which was around 95.8% of the original weight, meaning that 4.2% were lost as moisture during the drying process.

Table 3. Date seed retention amount.

Before Drying [g]	After Drying [g]	Retention [%]
1376.3	1318.7	95.8

Surface/Interfacial Tension

Toluene was used as a standard solution to calibrate surface tension measurements. At 20 ºC, toluene has a surface tension of 28.91 mN/m. The toluene-based correction factor was found to be 0.94. Both Table 4 and Fig. 2 display the results of the surface tension measurements of the different surfactant solutions. As expected, the higher the concentration of the surfactant regardless of the salinity of the brine, the lower the surface tension becomes. The most notable change in surface tension was that of sea water at 70 ºC. At 1 wt% of surfactant, the solution had a surface tension of around 49.6 mN/m which dropped to 43.1 mN/m at a surfactant concentration of 10 wt%. Overall, the best performing solution at both 1 and 5 wt% was formation water at 70 ºC, which was only slightly outperformed by 70 ºC sea water at 10 wt% surfactant concentration. The very low standard deviation values indicate the accuracy of the obtained results.

Table 4. Surface tension results for the different surfactant solutions.

	Surface Tension [mN/m] (± SD)					
	Distilled Water		Formation Brine		Sea Water	
Concentration [wt%]	23 °C	70 °C	23 °C	70 °C	23 °C	70 °C
1	51.8 ± 1.1	50.1 ± 0.9	51.9 ± 1.6	45.3 ± 0.7	50.2 ± 1.2	49.6 ± 0.3
5	50.7 ± 1.0	49.0 ± 1.7	50.8 ± 0.8	45.0 ± 1.5	47.1 ± 0.6	45.5 ± 2.1
10	50.1 ± 2.8	47.0 ± 0.9	49.7 ± 0.4	43.0 ± 0.7	45.4 ± 1.7	43.1 ± 0.6

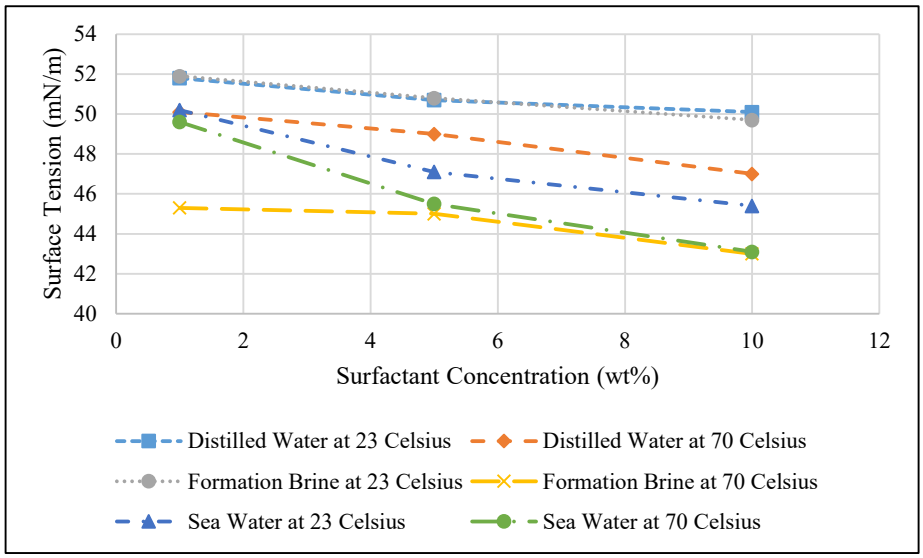

Fig. 2. Surface tension results for the different surfactant solutions.

Table 5. Interfacial tension results for the different surfactant solutions with Arabian medium oil (API= 26º).

	Surface Tension [mN/m]					
	Distilled Water		Formation Brine		Sea Water	
Concentration [wt%]	23 °C	70 °C	23 °C	70 °C	23 °C	70 °C
1	18.5	18.2	16.6	15.9	16.9	15.4
5	18.0	17.1	15.1	13.2	16.0	14.7
10	17.4	16.4	14.2	10.0	15.5	11.3

Table 6. Interfacial tension results for the different water types with Arabian oil without surfactant.

Interfacial Tension [mN/m]		
Distilled Water	Formation Brine	Sea Water
19.8	17.1	17.9

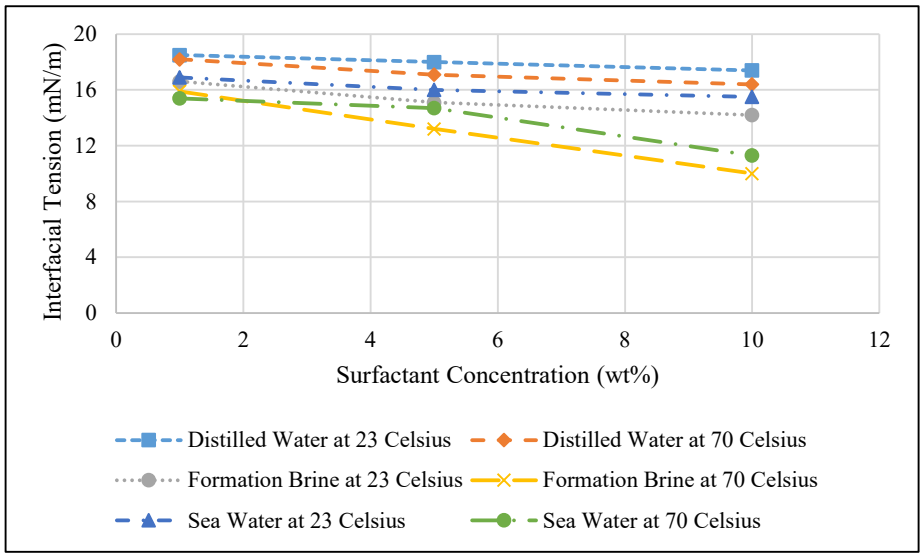

Fig. 3. Interfacial tension results for the different surfactant solutions.

pH and Density Measurement

The pH measurements are important for such novel materials to study their effect on the equipment and formations during the different applications in the oil industry. Low pH, which means high acidity solutions, can cause corrosion and harm the production and injection tubulars and can cause reactions in the reservoir rocks specially limestones reservoirs. This can be solved using multiple

approaches including, but not limited to, corrosion inhibitors. High pH means high alkalinity which can cause undesirable reactions with the reservoir fluids and cause undesirable results. pH also can affect the surfactant adsorption and hence the displacement efficiency.

Table 7. pH values for the different surfactant solutions.

	pH					
	Distilled Water		Formation Brine		Sea Water	
Concentration [wt%]	23 °C	70 °C	23 °C	70 °C	23 °C	70 °C
1	6.78	5.81	6.25	5.89	6.30	6.01
5	5.80	5.70	5.55	5.17	5.77	5.04
10	5.62	4.73	5.27	4.76	5.34	5.03

Table 8. pH values for the different water types.

pH		
Distilled Water	Formation Brine	Sea Water
7.4	6.65	7.2

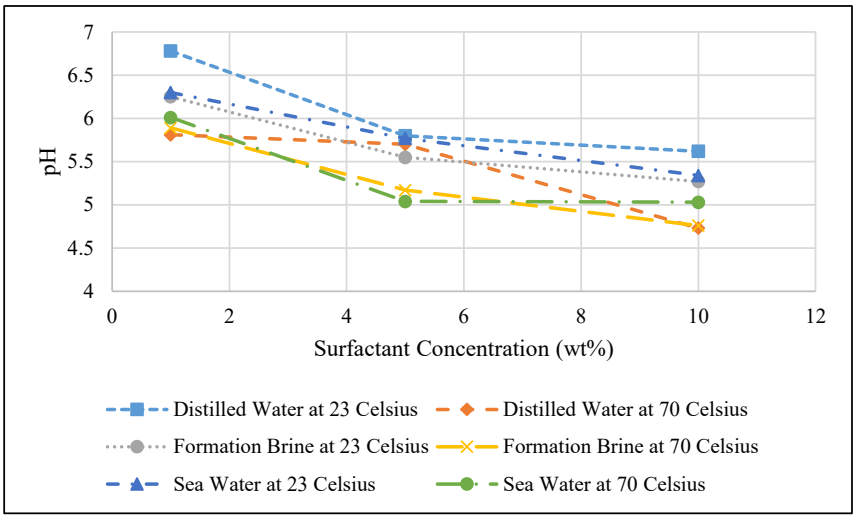

Fig. 4. pH results for the different surfactant solutions.

The pH decreases with increasing concentration of the solution. In addition, the pH level decreases as temperature increases in a solution. To put it into perspective, if we were to increase a solution's temperature, the pH of the solution would drop. However, if the temperature were to decrease, the opposite would happen, and the pH level would increase very slightly. Such reduction in pH may help with injection in carbonate reservoirs which may work, beside its function as a surfactant, as permeability stimulation as well.

Table 9. Density values for the different surfactant solutions.

	Density [g/cc]					
	Distilled Water		Formation Brine		Sea Water	
Concentration [wt%]	23 °C	70 °C	23 °C	70 °C	23 °C	70 °C
1	1.001	1.001	1.118	1.12	1.026	1.026
5	1.002	1.002	1.120	1.126	1.028	1.028
10	1.004	1.004	1.126	1.140	1.028	1.034

Table 10. Density values for the different water types.

Density [g/cc]		
Distilled Water	Formation Brine	Sea Water
1.000	1.116	1.026

Summary

The natural surfactant derived from date seeds demonstrates notable efficacy in reducing surface tension and interfacial tension, presenting a viable alternative to synthetic counterparts. Its non-toxic nature renders it environmentally benign, offering a significant advantage over conventional surfactants. Moreover, it proves economically advantageous for manufacturers seeking sustainable alternatives. This experimental study highlights several key findings: the successful evaluation of a promising, locally sourced, cost-effective green surfactant for oil field applications, particularly Enhanced Oil Recovery (EOR); its favorable attributes such as availability, affordability, local production, and environmental compatibility; its substantial reduction in surface tension (43%) and interfacial tension (49%) compared to seawater; and its stable density under varying conditions, obviating the need for special handling during injection or production.

Given the promising outcomes showcased in this study regarding the potential application of the innovative surfactant, several recommendations are proposed for future investigations. Firstly, further exploration is warranted under reservoir conditions encompassing elevated temperatures, salinity levels, and pressures. Additionally, comprehensive chemical analyses such as XRD and XRF are imperative to ascertain the composition and elucidate additional properties. Moreover, it is essential to broaden the scope of tested properties to include solution viscosity and compatibility with formation fluids, particularly oils. Furthermore, investigating the surfactant's impact on wettability alteration is crucial. Lastly, conducting core flooding experiments using limestone and sandstone core samples is recommended to assess the surfactant's efficacy in oil displacement.

References

[1] Afolabi RO, Oluyemi GF, Officer S, Ugwu JO. Hydrophobically associating polymers for enhanced oil recovery – Part A: A review on the effects of some key reservoir conditions. J Pet Sci Eng. 2019 Sep;180:681–98.

[2] Sabhapondit A, Borthakur A, Haque I. Water Soluble Acrylamidomethyl Propane Sulfonate (AMPS) Copolymer as an Enhanced Oil Recovery Chemical. Energy Fuels. 2003 May 1;17(3):683–8.

[3] Wever DAZ, Picchioni F, Broekhuis AA. Polymers for enhanced oil recovery: A paradigm for structure–property relationship in aqueous solution. Prog Polym Sci. 2011 Nov;36(11):1558–628.

[4] Li Z, Wu H, Hu Y, Chen X, Yuan Y, Luo Y, et al. Ultra-low interfacial tension biobased and catanionic surfactants for low permeability reservoirs. J Mol Liq. 2020 Jul;309:113099.

[5] Olayiwola SO, Dejam M. A comprehensive review on interaction of nanoparticles with low salinity water and surfactant for enhanced oil recovery in sandstone and carbonate reservoirs. Fuel. 2019 Apr;241:1045–57.

[6] Alzahid YA, Mostaghimi P, Walsh SDC, Armstrong RT. Flow regimes during surfactant flooding: The influence of phase behaviour. Fuel. 2019 Jan;236:851–60.

[7] Daghlian Sofla SJ, Sharifi M, Hemmati Sarapardeh A. Toward mechanistic understanding of natural surfactant flooding in enhanced oil recovery processes: The role of salinity, surfactant concentration and rock type. J Mol Liq. 2016 Oct;222:632–9.

[8] Sheng JJ. Enhanced oil recovery in shale reservoirs by gas injection. J Nat Gas Sci Eng. 2015 Jan;22:252–9.

[9] Alfarge D, Wei M, Bai B. IOR Methods in Unconventional Reservoirs of North America: Comprehensive Review. In: Day 3 Tue, April 25, 2017 [Internet]. Bakersfield, California: SPE; 2017 [cited 2023 Sep 25]. p. D031S008R005. Available from: https://onepetro.org/SPEWRM/proceedings/17WRM/3-17WRM/Bakersfield,%20California/195912

[10] Nowrouzi I, Mohammadi AH, Manshad AK. Chemical Enhanced Oil Recovery by Different Scenarios of Slug Injection into Carbonate/Sandstone Composite Oil Reservoirs Using an Anionic Surfactant Derived from *Rapeseed* Oil. Energy Fuels. 2021 Jan 21;35(2):1248–58.

[11] Gong L, Liao G, Luan H, Chen Q, Nie X, Liu D, et al. Oil solubilization in sodium dodecylbenzenesulfonate micelles: New insights into surfactant enhanced oil recovery. J Colloid Interface Sci. 2020 Jun;569:219–28.

[12] Yun W, Chang S, Cogswell DA, Eichmann SL, Gizzatov A, Thomas G, et al. Toward Reservoir-on-a-Chip: Rapid Performance Evaluation of Enhanced Oil Recovery Surfactants for Carbonate Reservoirs Using a Calcite-Coated Micromodel. Sci Rep. 2020 Jan 21;10(1):782.

[13] Deljooei M, Zargar G, Nooripoor V, Takassi MA, Esfandiarian A. Novel green surfactant made from L-aspartic acid as enhancer of oil production from sandstone reservoirs: Wettability, IFT, microfluidic, and core flooding assessments. J Mol Liq. 2021 Feb;323:115037.

[14] Shadizadeh SR, Seyedi Abandankashi SR, Moradi S. Experimental Investigation Used of Albizia Julibrissin Extract as a Plant Surfactant on Oil Recovery. Iran J Oil Gas Sci Technol [Internet]. 2021 Jan [cited 2023 Sep 25];(Online First). Available from: https://doi.org/10.22050/ijogst.2021.234857.1555

[15] Su L, Sun J, Ding F, Gao X, Zheng L. Effect of molecular structure on synergism in mixed zwitterionic/anionic surfactant system: An experimental and simulation study. J Mol Liq. 2021 Jan;322:114933.

[16] Groenendijk DJ, Van Wunnik JNM. The Impact of Micelle Formation on Surfactant Adsorption–Desorption. ACS Omega. 2021 Jan 26;6(3):2248–54.

[17] Kurnia I, Zhang G, Han X, Yu J. Zwitterionic-anionic surfactant mixture for chemical enhanced oil recovery without alkali. Fuel. 2020 Jan;259:116236.

[18] Esfandyari H, Moghani Rahimi A, Esmaeilzadeh F, Davarpanah A, Mohammadi AH. Amphoteric and cationic surfactants for enhancing oil recovery from carbonate oil reservoirs. J Mol Liq. 2021 Jan;322:114518.

[19] Khayati H, Moslemizadeh A, Shahbazi K, Moraveji MK, Riazi SH. An experimental investigation on the use of saponin as a non-ionic surfactant for chemical enhanced oil recovery (EOR) in sandstone and carbonate oil reservoirs: IFT, wettability alteration, and oil recovery. Chem Eng Res Des. 2020 Aug;160:417–25.

[20] Asl HF, Zargar G, Manshad AK, Takassi MA, Ali JA, Keshavarz A. Experimental investigation into l-Arg and l-Cys eco-friendly surfactants in enhanced oil recovery by considering IFT reduction and wettability alteration. Pet Sci. 2020 Feb;17(1):105–17.

[21] Do Vale TO, De Magalhães RS, De Almeida PF, Matos JBTL, Chinalia FA. The impact of alkyl polyglycoside surfactant on oil yields and its potential effect on the biogenic souring during enhanced oil recovery (EOR). Fuel. 2020 Nov;280:118512.

[22] Bahraminejad H, Manshad AK, Keshavarz A. Characterization, Micellization Behavior, and Performance of a Novel Surfactant Derived from *Gundelia tournefortii* Plant during Chemical Enhanced Oil Recovery. Energy Fuels. 2021 Jan 21;35(2):1259–72.

[23] Jiao K, Feng Q, Davarpanah A. Effect of anionic and non-anionic surfactants on the adsorption density. Pet Sci Technol. 2021 May 19;39(9–10):362–72.

[24] Chen W, Schechter DS. Surfactant selection for enhanced oil recovery based on surfactant molecular structure in unconventional liquid reservoirs. J Pet Sci Eng. 2021 Jan;196:107702.

[25] Atta DY, Negash BM, Yekeen N, Habte AD. A state-of-the-art review on the application of natural surfactants in enhanced oil recovery. J Mol Liq. 2021 Jan;321:114888.

[26] Holmberg K. Natural surfactants. Curr Opin Colloid Interface Sci. 2001 May;6(2):148–59.

[27] Sen R. Biotechnology in petroleum recovery: The microbial EOR. Prog Energy Combust Sci. 2008 Dec;34(6):714–24.

[28] Imanivarnosfaderani MR, Gomari SR, Dos Santos RG. Effects of rhamnolipid bio-surfactant and sodium dodecylbenzene sulfonate (SDBS) surfactant on enhanced oil recovery from carbonate reservoirs. Braz J Chem Eng. 2022 Sep;39(3):825–33.

[29] Kumar S, Kumar A, Mandal A. Characterizations of surfactant synthesized from Jatropha oil and its application in enhanced oil recovery. AIChE J. 2017 Jul;63(7):2731–41.

[30] Pal N, Kumar S, Bera A, Mandal A. Phase behaviour and characterization of microemulsion stabilized by a novel synthesized surfactant: Implications for enhanced oil recovery. Fuel. 2019 Jan;235:995–1009.

[31] Khandoozi S, Sharifi A, Riazi M. Enhanced oil recovery using surfactants. In: Chemical Methods [Internet]. Elsevier; 2022 [cited 2023 Sep 25]. p. 95–139. Available from: https://linkinghub.elsevier.com/retrieve/pii/B9780128219317000079

[32] Bachari Z, Isari AA, Mahmoudi H, Moradi S, Mahvelati EH. Application of Natural Surfactants for Enhanced Oil Recovery – Critical Review. IOP Conf Ser Earth Environ Sci. 2019 Mar 1;221:012039.

[33] Jahan R, Bodratti AM, Tsianou M, Alexandridis P. Biosurfactants, natural alternatives to synthetic surfactants: Physicochemical properties and applications. Adv Colloid Interface Sci. 2020 Jan;275:102061.

[34] Mujumdar S, Joshi P, Karve N. Production, characterization, and applications of bioemulsifiers (BE) and biosurfactants (BS) produced by *Acinetobacter* spp.: A review. J Basic Microbiol. 2019 Mar;59(3):277–87.

[35] Tackie-Otoo BN, Ayoub Mohammed MA. Experimental investigation of the behaviour of a novel amino acid-based surfactant relevant to EOR application. J Mol Liq. 2020 Oct;316:113848.

[36] Kumar P, Mittal KL, editors. Handbook of Microemulsion Science and Technology [Internet]. 1st ed. CRC Press; 2018 [cited 2023 Sep 25]. Available from: https://www.taylorfrancis.com/books/9781351442343

[37] Li Z, Wu H, Yang M, Jiang J, Xu D, Feng H, et al. Spontaneous Emulsification via Once Bottom-Up Cycle for the Crude Oil in Low-Permeability Reservoirs. Energy Fuels. 2018 Mar 15;32(3):3119–26.

[38] Vatanparast H, Alizadeh AH, Bahramian A, Bazdar H. Wettability Alteration of Low-permeable Carbonate Reservoir Rocks in Presence of Mixed Ionic Surfactants. Pet Sci Technol. 2011 Jul 28;29(18):1873–84.

[39] Nandwani SK, Chakraborty M, Bart HJ, Gupta S. Synergism, phase behaviour and characterization of ionic liquid-nonionic surfactant mixture in high salinity environment of oil reservoirs. Fuel. 2018 Oct;229:167–79.

[40] Pillai P, Mandal A. Synthesis and characterization of surface-active ionic liquids for their potential application in enhanced oil recovery. J Mol Liq. 2022 Jan;345:117900.

[41] AlAwad MNJ, Fattah KA. Superior fracture-seal material using crushed date palm seeds for oil and gas well drilling operations. J King Saud Univ - Eng Sci. 2019 Jan;31(1):97–103.

[42] Moawad TM, Al-Dhafeeri AM, Mohamed TI. Reservoir Management Tool-Kits in Offshore Khafji Field: Successful Solutions for Field Case Studies on Water Conning Problems in Sandstone Reservoirs. In: All Days. Cairo, Egypt: SPE; 2013. p. SPE-164642-MS. Available from: https://onepetro.org/SPENATC/proceedings/13NATC/All-13NATC/Cairo,%20Egypt/17779

Published in: Materials Science Forum
ISSN: 1662-9752, Vol. 1125, pp 65-69
doi:10.4028/p-BU7iac

Submitted: 2023-12-28
Revised: 2024-03-25
Accepted: 2024-03-26
Online: 2024-09-23

Comparative Study of Mechanical Behavior between an Adhesive Made from Date Palm Waste and FM-73 Adhesive

Sofiane MAACHOU[1*], Abdeldjalil BENBAKHTI[1,a], Abdelmadjid MOULGADA[2,b]

[1]University Centre of Maghnia, Al-Zawiya Road 13300, Maghnia, Tlemcen, Algeria

[2]University of Ibn Khaldoun Tiaret, City Zaaroura 14000 Tiaret, Algeria.

[a]Jalil7benbakhti@hotmail.com, [b]amoulgada@hotmail.fr, *Sofianemaachou@gmail.com

Keywords: Date palm waste, Adhesive, Crack propagation, Composite, Patch, NASGRO model.

Abstract. The thickness of the adhesive has a major influence on the shear strength of bonded assemblies. This work is based on a study of the fatigue behavior of two cracked aluminum (2024 T351) plates repaired by patch (graphite/epoxy) under cyclic loading. For this we used a computer code to study the propagation of fatigue cracks to predict the life of the plates repaired named AFGROW. The first plate was repaired using an adhesive made from date palm waste whereas the second plate was repaired using FM-73 adhesive. The results obtained from this study show that, despite the low shear modulus of the adhesive made from date palm waste and the very low film thickness, the joint bonded with the latter gives good joint strength and a lifetime (number of cycles) similar to the joint bonded with the FM-73 adhesive when the thickness of the joint of the adhesive is greater than that of the adhesive made by the waste of the date palm. This shows that the strength of the bonded joint increases rapidly from very low thicknesses (less than a few hundredths of a millimeter). Finally, we recommend using the adhesive made from date palm waste for patch repair as well as for applications such as lightweight construction, electric vehicles or solar panels.

Introduction

Repairing cracks by bonding a composite material patch is a reliable and economical method, which has proven its effectiveness in reducing the speed of crack propagation by reducing the stress intensity at the crack heads.

Several experimental studies, modeling or numerical simulations have been undertaken to better understand the evaluation of the lifespan of mechanical structures [1,2,3,4,5]. Generally, the prediction of this lifespan is based on the crack propagation speed.

Material and Geometric Model

In this modeling, we consider an aluminum plate (2024 T351) with a central crack and repaired by patch (graphite/epoxy). This crack of length 2a = 4mm located in the middle of the plate and perpendicular to the stress plane. The plate considered is stressed in uniaxial traction in the vertical direction Y. The adhesive joint used in the repair in the first case is the date palm waste adhesive, in the second case is FM73 adhesive. Fig. 1 presents the geometric model and the configuration of the crack investigated in this study. Fig. 2 shows the dimensions of the patch. Table 1 groups together the properties of the material used in this analysis as well as the properties of the patch, Fig. 3 shows the orientation of the 7 symmetrical plies with a thickness of 0.132mm per ply and Table 2 groups together the properties of the date palm waste adhesive and FM73 adhesive.

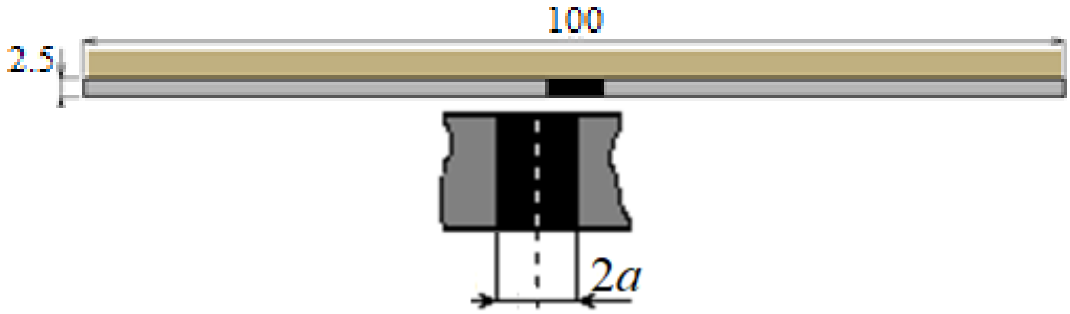

Fig. 1. Geometric model and the configuration of the crack.

Table 1. Properties of the aluminum (2024 T351) and of the graphite/epoxy.

	2024 T351	*graphite/epoxy*
E_L [N/mm^2]	73084.4	172369
E_T [N/mm^2]	---	10342,1
G_{LT} [N/mm^2]	---	4826,33
ν_{LT}	0.33	0,31
ν_{TL}	---	0,13
α_L[K^{-1}]	2.32.10^{-5}	-7.10^{-7}
α_T [K^{-1}]	---	3,6.10^{-5}

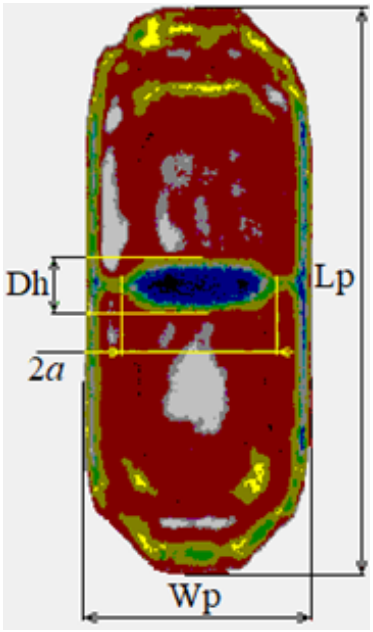

Fig. 2. Patch dimensions: width Wp = 90mm, length Lp = 100mm and Dh/2a = 0.

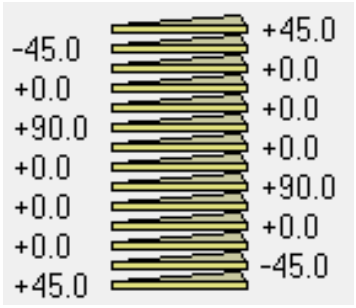

Fig. 3. Orientation des plies.

Table 2. Adhesive properties.

	Adhesive made from date palm waste	*FM73 adhesive*
G_{LT} [N/mm^2]	4	413.685
Thicknesses [mm]	1.10^{-5}	1.10^{-3}

Theoretical Model

We used a computer code to study the propagation of fatigue cracks to predict the life of metal structures named AFGROW. The NASGRO model is applied to predict crack propagation. The crack propagation equation used by NASGRO is:

$$\frac{da}{dN} = C\left[\left(\frac{1-f}{1-R}\right)\Delta K\right]^n \frac{\left(1-\frac{\Delta K_{th}}{\Delta K}\right)^p}{\left(1-\frac{K_{max}}{K_{cr}}\right)^q} \quad (1)$$

Or :

- ✓ C, n, p and q: material parameters (see table 3) ;
- ✓ R : load report;
- ✓ $\Delta K = K_{max} - K_{op}$;
- ✓ K_{max} : maximum stress intensity factor;
- ✓ K_{op} : crack opening stress intensity factor;
- ✓ K_c : critical stress intensity factor;
- ✓ The function f is $f = K_{OP}/K_{max}$.

Table 3. NASGRO equation parameters for Aluminum (2024 T351).

C	*n*	*p*	*q*
$1.7073.10^{-10}$	3.353	0.5	1

Results and Discussion

For a comparative study of the mechanical behavior of the date palm waste adhesive and the FM73 adhesive, we chose two cracked and patch-repaired (graphite/epoxy) aluminum plates (2024 T351) of identical geometric shapes under cyclic loading, one of the plates bonded by an adhesive made from date palm waste with a thickness T_{dpw}=10^{-2}mm and the other bonded by FM73 adhesive with a thickness of T_{FM}=1mm. The adhesive joint is loaded by applying forces to the ends of a joint with a load ratio R = 0.1.

Fig. 4 present the evaluation of patch (graphite/epoxy) β correction of the date palm waste adhesive and FM73 adhesive as a function of the crack length. A patching correction factor is proposed to account for the positive effects of the material and geometric properties of the patch and adhesive layer.

Fig. 5 shows the crack length as a function of the number of cycles of the date palm waste adhesive and FM73 adhesive.

For the variation of the length of the crack as a function of the number of cycles of the plate for the two adhesives which are FM-73 and that of date palm waste, we clearly see that the shape of the two curves is Almost confused with a difference almost infinitesimal, this lifespan of this crack propagation can reach $1.1.1O^5$ for that of the palm waste adhesive and $1.05.10^5$ for that of FM73.

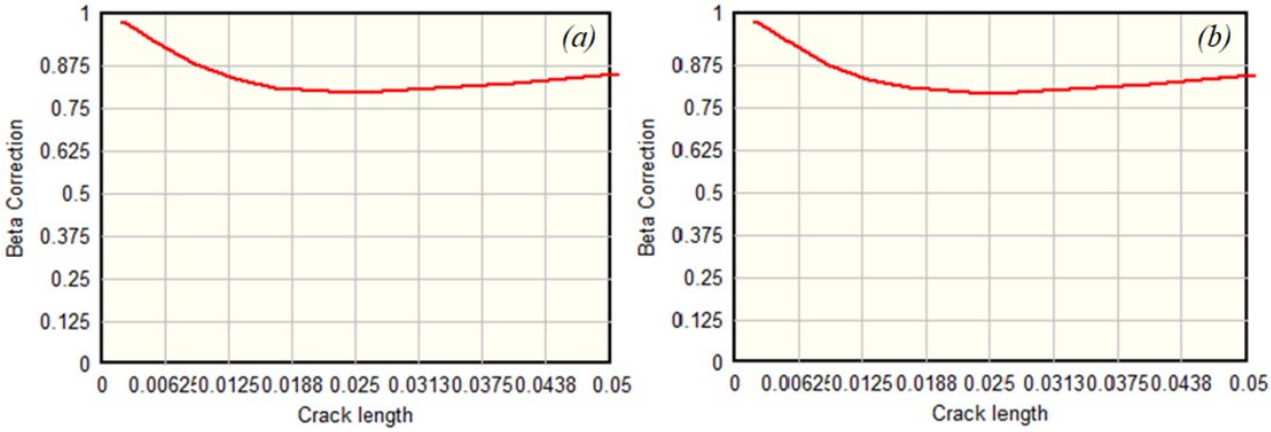

Fig. 4. Patch β correction factor: (a) date palm waste adhesive, (b) FM73 adhesive.

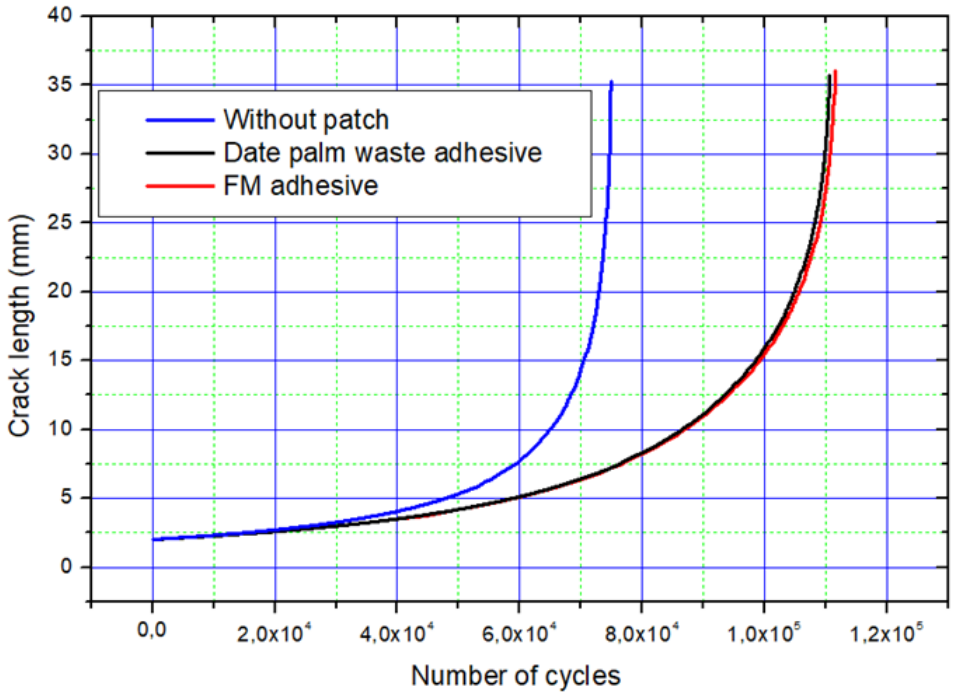

Fig. 5. The variation of crack length as a function of the number of cycles.

Conclusion

The thickness of the adhesive joint plays a very important role in the strength of bonded assemblies and has a direct influence on the service life of the structures. The best way to design such operations is to ensure good adhesion of the joint (structure-adhesive-patch) and reduce shear stresses in order to avoid patch decohesion as much as possible is to carefully study the thickness of the adhesive. This work presents a numerical approach to describe the comparison between date palm waste adhesive and FM73 adhesive.

The work that we carried out allowed us to deal with the influence of the thickness of the adhesive on the values of the fracture parameters calculated for a plate subjected to tension containing a central crack.

After this study, we can conclude that:

- ✓ The presence of a patch considerably reduces crack propagation which can delay the rate of cracking and subsequently increase the life of the structure.
- ✓ The evaluation of the correction factor β of the patch is almost identical for the two adhesives.
- ✓ The effectiveness of the date palm waste adhesive is comparable with that of FM73 and presents a very important natural contribution, because it uses natural and renewable materials and it could have a lower environmental impact compared to synthetic chemical-based adhesive, despite its physicochemical properties, and even more so by its mechanical properties, provided that it plays on the thickness.

References

[1] Moulgada et al. Study of mechanical behavior by fatigue of a cracked plate repaired by different composite patches, *Frattura ed Integrità Strutturale* 15 195-202. (2021)

[2] Maleki, et al. The fatigue failure study of repaired aluminum plates by composite patches using acoustic emission. *Engineering Fracture Mechanics* 210 300-311(2019)

[3] Maierhofer, R. Pippan, and H-P. Gänser Modified NASGRO equation for physically short cracks. *International Journal of fatigue* 59 200-207. (2014)

[4] L. Rezgani., K. Madani, M. Mokhtari, X. Feaugas, S. Cohendoz, S. Touzain, & S. Mallarino Hygrothermal ageing effect of ADEKIT A140 adhesive on the J-integral of a plate repaired by composite patch. *Journal of adhesion science and Technology* 32(13) 1393-1409. (2018)

[5] S. M. Khan, B. B. Bouiadjra, F. Benyahia, & A. Albedah Analysis of the single overload effect on fatigue crack growth in AA 2024-T3 plates repaired with composite patch. *Engineering Fracture Mechanics,* 202 147-161. (2018)

Keyword Index

Author Index